Finite Element Modelling and Updating of Structure of Sheet Metal with Bolted and Welded Joints

Thesis submitted in accordance with the requirements of
the University of Liverpool for the degree of Doctor in Philosophy

by

Mohd Azmi Yunus

July 27, 2011

To my parent and family

Abstract

A large and complex structure such as a car body-in-white typically consists of several major components that are produced from thin metal sheets. The components are joined together by different types of mechanical joints such as rivets, spot welds and bolted joints. These mechanical joints are highly influenced the overall dynamic behaviour of structures. The finite element method has been widely used for predicting the dynamic behaviour of structures. However, to model the local effects (such as slip, loosing, or clearance effect) arising from the joints is cumbersome and time consuming. Moreover, the predicted model is often found to be inconsistent with the measured data. The discrepancies are believed to be arisen from the invalid assumptions about the model and properties data of the initial finite element model. This thesis puts forward the idea of using a simple and practical bolted joint modelling considering local effects of the area of the bolted joints of thin metal sheet structures.

CFAST element and initial stress ratio are used in modelling the bolted joints and the local effects of the mating area between bolt, washer and surface of the structure. The properties of the parameters of the CFAST element and the initial stress ratio are used in the model updating procedure. The advantage of this technique allows the local effects of the bolted joints to be modelled in a simple way and it proved to be successful in modelling bolted joints.

The influence of the stiffness of suspension springs which is used in simulating free-free boundary conditions in the experimental work especially for the structure that is made from thin metal sheet is investigated as well in this thesis. In the investigation, CBUSH element is used to model the suspension springs and the stiffness of the spring is taken into account as the updating parameter for the finite element model of the full welded structure with free-free boundary conditions.

In this thesis, the use of the simple and practical modelling is adopted in the development of the finite element model of the full welded structure that consists of ten components made from thin metal sheets joined by spot welds and bolted joints. The model is updated using the results obtained from the experiments via the application of two model updating methods. They are iterative method and response surface method (RSM). In the iterative method, the NASTRAN SOL200 is used to improve the finite element models of the components and of the welded structures.

The work in the iterative method is divided into two parts. The first one, the finite element models of components are updated in order to reduce the discrepancies of the natural frequencies before they are assembled together. Meanwhile, the second part is the updating process of the finite element models of the welded structures by concentrating on joint modelling and updating.

Finally, the response surface method (RSM) is used in updating the model of the full welded structure with fixed boundary conditions due to bolted joints. The Latin hypercube sampling is used to generate numerical samples. The accuracy and efficiency of both methods (iterative method and RSM) are presented and discussed.

Acknowledgment

I would like to express my gratitude to my primary supervisor, **Prof. Huajiang Ouyang**, for his valuable advice, encouragement and supervision throughout this research. I also would like to thank **Dr. T. Shenton** for his valuable input and time serving as my second supervisor.

Special thanks to **Dr. Simon James** for his inspiring and valuable advice in performing experimental work. I would to express my appreciation **to Mr. Tommy Evans** in helping fabricated the welded structure.

Special appreciation to **Dr. Sham**, **Dr. Dan Stancioiu**, **Dr. Ruiqiang**, **Dr. Huaxia Deng** for their useful discussions and advice. I also would like to express my gratitude to former and present colleagues in the Dynamics and Control group **Dr. Haddad Khodaparast**, **Dr. N. Abu Hussain**, **Dr. Victor Weizhuo**, **Dr. M. Prandina**, **Mr. Shahrir**, **Ms.N.Hassan**, **Mr Y.Harmin** and **Mr. A.S Omar**.

Special thanks to my wife, **Noradauwiah Mohamad Nordin** and daughters, **Syahirah, Syasha and Batrisyia** for all their love moral support and patience. Without them I would not have had the courage to complete this thesis.

I am grateful to **Majlis Amanah Rakyat (MARA) of Malaysia** for providing the financial support.

Contents

List of Figures

List of Tables

List of Symbols and Abbreviations

NVH	noise, vibration and harness
EMA	experimental modal analysis
FEA	finite element analysis
BiW	Body-in-White
FEA	finite element analysis
FEM	finite element method
MAC	modal assurance criterion
FFT	Fast Fourier Transform
FRF	frequency response function
GA	genetic algorithm
RSM	response surface method
LHS	Latin Hyper Supercubic
CAD	computer aided design
RSW	resistance spot welding
ACM2	area contact model 2
SA	simulated annealing
RC	reinforced concrete
MS	main support
EXP	experiment
FE	finite element
SS	side support
CPU	Central processing unit
Z	vector of response variables

$\mathbf{S}$	sensitivity matrix
$\boldsymbol{\theta}$	structural parameter variable
$\mathbf{M}$	mass matrix
$\mathbf{K}$	stiffness matrix
$\mathbf{C}$	damping matrix
$\mathbf{H}(\omega)$	frequency response function
W	weighting coefficient
ω	frequency in rad / sec
$\boldsymbol{\phi}$	vector of eigenvectors
W	weighting coefficient
E	Young's modulus
G	shear modulus
ρ	Poisson's ratio
λ_i^{fe}	i^{th} numerical eigenvalue
λ_i^{exp}	i_{th} experimental eigenvalue
x_i^L ,	lower bound
x_i^U	upper bound
β_{ij}	coefficients of unknown parameter
ε	error

Chapter 1

Introduction

1.1 Introduction

The first chapter provides a general introduction of the research and problem areas, namely structural dynamic analysis (Section 1.1.1), modal analysis (Section 1.1.2), the finite element method (Section 1.1.3), and experimental modal analysis (Section 1.1.4) and model updating (Section 1.1.5). Research goal and objective is presented in Section 1.2. Section 1.3 presents list of publications. The preview of this thesis is presented in Section 1.4 and Section 1.5 shows the organisation of the thesis.

1.1.1 Structural dynamics analysis

Vibration phenomena can naturally occur in an engineering system. The effects of vibration can be unpleasant and harmful for many engineering systems. The effects of vibration present major hazards and high levels of vibration affect structures in the form of structural failure, system malfunction, reduced performance and even early breakdown. Consequently, a structure's integrity and safety can become jeopardised.

The earliest main contributions to the theoretical understanding of vibration phenomenon were made in late by 1600s by Hooke and then were formally defined in Newton's second law of motion. Later, significant contributions were made by people such as Bernoulli (1732), who used Bessel functions to describe modes of continuous systems, Kirchhoff (1850), on the theory of plate vibration, Rayleigh (1877), on the theory of sound, and Love (1926), who worked on the mathematical theory of elasticity which is the basis of today's vibration analysis. Then Timoshenko improved the theory of vibration of beams by considering the effects of rotary inertia and shear deformation and meanwhile a similar theory was

presented by Mindlin for the vibration analysis of thick plates which includes the effects of rotary inertia and shear deformation Rao (2004).

Apparently engineering structures have become more complex, flexible and lighter in order to become more economical. The weight reduction of structures such as in automotive and aerospace engineering has been pursued for higher speed and better fuel consumption. However, the complexity and weight of structures have given manufacturers a challenge to fulfil the design criteria that have been set by the industry or the authorities such as noise, vibration and harness (NVH), safety, ride comfort and the environmental legislation. Even though this phenomenon can be avoidable, it has been always a critical issue to engineers and designers in industry to overcome the problem that occurs from the effects of vibration. Therefore the understanding and analysis of the dynamic behaviour of structures has become essential and this can be accomplished through experimental and theoretical approaches or a combination of these approaches.

1.1.2 Modal analysis

Structural vibration testing and analysis contributes to progress in many industries such as aerospace, automotive and civil engineering. The analysis of the structures can be conducted on the physical objects or on models that represent certain aspects of the real structure. In general, simple structures such as beams or plates can be solved analytically by using the closed form solution that is available in various reference books and tables (Blevins, 1979) to predict the dynamic behaviour of the structure. However in order to evaluate the dynamics behaviour of more complex structures the analytical approach becomes impractical and more powerful tools are required in order to determine the vibration system, either numerically or experimentally, and subsequently produce a relatively accurate prediction of the structure's dynamic behaviour. Modal analysis can be used to investigate the dynamic behaviour of the structure by the application of experimental modal analysis (EMA) or numerical analysis (FE), respectively.

1.1.3 Finite element method (FEM)

The finite element analysis (FEA) rapidly developed as a useful numerical analysis tool because of advances in engineering such as civil, aerospace and automotives industries. The prediction of dynamic properties of the complicated structures such as car Body-in-White (BiW) has become more and more challenging. In addition to the manufacturing process, a variety of finite element analysis (FEA) packages is used to assist the engineers and designers to determine the dynamic behaviour of the structure and subsequently optimise overall demands on the structural system in the design stage prior to the construction of the real structure.

The finite element method (FEM) is one of those numerical methods that can be used to solve complex mathematical model of a continuous physical system. Theoretically, a structure is divided into small elements such as beam, plate and shell elements. Then the mass and stiffness matrices of the individual element are assembled to form global matrices by considering node connectivity and boundary conditions in order to reproduce the dynamic behaviour of the structure under study. The displacement field inside each element and along its edges can be obtained by polynomial functions which are commonly called shape functions (Knight, 1993).

Alternatively the FEM progressively takes place of practical dynamic tests and to limit the number of tests that need to be carried out especially in a condition where the structure is difficult to simulate by experiments. The simulation using FEM may reduce the cost and help to shorten the time in order to bring new product to the market and consequently give them a competitive edge. Originally in 1960s the finite element techniques had been used mainly in stress analysis and soon the potential of the FEM for dynamic analysis was significantly recognised. These days various finite element software packages such as MSC PATRAN / NASTRAN, ANSYS and ABAQUS are developed to solve the complex mathematical models that can be used to perform various types of analysis such as stress analysis, life time prediction, response prediction, etc. Therefore creating a correct numerical model that properly represents the area of interest is the most

important step in modelling process. The best numerical model is the one that adequately represents those real aspects of the real structures which are highly depending on the accuracy and the selection of the FEA package. However, finite element models can be inaccurate or incorrect because the input data are always based on assumptions and factors such as expensive and limited computational efforts, over simplification of boundary conditions, local geometry features and inadequate modelling of joints which are often difficult to model correctly in finite element models. These simplifications can lead to errors being introduced to the model (Mottershead and Friswell, 1993).

Availability of an accurate dynamic finite element model of a structure is very important to engineers or designers as it allows them to improve the dynamic design of the structure at computer level and results in an optimised design apart from savings in terms of money and time before using for further simulation work. Therefore the finite element model needs to be correlated with the experimental data to ensure its validity. The Modal Assurance Criterion (MAC) can be used to solve the mode shape pairing problem (Friswell and Mottershead, 1995b) and it is necessary that the natural frequencies and mode shapes be paired correctly and behave similarly to those of the physical structure under study. The model updating procedure is used to minimise the error produced between the finite element model and the measured data.

1.1.4 Experimental modal analysis (EMA)

The experimental modal analysis (EMA) has become a very interesting domain since 1940's. In early stage most applications of EMA were dominated by physical approach purposely to have better understanding of vibration problems. In the last three decades, the technology developments have created an increasing need for reliable dynamic analysis. Initially data acquisition systems were based on analogue systems which were expensive and cumbersome to use. Numerous measurement techniques have been developed continuously to improve the efficiency and accuracy of the system. The introduction of the Fast Fourier Transform (FFT) algorithm together with the availability of high performance

data acquisition system has significantly reduced the measurement time, human effort and concurrently improved the accuracy of measured data (Ewins, 2000).

In principle the EMA or modal testing process is used to extract the modal parameters (such as natural frequencies, damping factors, modal vectors and modal scaling) of the structure experimentally. The structure will be excited so that the modal properties such as natural frequencies, damping and mode shapes can be identified. There are two main excitation methods, single or multi–point excitations. In single–point excitation method, the structure will be excited at one coordinate using a shaker or impact hammer and the frequency response will be measured at the interested coordinate. Meanwhile the multipoint excitations are performed on two or more points and this method has been widely used especially in the aerospace industry. However the single point excitation method is more convenient to perform because it is faster and easier in comparison with the multipoint excitations which are more difficult, time consuming and expensive to implement.

The sensing mechanisms such as transducers (force transducers and accelerometers) are used to measure the input force from the exciter (hammer/ shaker) and the acceleration response of the structure. The electrical signals that are produced by these transducers will be analysed by a data acquisition system which is based on Fast Furrier Transform (FFT) algorithm and subsequently provides a set of frequency response functions (FRFs) of the measured structure.
The applications of modal testing have been rapidly expanding and into various objectives such as trouble shooting, structural modification, damage detection and updating of finite element models.

1.1.5 Model updating

Initially, the FE model of a structure is developed during design stages and will be used to predict the dynamic behaviour of the structure before fabrication of the structure. Once the structure is fabricated, then modal testing can be performed and the measured data are compared with its finite element model counterparts.

Understandably, finite element prediction is not always in good agreement with the experimental results because of limitation in the method which is merely based on assumption such as approximation of boundary condition, physical properties of the structure and meshing process. Therefore, the finite element prediction is not always reconciled with the experimental results.

In modal testing, the measurement of the modal properties such as natural frequencies, mode shapes and modal damping are obtained directly from a real structure. Therefore the experimental results are considered to be more reliable than those obtained from finite element model. Model updating is normally used to improve the correlation between finite element model and physical model by correcting the uncertainties in the model properties and boundary conditions of the finite element model. The basic principles of correlation that are applied to finite element model updating are to utilise advantages of the experimental data to correct the modal properties of the finite element model.

Model updating methods have been developed by a number of researchers over past 25 years (Zang et al., 2006b). Understandably, finite element model updating methods can be classified into two categories, namely one step methods and iterative methods (Brownjohn and Xia, 2000). Historically, the one step procedure of model updating is mainly based on a trial and error approach where the adjustments of physical parameters of the finite element model are done manually. Even though one step procedure offers less computational effort, however it highly depends on the individual's engineering judgement and experience. On the other hand it must be ensured that the most sensitive parameters are selected in the updating process.

In one step procedure, the updated mass and stiffness matrices that are regenerated from the response data are often not guaranteed to preserve the attributes of the finite element model. The values of the updated parameters used in the procedure cannot be controlled systematically and sometimes they may lose their physical meaning (Mottershead et al., 2011). However, one step procedure for model updating has become more difficult to be implemented, and more systematic approaches are required due to the increasing of complexity of the structures.

Alternatively, the iterative methods based on response sensitivity has appeared to be more popular due to its flexibility by allowing a wide choice of updating parameters and at the same time the physical meaning of updated finite element model are well preserved. In the iterative methods, the choice of algorithms with respect to the updating process is essential. This approach generally depends on minimising errors between the finite element model and experimental data as an objective function by making changes to the pre-selected set of the parameters of the finite element model (Modak et al., 2002a).

Most optimisation problems have constraints. For example, in the gradient based method, the constraints are defined through upper and lower bounds. A number of iterations of the respective system have to be computed to find an optimum value which has important influence on the produced result and the solution or set of solutions which are obtained as the final result of an evolutionary search must necessarily be feasible to satisfy all constraints. However, problems may occur if the objective function has several local minimums, which may cause not only intensive computation but also difficulty to converge due to ill conditioning (Khoo and Chen, 2001). The potential of probabilistic search algorithms such as genetic algorithm (GA), response surface method (RSM) etc, has been explored for model updating Levin and Lieven (1998) and Marwala (2004).

The RSM is modelling method that looks at various design variables and their response and identify the combination of design variables that give the best response. RSM attempts to replace implicit functions of the original design optimisation problem with an approximation model, which traditionally is polynomial and therefore is less expensive to evaluate (Pula and Bauer, 2007). This makes RSM useful in finite element model updating because to match measured data based on the traditional optimisation methods such as gradient methods is computationally expensive and often encounters numerical problems such as ill conditioning in the search of global minimum (Zabel and Brehm, 2009). RSM tends to be immune from such problems. This is largely because RSM is a crude approximation of the FE model rather than the full FE model which is of high dimensional order.

The GA works on the principle of genetic and natural selection based on Darwin's survival fitness strategy where the dominant members of population will compete with each other to survive and reproduce successfully. As a result, the combination of genes that confers this advantage is likely to breed successfully. Therefore GA has a higher probability of identifying a global optimum solution than gradient based approach However the main drawback with the GA is slow convergence speed at which solution is arrived at, making difficult to implement for a large–scale structure and furthermore, and it contains many choice and parameters that need to be selected Brian and Mark (1999) and Marwala (2010).

1.2 Research goal and objectives

The goal of this research is to perform an efficient method for improving the dynamic characteristic of finite element model of a complex structure that is made from thin metal sheets that are joined by spot welds and bolted joints. In order to reach this goal four objectives have been identified. The objectives of this research are as follows:

1. To develop a finite element model based on thin plate structure that are joined by spot welds and bolted joints.

2. To employ the finite element model updating method in order to improve the correlation of finite element model

3. To develop a simple technique for representing bolted joint.

4. To apply response surface method to the welded structure.

1.3 List of publications

1. YUNUS, M. A., RANI, M. N. A., OUYANG, H., DENG, H. and JAMES, S. 2011. Identification of damaged spot welds in a complicated joined structure. *Journal of Physics: Conference Series,* 305, 1-10.

2. ABDUL RANI, M. N. A., STANCIOIU, D., YUNUS, M. A., OUYANG, H., DENG, H. and JAMES, S. 2011. Model Updating for a Welded Structure Made from Thin Steel Sheets. *Applied Mechanics and Materials*, 70, 117-122.

1.4 Preview of the thesis

The scope of this research is to model and update the complex joined structure using experimental results. A full welded structure that consists of ten components was fabricated from thin metal sheets and joined by resistance spot welds are investigated. The FE models that represent components, welded structure and full welded structure are developed. Modal testing is carried out on each of individual components and subsequently the model updating process is performed individually in order to improve the correlation between the numerical models and physical components before they are assembled together by a number of resistance spot welds.

Model updating then is applied to the welded structures and to the full welded structure. The common parameters that used by Palmonella et al. (2005), for updating parameters of spot welds are used for updating the assembled FE models. However there is no significant improvement in the discrepancy. Although the requirements for model updating are well understood, and many methods of updating have been suggested in recent years, based on the author's best knowledge there is little work on model updating of complex thin metal sheet structures.

In this work, the imperfections of the structure due to the fabrication issues are taken into account. To address the fabrication issues such as local deformation and initial stress ratio (a ratio that represents the effect of residue stress) is introduced as an updating parameter. Different methods of model updating have been

investigated; firstly, the gradient based method is used to update the individual components, welded structures and the full welded structure. Then a Response Surface Method (RSM) is used to update the model of the full welded structure with fixed boundary condition due to bolted joints. A set of numerical samples are generated using the Latin hyper Supercubic (LHS). The obtained results from both model updating methods (Iterative method and response surface method) are compared to demonstrate the accuracy as well as computational efficiency.

1.5 Organisation of the thesis

Chapter 2 provides a literature review of different types of joints such as, weld joints and bolted joints. The advantages and disadvantageous of modelling techniques that represent weld joints are discussed.

Chapter 3 describes the fabrication of the components and the experimental modal analysis. The basic equipments and procedures utilised in this work are also described. Then chapter describes the experimental work performed on each of the components and assembled structures (welded structures and the full welded structure) also are investigated.

Chapter 4 reports the detailed numerical modelling, correlation and updating process. Firstly, FE model updating is performed on the components in order to minimise the errors between the FE results and the experimental data.

Chapter 5 presents finite element model updating of welded structures. Since the FE models of the components have been improved, therefore the errors in welded structures are assumed from the spot welds and the assembling procedure. The finite model of the welded structures is then updated in order to match the experimental data.

Chapter 6 presents finite element model updating of the full welded assembled structure. It also covers two methods for model updating of the full welded structure: (1) the gradient based method (SOL 200) is applied to the finite element

model of the full welded structure with free-free boundary conditions and the finite element model of the full welded structure with fixed boundary conditions due to bolted joints. (2) Then, response surface method is used to update the finite element model of the full welded structure with fixed boundary conditions due to bolted joints.

Chapter 7 summarises the main outcomes of this research and some suggestions for future research work on issues related to this thesis.

Chapter 2

Literature Review

2.1 Introduction

Understanding the dynamic behaviour of structures and structural components is becoming increasingly important in the design process of the structures. For instance, the quality and design of the vehicles in the automotive industries are improving rapidly from all perspectives due to high competition among automotive manufacturer and to meet the customer demands. This phenomenon has led the automotive manufacturers to produce lighter vehicles with better fuel efficient engines. Therefore, engineers and designers are continuously faced with various challenges of producing better products the lower cost. Computer aided engineering tools are intensively used in the automotive industries in order to speed up the product development process through which the cost of product development can be reduced.

In modern structural design, the finite element method has become significantly important and has been used intensively in almost all areas of engineering analyses due to its versatility and capability. Normally, finite element models which are constructed from computer aided design (CAD) models may not truly represent all aspects of physical structures very well. In other words, the finite element models are constructed based on assumptions on which the nominal standard values of the Young's modulus, shear modulus, density, and Poisson's ratio are used in the construction of the finite element models.

In many numerical analyses of large and complex structures such as body-in-white, the analyses are not an easy task (Donders et al., 2006). Typically, a vehicle is assembled with a few thousand spot welds and each spot weld varies geometrical and physical properties because of the variation of the electrode current, electrode contact region, welding duration, electrical current and welding pressure during the spot welding process. These variations are highly believed to

increase the complexity in predicting the dynamic behaviour of the structures (De Alba et al., 2009a).

According to the research work conducted by Palmonella et al. (2005) and Ahmadian et al. (2006) the discrepancies were originated from the uncertainty in simplifying assumption of the structural geometry, material properties and the boundary conditions. They acknowledged that the finite element model was only an approximation and there were always inaccuracies or uncertainties that were associated with the simplification of the model and they were incapable of demonstrating the behaviour of tested structures. Even though the dynamic behaviour of the structure can be predicted by the finite element method, however the need for confident results is very important because the significant discrepancies are often found in the comparison of results between the predicted and the measured data. The discrepancies between both results have led to a reconciliation process through which the finite element model is altered in order to provide closer agreement with the measured data (Blakely, 1991).

The discrepancies of the initial finite element model of the structure can be improved systematically using the measured data of the physical structure. They are normally performed by comparing between the modal properties of the predicted model and their experimental counterparts. The reconciliation technique is known as model updating has become predominantly a standard tool for structural analysis and assessment (Schulz and Inman, 1994; Hemez and Doebling, 2001; Brownjohn and Xia, 2000). In model updating the measured data is used as a benchmark for the updating process of the initial finite element model. The expectation of model updating process is to provide an improvement to the initial finite element model that is able to represent the dynamic behaviour of the tested structure.

Model updating can be classified into two categories, the direct methods and the iterative methods. In direct methods, the mass and the stiffness matrices of the initial finite element model are directly adjusted based on the measured data. Meanwhile, the iterative methods are also known as sensitivity methods. These methods are based on the minimisation of the penalty function that is based on the

error between the measured data and the predicted results from the model (Mottershead et al., 2011). The advantage of this method is that the updating parameters of the finite element models are updated at each iteration process during the reconciling process in order to match the measured data. The iterative method has emerged as the most widely used in general practical applications because its flexibility and also the sensitivity information is relatively easy to calculate (Imregun and Visser, 1991; Friswell and Mottershead, 2001). However, this method requires large computational efforts due to reconstruction of sensitivity matrices during each iteration process.

Despite the advancement in the computing power and speed, the computational cost of a large and complex structure has limited their usage in the numerical analysis such as the structural optimisation and the reliability analysis (Simpson et al., 2001b). Alternatively, a surrogate model analysis method such as response surface method (RSM) and the probabilistic search algorithms such as genetic algorithm (GA) have been widely used in the model updating (Levin and Lieven, 1998; Marwala, 2004) in order to minimise the computational costs. Response surface model (RSM) is a major surrogate model and was developed by (Box and Wilson, 1951) and initially was used to optimise the operating conditions in the chemical industry. Since then RSM has been progressively gained attention among researchers. Hill and Hunter (1966) and Myers et al. (1989) presented the basic principles and certain theoretical aspects of RSM and also the practical applications of RSM. RSM was successfully introduced into the reliability analysis and model validation of engineering fields such as aerospace, mechanical and civil structures (Rutherford, 2002; Stewart et al., 2002; Raich and Liszkai, 2007; Khodaparast, 2010 and Ren et al., 2011).

Latin hypercube sampling (LHS) is a method of sampling that can be used to sample the regions of interest (design spaces) which is bounded by the upper and lower limits of each of the design variable (McKay et al., 1979). Olsson et al. (2003) revealed that LHS provided an efficient and generally applicable tool in generating numerical sampling for structural reliability analysis. In LHS, variables are sampled using an even sampling method, and then are randomly combined with sets of those variables used for the calculation of the target function. The

sampling algorithm of LHS ensures that distribution function is sampled evenly, but still with the same probability trend (Stein, 1987). On top of that, it provides explicit functions expressing the relationships between inputs and outputs, which are the two most advantages of this method.

Evolutionary optimisation algorithms have gained attention among many researchers in the last two decades. GA works on the principle of genetic and natural selection based on Darwin's survival fitness strategy where selection, mutation and crossover play a major role (Chambers, 2001). The dominant members of population will compete with each other to survive and reproduce successfully. As a result, the combination of genes that confers this advantage is dominantly to across the population. GA methods have the advantage of being robust, having an increased chance of finding a global minimum, being easy to implement and being well suit for discrete optimisation problem (Haupt, 1995).

The purpose of this chapter is to provide the background information on the domain of structural modelling, structural joints and the finite element model updating methods. A review of literature related to the global search algorithm such as, genetic algorithm (GA) and surrogate model such as response surface method (RSM) is discussed and presented.

2.2 Structural modelling

The development of the reliable model for the dynamic behaviour of engineering structures is very crucial. The reliable model is essential in terms of the structural dynamics because it is used to represent the dynamic behaviour of the physical structure and will be used for further analyses such as structural modification, damage identification, structural control and structural heath monitoring (Sinha et al., 2002; Ren and Chen, 2010). Typically, the analytical solution can be used to describe the dynamic behaviour of the structure if the structure has a simple geometry shape and the physical properties are uniform. However, large and complex structures such as automotive structures, the analytical solutions are

often impractical because the analytical solutions are not capable of describing their dynamic characteristics accurately.

Computational methods such as the finite element method are widely used to solve a system of governing equations over the domain of a continuous physical system. The early development of the finite element method was dated in early 1950's and it was used to analyse the complex aeroplane structures (Cook, 1983). A paper by Argyris (1954) laid the foundations for the finite element method as it is used today. Meanwhile, the term finite element was first used by Clough (1960). The summaries of the work of several authors which are associated with the invention of the finite element method have been presented briefly by (Gupta and Meek, 1996; Samuelsson and Zienkiewicz, 2006). There are a vast amount of literatures that has provided a comprehensive coverage of the topic of the finite element analysis (Bathe, 1982 and Zienkiewicz et al., 2005).

The finite element method has become a dominant tool of engineering analyses especially in mechanical and aerospace engineering (Komzsik, 2005). The requirement for a more generalised method of modelling the dynamics of complex structures with non-homogeneous physical properties has brought about the development of different types of analyses in the finite element method. The finite element method has been used in various engineering analyses such as stress analysis, structural dynamic modification, geo-mechanic and vibration problems. However, this method offers many choices for engineers in the construction of finite element models (Sinha and Friswell, 2002). Furthermore, the estimation of the properties of material and geometric performed by engineers usually has a high tendency towards the use of textbook values and the initial design rather than the measured data. As a result, the finite element model can be inaccurate or even incorrect due to inadequate modelling details, geometrical over-simplification and uncertainties on the finite element model input data (Lee, 2001).

A survey carried out by Ewins and Imregun (1986) and Maguire (1996) to assess the reliability of structural dynamic analysis capabilities showed that the finite element analysis of the structural dynamic properties were not always as reliable as they were generally believed to be and it was found that if an analysis was

performed by different sites independently of each other, the computed results could differ considerably. At this point the need for vibration tests on the structure is crucially important in order to confirm the validity of the finite element model before it is used for subsequent design analyses.

2.3 Finite element model updating

The finite element method has been identified as the most appropriate tool for analysing engineering structures today. In the finite element method, a mathematical model is used to represent the physical behaviour of the actual structure. The availability of an accurate dynamic finite element model is very important to designers and engineers as it allows them to investigate and to improve the dynamic design of the structure utilizing computerized methods. However it is often observed that the initial finite element model is not well-matched to represent the description of the dynamic behaviour of the physical structure under study.

Inaccuracies arise in a finite element model because of simplification and assumptions that are made in defining the finite element model. The elimination of all errors in the finite element model seems to be impossible even though well rounded selection of data including the use of practical and measured parameters in the process of constructing the finite element model is used. For the success of the construction of a reliable finite element model, comparative evaluation of both the predicted results and the measured results is vital because the results of the comparison provide some insights into the likely sources of inaccuracies in the finite element model.

With increasing reliability and confidence in measurement technology, the need to improve the numerical model representations initiated the development of the model updating algorithms in the 1970s. In the paper written by Imregun and Visser (1991), a comprehensive review was given of most related previous works on the model updating techniques and potential problems identified for each model updating method. Meanwhile in a survey paper by Mottershead and

Friswell (1993), the basic knowledge and technique on the structural model updating was discussed and presented. Later on, Friswell and Mottershead (1995b) elaborated an essential introduction theory of the finite element model updating and a wide range of model updating methods.

2.3.1 Direct method

Generally, the model updating can be categorised into two groups; firstly direct methods and secondly iterative methods. The direct methods are known as the earliest methods that are used in model updating which is directly used to update the global system mass and stiffness matrices by a single iteration. The updated model is expected to match a reference data and these approaches are known as direct or representation models (Zhang and Lallement, 1987). Berman and Flannelly (1971) and Baruch (1978) are among the first authors who presented direct methods in model updating by altering the stiffness and mass characteristics of the finite element model. In their studies, the improvement was only achieved through the mass matrix, but not through the stiffness matrix because in this case it did not resemble a true stiffness matrix. The same approach was used by Berman and Nagy (1983) in the attempt to update a large analytical model. In this method, the updating of the finite element model was performed in two steps. Firstly the mass matrix was updated subject to the orthogonality constraint and followed by the stiffness matrix.

Even though these methods require less computational effort, but from an engineering point of view, direct methods present several drawbacks when compared to the iterative methods because the high quality measurements and accurate modal analysis are needed as a reference. The updated structural matrices are difficult to interpret and may lose their physical meaning and furthermore, there is no guarantee the positive definiteness of the updated and stiffness matrices (Ceaser, 1987; Mottershead and Friswell, 1993 and Arora, 2011).

2.3.2 Iterative methods

Alternatively, the iterative methods become popular and acceptable due to its flexibility by allowing a wide choice of the updating parameters and at the same time the physical meanings of the updated finite element model are well preserved. Most of the iterative methods use partial derivatives which are called the sensitivities of properties with respect to physical parameters of the model. The main idea of the iterative methods is to use the sensitivity in minimising the error between the predicted and the measured eigenvalues and eigenvectors (Fox and Kapoor, 1968).

In the 1980s the correction of the analytical stiffness and the mass matrices of a vibration structure via iterative methods gained attention among researches. Sidhu and Ewins (1984) and He and Ewins (1986) revealed that the iteration process was able to bring a dramatic improvement in the correction of the analytical stiffness matrix and the mass matrices of the structure. Furthermore the updated models via iterative methods are able to represent physically meaningful to updated parameters if their convergence was achieved (Ceaser, 1987).

Almost all sensitivity based methods compute a sensitivity matrix by considering the partial derivatives of modal parameters with respect to structural parameters via truncated Taylor's expansion (Imregun and Visser, 1991) The variation of analytical response due to parameter variations can be expressed as a Taylor's series expansion limited to the first two terms

$$\mathbf{Z}_m = \mathbf{Z}_j + \mathbf{S}_j \left(\boldsymbol{\theta}_{j+1} - \boldsymbol{\theta}_j \right) \tag{2.1}$$

where, $\mathbf{Z}_m$ is the vector of measured data involving eigenvalues or eigenvectors, $\mathbf{Z}_j$ is the vector of analytical response at j^{th} iteration and $\boldsymbol{\theta}$ is the vector of structural updating parameters which probably belong to one of these: geometrical and material properties or boundary conditions. The application of structural updating parameters has been thoroughly discussed and demonstrated in chapter 5, chapter 6 and chapter 7. The solution vector in Equation (2.1) is obtained by

solving the vector of structural updating parameters $\boldsymbol{\theta}_{j+1}$. The resulting parameter changes are used to calculate the structural system matrices of mass and stiffness yielding a new eigensolution which matches the measured data more closely. The calculation is iteratively carried out until the target modal properties are satisfactorily achieved.

The relative merits of iterative methods of finite element model updating used in practical application examples were demonstrated by Dascotte (1990) in which real-life structural dynamic problems were solved by characterising and optimising the properties of material and geometry. Link (1990) presented the classification of possible error sources in analytical models and discussed their influence on the accuracy of predicted results. In addition, the author also presented the guidelines for identifying the source and the location of errors prior to performing model updating. Meanwhile, Schulz and Inman (1994) developed the model updating using the eigen-structure assignment method which was developed from the control theory. In this method, a feedback system was used to manipulate the mass and stiffness matrices to the inputs system in order to obtain the desired eigenvalues and eigenvectors. David-West et al. (2010) applied model updating to update a thin wall enclosure using imaginary point element on the base boundary nodes to control the linear and rotational stiffnesses. The updated model showed good correlation with the experimentally derived data.

The dynamic characteristic of the automotive structure is highly influent by the integrity and rigidity of the joints. However they are also highly susceptible to damage because of operational and environmental issues. The capability of iterative methods based model updating in damage identifications was demonstrated by Fritzen et al. (1998); Abu Hussain et al. (2009); Abu Hussain et al. (2010) and Yunus et al. (2011). However, uncertainties in the finite element models and the measured data can limit the success of the method (Friswell et al., 1997). Model updating of joints was studied by Palmonella et al. (2003) ; Abu Husain et al. (2010) and also Abdul Rani et al. (2011) in which the results and discussion of the latest updated model can be referred from chapter 5 and 6.

2.4 Structural joint modelling

Automotive components are mainly fabricated from thin metal sheets and they are assembled by a variety of jointing methods such as spot welds, bolted joints and adhesive in order to form automotive structures. The selection of modelling the jointing methods is very important in ensuring the overall dynamic behaviour of the assembled structure. This is because the connecting elements that are used to represent the joints are significantly affecting the overall dynamic behaviour of the assembled structure (Maloney et al., 1970 and Ewins et al., 1980). Cook (1983) revealed that the fundamental design consideration for an automobile is the overall dynamic behaviour in bending and torsion and these important issues can be due to a variety of structural design considerations which are highly influenced by these joints.

With the increase in computing performance such as speed and processing storage, the joint modelling has become easier and faster. However, the constructions of the predictive model of joints are still in doubt due to non-linearity and complex behaviour of the joints itself. Therefore, constructing a simple and reliable model of joints remains to be seen difficult tasks. The local effects that are produced by these joints (such as loosening effect, frictions and contact force) are difficult to be modelled numerically. A detailed model of these joints can be costly and impractical to develop. The measured data that is obtained from a particular type of joints on a given structure often cannot be confidently extrapolated in different structure designs or even, in many cases, to a different location on the same structure. Therefore a simple and reliable model of joints is crucially required by engineers in order to construct complex structures that usually have a large number of joints. For instance, a typical car body-in-white comprising at least 4000 to 5000 spot welds. Realising this issue which has been of central important since 1970, a large effort has been made either by creating new methods or improving and enhancing theoretically the existing methods or applying the available methods with the combination of other methods systematically.

2.4.1 Bolted joint modelling

As it has been highlighted in the previous section, finite element modelling of boundary conditions and joints is generally very difficult to perform. Bolted joints are one of the joint types for connecting structural components and they are widely used in joining the components because they can be easily dissembled, maintained and inspected. Therefore, bolted joints have become one of the prevailing joint types in engineering industries. Since year 1970, a large amount of research on joints has been carried out by scientists and engineers. On top of that, they have tried to understand the characteristics of joints and to simulate their findings into analytical modelling. Attempts to understand and investigate the behaviour of joints have been addressed by several authors. For instance, Chang (1974) demonstrated and discussed the importance of joint flexibility on the structural response analysis. Through the static analysis, the author discovered that the structural response was significantly sensitive to the level of joint stiffness.

On the modelling work, Rao et al. (1983) had improved modelling techniques and determined joint stiffness based on an instantaneous centre of rotation approximation. Similar work dealing in region of interest of the modelling techniques, Moon et al. (1999) developed a method for modelling joints and calculating the stiffness value of joints by using static load test data. Similar investigation was carried out by Rao et al. (1983) and Moon et al. (1999), they used rigid and rotational spring joints to improve the stiffness value of the joints. However, good dynamic analysis results were achieved through the latter. Friction behaviour that was inherent in bolted joints was complicated and found to be a nonlinear phenomenon. Gaul and Nitsche (2001) provided an extensive source of information on the friction laws of bolted joints and modelling issues of bolted joints. Oldfield et al. (2005) used Jenkins element model and Bouc-Wen model to illustrate the dynamic response of the finite element model of the bolted joints. The results calculated from the proposed simplified models showed very good agreement with those calculated from a detailed 3D finite element model and also showed a huge reduction in the computational effort in comparison with 3D finite element model.

Ibrahim and Pettit (2005) provided comprehensive information on bolted joints, particularly in the issues pertaining to structural dynamics with bolted joints, such as the energy dissipation of bolted joints, linear and non-linear identification of the dynamic properties of the joints, parameter uncertainties and relaxation, and active control of the joint preload. Moreover, they also covered the issues relating to design of fully and partially restrained joints, sensitivity to variations of joint parameters, and fatigue prediction for metallic and composite joints. Obviously, bolted joints have many complexities such as pretension, nonlinear frictional behaviour, etc., which are very difficult to investigate and compute yet important for joints (Ouyang et al., 2006). As a result, bolted joint modelling will be a major challenging problem for engineers.

Kim et al. (2007) studied modelling techniques for structures with bolted joints by constructing four types of finite element models which were a solid bolt model (Figure 2.1a), a coupled bolt model (Figure 2.1b), a spider bolt model (Figure 2.1c) and a non-bolt model (Figure 2.1d). The comparisons of analysis were performed with the consideration of pretension effects and also contact behaviour between joint components. It was found that the most accurate model was the solid bolt model and the most efficient model was the coupled model.

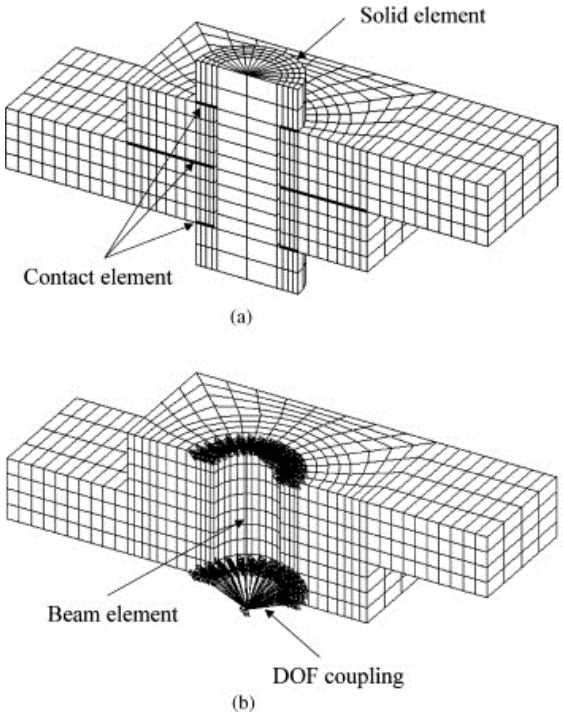

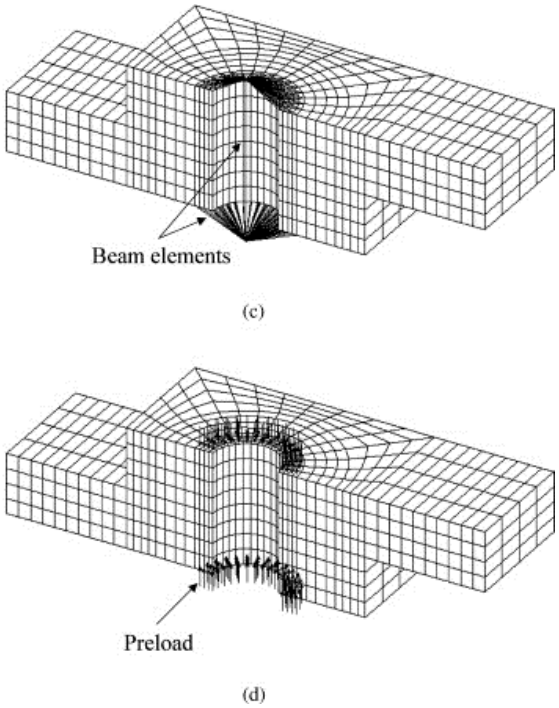

Figure 2.1: Finite element models for a structure with a bolted joint. (a) Solid bolt model, (b) coupled bolt model, (c) spider bolt model and (d) no-bolt model (Kim et al., 2007).

Yoo et al. (2009) used the concept of the cone-frusta method for the jointed parts and a number of spring elements were used to represent the contact effects exhibited in the interfaced area. On the other hand, Rutman et al. (2009) presented the modelling techniques of the bolted joint used to connect with different types of components. Combination of several elements in NASTRAN such as spring elements (CELAS and CBUSH), connector elements (CBAR and CBEAM) and rigid connection element (RBE2) are used to idealise the bending and shear of the fastener shank, elastic bearing stiffness of the plate and fasteners at the contact surface and also compatibility of displacement of fastener and the connected plates in the joint. Moreover, MSC.NASTRAN (2005), introduced a model of connector element that can be used to represent bolted joints based on the enhancement of the CWELD element which is known as CFAST element. However, the versatility of this connector element is not highly utilised in modelling of bolted joints.

2.4.2 Weld joint modelling

Resistance spot welding (RSW) is one of the electric welding techniques and widely used by automotive industries because of its easier and faster to operate and easy automation to adapt for mass production. The welding process is made by a combination of heat, pressure, and time. The geometry and material properties of the metal sheets are changed locally due to current and pressure applied during the welding process as shown in Figure 2.2. Meanwhile the quality and strength of spot welds are highly based on the resistance of metal surfaces and the amount of current flowing to produce the heat that are necessary to make spot welds.

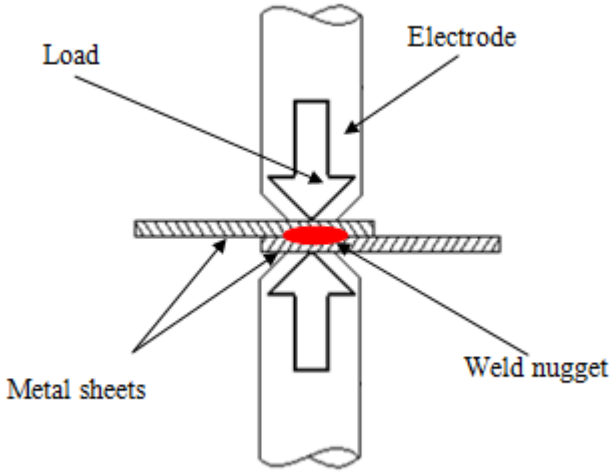

Figure 2.2: Illustration of resistance spot welding process

Typically, the automotive structure contains a large number of spot welds. A variability of spot welds (due to pressure, current and defects) are inherited to the behaviour of the dynamic behaviour of the structure. The electrode force can leave a surface print that makes the geometry of metal sheets become complex. As a result, the material properties are changed locally due to the heat produced during the spot welding process. Therefore, to incorporate the local effects of each spot weld in details, it can be cumbersome and time consuming (Mottershead et al., 2006).

However, only practical procedures and methods that could be used to represent spot weld joints in simplest way, without penalising the accurate of the model. In other words, simplified models should be able to deliver reliable results of any analyses of interest.

The theoretical modelling of the spot weld was well emerged in early 1980. For example, publications of theoretical modelling of the resistance spot welding in the decade of 1967 to 1977 were sparse (Nied, 1984). A various approaches have been used to describe the physical phenomena of spot welds and most of the work was mainly focused either on the fatigue and the static strength of spot welds and was performed by experimentally (Orts, 1981 and Rossetto et al., 1987). However, due to advancement of computing facilities in the early 1990s, a large amount of research on improving the previous approaches by adopting numerical techniques for modelling spot welds was carried out by many researchers and among them are Lim et al. (1990); Blot (1996); Vopel and Hillmann (1996); Heiserer et al. (1999); Palmonella et al. (2003); De Alba et al. (2009b); Abu Husain et al. (2010) and etc.

There many different types of the spot weld models that have been developed for different fields of analyses such as stress analysis, crash simulation and structural dynamics (Deng et al., 2000; Fang et al., 2000 and Xu and Deng, 2004). Each of these analyses has different requirement on modelling procedures, for instance a model for stress analysis and crash analysis requires an adequate numbers of elements in order to capture the local effects. However, these features are not important in modelling procedures of structural dynamic analysis which the overall stiffness and mass play a much more important role in the determination of structural characteristics. Vibrational analysis is usually treated as a global issue rather than a local issue. The eigenproblem is typically a function of the structural mass and stiffness and of boundary conditions as well. Therefore in analysing eigenproblem of the welded structures, emphasis should not only be on modelling work of the structure but also be on spot weld modelling. This is because the properties and characteristics of spot welds play a significant role in the dynamic behaviour of welded structures.

The dynamic characteristics of numerical models of welded structures are highly depend on the quality and reliability of spot weld models. In past twenty years, there many types of spot weld models have been developed and extensive research has been done with the aim to produce an easy and reliable model of spot welds that is able to represent the physical spot weld (Vopel and Hillmann, 1996; Blot, 1996 and Fang et al., 2000).

Initially, spot weld are modelled using elastic element, rigid bar and beam elements and these elements are required coincident nodes approach for element connections (Lardeur et al., 2000). For example, Pal and Cronin (1995) used rigid bars and elastic rod elements to model the spot welds on a simple welded beam for investigating the effects of the spot welds spacing on the dynamic behaviour of the welded beam that consists of a hat and a box welded together. However, large deviations from the elastic rod elements based model were still observed in the comparison. In addition, none of the aforementioned attempts, using single beam elements to model the spot welds have produced satisfactory results of dynamic behaviour of welded structures. For instance, Palmonella et al. (2003) revealed that elastic elements, rigid bars and beam elements tend to underestimate the stiffness and do not represent the spot welds in an appropriate way. On the other hand, Pal and Cronin (1995) used elastic solid element namely CHEXA for representing the spot welds and in their analysis they concluded that the CHEXA element based model produced the best results of comparison to the experimental data of the welded beam. However, this model requires congruent meshes and all eight nodes of the elastic solid element are connected to the plate shell elements using beam elements. Therefore the congruent meshed model is required if the type of element was chosen to represent spot welds.

Heiserer et al. (1999) proposed another type of spot weld model namely Area Contact Model 2 (ACM2) as shown in shown in Figure 2.3. This model is constructed based on HEXA solid element which is represented as a nugget at the position of the spot weld.

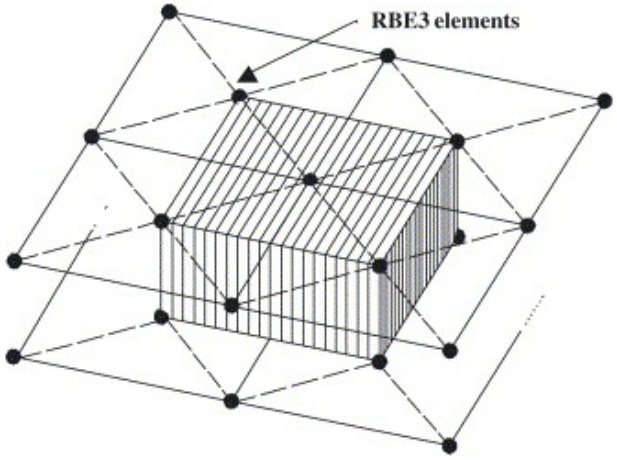

Figure 2.3: ACM2 spot weld model

The RBE3 interpolation elements are used to link the HEXA model with the nodes of shell elements. The advantages of this spot weld model are that it allows the model to be used for congruent and non-congruent component meshes and can be used for both limit capacity analysis and dynamic analysis. The advantages of the model in several aspects have caused an attention to a large number of the people either from academia or industry to use it in their research. For example, Lardeur et al. (2000) and Palmonella et al. (2003) successfully used ACM2 to represent physical spot welds and predicted the dynamic behaviour of both academic welded structure and automotive welded structure in comparison with the measured results. Apart from using ACM2 to represent the spot welds, they also demonstrated model updating work on the spot weld model and the effect of considering patch as updating parameter on the accuracy of the updated model. Meanwhile, a compressive overview of ACM2 in terms of the application of the model in NVH and durability analysis in automotive industry was presented by Donders et al. (2005) and Donders et al. (2006). The effect of refinement of the welded structure meshes on the accuracy of the analysis results calculated from ACM2 was discussed by Torsten and Rolf (2007.)

The CWELD element was proposed by Fang et al. (2000) and it was then introduced by MSC.NASTRAN in 2001. This model is a type of spot weld model whose element is represented by a sheer flexible Timoshenko type element with

two nodes at the end of element and has 12 degrees of freedom. The properties of CWELD element which are required to be defined as those of physical spot welds are the diameter and the Young's modulus of spot welds. Since no additional material is required in the spot welding process, therefore the Young's modulus of parent material is used for that of CWELD element.

Fang et al. (2000) demonstrated the application of three types of CWELD element connections in investigating the numerical problems with the modelling techniques of spot welds. The authors applied the modelling techniques of spot welds to two different types of connections which were a point to a point connection and a patch to a patch connection. Both types of connections could be used for connecting non-congruent meshes. The authors also took the areas of spot welds into account and proved that the ratio between the diameter of spot weld model and the size of mesh should be less than one. In other words, in order to avoid the stiffness of connections being underestimated, the diameter of spot weld model should not be bigger than the size of patch which is normally 3x3 elements per patch.

Palmonella et al. (2003); Palmonella et al. (2004) and Palmonella et al. (2005) used the same spot weld modelling technique for investigating and improving dynamic behaviour of a welded beam comprising a hat and a plate welded together by twenty spot welds. CWELD elements with the type of connection of patch to patch were used to model the spot welds. The discrepancies between the initial model of the welded beam and the tested structure were assumed to be due to the invalid assumptions of the parameters of spot welds. In the investigation, they concluded that CWELD modelling technique showed a high capability of and the simplest method for representing spot welds. Obviously, the optimum size and also the Young's modulus of patch of CWELD element played a significant role in improving the accuracy of the predicted results through the application of model updating.

The work related to using CQUAD4 and CWELD elements in the development of finite element models was reported in Horton et al. (1999); Palmonella et al. (2004); Mares et al. (2004) and Palmonella et al. (2005). These papers merely

dealt with model updating procedures for minimising the errors introduced in the finite element models which were mainly due to the inaccurate assumptions of the properties of materials, elements and patches. However, a structure with a large surface area made from thin metal sheets is susceptible to initial curvature due to its low flexible stiffness or manufacturing or assembling errors.

Initial stress can arise when components are assembled either by means of welded or bolted joints. For a structure with a large surface of low thickness with initial curvature, stiffeners can be intentionally added to remove it and they may also unintentionally remove it. When the initial curvature is suppressed after addition of stiffeners, initial stress arises (Abdul Rani et al., 2011). Initial stress can also arise as a result of fabrication and heat treatment. However, such initial stress is very difficult to estimate by theoretical analysis or to measure, unless the unstressed configuration is first measured in the latter case, which is very rare in reality. In general, initial stress state is rarely completely known (De Faria and De Almeida, 2006). The influence of initial curvature and initial stress on the natural frequencies of structures was investigated and found to be noticeable in Leissa and Kadi (1971); Fong (2005) and Liu et al. (2008). Furthermore work on the effect of initial curvature was carried out in (Yu et al., 1994) and Rao (2004). It was also pointed out (Yu et al., 1994) that finite element commercial software treats membrane and bending deformation as being independent and this approximation was only reasonable for structures with a small initial curvature and small deflection, however, for a moderate initial curvature and a small deflection the interaction between membrane and bending deformations should not be neglected. Abdul Rani et al. (2011) used the initial stress (which have a large effect on natural frequencies) as an updating parameter for improving the performance of the finite element model of a structure made from thin steel sheets with a large surface area.

2.5 Non-deterministic methods

In science and engineering, numerical simulation is a powerful tool that predicts the behaviour of physical systems. Despite the advancement of the computing

capabilities such as power and speed, the numerical prediction of the dynamic behaviour of structure via the finite element method is still incapable of representing the behaviour of physical structure accurately. Model updating techniques have been used to improve the finite element models to closely characterise the physical behaviour of the actual structure. Most of the model updating methods is based on the minimisation of structural parameters by minimising the error function between the measured data and numerical model.

Teughels et al. (2003) revealed that the success of the application of the finite element model updating method depends on the numerical finite element model, quality of the measured data, definition of the optimisation problem and the mathematical capabilities of the optimisation algorithm. Zingg et al. (2008) showed that the computation of the optimisation problem is typically proportional to the number of design variables and constraints because a large number of iterations of the respective system had to be computed in order to find an optimum value. This is because most of the local optimisation algorithms are based on the iterative method and they are widely used for solving a variety of optimisation problem such as model updating, because these methods are easy to perform, fast and robust (Zabel and Brehm, 2009). However, the gradient based method highly depends on the given starting point and if the objective function has several local minimums, the search algorithm may get stuck in the local minimum rather than the global optimum (Ren et al., 2011). The sensitivity based finite model updating methods are determined on the construction of sensitivity matrices which can affect the optimisation process due to large computational efforts.

Alternatively, there are many alternatives methods that have been developed through which the finite element models of structures are adjusted by varying the parameters of numerical models to fit the experimental data (Venter, 2010). Recently, the alternative methods such as the evolutionary algorithms (genetic algorithms (GA) and simulated annealing (SA)) and model replacement designs (RSM) and statistical method (Monte Carlo) have attracted the attention of the engineering communities. Response surface method (RSM) is based on the replacement model of the finite element model of the system/structure which requires less computational efforts. Meanwhile, the evolutionary algorithms such

as genetic algorithms (GA) and simulated annealing (SA) are gained attention by researcher because its capability in finding globally optimum results to complicated optimisation problems (Khan and Prasad, 1997; Baumal et al., 1998 and Correia et al., 2005).

Meanwhile, Mares et al. (2004) and Mottershead et al. (2006) presented a stochastic model updating method using inverse Monte-Carlo propagation of actual structure variability and model uncertainty together with multivariate multiple regression for optimisation by the gradient method. Abu Husain et al. (2012) demonstrated the stochastic model updating using perturbation method to update flat plates and hat shape structures.

2.5.1 Response surface method

The RSM that was originally developed by Box and Wilson (1951) is the combination of mathematical and statistical technique. The RSM approach is to create the response surface by replacing the expensive computer analyses as the approximated model by utilising the generated numerical sample (Myers and Montgomery, 2002 and Carlo et al., 2002) found that the RSM has become popular and been widely used because RSM is insensitive to numerical noise such as round-off errors and can be efficiently used with other computer programme.

The RSM has been widely used in different applications such as engineering, biological and food science (Myers et al., 1989). For instance, Giunta et al. (1997) applied RSM to the analysis and design of aircraft. He used stepwise regression to obtain the optimal model. Meanwhile, Stewart et al. (2002) applied the RSM for the development of aerospace simulations. The response surface was used to attain a real time and useable accurate response for complex aerospace component simulations. Nicolai et al. (2004) used the automated setting of RSM in optimisation exercise when there was a little information about the objective function and they used the stochastic objective functions with unknown variance and objective function that were very time consuming to evaluate for every solution. On the other hand, the RSM also has been used for damage

identification. In civil engineering (Fang and Perera, 2009) used an RSM to predict damage on a beam that made of reinforced concrete (RC) and the full scale bride structure.

2.5.2 Numerical sampling

The main components of the RSM are normally coupled to design of experiment (DOE) for the computer analysis and the response surface analysis. A set of numerical sampling data is generated based on appropriate DOE. These numerical samples will be used to generate the response surface based on polynomial approximation functions. The goal of the numerical sampling is to compute the values of design variables which are considered in the design constraints. The quality of numerical sampling is essential in order to obtain an accurate model of the function and also to reduce computational effort (Chaloner and Verdinelli, 1995; Helton and Davis, 2003).

A design optimal distribution can be created using the space filling sampling, in the sense that all areas of the parameter space are randomly sampled. Several space-filling methods requiring only information on the domain are available in the literature, such as Monte Carlo (Metropolis and Ulam, 1949), Latin hypercube sampling (LHS) (Stein, 1987) and Sobol (Kocis and Whiten, 1997). On top of that, Simpson et al. (2001a) and Rutherford et al. (2006) provided a comprehensive overview of a few types of space filling design and sampling methods. The space-filling method such as LHS is used to generate numerical sampling in order to find the output features. This method which is the most ambitious is about ensuring a good coverage of the random parameter space (McKay, 1992).

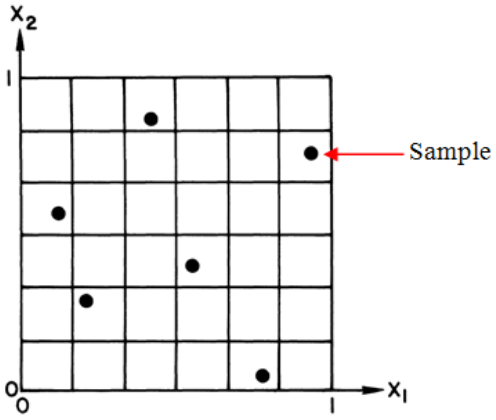

Figure 2.4: Latin hypercube sampling (Stein, 1987)

Figure 2.4 illustrates how the LHS can be used to draw samples from this bi-dimensional parameter space. As shown in the figure, the samples are taken randomly from each subspace and they are distributed uniformly on the parameter space.

2.5.3 Evolutionary algorithm

The generated surface of the response can be complex and it is also very difficult to obtain the optimal value due to many local optima points. Therefore, it is difficult to apply traditional optimisation methods such as the steepest ascent for searching the global optimum due to many local optima (Alvarez et al., 2009). The optimisation can be performed on the response surface by applying gradient based method or evolutionary algorithms such as genetic algorithm (GA) and simulated annealing (SA) (Raphael and Smith, 2000). The basic GA was introduced by Holland (1975). GA works on the principle of genetic and natural selection based on Darwin's survival fitness strategy where the dominant members of population will compete with each other to survive and reproduce successfully. As a result, the combination of dominant genes is likely to across the populations. GA has a higher probability of identifying a global optimum solution than the gradient based approach especially finite element model updating which produces a non-smooth objective function that makes the process of searching a global minimum become extremely difficult.

GA has been widely used in mechanical and civil engineering, (Coley, 1999; Chambers, 2001 and Kwak and Kim, 2009). For example, Kim et al. (2002) applied GA on RSM to determine the optimal conditions of welding processes. Akula and Ganguli (2003) utilised the finite element model updating based on GA to update the helicopter rotor blade design. Canyurt et al. (2008) used GA to estimate the strength of laser hybrid welded joint. Meanwhile, Perera and Ruiz (2008) successfully applied a GA based on the finite element model updating for damage identification of a bridge.

Despite having several attractive features, GA algorithm also have a several weaknesses and drawbacks like slow convergence at which solution is arrived at, making incredibly difficult to implement for a structure that contained many choices and parameters (Marwala, 2010). Levin and Lieven (1998) used a combination of GA and SA for the finite element model updating and it was revealed that the GA had led to high computational efforts and to slow rate of convergence, especially near an optimum making it incredibly difficult to implement for a large scale structure.

2.6 Conclusions

This chapter reviews the modelling work on structures, bolted joints, spot welds and model updating methods. It has shown that the finite element method has been widely used by engineering communities in predicting the dynamic behaviour of structures. The method can be used to analyse large and complex structures and is also able to perform different types of analyses. However, the computed results from initial finite element model are often found to be different from the measured data. The discrepancies are because the finite element model is developed based on assumptions and the predicted results highly depends on the validity of the assumptions made on the parameters of the finite element model such as material properties, geometry and boundary conditions.

Furthermore, the construction of the finite element model highly depends on the engineering judgments. As a result, there are possibilities that engineers and

designers may have overlooked and misjudged some important aspects of material properties, geometry and boundary conditions of the actual structure. The reconciliation technique such as finite element model updating is used to improve the correlation between the finite element model and the measured data. The model updating based on iterative methods is more preferable than direct methods because the iterative methods are more versatile and can be used in updating large and complex structures with a large number of parameters and a large number of degrees of freedom. On top of that physical meaning of the updated parameters is well preserved.

The sensitivity based model updating methods require a huge computational effort due to the construction of the sensitivity matrices at each iteration process. In addition, the gradients method is highly depend on the initial starting point and gradient based algorithms are often get stuck in local minimum rather than global minimum if the initial starting point are poorly selected. The probabilistic algorithms such as RSM can be used to reduce the computational burden.

Discrepancies between measured data and the finite element model of assembled structures can be primarily due to the modelling errors of the joints. The influence of mechanical joints on dynamic characteristics is highly depended on the variation of joints and jointing process. Joints such as spot welds and bolted joints, in practice, will introduce additional stiffness to the assembled structure and also alter the dynamic behaviour of the structure. This is because the geometry of metal sheets and material properties are already changed locally during the joining process because of the heat that has been applied during spot welding process.

Different types of elements are used to represent the spot weld such as ACM2 and CWELD. However, CWELD element has been widely used by engineering communities. The CWELD element seems to be more versatile as compared with the ACM2 model for spot weld modelling.

Chapter 3

Experimental Modal Analysis (EMA) and Fabrication

3.1 Introduction

Generally, vibration testing is used to identify the dynamic properties of a structure in response to an external excitation. The data from the experiment is then used for updating the finite element models. In this chapter, an overview of the experimental modal analysis (EMA) and its theoretical background are presented. For experiment purposes, a complex structure that is based on a simplified structure of Natural GAS Vehicles (NGV) compartment is fabricated. The structure consists of ten components, which are made from cold roll thin metal sheets. These components are then joined together by seventy two spot welds. The experiments are carried out on every component. The experimental results components are then used in the updating process in order to reduce the error in the finite element models. The experiments on component level are firstly performed so that the discrepancies between the predicted and measure results of the structure can be assumed arising from the errors in the joint modelling such as spot welds and bolted joints. The components are assembled together to form the welded structures (Figure 3.7) after their natural frequencies and mode shapes are measured. Meanwhile, the full welded structure which is a result of the combination of all components is shown in Figure 3.10.

3.1.1 Component and structure fabrication

A simplified test structure is developed based on a natural gas compartment that is normally used in natural gas vehicles (NGV) as shown in Figure 3.1. The assembled structure of natural gas cylinder platform consists of ten components. The computer aided design (CAD) is used to develop component and assembly

drawings for fabrication purposes. The CAD models of the components and assembled structures are utilised for the construction of the finite element models.

3.1.2 Description of components

The components are fabricated from a batch of cold roll thin steel sheets with the nominal thickness of 1.2 mm. The nominal values of the material properties are given in Table 3.1.

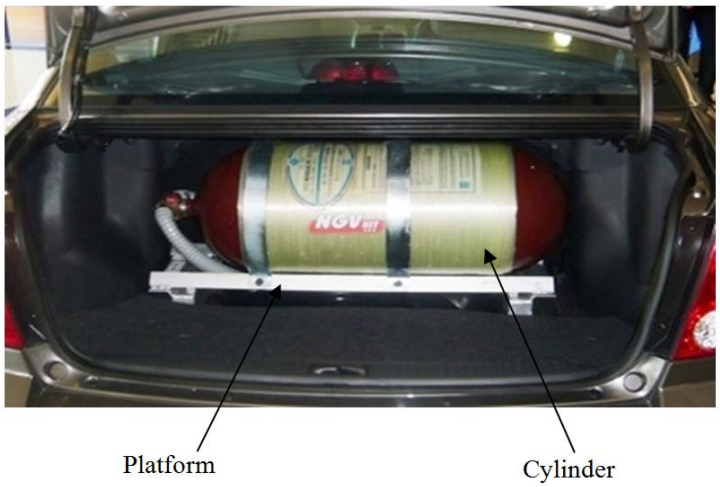

Figure 3.1: NGV cylinder compartment

Firstly, the steel sheets are cut and fabricated based on the CAD drawings of the components. The parameters of physical (dimension and mass) components are measured and weighed. Any discrepancies between the tested components and CAD drawings will be taken into account in FE modelling. This will be done by changing the related parameters in FE models so that the FE models will represent as closely as possible the tested components. It was found that the thickness of the plate varied from 1.10 mm to 1.30 mm (the nominal thickness of 1.20 mm). However, the thickness of 1.18 mm is used based on the average of measurement that has been performed on the plates.

Table 3.1: Nominal values of material properties

Material Properties	Nominal Values
Young's modulus (E)	210 GPa
Shear modulus (G)	81 GPa
Poisson's ratio (ν)	0.3
Mass density (ρ)	7850 kg/m^3

3.1.3 Main support

The main support is the biggest components of the full assembled structure in the NGV platform. Figure 3.2 shows the angle and side view of the main support with dimensions 600 x 147 x 68 mm. There are two main supports in the assembled structure. Therefore, the main support is fabricated for two sets and the average weight of these components is about 1.2 kg.

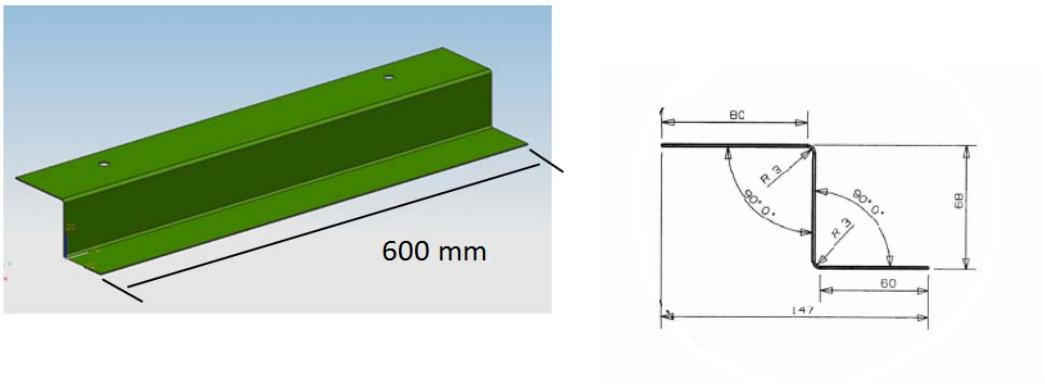

Figure 3.2: Main support

3.1.4 Base bent support

Figure 3.3 shows the side view of the base bent support with dimensions 284 x 147 x 68 mm. There are two sets of base bent support components that are required for the fabrication. The weight of each component is about 0.5 kg.

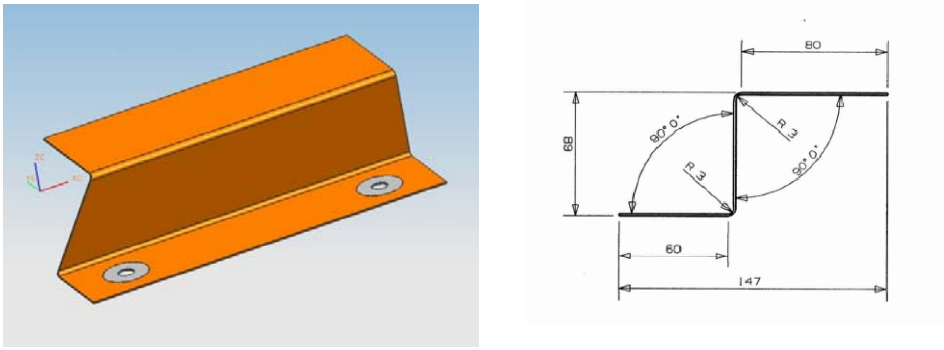

Figure 3.3: Base bent support

3.1.5 Bracket

The bracket as shown in Figure 3.4 is the smallest component in the full assembled structure with dimensions 83 x 64 x 63 mm. There are four bracket components that are required in the full assembled structure. The fabrication of the component is the most difficult task due to its size and shape. The information on the component is given in Table 3.2.

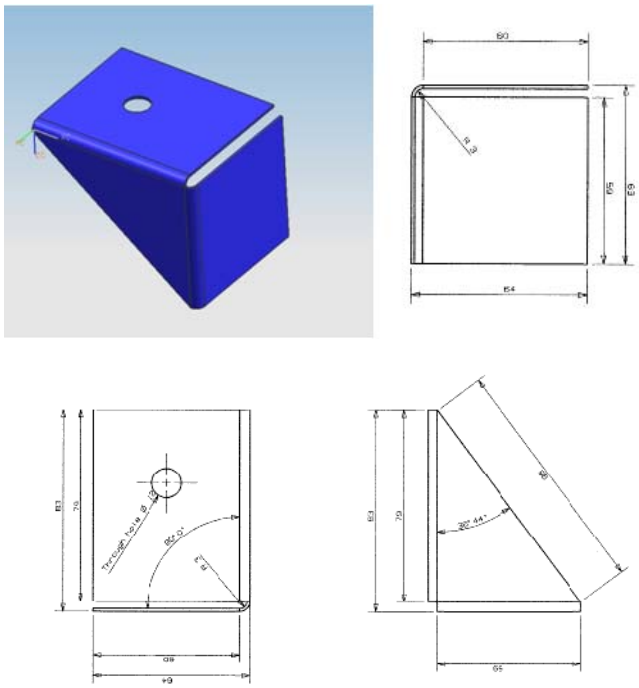

Figure 3.4: Bracket

Table 3.2: Information on bracket

Item	Description	Component ID	Quantity	Measured (kg)
1	Bracket A	05A	1	0.1025
2	Bracket AA	05AA	1	0.1013
3	Bracket B	05B	1	0.1020
4	Bracket BB	05BB	1	0.1014

3.1.6 Side support

The side support component as shown in Figure 3.5 (a) is used to reinforce the assemble structure (AC1). Therefore, two components are required to be fabricated. Figure 3.5 (b) shows the details of the side support with dimensions 410 x R 171 mm and the average weight of these components is about 0.2 kg each.

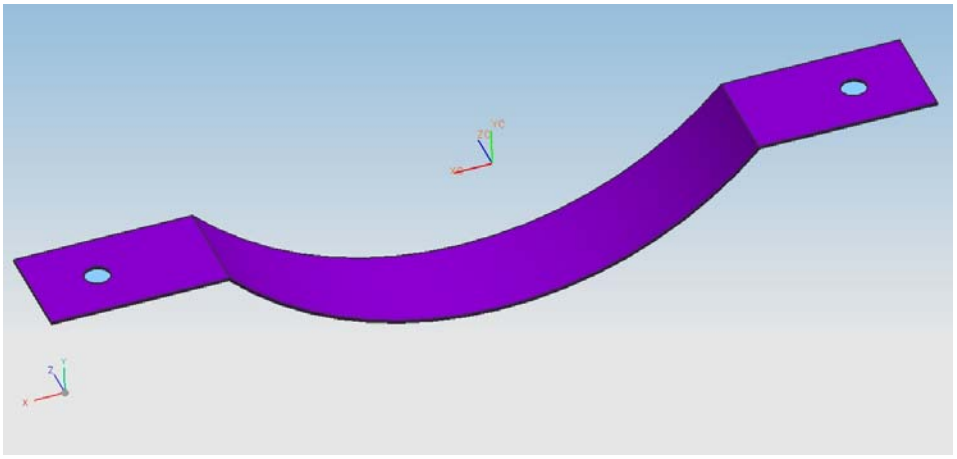

Figure 3.5 (a): Side support

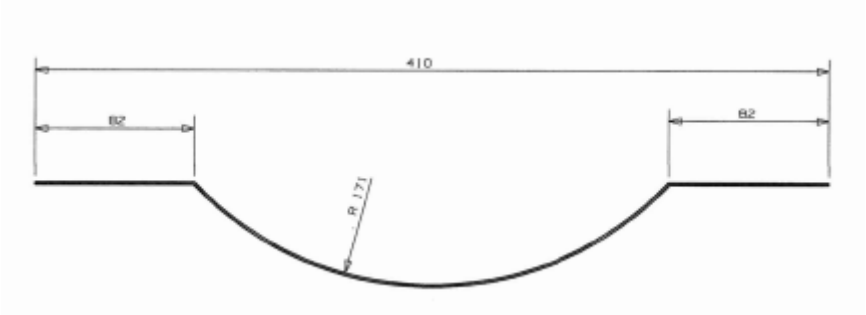

Figure 3.5 (b): Information of side support

3.2 Assembled structure

Modal tests on the components are performed before they are assembled together to form the structure. The test results of the components are compared with those calculated from the FE models of the components. The discrepancy between the FE models and the tested components that is believed to arise as a result of invalid assumptions in the FE models is firstly minimised before the components are welded together. It is essential to ensure that the reduction in the discrepancy is within the acceptable range so that the error found in the FE model of the assembled structure can be assumed to be as a consequence of welded joints. The components are assembled together by a number of spot welds using the portable resistance spot weld machine as shown in Figure 3.6. The overall dimensions of the assembled structure are 660 mm long and 410 mm wide.

3.2.1 Spot welding

The portable resistance spot welding as shown in (Figure 3.6) is used to assemble the components. In order to ensure the quality of spot welds, the components need to be cleaned from any dirt and oils before they are welded. In order to ensure the assembled structure is in good rigidity and dimensional accuracy, the components are clamped over the flanges in each welding process. This is because, the accuracy of the final assembly process highly depends on each stage of spot welding process. Therefore, spot welding process is carried out in a geometrical sequence in order to minimise the potential susceptibility of the structure to residual stress, geometrical irregularity and also distortion (Bhatti et al., 2011).

In addition, having the right settings for welding process is one of the important steps in order to achieve a good welding quality. Therefore, the parameters of the welding machine such as current, clamping force and welding time are set based on the recommendations of the equipment manufacturer. The electrode tip needs to be shaped regularly in order to obtain the right diameter of spot weld required.

This is because the electrode tip tends to deform due to heat and pressure during the spot welding process.

Figure 3.6: Resistance spot welding machine

3.2.2 Welded structures (welded main support structure)

The main support structures as shown in Figure 3.7 are constructed by assembling two brackets with the main support component. Each bracket is joined by eight spot welds as depicted in Figure 3.8.

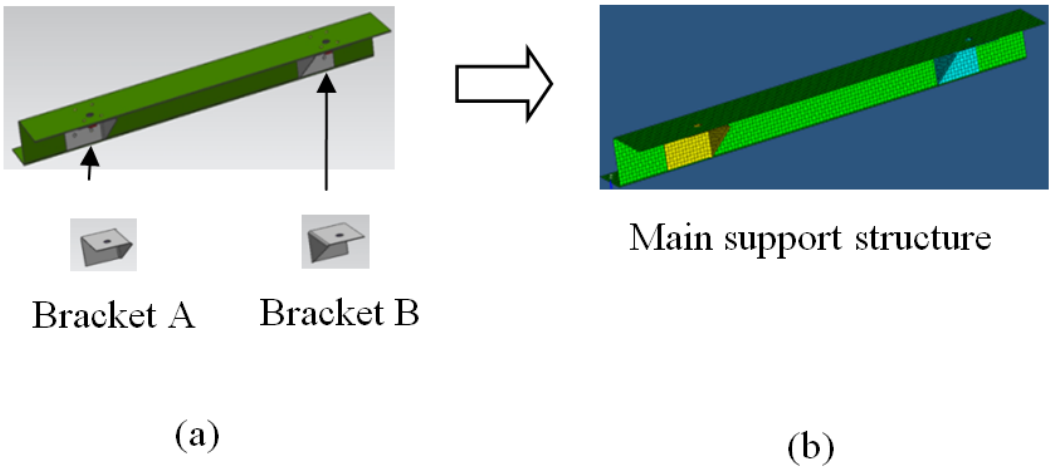

Figure 3.7: Assembly process of main support structure (welded structures)

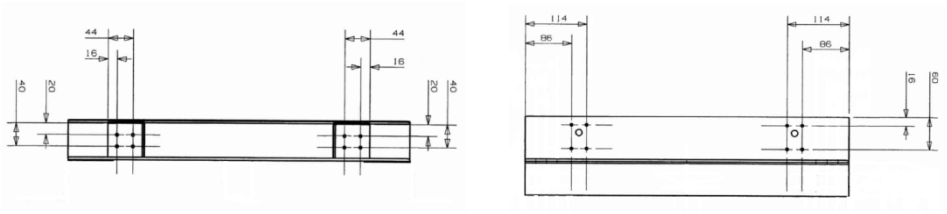

(a) (b)

Figure 3.8: (a) Side view and (b) top view of spot welds location of main support structures

Modal test is performed on both main support structures and the test results are compared with the FE results. The structures are then sent to the assembly process once the experiments are completed. Model updating is performed on the FE model in order to minimise the error between the FE and measured results.

3.2.3 Full welded Structure

The welded structures (Figure 3.7) then are spot welded with another component namely base bent support (Figure 3.3) and side support (Figure 3.5) in order to form the assembled structure (Figure 3.9). They are assembled to the existing structure (welded main support structure) by using twenty four spot welds as shown in Figure 3.9.

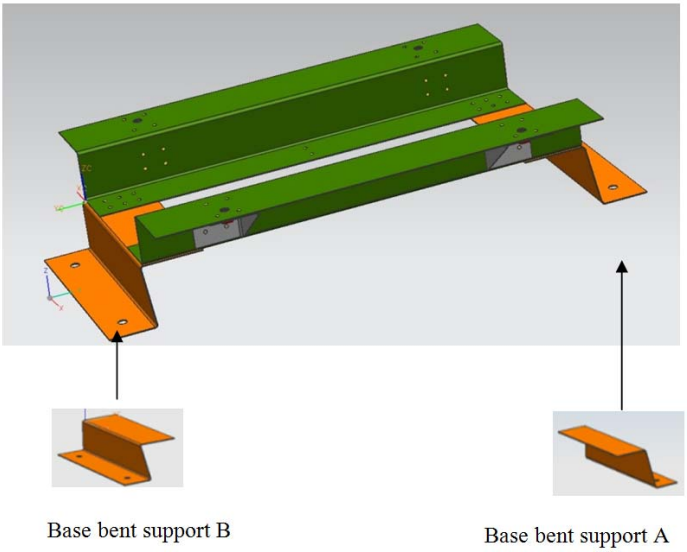

Figure 3.9: Assembly process of full welded structure

The full assembled structure (Figure 3.10) consists of ten components which are joined by seventy two spot welds as shown in Figure 3.11. The total weight of the full assembled structure is 4.24 kg.

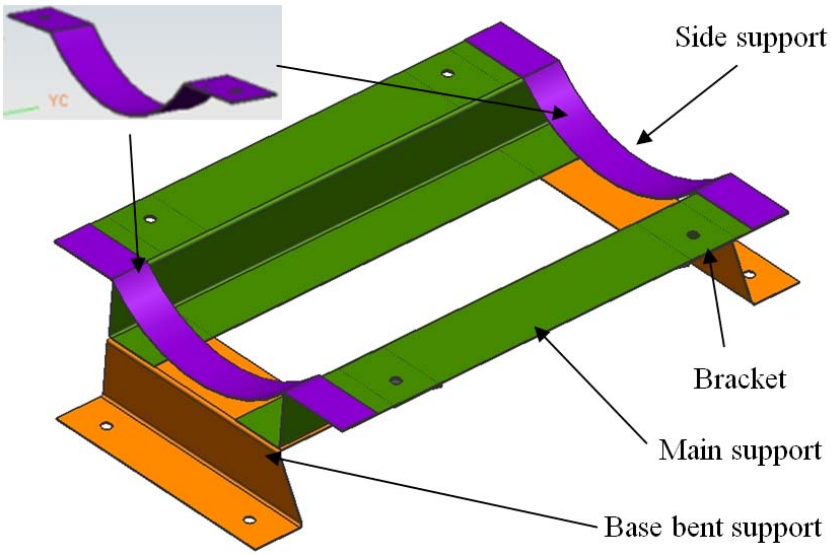

Figure 3.10: Full assembled of simplified Gas Cylinder Platform

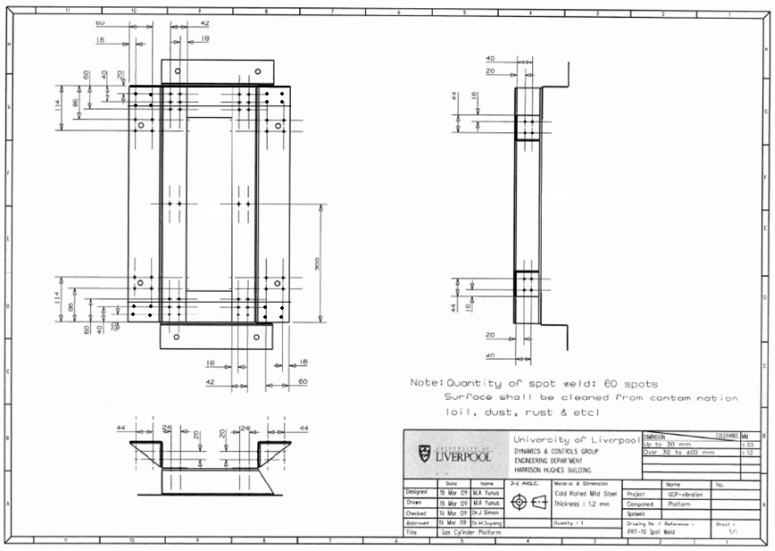

Figure 3.11: Spot welds location of full assembled structure

3.3 Experiment modal analysis

The experimental modal analysis (EMA) is to obtain a mathematical description of the dynamic behaviour of a structure. The theoretical basis of modal testing is established on the relationship between the vibration response at one location and excitation at the same or another location as a function of excitation frequency. These are normally performed by measuring response and excitation applied to the test structure.

In modal testing, the test structure is virtually presented in a geometrical form. The structure is meshed into grids on the display window of the hardware. The predicted results of the finite element analysis are used to determine the number of measurement points and the excitation point of a structure. The numbers of measurement points are normally determined by the size, complexity of a structure and also the number of modes of interest. For instance, higher frequency requires a larger number of measurement points in order to have better representation of the measured mode shapes.

The modal properties of the test structure such as natural frequencies, damping ratios and mode shapes can be identified through three stages as illustrated in Figure 3.12. From the analytical point of view (Figure 3.12 (a)), a mode of vibration is characterised by modal frequencies and mode shapes also known as a modal model. On the other hand, from an experimental point of view, the starting point is in the reversed direction from the theoretical route (Figure 3.12 (b)). In practice, the experiment is done based on several measurements that are required to adequately cover enough DOFs and vibration modes within the interested frequency range.

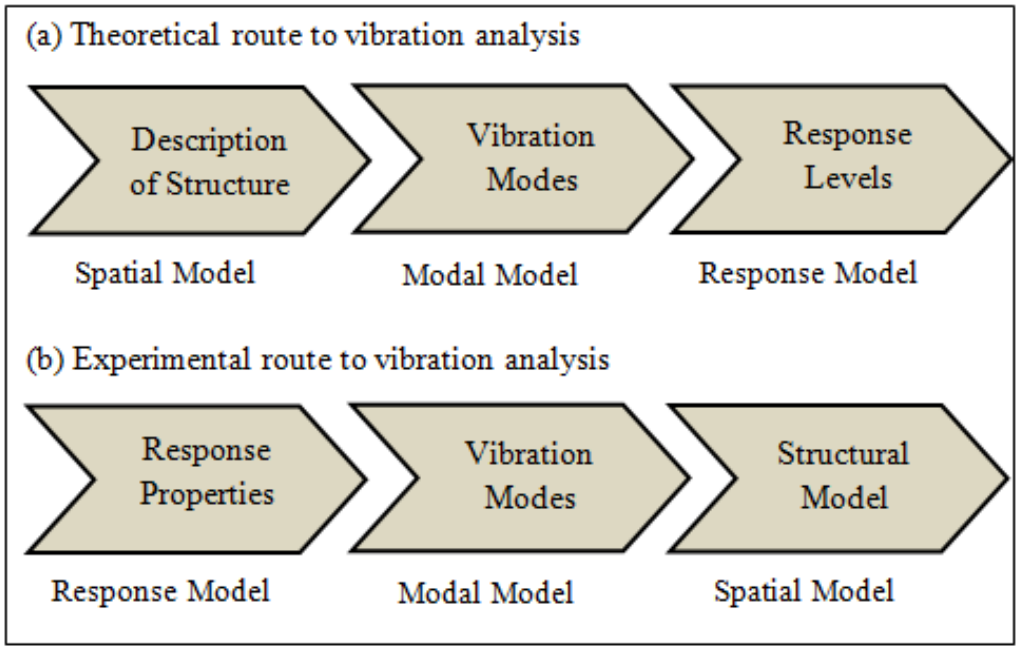

Figure 3.12: Theoretical and experimental route to vibration analysis (Ewins, 2000)

In modal testing, there are two common methods that are widely used to excite the test structure, impact hammer (Figure 3.13) and electro-dynamic shaker (Figure 3.14 (a)). The impact hammer testing is the most popular method and widely used in modal test because the test set-up is quicker compared with shaker test set-up.

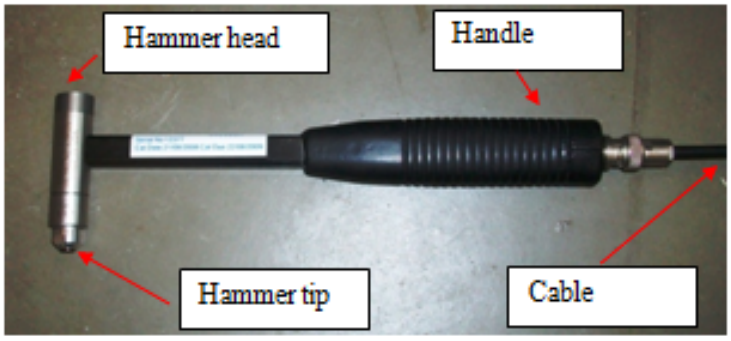

Figure 3.13: Impact hammer

An impact hammer is often used for modal analysis of structures, where the use of an electro shaker is not convenient especially for light weight and small structure. Meanwhile for a large structure such as a body-in-white (BiW) and an aircraft fuselage, the shaker test is preferable because high input force is required to excite the structure. Meanwhile the excitation force is transferred to the test structure via stinger rod as shown in Figure 3.14 (b).

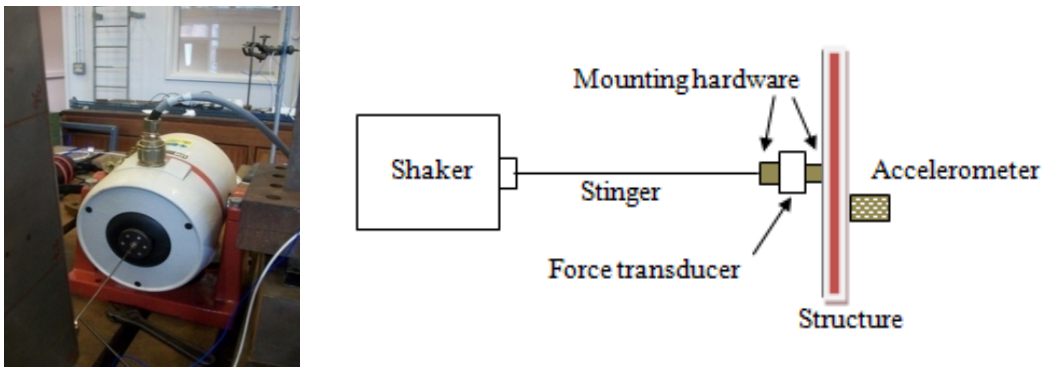

(a) (b)

Figure 3.14: (a) Shaker and (b) Schematic of shaker test layout

A computer based controller usually drives a shaker by generating a controlled voltage signal through the amplifier. This voltage signal is then sent to the shaker to vibrate the test structure. The excitation signal of the shaker can be assigned a variety of excitation signals such as harmonic, random, and periodic (Heylen et al., 1998).

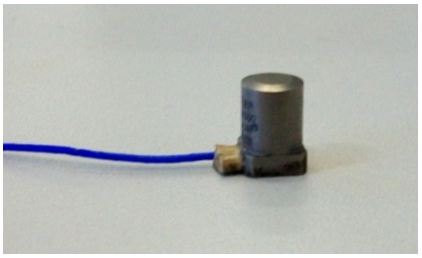

Figure 3.15: Accelerometer

The response of a structure can be measured at one or more points using accelerometers. Accelerometers (Figure 3.15) are normally made from piezoelectric materials and the electrical signals from accelerometers are channelled to a data acquisition system to derive a mathematical model of the structure in the time-history domain. Therefore the sensitivity of the accelerometer has a significant impact on the quality of the measured signal (Maia and Silva, 1997).

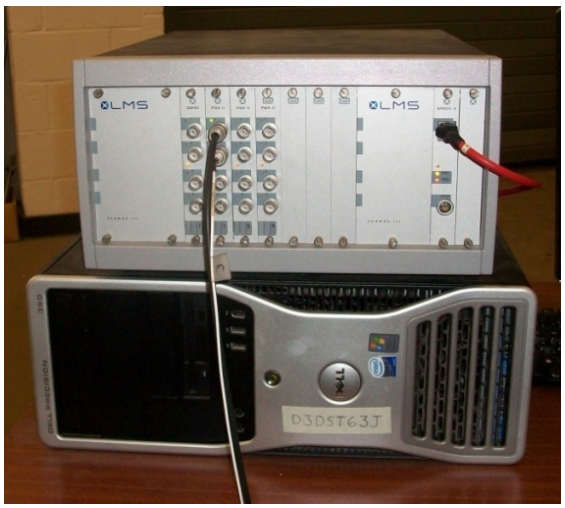

Figure 3.16: Data acquisition system

The data acquisition system is normally used to convert the analogue signals from transducers into digital format via an analogue to digital converter (ADC). The digital signal processor (DSP) as shown in Figure 3.16 performs all required calculations, including filtering, computation of time and frequency measurements that are obtained from force and response signals. The mathematical technique, which is based on the Fast Fourier Transform (FFT) algorithm, is utilised to compute FRFs of interested frequency range. These then are followed by curve fitting technique which is utilised to determine the modal properties such as natural frequencies, damping and mode shapes of the test structure.

The FRF describes relationship between excitation input and output signal of a measuring point on mechanical system as shown in Figure. 3.17.

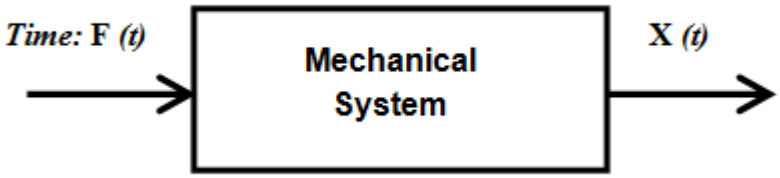

Figure 3.17: Block diagram of FRFs (Brian and Mark, 1999)

$$\{\mathbf{X}(\omega)\} = [\mathbf{H}(\boldsymbol{\omega})]\{F(\boldsymbol{\omega})\} \qquad (3.1)$$

From Eq. (3.1) indicates that FRF $\mathbf{H}(\omega)$ is defined as the ratio of the output response $X(\boldsymbol{\omega})$ divided by the input force $F(\boldsymbol{\omega})$. Therefore the relationships between the response model $\mathbf{H}(\omega)$ to spatial and modal model can be represented by;

$$\mathbf{H}(\omega) = (-\omega^2\mathbf{M} + i\omega\mathbf{C} + \mathbf{K})^{-1} \qquad (3.2)$$

where, **M**, **C** and **K** represent the mass, damping and stiffness matrices the spatial model.

Since the input force to the structure and dynamic response of the structure are obtained from physical measurement, it is theoretically possible to obtain a mathematical description of the structure through experiment.

3.3.1 Implementation of experimental work

Prior to an experiment, the locations of the excitation point and measurement points of the components/structures are determined from the mode shapes that are calculated from the initial finite element model. Therefore before the experiment is performed, it is necessary to decide how many measurement locations are required, where they should be located, and where the excitation should be applied (Penny et al., 1994). This is to ensure the excitation point is able to excite all modes of interest and also to obtain reliable mode shapes of the structure.

The information of initial finite element model is then used in modelling the geometry of components/structure in LMS data acquisition system. The grid lines and points are virtually assigned to represent the geometric shape of the test components/structures. The measurement of the dynamic force and response of a structure, in terms of FRFs, often involves the use of force transducer and accelerometers. In the experiment an impact hammer (PCB 06C03) and Kistler (type 8728A500) accelerometers are used on the component level of experiment. Meanwhile, impact hammer and electromagnetic shaker (LDS V201) are used in the experiment of structure.

Responses of the experiment are measured using a 12-channel LMS system and extracted using the LMS PolyMAX curve-fitting procedure. The advantage of the LMS PolyMAX curve fitting is that the selection of modal parameters are easier since the spurious numerical poles will not stabilise at all during this process and can be sorted out of the modal parameter data set more easily (Peeters et al., 2004) (Bart and Herman, 2004). Usually, FRFs can be processed globally and individually from stabilization chart by applying the measurement processing procedure which is displayed on desktop window.

As the components are fabricated from thin metal sheets, they have a high tendency to snap through when it is excited by an impact hammer and therefore, roving accelerometer method is used in the experiment (Yunus et al., 2011). In this method, one accelerometer is fixed at the excitation point as a reference for

each run. Meanwhile, other accelerometers are roved around measuring points on components/structures. The numbers of accelerometers are kept as small as possible in order to avoid mass loading issue to the component/structure during the measurement process. A general rule is that the total weight of accelerometers should be less than one-tenth of the weight of the component/structure to which they are attached (Dyer, 2001). The additional mass may significantly alter the modal parameters of the test structure.

3.3.2 Experimental work with free-free boundary conditions

Experiments with free-free boundary conditions are performed to the test components and structures. The free-free boundary can be achieved by suspending the test component/structure with very soft springs as shown in Figure 3.18. The six rigid body modes no longer have zero natural frequencies, but they have values which are significantly lower than that of the first elastic mode of the structure (Agilent technologies, 2000).

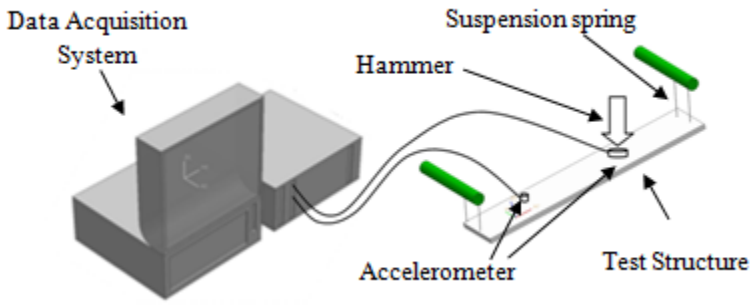

Figure 3.18: General experimental set-up for free-free boundary conditions

3.3.3 Experimental work of the main support

Test component main support (component 01A and 01B) is the biggest component of the natural gas cylinder compartment. The component dimension is 147mm x 600 mm x 60 mm height and fabricated from cold roll mild steel sheets with the thickness 1.18 mm. The experiments are performed with free-free boundary conditions as shown in Figure 3.19 and components are hanged using two soft springs during testing. Meanwhile Figure 3.20 illustrates the details of measurement points.

Figure 3.19: Experimental set-up for the main support (Component 01A and 01B)

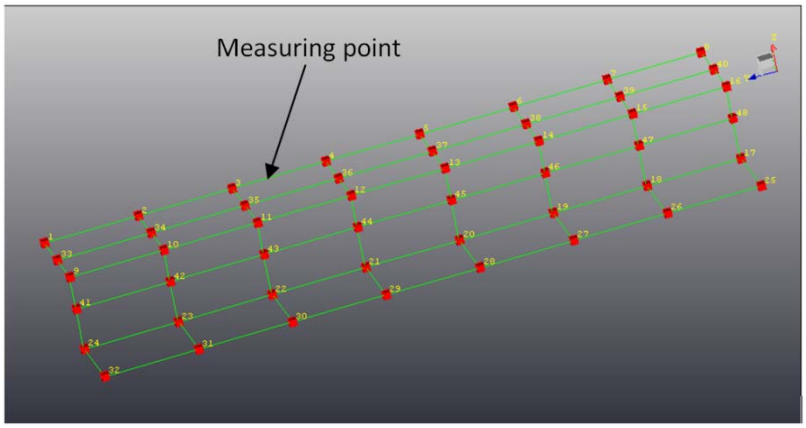

Figure 3.20: Experimental model of the main support and measuring points (Component 01A and 01B).

There are five accelerometers used to measure the response of the component. One of the accelerometers is fixed and another four are roved around to measure the dynamic response of 64 degrees of freedom of the structure that cover 98

degrees of freedom through a master-slave relationship as shown in Table 3.3 with the frequency range of interest is from 0 to 270 Hz. The ten measured natural frequencies and mode shapes of the main support A (Component 01A) are shown in Figure 3.21. Meanwhile the first ten measured natural frequencies and mode shapes of the main support B (Component 01B) are shown in Figure 3.22.

Table 3.3: Information of the excitation point and accelerometers used in experiment the main support (Component 01A and 01B)

Run	Accelerometers									
	8879		8881		8882		8891		7226	
	Point /Direction		Point /Direction		Point /Direction		Point /Direction		Excitation Point	
1	1	+Z	13	+Z	22	-Z	47	-X	39	-Z
2	2	+Z	14	+Z	21	-Z	45	-X	39	-Z
3	3	+Z	15	+Z	20	-Z	46	-X	39	-Z
4	4	+Z	16	+Z	19	-Z	43	-X	39	-Z
5	5	+Z	9	+Z	18	-Z	44	-X	39	-Z
6	6	+Z	10	+Z	17	-Z	21	+X	39	-Z
7	7	+Z	11	+Z	24	-Z	19	+X	39	-Z
8	8	+Z	12	+Z	23	-Z	18	+X	39	-Z
9	9	-X	20	+X	38	+Z	48	-X	39	-Z
10	10	-X	17	+X	29	-Z	24	+X	39	-Z
11	11	-X	14	-X	23	+X	26	-Z	39	-Z
12	33	+Z	30	-Z	27	-Z	13	-X	39	-Z
13	40	+Z	41	-X	25	-Z	22	+X	39	-Z
14	35	+Z	28	-Z	31	-Z	15	-X	39	-Z
15	36	+Z	32	-Z	34	+Z	16	-X	39	-Z
16	12	-X	37	+Z	42	-X			39	-Z
17									39	-Z

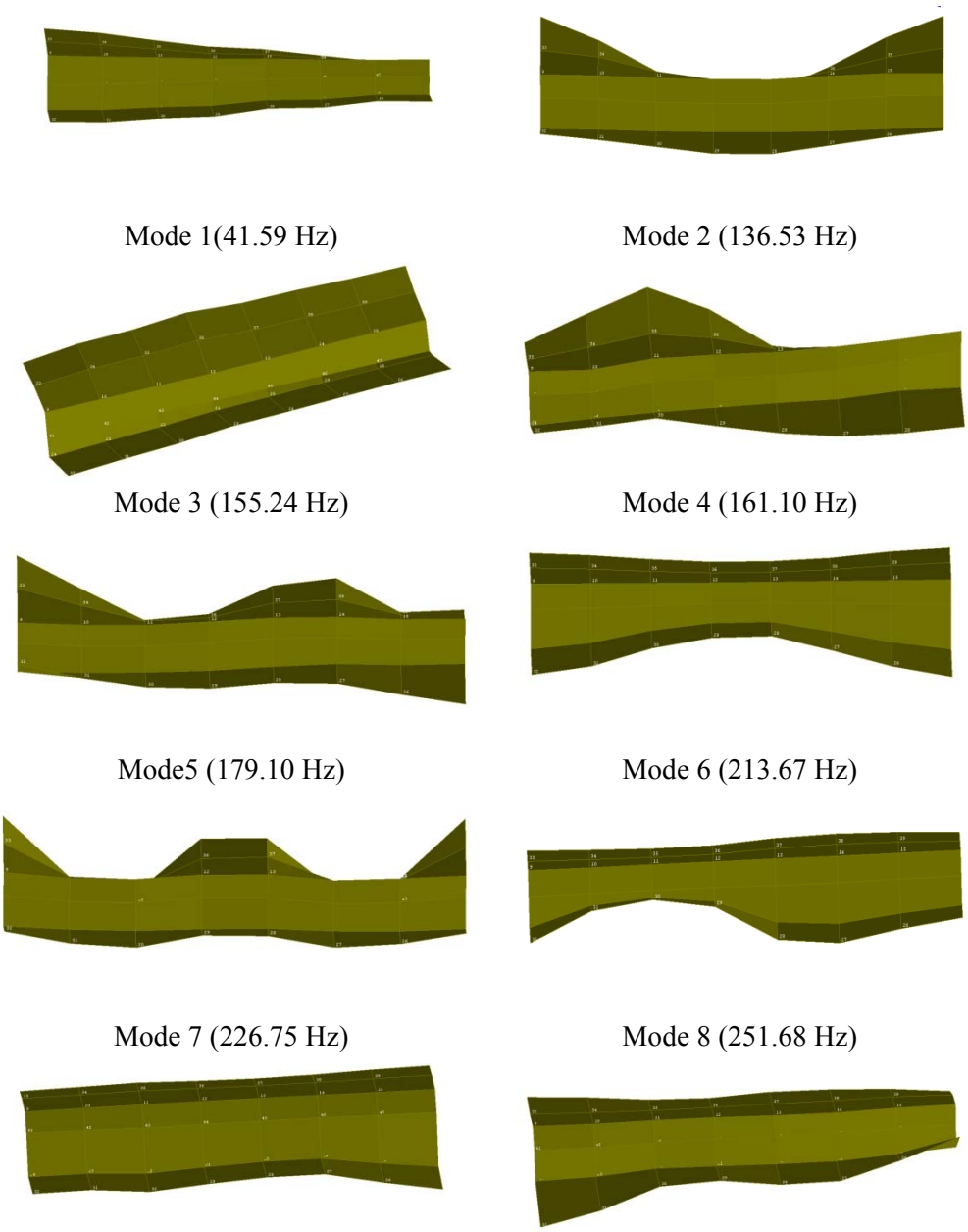

Figure 3.21: Experimental natural frequencies and mode shapes of the main support A (Component 01A)

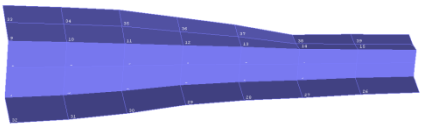

Mode 1 (41:58 Hz)

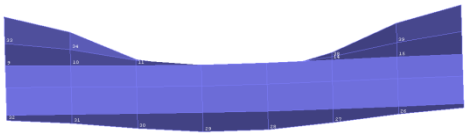

Mode 2 (135.34 Hz)

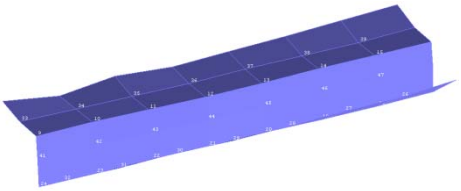

Mode 3 (154.41 Hz)

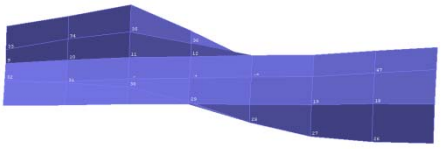

Mode 4 (160.22 Hz)

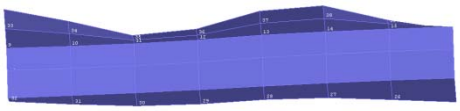

Mode 5 (178.40 Hz)

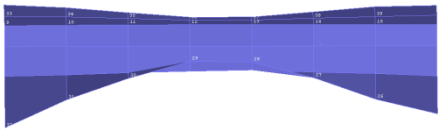

Mode 6 (213.66 Hz)

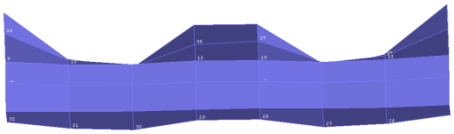

Mode 7 (226.31 Hz)

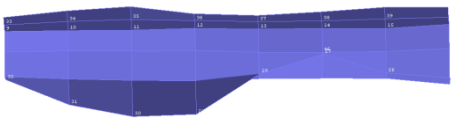

Mode 8 (249.50 Hz)

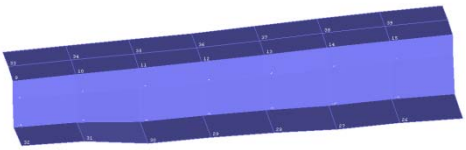

Mode 9 (255.14 Hz)

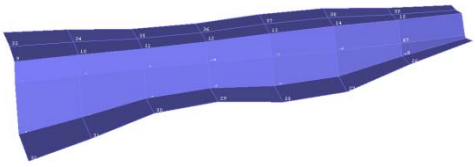

Mode 10 (262.90 Hz)

Figure 3.22: Experimental natural frequencies and mode shapes of the main support B (Component 01B)

3.3.4 Experimental work of the base bent support

Base bent support (Component 02A and 02B) is used to support the full assembled natural gas cylinder compartment. The base bent support is fabricated from cold roll mild steel sheets with the overall 284mm x 147 mm x 68 mm height. The experiments are performed with free-free boundary conditions with two soft springs are used to hang test component as shown in Figure 3.23. Meanwhile Figure 3.24 illustrates the details of measurement points.

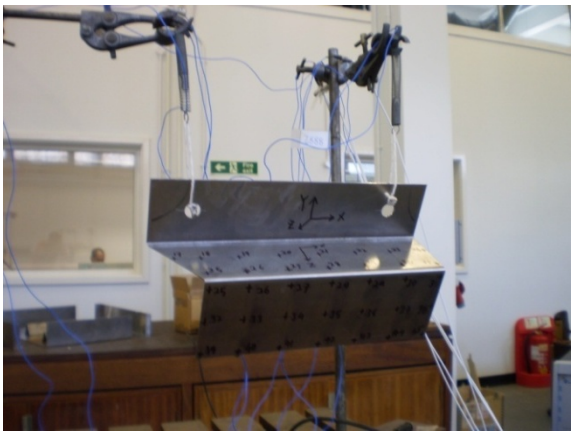

Figure 3.23: Experimental set-up for the base bent support (Component 02A and 02B)

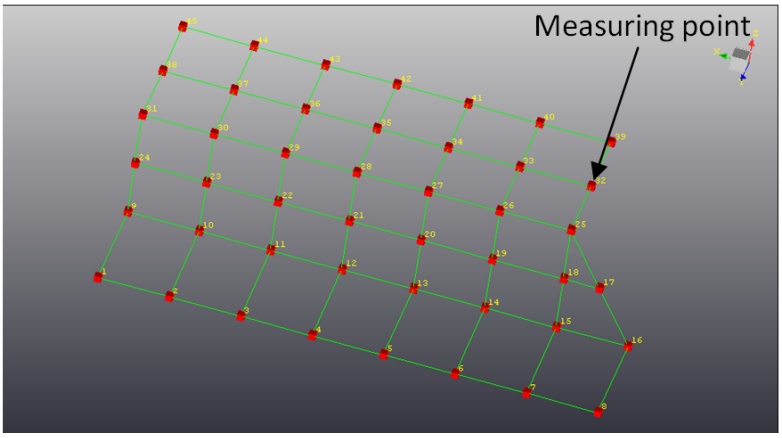

Figure 3.24: Experimental model of the base bent support and measuring points (Component 02A and 02B)

There are three accelerometers used to measure the response of the component. One of the accelerometers is fixed and other two are roved around to measure the response of 60 degrees of freedom of the structure that cover 92 degrees of freedom through a master-slave relationship as shown in Table 3.4 and Table 3.5. The frequency range of interest is from 0 to 670 Hz. The first ten measured natural frequencies and mode shapes of the base bent support A (Component 02A) are shown in Figure 3.25. Meanwhile the first ten measured natural frequencies and mode shapes of the base bent support B (Component 02B) are shown in Figure 3.26.

Table 3.4: Information of the excitation point and accelerometers used in the experiment the base bent support from run 1 up to run 15 (Component 02A and 02B).

Run	Accelerometers					
	8879		8881		7226	
	Point /Direction		Point /Direction		Excitation Point	
1	1	-*Y*	12	-*Y*	25	-*Z*
2	2	-*Y*	13	-*Y*	25	-*Z*
3	3	-*Y*	14	-*Y*	25	-*Z*
4	4	-*Y*	15	-*Y*	25	-*Z*
5	5	-*Y*	16	-*Y*	25	-*Z*
6	6	-*Y*	9	-*Y*	25	-*Z*
7	7	-*Y*	10	-*Y*	25	-*Z*
8	8	-*Y*	11	-*Y*	25	-*Z*
9	9	-*Z*	33	+*Z*	25	-*Z*
10	10	-*Z*	26	+*Y*	25	-*Z*
11	11	-*Z*	27	+*Y*	25	-*Z*
12	12	-*Z*	28	+*Y*	25	-*Z*
13	13	-*Z*	29	+*Y*	25	-*Z*
14	14	-*Z*	30	+*Y*	25	-*Z*
15	15	-*Z*	31	+*Y*	25	-*Z*

Table 3.5: Information of the excitation point and accelerometers used in the experiment the base bent support from run 16 up to run 31 (Component 02A and 02B).

Run	Accelerometers					
	8879		8881		7226	
	Point /Direction		Point /Direction		Excitation Point	
16	21	+*Y*	25	+*Z*	25	-*Z*
17	22	+*Y*	26	+*Z*	25	-*Z*
18	23	+*Y*	27	+*Z*	25	-*Z*
19	24	+*Y*	28	+*Z*	25	-*Z*
20	17	+*Y*	42	+*Z*	25	-*Z*
21	18	+*Y*	43	+*Z*	25	-*Z*
22	19	+*Y*	44	+*Z*	25	-*Z*
23	20	+*Y*	45	+*Z*	25	-*Z*
24	38	+*Z*	29	+*Z*	25	-*Z*
25	39	+*Z*	30	+*Z*	25	-*Z*
26	40	+*Z*	31	+*Z*	25	-*Z*
27	41	+*Z*	36	+*Z*	25	-*Z*
28	16	-*Z*	32	+*Z*	25	-*Z*
29	35	+*Z*	37	+*Z*	25	-*Z*
30	34	+*Z*			25	-*Z*
31					25	-*Z*

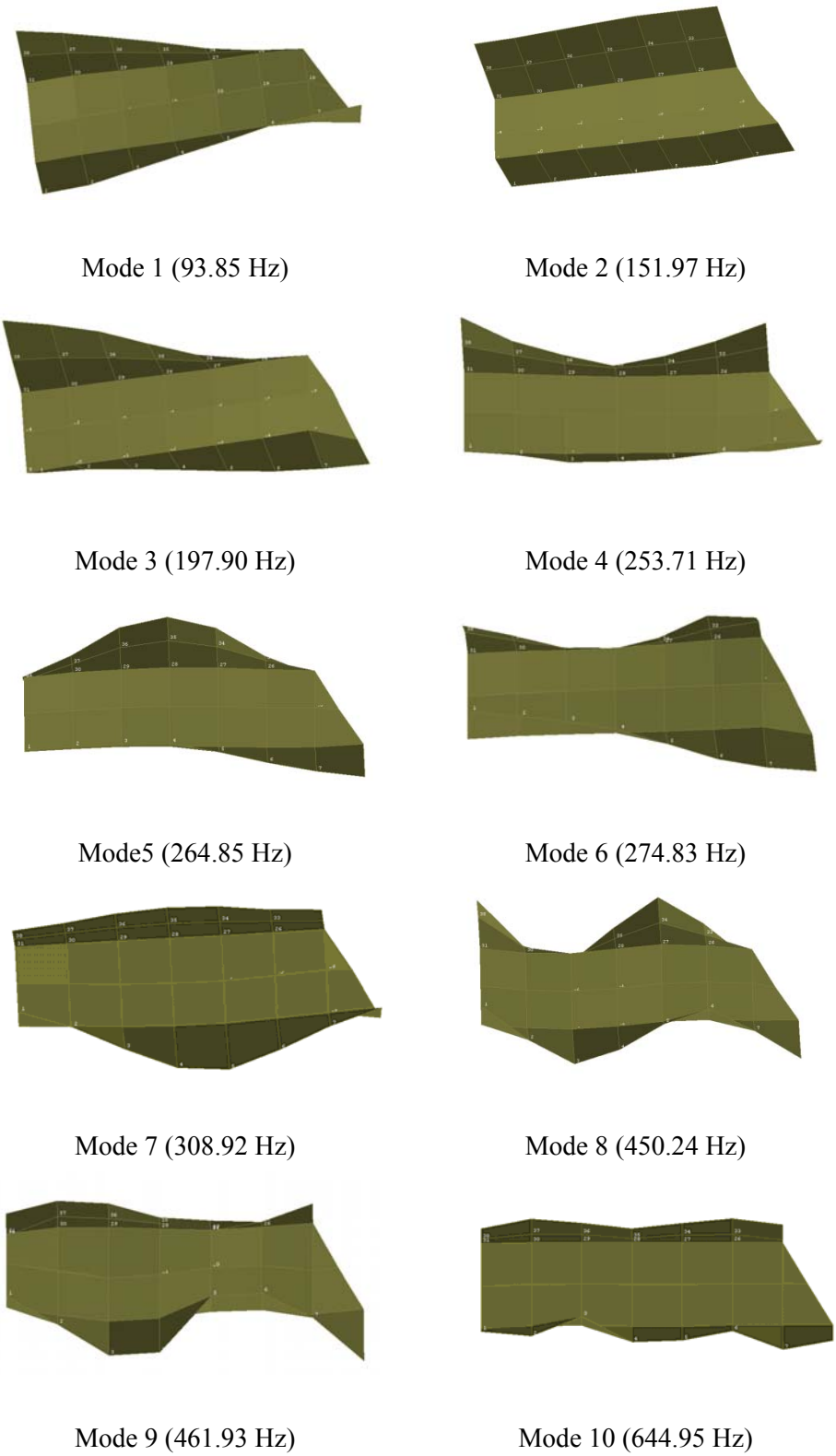

Figure 3.25: Experimental model of the base bent support A (Component 02A)

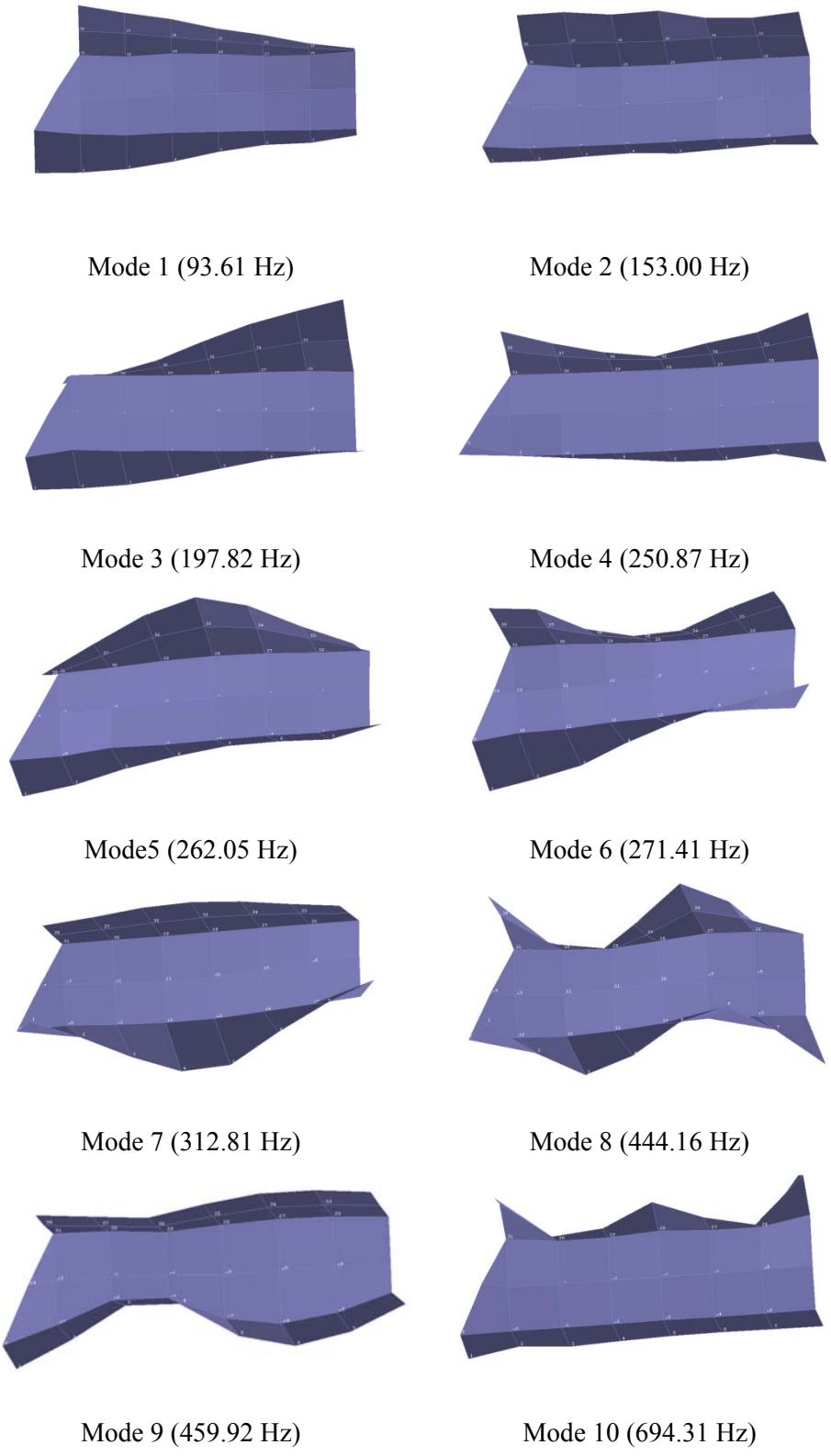

Figure 3.26: Experimental model of the base bent support B (Component 02B)

3.3.5 Experimental work of bracket

There are four similar brackets (Component 05A, 05B, 05AA and 05BB), and they are used to reinforce the main support of the natural gas cylinder compartment. The dimension of bracket is 83mm x 64 mm x 64 mm height and it is fabricated from cold roll mild steel sheets with 1.2 mm thickness. The test is performed with free-free boundary conditions by hanging it using a single soft spring as shown in Figure 3.27

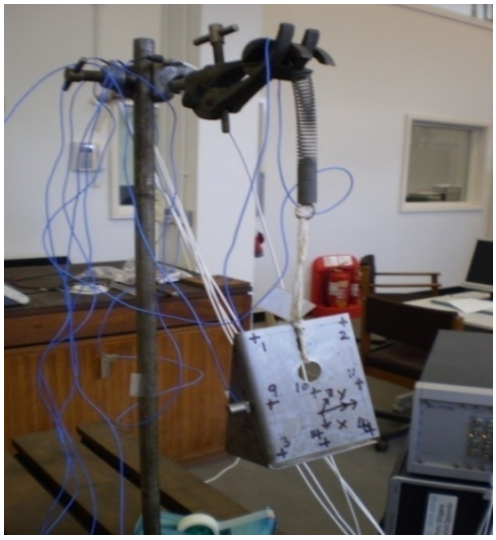

Figure 3.27: Experimental set-up for the bracket

For the experiment of bracket the number of accelerometers is kept as small as possible in order to avoid a mass loading issue. Therefore two accelerometers are used to measure the response of the bracket. One of the accelerometers is fixed and another accelerometer is roved around to measure the response of 24 degrees of freedom of the structure that cover 56 degrees of freedom through a master-slave relationship. The frequency range of interest is from 0 to 700 Hz. The first four measured natural frequencies and mode shapes of the brackets are shown in Figure 3.28.

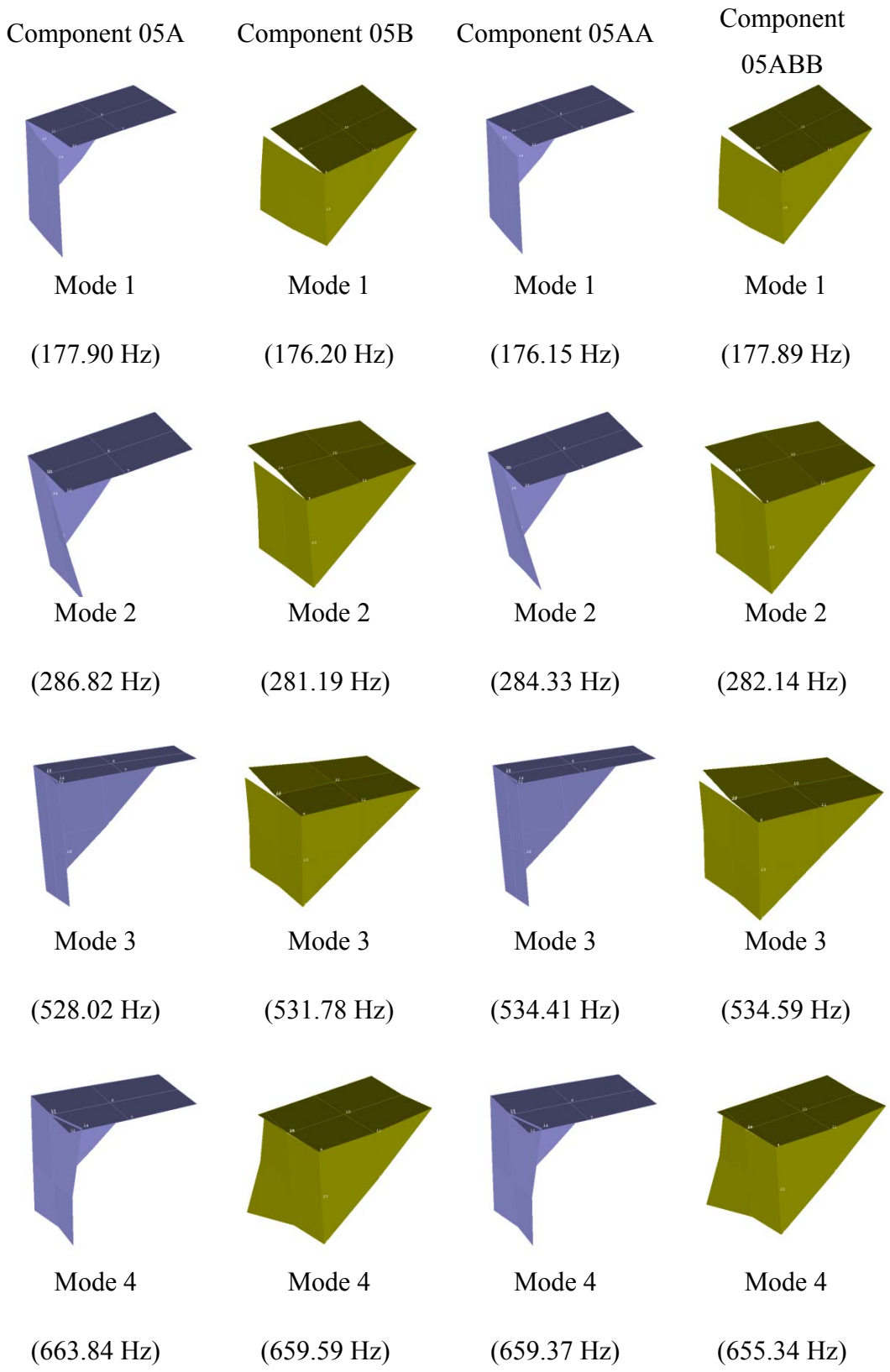

Figure 3.28: Experimental mode shapes and natural frequencies of the bracket (Component 05A, Component 05B, Component 05AA and Component 05BB).

3.3.6 Experimental work of side support (Component 07A and 07B)

There are two components of side support (Component 07A and Component 07B), and they are assembled to welded structures as shown in Figure 3.10. The dimension of the side support is 410mm x 48 mm x 55 mm height. The experiments are performed with free-free boundary conditions using a single soft spring as shown in Figure 3.29

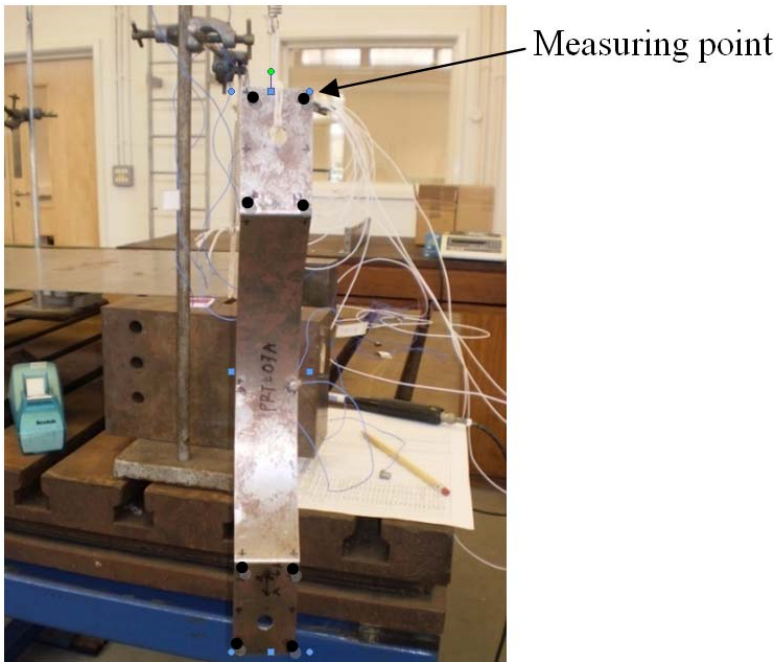

Figure 3.29: Experimental set-up for the side support (Component 07A and Component 07B)

Two accelerometers are used to measure the response of the component. One accelerometer is fixed while another accelerometer is used to measure the response of 10 degrees of freedom of the structure. The frequency range of interest for side support is from 0 to 170 Hz. The first five measured natural frequencies and mode shapes of the side support (Component 07A and Component 07B) are shown in Figure 3.30.

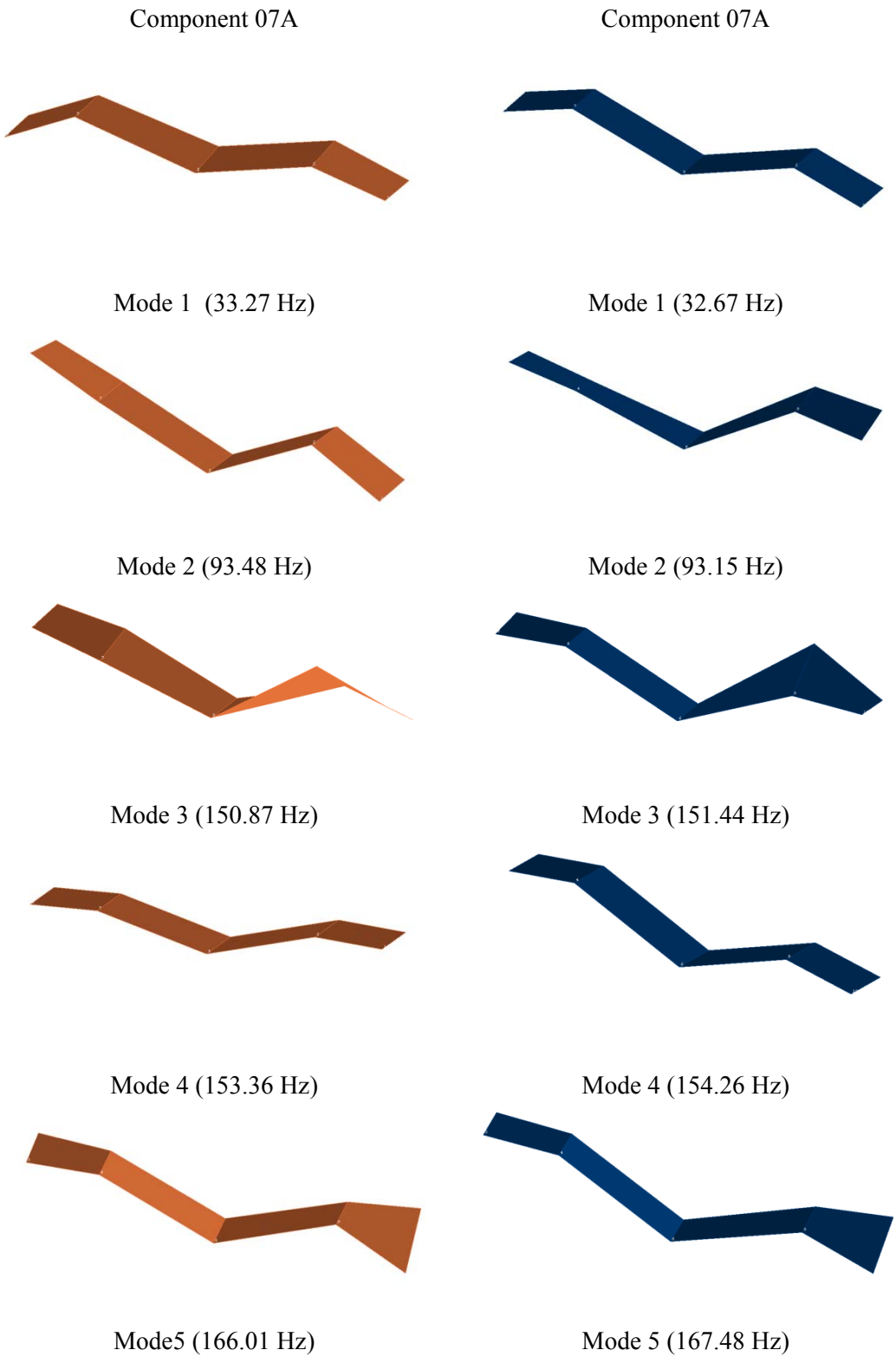

Figure 3.30: Experimental natural frequencies and mode shapes of the side support (Component 07A and Component 07B)

3.4 Experimental work of welded structures (free-free boundary conditions)

3.4.1 Main support structures (Structure 01A5AA and 01B5BB)

Main support structures (Structure 01A5AA and 01B5BB) are fabricated by spot welding two brackets onto the main support component as shown in Figure 3.7. Two structures are fabricated and the experiments are performed with free-free boundary conditions. Two soft springs are used to hang test structure as shown in Figure 3.31.

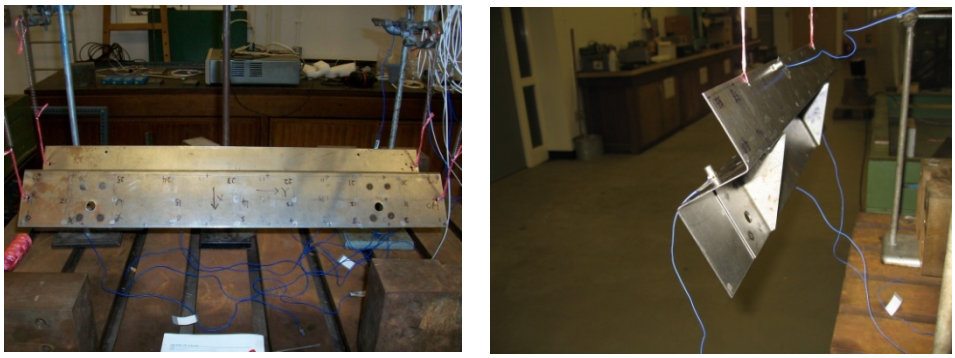

Figure 3.31: Experimental set-up for test structures (Structure 01A5AA and 01B5BB)

There are four accelerometers used to measure the response of the component. One of the accelerometer is fixed and another three are roved around to measure the dynamic response of 84 degrees of freedom of the structure that cover 149 degrees of freedom through a master-slave relationship as shown in Table 3.6. Figure 3.32 illustrates the details of measurement points.

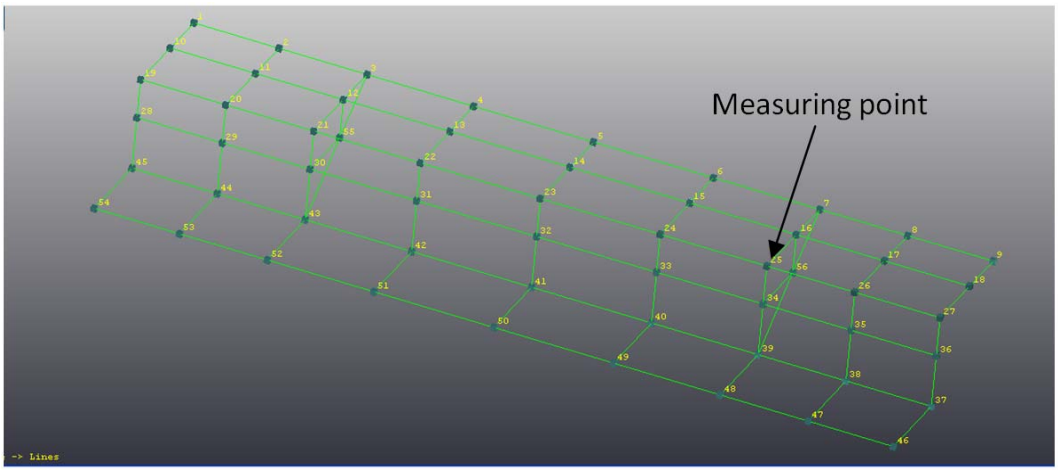

Figure 3.32: Experimental model and measuring points of welded structures (Structure 01A5AA and 01B5BB).

The frequency range of interest is from 0 to 150 Hz. The first ten measured natural frequencies and mode shapes of the welded structure main support A (Structure 01A5AA) are shown in Figure 3.33. Meanwhile for the first ten measured natural frequencies and mode shapes of the welded structure main support B (Structure 01B5BB) are shown in Figure 3.34.

Table 3.6: Information of the excitation point and accelerometers used in experiment the main support structures (Structure 01A5AA and 01B5BB)

Run	Accelerometers							
	8879		8881		8882		7226	
	Point/Direction		Point/Direction		Point/Direction		Excitation point	
1	1	+Z	23	+X	37	-Z	17	-Z
2	2	+Z	24	+X	38	-Z	17	-Z
3	3	+Z	25	+X	39	-Z	17	-Z
4	4	+Z	26	+X	40	-Z	17	-Z
5	5	+Z	27	+X	41	-Z	17	-Z
6	6	+Z	19	+X	42	-Z	17	-Z
7	7	+Z	20	+X	43	-Z	17	-Z
8	8	+Z	21	+X	44	-Z	17	-Z
9	9	+Z	22	+X	45	-Z	17	-Z
10	14	+Z	28	+X	46	-Z	17	-Z
11	15	+Z	29	+X	47	-Z	17	-Z
12	16	+Z	30	+X	48	-Z	17	-Z
13	18	+Z	31	+X	49	-Z	17	-Z
14	19	+Z	32	+X	50	-Z	17	-Z
15	20	+Z	33	+X	51	-Z	17	-Z
16	21	+Z	34	+X	52	-Z	17	-Z
17	22	+Z	35	+X	53	-Z	17	-Z
18	23	+Z	36	+X	54	-Z	17	-Z
19	24	+Z	41	-X	10	+Z	17	-Z
20	25	+Z	42	-X	11	+Z	17	-Z
21	26	+Z	43	-X	12	+Z	17	-Z
22	27	+Z	44	-X	13	+Z	17	-Z
23	3	+Y	45	-X	7	-Y	17	-Z
24	12	+Y	37	-X	16	-Y	17	-Z
25	21	+Y	38	-X	25	-Y	17	-Z
26	30	+Y	39	-X	34	-Y	17	-Z
27	43	+Y	40	-X	39	-Y	17	-Z
28	55	+Y			56	-Y	17	-Z
29							17	-Z

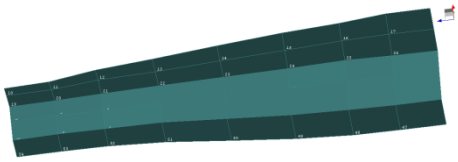

Mode 1 (43.47 Hz)

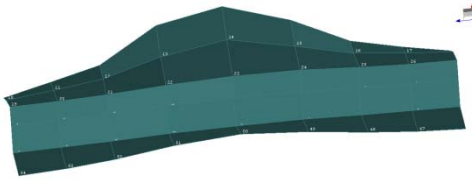

Mode 2 (144.05 Hz)

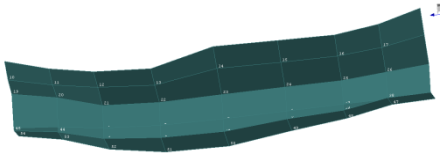

Mode 3 (197.16 Hz)

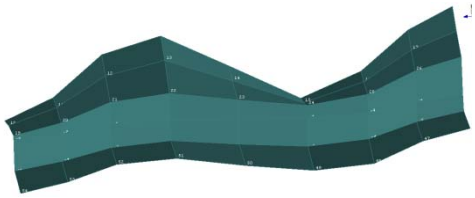

Mode 4 (201.93 Hz)

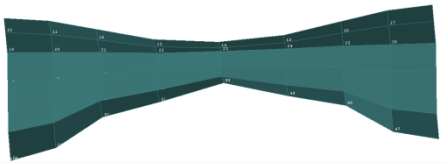

Mode 5 (215.83 Hz)

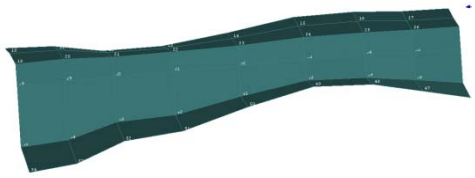

Mode 6 (219.01 Hz)

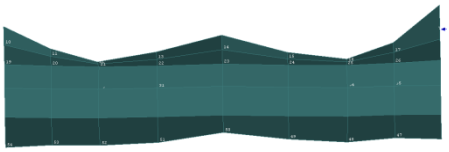

Mode 7 (252.95 Hz)

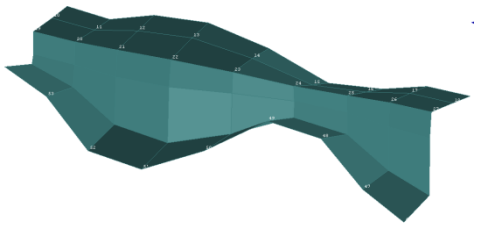

Mode 8 (264.30 Hz)

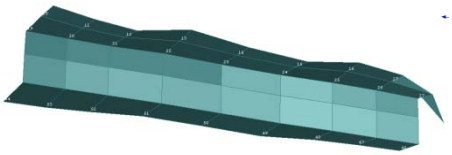

Mode 9 (276.43 Hz)

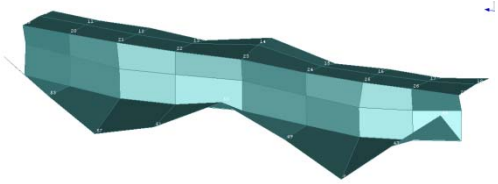

Mode 10 (307.78 Hz)

Figure 3.33: Experimental natural frequencies and mode shapes of the welded support structure (Structure 01A5AA)

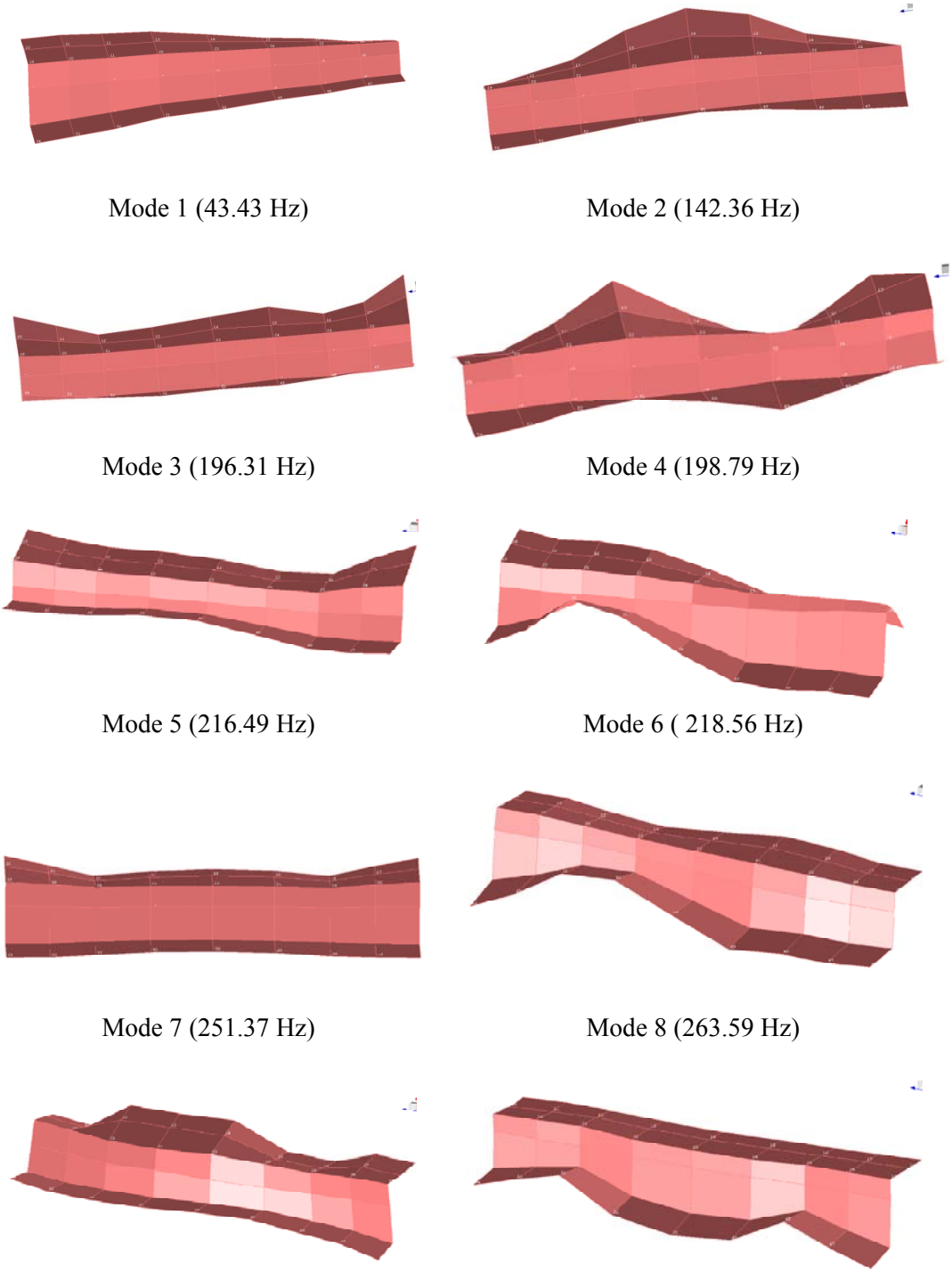

Figure 3.34: Experimental natural frequencies and mode shapes of the welded support structure (Structure 01B5BB)

3.4.2 Linearity check of full welded structure

Prior to the experiment of the full welded structure, the homogeneity test is firstly performed. The experiment is carried out in free-free boundary condition as shown in Figure 3.35. The purpose of this test is to check the linearity of the full welded structure due to complexity and fabrication process of the structure. Whilst there was no intention of studying non-linearity in detail, the ability to examine the degree of non-linearity in the test structures under low-level vibration was considered worthwhile. The non-linearity in the structure can be identified using shaker because normally a test structure cannot be excited sufficiently using impact hammer.

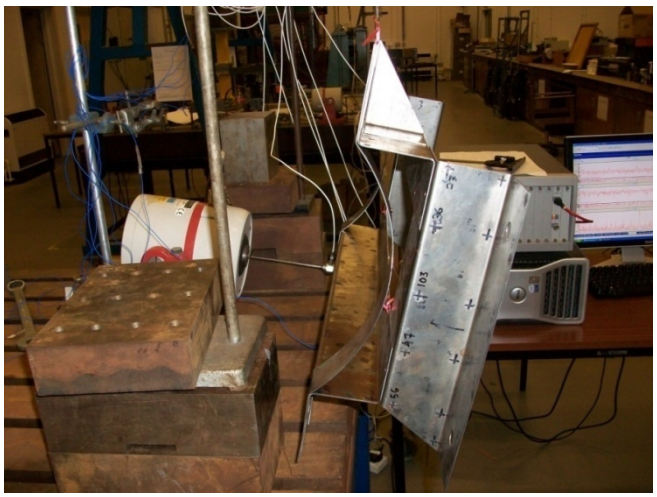

Figure 3.35: Experimental set-up for linearity check of full welded structure

The measurements are performed using stepped sine excitation because this type of excitation is the best form for quantifying any non-linear behaviour in a test structure (Farrar et al., 2007).

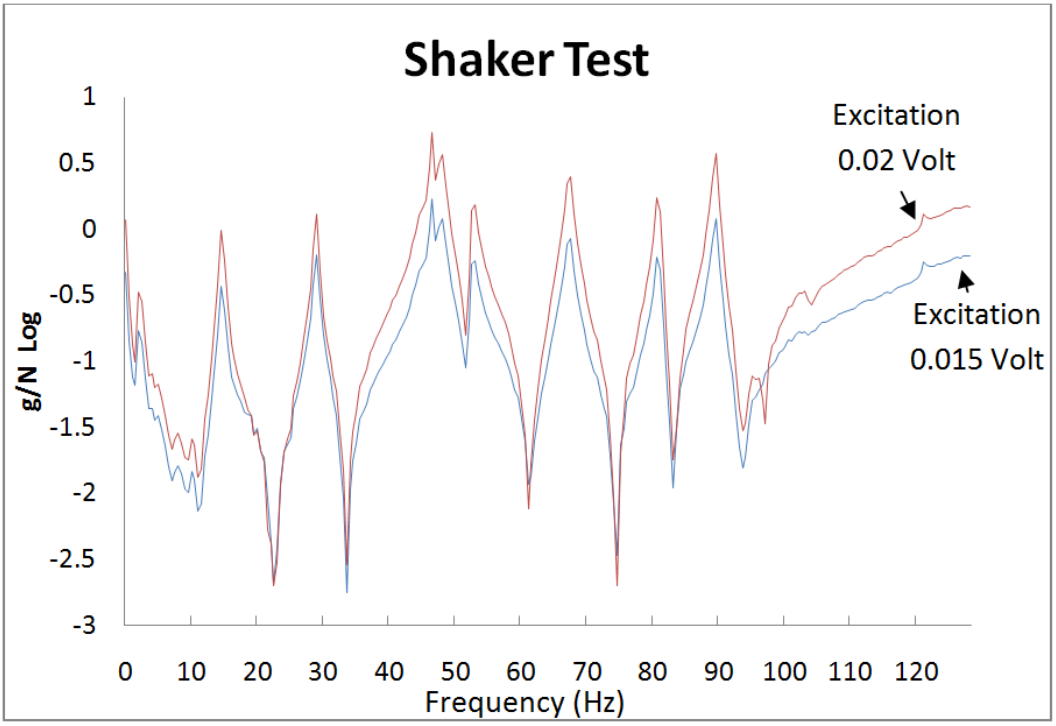

Figure 3.36: The linearity test FRF magnitude of the full welded structure

The non-linearity of the structure can be identified by shifting of any peak of FRFs assembly with the level of energy applied to the excitation input. This can be done by increasing level of input energy to the shaker. However, the test shows that the structure is almost linear within the measured frequency range as shown in Figure 3.36.

3.4.3 Experimental modal analysis of full welded structure

The experimental work of the full welded structure (Figure 3.37 (a)) is performed with free-free boundary condition as shown in Figure 3.37(b). The test structure is hanged using four soft springs. The measuring points are illustrated in Figure 3.38. There are five accelerometers used to measure the response of the component. One of the accelerometer is fixed and another four are roved around to measure the dynamic response of 111 degrees of freedom of the structure that

cover 324 degrees of freedom through a master-slave relationship as shown in Table 3.7 and Table 3.8. The frequency range of interest is from 0 to 160 Hz. The first ten measured natural frequencies and mode shapes of the full welded structure are shown in Figure 3.39.

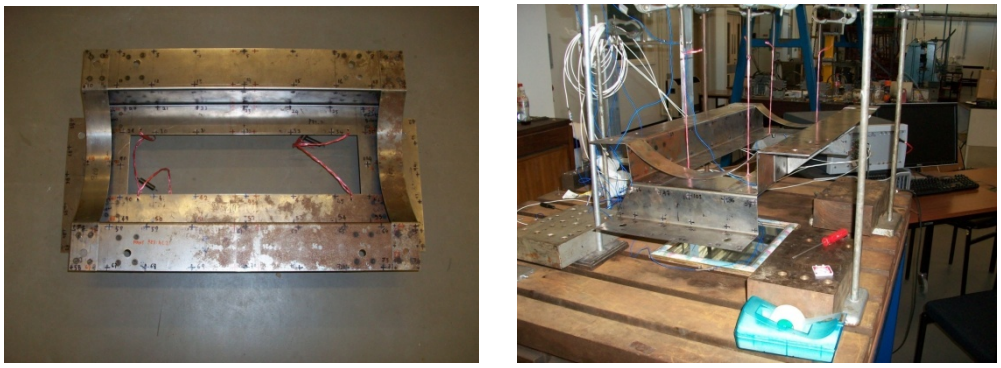

(a) (b)

Figure 3.37: Test of full structure (a) and (b) experimental set-up for the test structure

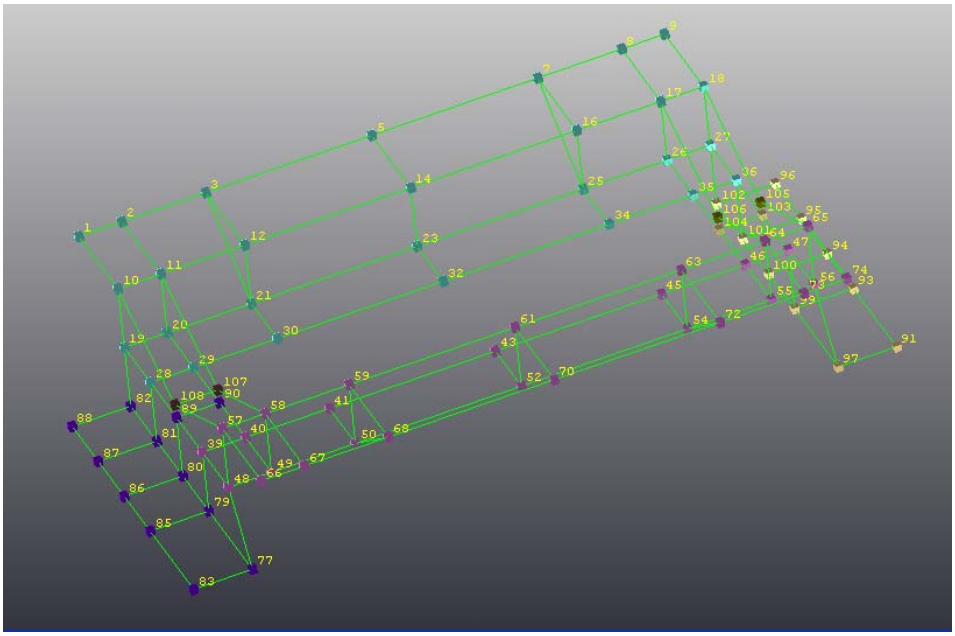

Figure 3.38: Experimental model and measuring points of full welded structure.

Table 3.7: Information of the excitation point and accelerometers used in experiment the test structures run 1 up to run 22

Run	Accelerometers									
	8879		8881		8882		8891		7226	
	Point		Point		Point		Point		Excitation Point	
1	10	-*X*	107	+*Z*	1	+*Z*	91	+*Z*	40	-*Z*
2	11	-*X*	108	+*Z*	2	+*Z*	93	+*Z*	40	-*Z*
3	12	-*X*	90	+*Z*	3	+*Z*	94	+*Z*	40	-*Z*
4	14	-*X*	89	+*Z*	5	+*Z*	95	+*Z*	40	-*Z*
5	16	-*X*	39	+*Z*	7	+*Z*	96	+*Z*	40	-*Z*
6	17	-*X*	83	+*Z*	8	+*Z*	47	+*Z*	40	-*Z*
7	18	-*X*	85	+*Z*	9	+*Z*	36	+*Z*	40	-*Z*
8	59	+*Z*	86	+*Z*	10	+*Z*	103	+*Z*	40	-*Z*
9	61	+*Z*	87	+*Z*	11	+*Z*	104	+*Z*	40	-*Z*
10	63	+*Z*	88	+*Z*	12	+*Z*	105	+*Z*	40	-*Z*
11	64	+*Z*	7	+*Y*	14	+*Z*	106	+*Z*	40	-*Z*
12	65	+*Z*	16	+*Y*	16	+*Z*	3	-*Y*	40	-*Z*
13	66	+*Z*	25	+*Y*	17	+*Z*	12	-*Y*	40	-*Z*
14	67	+*Z*	54	+*Y*	18	+*Z*	21	-*Y*	40	-*Z*
15	68	+*Z*	63	+*Y*	29	+*Z*	50	-*Y*	40	-*Z*
16	70	+*Z*	72	+*Y*	30	+*Z*	59	-*Y*	40	-*Z*
17	72	+*Z*	97	-*Y*	32	+*Z*	68	-*Y*	40	-*Z*
18	73	+*Z*	99	-*Y*	34	+*Z*	77	+*Y*	40	-*Z*
19	74	+*Z*	100	-*Y*	35	+*Z*	79	+*Y*	40	-*Z*
20	41	+*Z*	101	-*Y*	50	+*X*	80	+*Y*	40	-*Z*
21	43	+*Z*	102	-*Y*	52	+*X*	81	+*Y*	40	-*Z*
22	45	+*Z*	19	-*X*	54	+*X*	82	+*Y*	40	-*Z*

Table 3.8: Information of the excitation point and accelerometers used in experiment the test structures run 23 up to run 29

Run	Accelerometers									
	8879		8881		8882		8891		7226	
	Point		Point		Point		Point		Excitation Point	
23	46	+*Z*	20	-*X*	55	+*X*	27	+*Y*	40	-*Z*
24	57	+*Z*	21	-*X*	58	+*X*	36	+*Y*	40	-*Z*
25	58	+*Z*	23	-*X*	59	+*X*	103	+*Y*	40	-*Z*
26	63	+*X*	25	-*X*	61	+*X*	47	+*Y*	40	-*Z*
27	64	+*X*	26	-*X*	65	+*X*	56	+*Y*	40	-*Z*
28	57	+*X*	27	-*X*					40	-*Z*
29									40	-*Z*

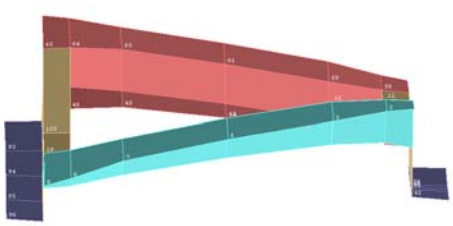

Mode 1 (14.55 Hz)

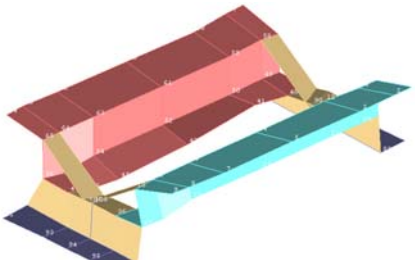

Mode 2 (28.96 Hz)

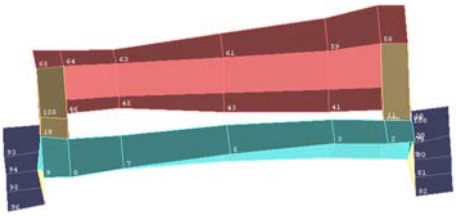

Mode 3 (44.92 Hz)

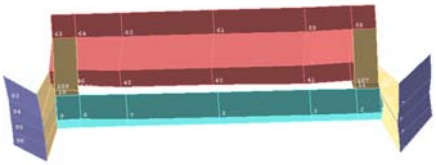

Mode 4 (46.92 Hz)

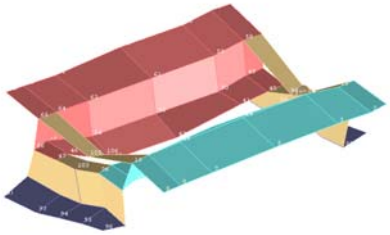

Mode 5 (47.96 Hz)

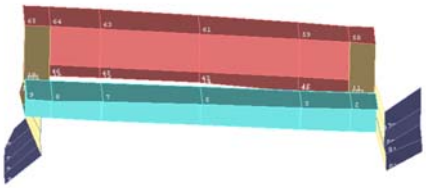

Mode 6 (52.66 Hz)

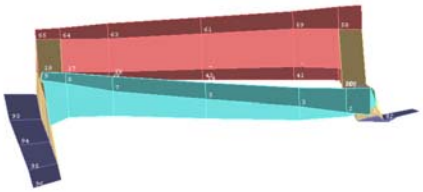

Mode 7 (67.35 Hz)

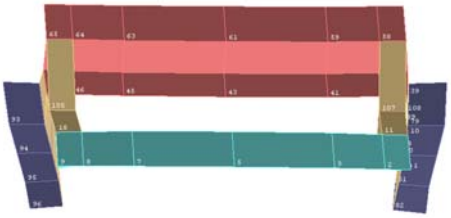

Mode 8 (80.74 Hz)

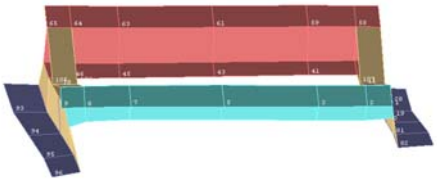

Mode 9 (89.48 Hz)

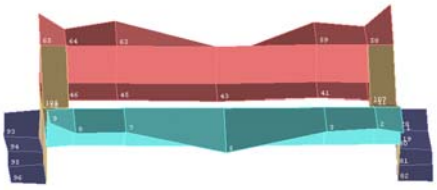

Mode 10 (137.833)

Figure 3.39: Experimental natural frequencies and mode shapes of the full welded structure

3.4.4 Experimental work of the full welded structure (fixed boundary conditions)

The purpose of this experiment is to identify the dynamic behaviour of the full welded structure with fixed boundary conditions. Model test on the full structures with fixed boundary conditions is performed and it is shown in Figure 3.40. The full welded structure is mounted on the test bed by four bolts (Figure 3.41). The bolts are tightened by a torque wrench with a force of 40 N/ m. The tightening process is done carefully to avoid any local deformation to the structure.

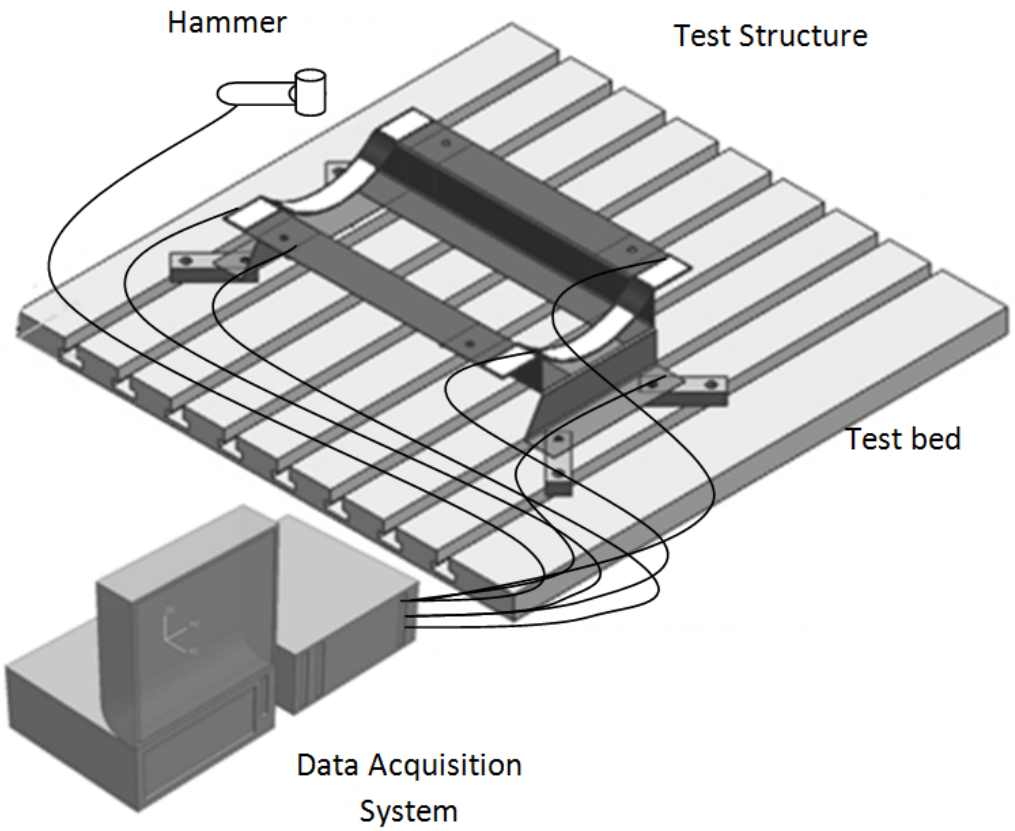

Figure 3.40: Schematic diagram for the experimental set-up for fixed boundary conditions

Figure 3.41: Experimental set-up for the full welded structure with bolted joints.

The details of measured points are based on Table 3.7. There are five accelerometers used to measure the response of the component. One of the accelerometers is fixed and the rest is roved over in order to measure the dynamic response of 324 degrees of freedom of the structure. The data acquisition system (LMS Scada III) has an option which is called slave-master through which it allows the response of the slave points to be referred to those measured at the master points. With this option, the number of measurements can be reduced and it helps to expedite the experimental work. In this work, only 111 degrees of freedom of the structure are measured. The frequency range of interest is within 0 to 130 Hz. The first ten measured natural frequencies and mode shapes are shown in Figure 3.42.

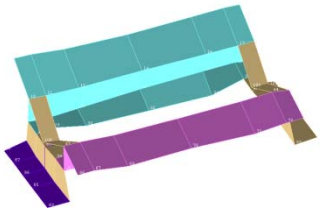

Mode 1 (26.40 Hz)

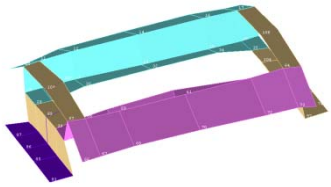

Mode 2 (28.41 Hz)

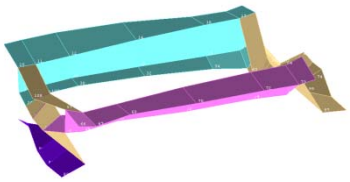

Mode 3 (34.61 Hz)

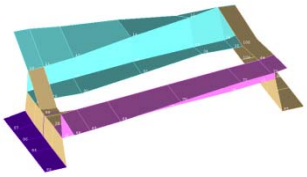

Mode 4 (43.50 Hz)

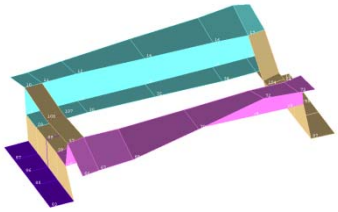

Mode 5 (45.02 Hz)

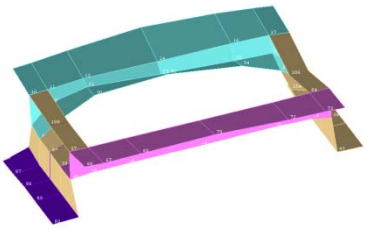

Mode 6 (68.67 Hz)

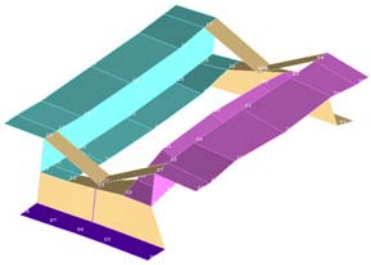

Mode 7 (84.64 Hz)

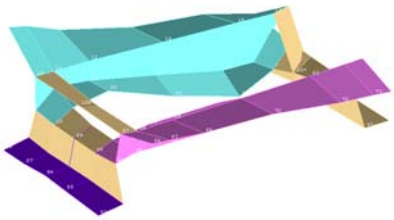

Mode 8 (101.48 Hz)

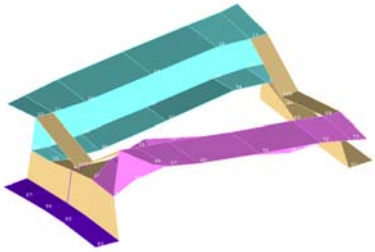

Mode 9 (124.76 Hz)

Figure 3.42: Experimental natural frequencies and mode shapes of the full welded structure of bolted joints

3.5 Closure

The fabrication process and the experimental modal analysis have been explained, and discussed in this chapter. Based on the observation, the quality, and diameter of spot welds are varied from each other. This is because the spot welding process are performed by a portable spot welding machine and highly depend on the spot welder the operator itself. To ensure the accuracy of the experiment results, several factors have been considered in the experimental such as mass loading issue, number of measurement points, accelerometers, and excitation method.

The location of excitation point and measuring points of components and structures are determined from finite element analyses in order to obtain reliable results and to avoid nodes. The experiments are systematically performed to components, welded structures and the full welded structure.

Due to complexity of the full welded structure, the linearity test is performed in order to check non-linearity of the structure.

The experimental data will be utilised in the next chapter to validate and update the initial finite element models.

Chapter 4

Finite Element Modelling and Model Updating of the Components

4.1 Introduction

Modal analysis is known as a process to determine the dynamic behaviour of the system in terms of natural frequency, mode shapes and damping ratio. Modal analysis can be performed either by experimental or numerical analysis. However, the accuracy of the finite element model alone cannot be verified without comparing with the experimental data of test structures. The accuracy of the dynamic behaviour of the finite element model of a structure is very important to designers and engineers as it allows them to improve the dynamic design of the structure as early as in design stage. Therefore, much effort is made to develop accurate finite element models. However, to perform finite element analyses especially to a large complex structure has become very challenging tasks.

Simplifications are normally made to a structure in order to reduce the computational time. Therefore, the finite element model may contain inaccuracy or uncertainty such as material properties, boundary conditions and geometrical tolerances (Modak et al., 2002b). For instance, (He and Zhu, 2011) found a significant difference between the initial numerical natural frequencies and their experimental counterparts when investigating the structures with L shape beam with bolted joint. Meanwhile, Chellini et al. (2008) and Arora (2011) and found significant differences between the initial finite element natural frequencies and experiment of the measured frequencies when investigating a steel-concrete composite frame structure. Therefore, correlation of finite element model and experimental data are important to reflect the physical dynamic behaviour of the structure.

For validation purpose, the developed finite element model is normally compared with experimental data and these comparisons usually disclose the discrepancies between these two models.

Model updating is used to improve the accuracy of a finite element model by correcting the invalid assumptions that have been made to the finite element model (Mottershead et al., 2000). This is done by changing some uncertain finite modelling parameters, which have the potential to influence modal properties and subsequently to improve the accuracy of the model (Živanović et al., 2007). The modal assurance criterion (MAC) is normally used to quantify modes between finite element model and experiment. Consequently, the data from experiment can be used in many applications such as optimisation, design, damage identification, structural control and health monitoring.

This chapter presents the finite element modelling and model updating procedure, including formulation used in finite element method, model updating and followed by design sensitivity and optimisation (SOL 200) that are available in NASTRAN. The development of finite element models of components and structures are also described in this chapter. The initial and updated natural frequencies and mode shapes are compared with the experimental values presented in Chapter 3. The updated parameter values then are used for the development of the finite element model of the structures.

4.2 Finite element modelling

The tough competition between automotive manufactures and more stringent requirements by government regulations have put a pressure on the automotive industries to develop energy efficient and improve safety standard vehicles than the past. Engineers and designers must have better testing and analysis tools to assist them to meet the stringent requirements of the products. The finite element method (FEM) is commonly referred to as modelling tools in structural

engineering and rapidly become an important tool for engineers and designers since it was introduced in the 1950s.

Essentially, any complex geometrical shape can be divided into standard elements such as beams and shells. These elements are connected to each other at their nodes. Deformations within the elements are assumed to follow predefined functions known as shape functions (Zienkiewicz et al., 2005 and Mottram and Zheng, 1996).

The general governing equation of motion for the system is given as

$$\mathbf{M}\ddot{\mathbf{x}}(t) + \mathbf{C}\dot{\mathbf{x}}(t) + \mathbf{K}\mathbf{x}(t) = \mathbf{f}(t) \qquad (4.1)$$

where, **M**, **C** and **K** are known as *n* x *n* mass, damping and stiffness matrices of the system. Meanwhile $\mathbf{x}$, $\dot{\mathbf{x}}$ and $\ddot{\mathbf{x}}$ are the *n* x 1 vectors of displacement, velocities and accelerations respectively and $\mathbf{f}(t)$ is *n* x 1 vector of external forces.

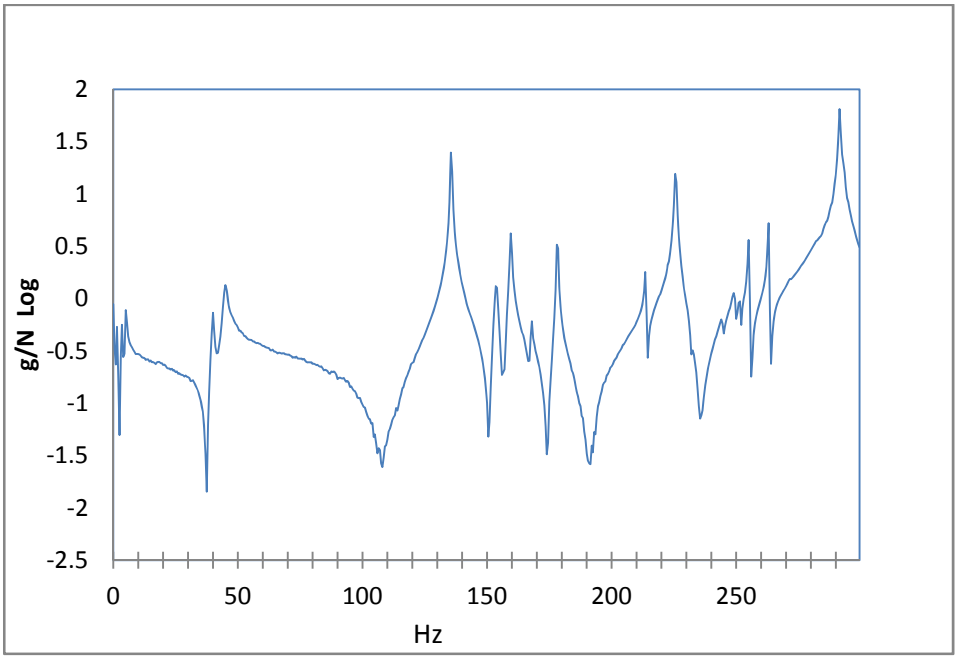

(a)

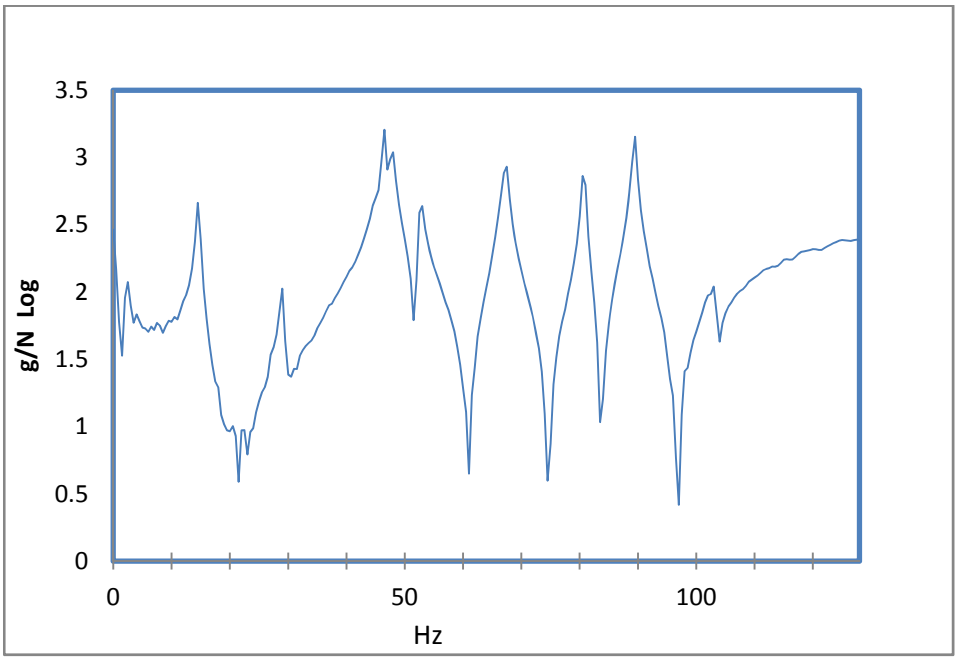

(b)

Figure 4.1: (a) FRFs of the component 01A and (b) the assembled structure 01A5AA

Based on the narrow peaks in the FRFs that are shown in Figure 4.1 (a) and Figure 4.1 (b), the component and assembled structure are considered having light damping. Therefore for free undamped vibration analysis of multi degree of freedom (MDF) systems, the equation of motion for free vibration can be written from, (Eq. (4.1)), as

$$\mathbf{M}\ddot{\mathbf{x}}(t) + \mathbf{K}\mathbf{x}(t) = 0 \tag{4.2}$$

Assuming a trial solution of the form

$$\mathbf{u} = \boldsymbol{\phi} \sin \omega t \tag{4.3}$$

where, $\boldsymbol{\phi}$ is the eigenvector or mode shape, ω is the natural frequency of the structure in rad /sec, and t represents the time. Equation (4.3) is then can be simplified form of eigen-equation, as follows.

$$(\mathbf{K} - \omega^2\mathbf{M})\boldsymbol{\phi} = 0 \tag{4.4}$$

In order to calculate the natural frequencies and mode shapes of complex structure, it is necessary to use an iterative solver due to its practicality. The natural frequencies and mode shapes of the structure are obtained by solving the (Eq. (4.4)). In this work, the calculation of the natural frequencies and mode shapes is performed using the Normal Modes analysis (SOL 103) that is available in MSC.NASTRAN.

The natural frequencies and mode shapes of the initial finite element are compared with those from experimental data in order to validate the accuracy of the finite element model. However, to evaluate the accuracy of mode shapes, it is necessary to pair modes between experimental modes and finite element modes correctly.

The modal assurance criterion (MAC) can be used to indicate the level of correlation of mode shapes between finite element model and experimental model.

It is normally used to calculate experimental (ϕ_m) and finite element modes (ϕ_a) and presented in matrix form, which can be calculated from Equation (4.5) (Brehm et al., 2010).

$$\mathrm{MAC} = (\phi_m \phi_a) = \frac{\left|\phi_m^{\mathrm{T}} \phi_a\right|^2}{\left(\phi_a^{\mathrm{T}} \phi_a\right)\left(\phi_m^{\mathrm{T}} \phi_m\right)} \tag{4.5}$$

The mode shape correlation generally is displayed in matrix form which may take a scalar value between 0 and 1. The value of 1 in diagonal terms indicates that the correlations of the mode shapes are perfect. Meanwhile the value of 0 is indicated that mode shapes are completely unrelated.

4.3 Finite element model updating

Generally, the finite element method is proven to be an efficient tool for engineers and designers to predict the dynamic behaviour of the structures in many industrial fields such as automotive, aerospace and civil structures. As a structure becomes more complex, the accurate prediction and simulations of the structures based on numerical models become more challenging. The demand for reliable finite element models with respect to experimental data is crucial. However, the predicted result of finite element models often differ from measure data that contain the actual information of the real structure. The deviations between experimental and numerical analysis will allow the engineer to evaluate the accuracy of the initial finite element model (Schedlinski et al., 2005). If the deviations between the experimental and analysis are not acceptable, the initial finite element model needs to be reviewed and corrected based on experimental data.

Model updating methods have been recognised as a systematic way to enhance or to improve an existing finite element model using experiment data. An improved finite element model is obtained by altering parameters of the model such as

Young's modulus and shear modulus of the structure. Finite element model updating has gained attention among researchers for the past twenty years (Friswell et al., 2001). For instance, Ziaei-Rad and Imregun (1996) and Asma and Bouazzouni (2005) investigated FRFs based model updating techniques and use the measured data directly as their reference. Zang et al. (2006a) presented the optimally selected DOFs for effective model updating with multiple design parameters. Meanwhile, Marwala and Heyns (1998) introduced a multi-criterion updating method that minimised the discrepancy based on modal properties and FRFs. On top of that, different applications of finite element model updating have been made such as in civil and mechanical and engineering. For instance, Brownjohn and Xia (2000) and Cunha et al. (2001) investigated of footbridges. Ventura et al. (2001) attempted to correlate experimental and analytical modal properties of the building using a manual updating process. Burnett and Young (2008) and Abu Husain et al. (2010) employed the model updating method for updating automotive structures.

Model updating methods can be classified into two categories, namely direct methods and iterative methods. Direct updating method is capable of replicating the measured natural frequencies and mode shapes with one step (Brownjohn et al., 2000). Even though, direct methods required less computational efforts, however the major drawback is the final value of the updated parameters may lose their physical meaning and does not allow for a physical interpretation (Mottershead et al., 2011). Meanwhile, the iterative methods are more versatile compared with direct methods because it allows a wide choice of parameters to be updated. The iterative methods are used to minimise the error between the numerical and the experimental data based on minimisation of the objective function which are involving modal data such as frequencies and mode shapes. The iterative methods are generally based on sensitivity analysis. In sensitivity analysis, the modal data are often used because relatively sensitivity information is easy to calculate. The sensitivity analysis is performed to select the most sensitive parameters for the finite element model (Mordini et al., 2007). The sensitivity matrix is calculated by considering the partial derivatives of modal

parameters with respect to structural parameters via a truncated Taylor's expansion. This expansion is often limited to the first two terms, in order to produce the linear approximation as follows (Friswell and Mottershead, 1995b).

$$\delta \mathbf{Z} = \mathbf{S}_j \delta \boldsymbol{\theta} \tag{4.6}$$

where, $\mathbf{S}_j$ is the sensitivity matrix, contains the first derivative of the eigenvalues and mode shapes with respect to parameters j^{th} iteration, and $\delta \mathbf{Z}$ is the differences between measured and predicted output vectors. Meanwhile $\delta \boldsymbol{\theta}$ is the vector of perturbation in the updating parameters such as Young's modulus, shear modulus, diameter, etc. The rate of change of the i^{th} eigenvalues (λ_i) with respect to the j^{th} parameters, $\boldsymbol{\theta}_j$ can be calculated from Equation (4.7) (Mottershead and Friswell, 1993).

$$\mathbf{S}_{ij} = \frac{\partial \lambda_i}{\partial \boldsymbol{\theta}_j} = \boldsymbol{\phi}_i^{\mathrm{T}} \left[\frac{\partial \mathbf{K}}{\partial \boldsymbol{\theta}_j} - \lambda_i \frac{\partial \mathbf{M}}{\partial \boldsymbol{\theta}_j} \right] \boldsymbol{\phi}_i \tag{4.7}$$

4.4 Finite element model updating via MSC NASTRAN (SOL200)

The NASTRAN optimisation code (SOL 200) is used to perform model updating. The optimisation algorithm, which is a sensitivity-based iterative procedure, allows the objective function (J) to be minimised by adjusting the eigenvalues of initial finite element model until objective function (J) is converged. The objective function based on eigenvalues is defined as follows (Friswell and Mottershead, 1995b).

$$J = \sum_{i=1}^{n} W_i \left(\frac{\lambda_i^{\text{fe}}}{\lambda_i^{\text{exp}}} - 1 \right)^2 \tag{4.8}$$

where, $\lambda_i^{\exp}$ is the i^{th} experimental eigenvalue and λ_i^{fe} is the i^{th} predicted eigenvalue from finite element model and *n* is the number of eigenvalues involved in updating.

4.5 Design sensitivity and optimisation

The approximate optimization problem of MSC.Nastran is constructed using a first-order approximation which is based on Taylor series expansions as indicated below (MSC.NASTRAN, 2005b),

$$z(\theta+\Delta\theta) = z(\theta) + \left.\frac{dz}{d\theta}\right|_{\theta} \Delta\theta + \left.\frac{d^2z}{d\theta^2}\right|_{\theta} \frac{\Delta\theta^2}{2!} + \left.\frac{d^3z}{d\theta^3}\right|_{\theta} \frac{\Delta\theta^3}{3!} + ... \tag{4.9}$$

In the iterative process, the numerical optimiser is used to search the best configuration within a set of design spaces of the parameters which are limited by design constraints. Design constraints consist of boundaries imposed over the values of design variables, given by

$$x_i^L \le x_i \le x_i^U \tag{4.10}$$

where, x_i^L , the lower bound on the i^{th} design variable and x_i^U is the upper bound

The design variables are subsequently updated at each iteration in order to find best combination value to fit the objective function (Eq. (4.8)). This process is repeated until the design variables converge to the optimal values.

4.6 Implementation of finite element modelling

A mechanical structure normally consists of many components. They are joined together by mechanical joints or adhesive to form a more complex structure. The meshes of the structure are getting finer in order to achieve a higher accuracy. Moreover, process of meshing can be time consuming especially for a large and complex structure. Therefore, the specific considerations such as type and size of elements for finite element modelling are important.

In order to generate a finite element model of components and the structure with spot welds joints, the MSC PATRAN/NASTRAN finite element software is employed in this research to perform the dynamic analysis.

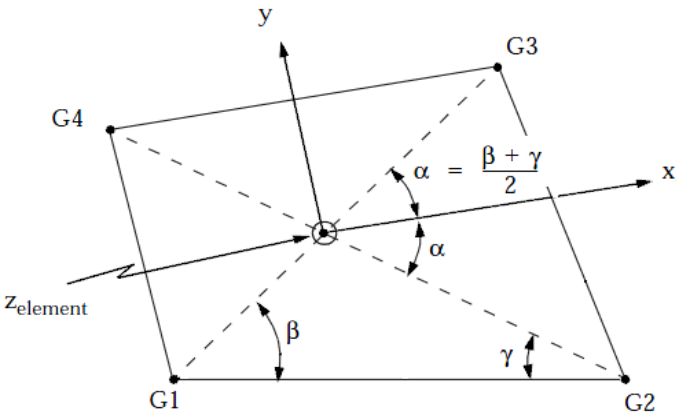

Figure 4.2: CQUAD4 Element geometry and coordinate system (MSC.NASTRAN, 2001).

CQUAD4 element is employed to model components and assembled structures. The element is based on shell theory and is ideal for representing shell like structures such as thin plates, and thin walled structures as shown in Figure 4.2. The element geometry is specified by four corner nodes (G1, G2, G3 and G4) which have three translations and two rotationals as their degrees-of-freedom. The orientation of the element coordinate system is determined by the order of the connectivity for the grid points. However the rotation about an axis (z-axis) perpendicular to the plane of the element is not allowed. The element z-axis, often referred to as the positive normal, is determined using the right-hand rule as shown in Figure 4.2.

The finite element models are developed based on the initial CAD drawings that were utilised for fabrication process. The geometry of CAD model needs to be idealized in order to reduce the complexity of the finite element model. The developed finite element model of components will be validated with the measured data in order to evaluate their accuracy.

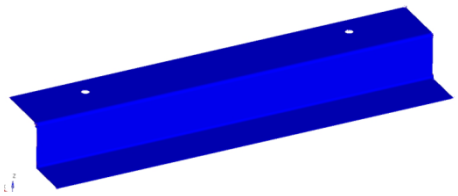

(a) CAD model

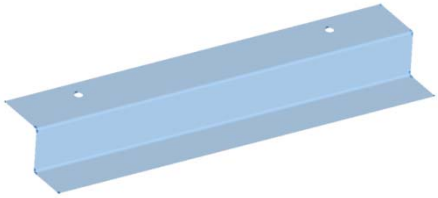

(b) Mid-surface model

(c) CAE model

Figure 4.3: Visual model of main supports

The main requirement to develop the 2-D shell elements is to use mid-surface of the solid models of the structure. The pre/post processing tool PATRAN is utilised to extract the mid-surface (Figure 4.3 (a)) and meshing process (Figure 4.3 (b)) of the components. The parameters of fabricated components and structures such as dimension and thickness are inspected once again. The goal is to develop an accurate representation of physical components/structures. The final amendments are performed on components and structures in final CAD drawing prior to be used for the Finite Element models (Figure 4.3 (c)). The material properties of mild steel are used in the finite element model with nominal values as tabulated in (Table 3.1). The discrepancy of the fabricated components must be taken into account. Measurements are performed and revealed the actual thickness is 1.18 mm instead of nominal value 1.2 mm. Therefore thickness of 1.18 mm is used in modelling of the components and structures instead of nominal value of 1.2 mm. Generally, the basic concept of finite element analysis is one of discretisation. In this process, a mid surface of CAD model of the component (Figure 4.3 (b)) is

divided into smaller segments, commonly known to as a mesh (Figure 4.3 (c)) and each mesh contains a number of finite points are identified as nodes. In structural dynamics analysis of a large and complex structure, the choice of element type, the size of mesh, material properties and the selection of boundary conditions must all be carefully determined in order for simulation results to have a physical meaning. On top of that, the selection of finite element package is important that the pre-processor be capable of reading the CAD drawing files. The most general finite element analysis package includes a pre-processor, a solver and a post-processor.

PATRAN is the pre-and post-processing in MSC.NASTRAN, and the finite element models of the components and structures are modelled using CQUAD4 elements available PATRAN. The CQUAD4 is a general-purpose plate element capable of carrying in-plane force, bending forces, and transverse shear forces (MSC.NASTRAN, 2001). NASTRAN solution 103 is used to compute the natural frequencies and the mode shapes of the initial finite element models. The natural frequencies and mode shapes of initial finite element models are then compared with the experimental counterparts. Model Assurance Criterion (MAC) is used to quantify the correlation of the mode shapes.

4.7 Finite element modelling and updating of main support A and main support B

The finite element model of main support A (MS A) and main support B (MS B) is using the procedures in the preceding section. The finite element models of main support components are modelled by 8240 CQUAD4 elements. The normal mode analysis of NASTRAN SOL 103 is used to calculate the first ten natural frequencies and mode shapes of the initial finite element model of the components. The computed natural frequencies are compared with the experimental natural frequencies as shown in Table 4.1 and Table 4.2. The total of the relative errors for the main support A is 19.03 percent. Meanwhile, for main support B the total relative error is 15.16 percent.

Table 4.1: Comparison between measured and FE natural frequencies of main support A

Mode	I Experiment Frequency (Hz)	II Initial F.E Frequency (Hz)	III Relative Error [%] [I-II/I]	IV Initial FE MAC
1	41.59	41.42	0.41	0.92
2	136.59	133.26	2.39	0.93
3	155.24	152.78	1.58	0.87
4	161.09	159.04	1.28	0.89
5	179.10	174.52	2.56	0.92
6	213.67	207.63	2.83	0.97
7	226.75	221.67	2.24	0.98
8	251.68	244.86	2.71	0.90
9	255.75	252.60	1.23	0.88
10	263.62	258.87	1.80	0.95
Total Error			19.03	

Table 4.2: Comparison between measured and FE natural frequencies of main support B

Mode	I Experiment Frequency (Hz)	II Initial F.E Frequency (Hz)	III Relative Error [%] [I-II/I]	IV Initial FE MAC
1	41.58	41.42	0.39	0.92
2	135.34	133.26	1.54	0.90
3	154.41	152.78	1.06	0.95
4	160.22	159.04	0.73	0.98
5	178.40	174.52	2.18	0.92
6	213.66	207.63	2.82	0.87
7	226.31	221.67	2.05	0.98
8	249.50	244.86	1.86	0.82
9	255.14	252.60	1.00	0.83
10	262.90	258.87	1.53	0.96
Total Error			15.16	

Obviously the result shows that the initial finite element needs to be update in order to reduce the errors. On the other hand, the MAC analysis is performed to identify the mode shapes correlation between measured points of the component and the finite element model. The mode shapes of the initial finite element model are found to have reasonable correlation with the experiment data with more than 0.8.

The parameterisation of the main support A and main support B is performed using a sensitivity analysis. The sensitivity analysis which is based on NASTRAN SOL200 is used to identify the most sensitive parameters by calculating the changes (sensitivity coefficient) of the structure response (such as, natural frequency, displacement, etc) relative the unit design variable through the computation and the results are shown in Table 4.3. Several potential parameters such as the thickness, Young's modulus, shear modulus, density and Poisson's ratio are considered in the sensitivity analysis.

In the sensitivity analysis, the values of updating parameters (such as the thickness, Young's modulus, Shear modulus, Poisson's ratio and density) which are set with the design constraints are normalised to the initial value of the updating parameters. It can be seen that, from Table 4.3 the sensitivity coefficients of the Young's modulus and density of the component of the main support show the same coefficients. However, only one of these two parameters is selected for updating due to their direct relation in the calculation of the natural frequency.

Table 4.3: Summarised results of the sensitivity analysis with respects to the normalised parameters of main support A and main support B.

Mode	Frequency	Parameters				
		Thickness	Young's Modulus	Shear Modulus	Poisson's Ratio	Density
1	4.21E+01	3.90E+01	1.98E+01	2.91E-02	-4.32E+00	-2.05E+01
2	1.35E+02	1.17E+02	6.18E+01	8.21E-02	-1.69E-01	-6.78E+01
3	1.55E+02	1.36E+02	6.99E+01	1.33E-02	1.32E+01	-7.41E+01
4	1.62E+02	1.43E+02	7.36E+01	5.48E-02	6.14E+00	-7.82E+01
5	1.77E+02	1.58E+02	8.21E+01	1.33E-01	-2.53E+00	-8.77E+01

The comparisons are made to choose most suitable parameters for updating procedure. Based on the sensitivity data, it can be summarised that the frequencies are more sensitive to the thickness of the plate and Young's modulus of the component. Meanwhile, the Poisson's ratio is proved less sensitive to the all frequencies.

Although, the thickness of components shows the highest coefficient, the correction of thickness is normally performed manually rather than included as an updating parameter. Hence, the thickness is assumed to have already been corrected. Obviously, the value of the Young's modulus is assumed not well

known. Therefore, the Young's modulus is used as an updating parameter for both main base support A and main support B. The initial value of the Young's modulus is set to be 210 GPa and it is allowed to vary from 190 GPa to 220 GPa in which the range of Young's modulus of mild steel is standardised.

The updating is performed by minimising the objective function (Eq. (4.8)) which is based on the first five measured frequencies. The updated natural frequencies of the finite element model of main support A is compared with those of the experimental results in Table 4.4 (column III) together with their MAC value. The discrepancies of the frequencies are reduced significantly from 19.03 percent to 6.98 percent.

Table 4.4: Three comparisons of results between the tested and finite element (FE) model of main support A

Mode	I Experimental Main Support A (Hz)	II Initial FE Main Support A (Hz)	III Error (%) [I-II/I]	IV Updated FE Main Support A (Hz)	V Error (%) [I-IV/I]	VI Updated FE MAC
1	41.59	41.42	0.41	42.13	1.30	0.94
2	136.53	133.26	2.39	135.45	0.79	0.95
3	155.24	152.78	1.58	155.25	0.01	0.90
4	161.09	159.04	1.28	161.65	0.34	0.91
5	179.10	174.52	2.56	177.43	0.93	0.92
6	213.67	207.63	2.83	210.87	1.31	0.98
7	226.75	221.67	2.24	225.44	0.58	0.99
8	251.68	244.86	2.71	248.74	1.17	0.94
9	255.75	252.60	1.23	256.39	0.25	0.90
10	263.62	258.87	1.80	262.84	0.29	0.94
	Total error		19.03		6.98	

This is shown that the selection of the updated parameter of the Young's modulus is able to improve the first ten frequencies even though only first five frequencies are used as a reference. On top of that, the updated MAC value (Column VI) for all modes also shows better correlation. The comparison between the initial finite element mode shapes and the updated mode shapes is shown in Figure 4.6 and Figure 4.7. Table 4.5 shows the changes of the initial and updated value of the Young's modulus with the increment of 4.8 percent from the initial value. Meanwhile Figure 4.4 shows the initial changes of the updating parameters from the initial normalised value to convergent value.

Table 4.5: Updated value of parameter of main support A

Parameters	Initial Value	Updated Value	Unit
Young's Modulus	210000	220080	MPa

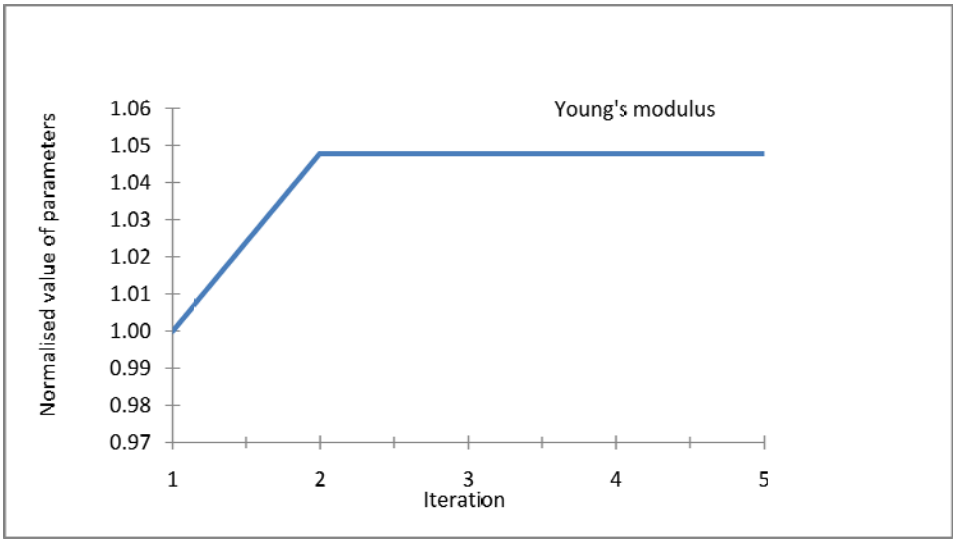

Figure 4.4: The convergence of the updating of main support A

The initial finite element results of main support A and main support B are compared (Table 4.1 and Table 4.2) with their experimental counterparts. The

results (Table 4.1 and Table 4.2) it reveals that the error in each component is different even though the components are considered identical and fabricated from the same batch of material. Therefore, the model updating also must be performed to improve the accuracy of the initial finite element model of main support B.

Table 4.6: Three comparisons of results between the tested and finite element (FE) model of main support B

Mode	I Experimental Main Support A (Hz)	II Initial FE Main Support A (Hz)	III Error (%) [I-II/I]	IV Updated FE Main Support A (Hz)	V Error (%) [I-IV/I]	VI Updated FE MAC
1	41.58	41.42	0.39	41.75	0.40	0.92
2	135.34	133.26	1.54	134.28	0.79	0.91
3	154.41	152.78	1.06	153.93	0.31	0.96
4	160.22	159.04	0.73	160.25	0.02	0.94
5	178.40	174.52	2.18	175.87	1.42	0.95
6	213.66	207.63	2.82	209.13	2.12	0.89
7	226.31	221.67	2.05	223.42	1.28	0.90
8	249.50	244.86	1.86	246.67	1.14	0.88
9	255.14	252.60	1.00	254.36	0.31	0.90
10	262.90	258.87	1.53	260.72	0.83	0.95
	Total error		15.16		8.60	

In order to minimise the error between the initial finite element model and the experiment counterpart, the model updating is performed to the counterpart and the Young's modulus is again used for the updating parameters of component main support B. The total error between the updated finite element model and its experiment counterpart is reduced from 15.16 percent to 8.60 percent and the MAC value is improved above 0.8 as shown in Table 4.6.

Table 4.7 shows the changes of the initial and updated value of the Young's modulus with the increment of 4.8 percent from the initial value. Meanwhile, Figure 4.5 shows the initial changes of the updating parameters from the initial normalised value to convergent value.

Table 4.7: Updated value of parameter of main support B

Parameters	Initial Value	Updated Value	Unit
Young's Modulus	210000	220080	MPa

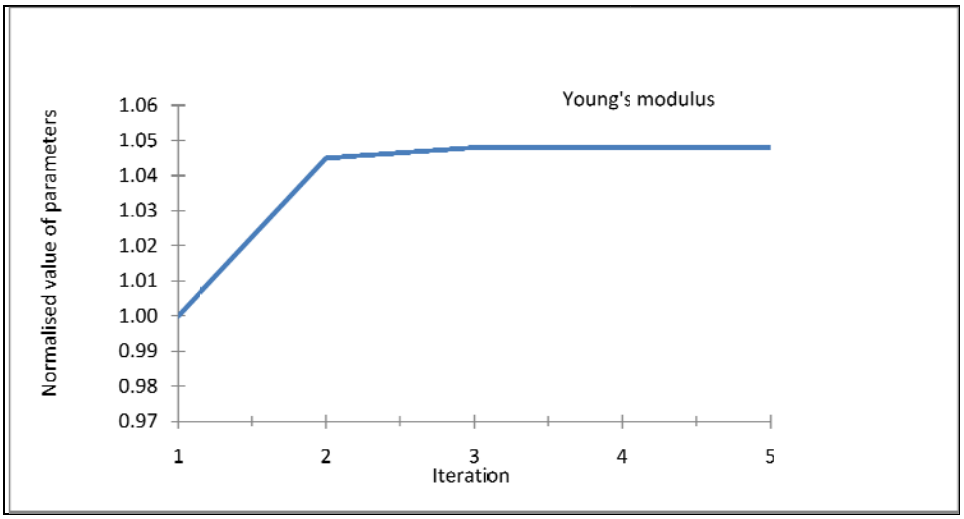

Figure 4.5: The convergence of the updating of main support B

Tables 4.8 up to Table 4.11 shows the comparison of the results of main support A and main support B calculated based on the different number of the measured frequencies defined in the objective function as shown in Equation (4.8). Column I and II represent for the experimental results and the results calculated from the initial finite element model. Meanwhile, column III gives the results calculated from the updated finite element model. These tables show that the larger the

numbers of measured frequencies used in the objective function, the better the results are obtained.

Table 4.8: The comparison of results calculated using different numbers of measured frequencies (1^{st} to 5^{th}) of main support A in the objective function multiply by 100

Mode	I	II	III				
	Exp (Hz)	Initial FE (Hz)	Number of the measured frequencies				
			1 (Hz)	2 (Hz)	3 (Hz)	4 (Hz)	5 (Hz)
1	41.59	41.42	41.59	42.01	42.04	42.03	42.13
2	136.53	133.26	133.77	135.08	135.19	135.15	135.45
3	155.24	152.78	153.35	154.83	154.95	154.91	155.25
4	161.10	159.04	159.65	161.20	161.33	161.28	161.65
5	179.10	174.52	175.19	176.93	177.08	177.02	177.43
6	213.67	207.63	208.38	210.31	210.48	210.41	210.86
7	226.75	221.67	222.54	224.79	224.98	224.91	225.44
8	251.68	244.86	245.76	248.07	248.27	248.19	248.73
9	255.75	252.60	253.48	255.74	255.93	255.85	256.39
10	263.62	258.87	259.79	262.16	262.36	262.27	262.83
Total Error		0.41687	0.29141	0.09277	0.08374	0.08723	0.06895

Table 4.9: The comparison of results calculated using different numbers of measured frequencies (6^{th} to 10^{th}) of main support A in the objective function multiply by 100

Mode	I	II	III				
	Exp (Hz)	Initial FE (Hz)	Number of the measured frequencies				
			6 (Hz)	7 (Hz)	8 (Hz)	9 (Hz)	10 (Hz)
1	41.59	41.42	42.22	42.24	42.29	42.26	42.26
2	136.53	133.26	135.73	135.81	135.95	135.87	135.87
3	155.24	152.78	155.57	155.65	155.82	155.73	155.72
4	161.10	159.04	161.98	162.06	162.24	162.15	162.14
5	179.10	174.52	177.80	177.89	178.09	177.98	177.98
6	213.67	207.63	211.27	211.38	211.60	211.48	211.48
7	226.75	221.67	225.92	226.05	226.31	226.16	226.16
8	251.68	244.86	249.23	249.35	249.62	249.47	249.47
9	255.75	252.60	256.87	256.99	257.25	257.11	257.11
10	263.62	258.87	263.34	263.47	263.74	263.58	263.59
Total Error		0.41687	0.06066	0.05954	0.05978	0.05928	0.05918

Table 4.10: The comparison of results calculated using different numbers of measured frequencies (1st to 5th) of main support B in the objective function multiply by 100

Mode	I	II	III				
	Exp (Hz)	Initial FE (Hz)	Number of the measured frequencies				
			1 (Hz)	2 (Hz)	3 (Hz)	4 (Hz)	5 (Hz)
1	41.58	41.42	41.58	41.83	41.85	41.83	41.93
2	135.34	133.26	133.74	134.55	134.59	134.51	134.84
3	154.41	152.78	153.32	154.23	154.28	154.19	154.56
4	160.22	159.04	159.61	160.57	160.63	160.52	160.92
5	178.40	174.52	175.15	176.22	176.29	176.18	176.62
6	213.66	207.63	208.34	209.53	209.60	209.47	209.97
7	226.31	221.67	222.49	223.87	223.96	223.82	224.39
8	249.50	244.86	245.71	247.13	247.23	247.07	247.66
9	255.14	252.60	253.43	254.82	254.91	254.76	255.34
10	262.90	258.87	259.74	261.19	261.29	261.13	261.73
Total Error		0.27878	0.29781	0.15168	0.14494	0.15694	0.11496

Table 4.11: The comparison of results calculated using different numbers of measured frequencies (6^{th} to 10^{th}) of main support B in the objective function multiply by 100

Mode	I	II	III				
	Exp (Hz)	Initial FE (Hz)	Number of the measured frequencies				
			6 (Hz)	7 (Hz)	8 (Hz)	9 (Hz)	10 (Hz)
1	41.58	41.42	42.05	42.08	42.11	42.09	42.09
2	135.34	133.26	135.21	135.32	135.39	135.33	135.33
3	154.41	152.78	154.98	155.11	155.18	155.11	155.12
4	160.22	159.04	161.36	161.49	161.57	161.49	161.51
5	178.40	174.52	177.11	177.26	177.34	177.26	177.27
6	213.66	207.63	210.51	210.67	210.77	210.68	210.70
7	226.31	221.67	225.02	225.22	225.33	225.21	225.24
8	249.50	244.86	248.31	248.51	248.62	248.51	248.53
9	255.14	252.60	255.97	256.16	256.28	256.17	256.19
10	262.90	258.87	262.39	262.60	262.72	262.60	262.63
Total Error		0.27878	0.08238	0.07490	0.07192	0.07528	0.07452

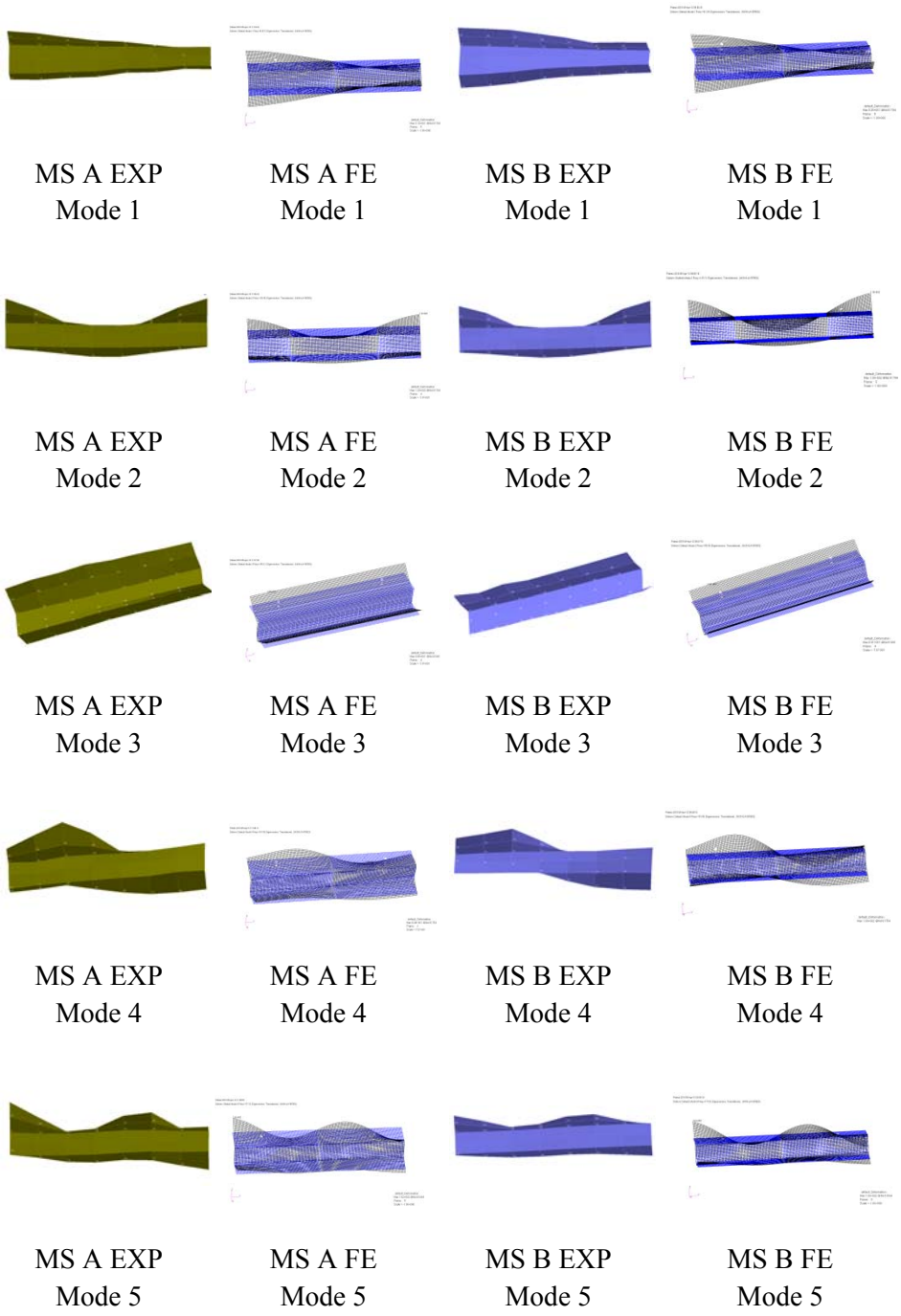

Figure 4.6: Comparison results of mode shapes (1st to 5th) between test and updated FE models of the main support A (MS A) and main support B (MS B).

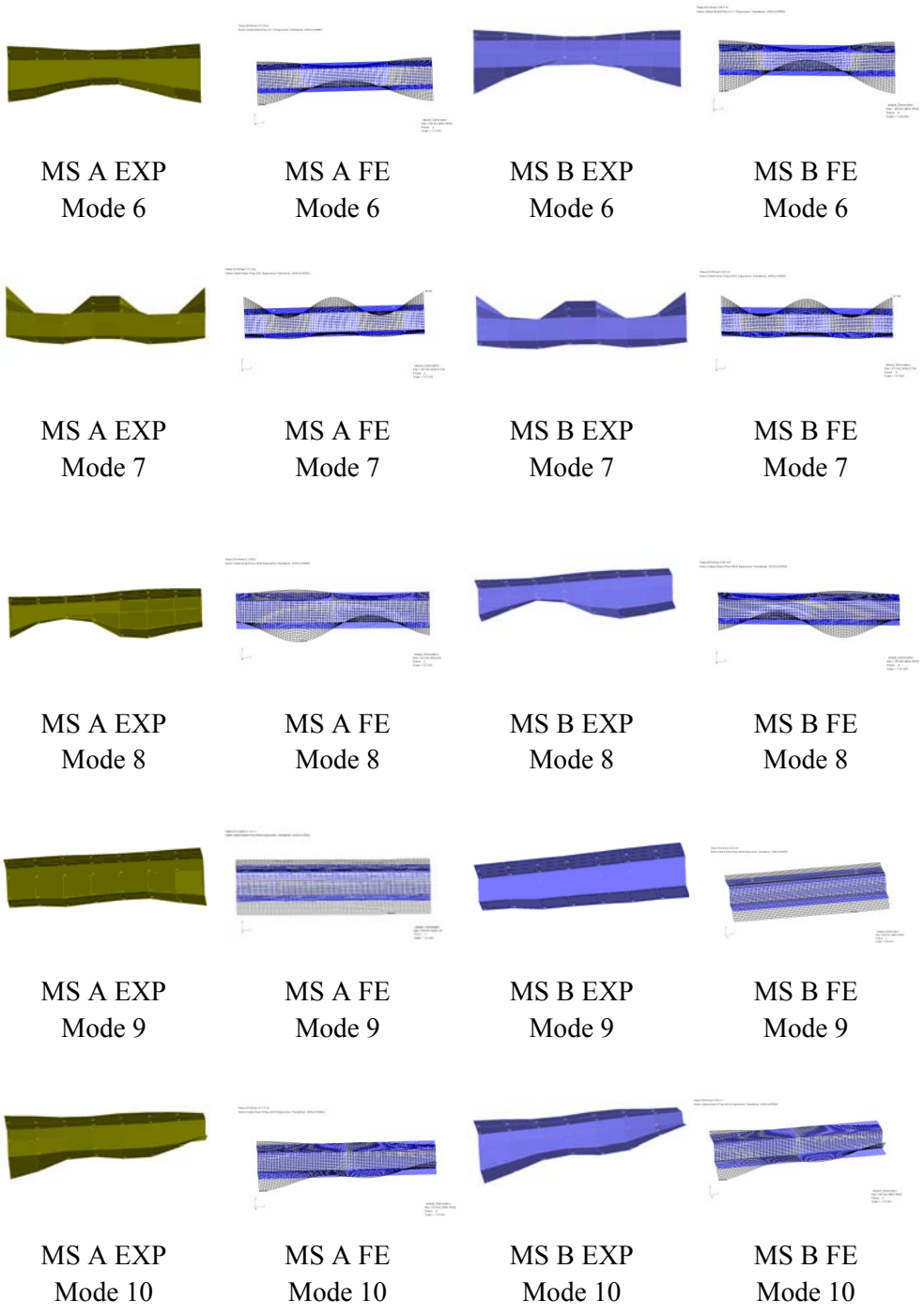

Figure 4.7: Comparison results of mode shapes (6^{th} to 10^{th}) between test and updated FE models of the main support A (MS A) and main support B (MS B).

4.8 Finite element modelling of the base bent support

The base bent support A and base bent support B are modelled by 3946 CQUAD4 elements (Figure 4.8) and the nominal values for the material properties of base bent support is shown in Table 3.1. The normal mode analysis of NASTRAN SOL103 is used to calculate the first ten natural frequencies and mode shapes of the initial finite element model of the components.

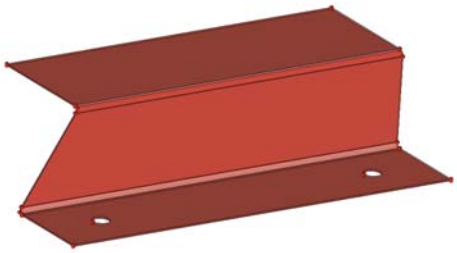

(a) CAD model

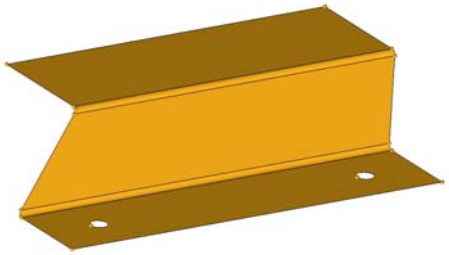

(b) Mid-surface model

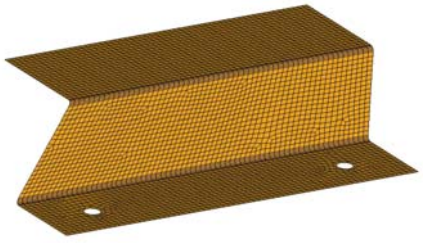

(c) CAE model

Figure 4.8: Visual model of base bent supports

The computed natural frequencies are compared with the experimental natural frequencies. The total of relative error for the base bent support A (Table 4.12) is 23.73 percent. Meanwhile the total relative error for base bent support B (Table

4.13) is 20.47 percent. The comparison between the initial finite element mode shapes and the updated mode shapes is made in Figure 4.11 and Figure 4.12.

Table 4.12: Comparison between measured and FE natural frequencies of base bent support A

Mode	I Experiment Frequency (Hz)	II Initial F.E Frequency (Hz)	III Relative Error [%] [I-II/I]	IV Initial FE MAC
1	93.85	90.87	3.17	0.87
2	151.97	151.05	0.60	0.90
3	197.90	194.83	1.55	0.97
4	253.71	246.90	2.68	0.94
5	264.85	259.98	1.84	0.96
6	274.83	267.74	2.58	0.93
7	308.92	303.42	1.78	0.98
8	450.24	442.27	1.77	0.93
9	461.93	453.35	1.86	0.66
10	695.83	654.87	5.89	0.75
Total error			23.73	

Table 4.13: Comparison between measured and FE natural frequencies of base bent support B

Mode	I Experiment Frequency (Hz)	II Initial F.E Frequency (Hz)	III Relative Error [%] [I-II/I]	IV Initial FE MAC
1	93.62	90.87	2.94	0.96
2	153.06	151.05	1.32	0.94
3	197.80	194.83	1.50	0.93
4	250.86	246.90	1.58	0.92
5	262.03	259.98	0.78	0.85
6	271.81	267.74	1.50	0.93
7	312.87	303.42	3.02	0.85
8	444.16	442.27	0.43	0.87
9	461.26	453.35	1.71	0.74
10	694.37	654.87	5.69	0.81
Total error			20.47	

The updating is performed on the basis of the first five measured frequencies by minimising the objective function (Eq. 4.8). The NASTRAN SOL200 is employed to identify the most sensitive parameters. The potential parameters such as the thickness, Young's modulus, shear modulus, density and Poisson's ratio have been studied in the sensitivity analysis. The sensitivities are given in Table 4.14.

Table 4.14: Summarised results of the sensitivity analysis with respects to the normalised parameters of base bent support A and base bent support B

Mode	Frequency	Parameters				
		Thickness	Young's Modulus	Shear Modulus	Poisson's Ratio	Density
1	9.24E+01	9.23E+01	4.61E+01	7.20E-02	-9.52E+00	-4.62E+01
2	1.54E+02	1.54E+02	7.68E+01	3.09E-02	1.34E+01	-7.68E+01
3	1.98E+02	1.98E+02	9.89E+01	1.44E-01	-1.19E+00	-9.91E+01
4	2.51E+02	2.51E+02	1.25E+02	1.57E-01	1.17E+01	-1.26E+02
5	2.64E+02	2.64E+02	1.32E+02	2.24E-01	4.14E+00	-1.32E+02

Table 4.14 shows the Young's modulus is most sensitive to the frequency after the thickness of the component. Therefore the Young's modulus is used as the updating parameter for both base bent support A and base bent support B. The updated natural frequencies of the finite element model of base main support A is compared with those of the experimental result in Table 4.15 (column V) together with MAC values. The error between the initial updated finite element model and experiment is reduced significantly from 23.73 percent to 9.01 percent.

Table 4.15: Three comparisons of results between the tested and finite element (FE) model of base bent support A

Mode	I Experimental base bent support A (Hz)	II Initial FE base bent support A (Hz)	III Error (%) [I-II/I]	IV Updated FE base bent support A (Hz)	V Error (%) [I-IV/I]	VI Updated FE MAC
1	93.85	90.87	3.17	92.69	1.23	0.91
2	151.97	151.05	0.60	154.07	1.38	0.95
3	197.90	194.83	1.55	198.73	0.42	0.97
4	253.71	246.90	2.68	251.83	0.74	0.95
5	264.85	259.98	1.84	265.18	0.12	0.98
6	274.83	267.74	2.58	273.09	0.63	0.94
7	308.92	303.42	1.78	309.47	0.18	0.99
8	450.24	442.27	1.77	451.10	0.19	0.96
9	461.93	453.35	1.86	462.40	0.10	0.82
10	695.83	654.87	5.89	667.95	4.01	0.90
Total error			23.73		9.01	

Table 4.16 shows the changes of the initial and updated value of the Young's modulus with the increment of 4.04 percent from the initial value. Meanwhile, Figure 4.9 shows the initial changes of the updating parameters from the initial normalised value to convergent value.

Table 4.16: Updated value of parameter of base bent support A

Parameters	Initial Value	Updated Value	Unit
Young's Modulus	210000	218484	MPa

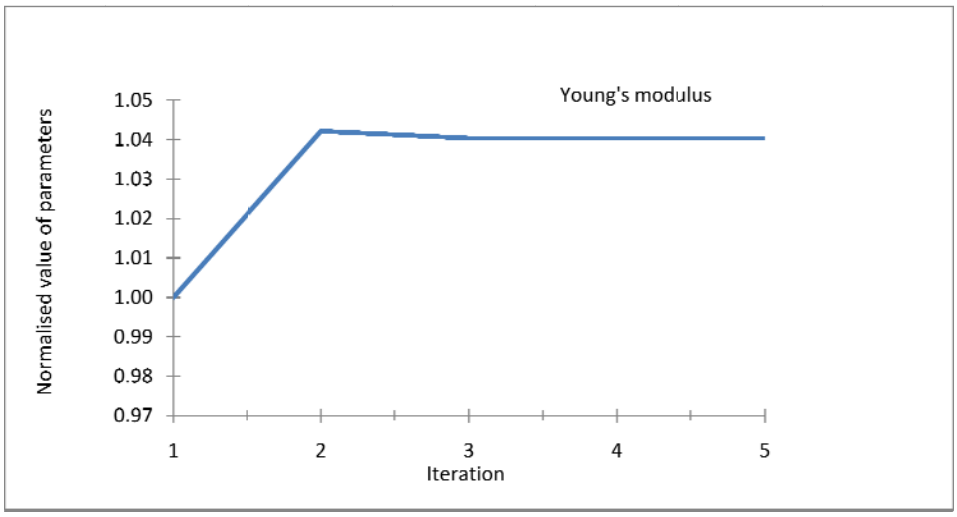

Figure 4.9: The convergence of the updating of base bent support A

Similar updating procedure is applied to the component base bent support B and Young's modulus is used as the updating parameter. Table 4.17 (column V) shows the reduction in the error which is from 20.47 percent to 10.96 percent and the MAC values are now above 0.8.

Table 4.17: Measured natural frequencies and finite element (FE) predictions in Hz for the base bent support B

Mode	I Experimental base bent support B (Hz)	II Initial FE base bent support B (Hz)	III Error (%) [I-II/I]	IV Updated base bent support B (Hz)	V Error (%) [I-IV/I]	VI Updated FE MAC
1	93.62	90.87	2.94	92.70	0.99	0.98
2	153.06	151.05	1.32	154.10	0.68	0.96
3	197.80	194.83	1.50	198.76	0.48	0.94
4	250.86	246.90	1.58	251.87	0.40	0.93
5	262.03	259.98	0.78	265.22	1.22	0.94
6	271.81	267.74	1.50	273.14	0.49	0.89
7	312.87	303.42	3.02	309.52	1.07	0.94
8	444.16	442.27	0.43	451.17	1.58	0.91
9	461.26	453.35	1.71	462.48	0.26	0.83
10	694.37	654.87	5.69	668.05	3.79	0.86
Total error			20.47		10.96	

Table 4.18 shows the changes of the initial and updated value of the Young's modulus with the increased of 4.08 percent from the initial value. Meanwhile, Figure 4.10 shows the initial changes of the updating parameters from the initial normalised value to convergent value.

Table 4.18: Updated value of parameter of base bent support B

Parameters	Initial Value	Updated Value	Unit
Young's Modulus	210000	218568	MPa

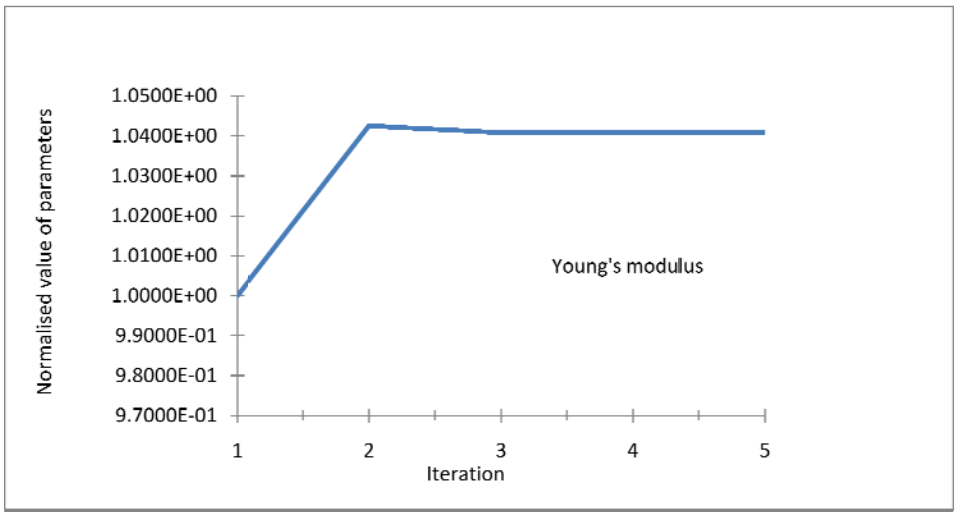

Figure 4.10: The convergence of the updating of base bent support B

Table 4.19 up to Table 4.22 show the results of base bent support A and base bent support B calculated based on the different numbers of the measured frequencies defined in the objective function as shown in Equation 4.8. Column I and II represent the experimental results and the results calculated from the initial finite element model. Meanwhile, column III gives the results calculated from the updated finite element model. Tables shown that the larger the numbers of measured frequencies used in the objective function, the better the results are obtained.

Table 4.19: The comparison of results calculated using different numbers of measured frequencies (1st to 5th) of base bent support A in the objective function multiply by 100

Mode	I	II	III				
	Exp (Hz)	Initial FE (Hz)	Number of the measured frequencies				
			1 (Hz)	2 (Hz)	3 (Hz)	4 (Hz)	5 (Hz)
1	93.85	90.87	93.03	92.61	92.51	92.72	92.69
2	151.97	151.05	154.64	153.93	153.76	154.13	154.08
3	197.90	194.83	199.45	198.54	198.33	198.79	198.73
4	253.71	246.90	252.75	251.60	251.32	251.91	251.83
5	264.85	259.98	266.14	264.93	264.64	265.26	265.10
6	274.83	267.74	274.08	272.84	272.54	273.18	273.09
7	308.92	303.42	310.59	309.18	308.84	309.56	309.47
8	450.24	442.27	452.74	450.68	450.19	451.12	451.10
9	461.93	453.35	464.07	461.97	461.47	462.55	462.40
10	695.83	654.87	670.36	667.32	666.60	668.15	667.94
Total Error		0.74487	0.19130	0.21531	0.22713	0.20480	0.20730

Table 4.20: The comparison of results calculated using different numbers of measured frequencies (6^{th} to 10^{th}) of base bent support A in the objective function multiply by 100

Mode	I	II	III				
	Exp (Hz)	Initial FE (Hz)	Number of the measured frequencies				
			6 (Hz)	7 (Hz)	8 (Hz)	9 (Hz)	10 (Hz)
1	93.85	90.87	92.79	92.75	92.72	92.71	93.02
2	151.97	151.05	154.23	154.17	154.13	154.10	154.63
3	197.90	194.83	198.94	198.86	198.79	198.87	199.45
4	253.71	246.90	252.10	251.99	251.92	251.87	252.74
5	264.85	259.98	265.45	265.34	265.26	265.22	266.14
6	274.83	267.74	273.38	273.27	273.18	273.14	274.08
7	308.92	303.42	309.79	309.67	309.57	309.52	310.59
8	450.24	442.27	451.57	451.39	451.25	451.17	452.73
9	461.93	453.35	462.88	462.70	462.55	462.48	464.07
10	695.83	654.87	668.60	668.37	668.16	668.05	670.36
Total Error		0.74487	0.20016	0.20243	0.20476	0.20633	0.19126

Table 4.21: The comparison of results calculated using different numbers of measured frequencies (1^{st} to 5^{th}) of base bent support B in the objective function multiply by 100

Mode	I	II	III				
	Exp (Hz)	Initial FE (Hz)	Number of the measured frequencies				
			1 (Hz)	2 (Hz)	3 (Hz)	4 (Hz)	5 (Hz)
1	93.62	90.87	93.02	92.84	92.64	92.56	92.36
2	153.06	151.05	154.63	154.31	153.99	153.86	153.53
3	197.80	194.83	199.45	199.03	198.62	198.46	198.03
4	250.86	246.90	252.74	252.22	251.69	251.49	250.95
5	262.03	259.98	266.14	265.58	265.03	264.81	264.24
6	271.81	267.74	274.08	273.52	272.94	272.72	272.14
7	312.87	303.42	310.59	309.95	309.30	309.04	308.38
8	444.16	442.27	452.73	451.79	450.86	450.48	449.52
9	461.26	453.35	464.07	463.11	462.15	461.76	460.78
10	694.37	654.87	670.36	668.97	667.58	667.02	665.60
Total Error		0.62581	0.22455	0.21635	0.21730	0.22018	0.23344

Table 4.22: The comparison of results calculated using different numbers of measured frequencies (6^{th} to 10^{th}) of base bent support B in the objective function multiply by 100

Mode	I	II	III				
	Exp (Hz)	Initial FE (Hz)	Number of the measured frequencies				
			6 (Hz)	7 (Hz)	8 (Hz)	9 (Hz)	10 (Hz)
1	93.62	90.87	92.35	92.53	92.37	92.38	92.75
2	153.06	151.05	153.51	153.82	153.55	153.56	154.18
3	197.80	194.83	197.99	198.39	198.05	198.07	198.86
4	250.86	246.90	250.90	251.41	250.97	250.99	251.99
5	262.03	259.98	264.19	264.73	264.27	264.30	265.35
6	271.81	267.74	272.09	272.64	272.16	272.19	273.27
7	312.87	303.42	308.33	308.95	308.41	308.44	309.67
8	444.16	442.27	449.43	450.34	449.56	449.60	451.39
9	461.26	453.35	460.69	461.63	460.82	460.87	462.70
10	694.37	654.87	665.47	666.82	665.67	665.73	668.38
Total Error		0.62581	0.23481	0.22150	0.23262	0.23180	0.21585

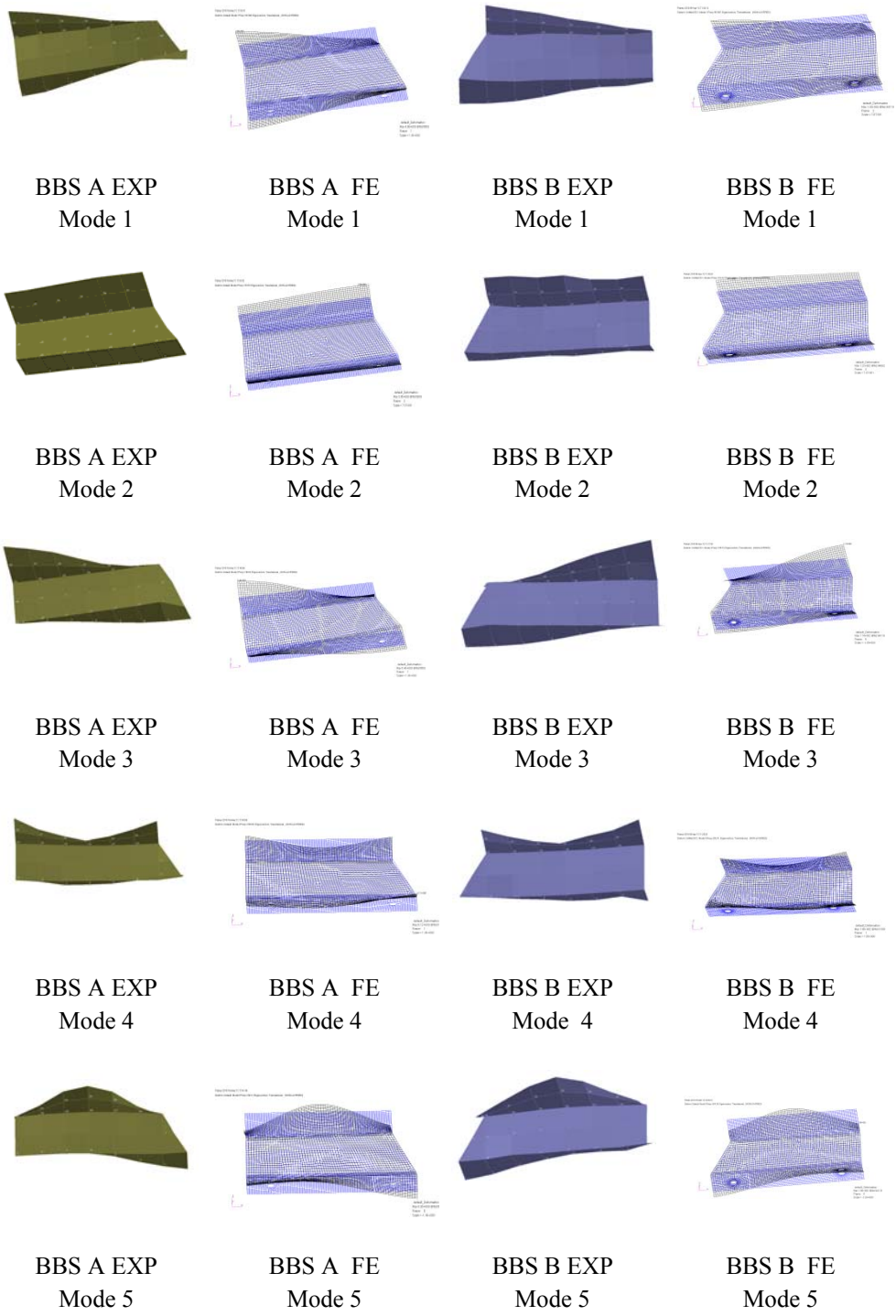

Figure 4.11: Comparison results of mode shapes (1st to 5th) between test and updated FE models of the base bent support A (BBS A) and base bent support B (BBS B).

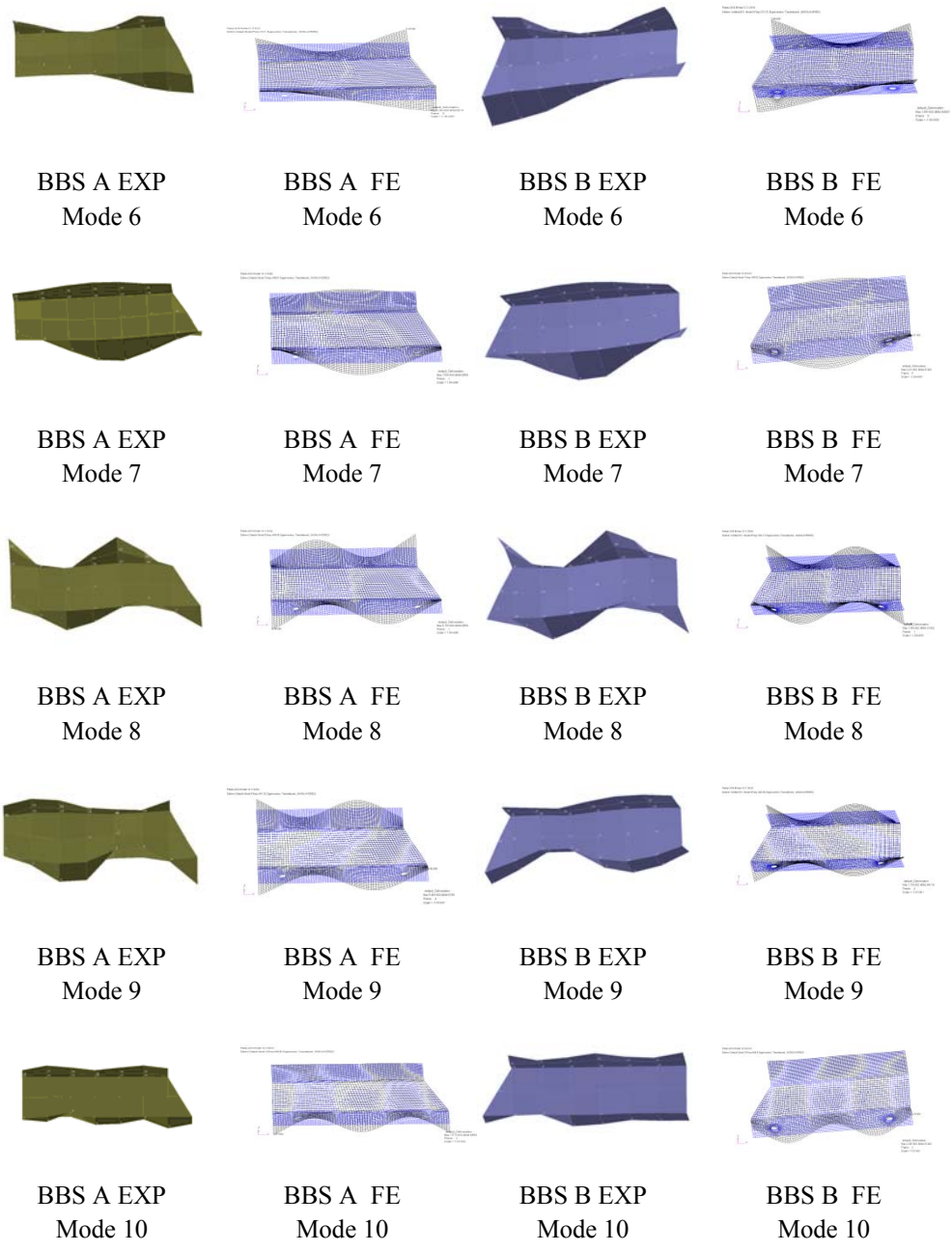

Figure 4.12: Comparison results of mode shapes (6^{th} to 10^{th}) between test and updated FE models of the base bent support A (BBS A) and base bent support B (BBS B).

4.9 Finite element modelling of the brackets

The finite element models of brackets are developed using 779 of CQUAD4 elements and they are shown in Figure 4.13. Meanwhile, the nominal values of the material properties of the brackets are shown in Table 3.1. There are four finite element models used in this work, namely bracket 1A (B 1A), bracket 1B (B 1B), bracket 2A (B 2A) and bracket 2B (B 2B).

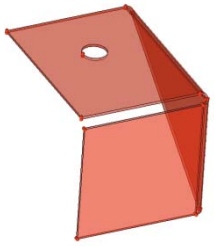

(a) CAD model

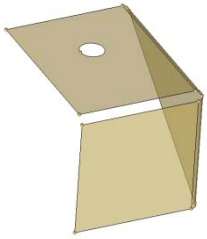

(b) Mid-surface model

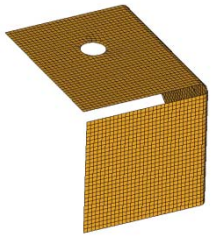

(c) CAE model

Figure 4.13: Visual model of brackets

Table 4.23 to Table 4.26 shows a series of the comparison results of the first three frequencies from the test and the initial finite element models of the brackets. The lowest of total relative error is 4.85 percent (Table 4.26). Meanwhile, comparison

between the initial finite element mode shapes and the updated mode shapes is shown in Figure 4.18 and Figure 4.19.

Table 4.23: Comparison between measured and FE natural frequencies of bracket 1A

Mode	I Experiment Frequency (Hz)	II Initial F.E Frequency (Hz)	III Relative Error [%] [I-II/I]	IV Initial FE MAC
1	172.14	165.71	3.73	0.93
2	273.38	268.69	1.71	0.83
3	501.76	494.08	1.53	0.79
	Total Error		6.98	

Table 4.24: Comparison between measured and FE natural frequencies of bracket 1B

Mode	I Experiment Frequency (Hz)	II Initial F.E Frequency (Hz)	III Relative Error [%] [I-II/I]	IV Initial FE MAC
1	171.55	165.71	3.40	0.82
2	271.57	268.69	1.06	0.88
3	497.71	494.08	0.73	0.86
	Total Error		5.19	

Table 4.25: Comparison between measured and FE natural frequencies of bracket 2A

Mode	I Experiment Frequency (Hz)	II Initial F.E Frequency (Hz)	III Relative Error [%] [I-II/I]	IV Initial FE MAC
1	171.01	165.71	3.10	0.90
2	274.37	268.69	2.07	0.76
3	492.73	494.08	0.27	0.88
	Total Error		5.44	

Table 4.26: Comparison between measured and FE natural frequencies of bracket 2B

Mode	I Experiment Frequency (Hz)	II Initial F.E Frequency (Hz)	III Relative Error [%] [I-II/I]	IV Initial FE MAC
1	171.31	165.71	3.27	0.91
2	271.16	268.69	0.91	0.81
3	497.42	494.08	0.67	0.92
	Total Error		4.85	

The updating is performed on the basis of the first two measured frequencies by minimising the objective function (Eq. 4.8). NASTRAN SOL 200 is employed to identify the most sensitive parameters of all brackets. The potential parameters such as the thickness, the Young's modulus, the shear modulus, density and Poisson's ratio have been considered in the sensitivity analysis. The results of the sensitivity analysis are tabulated in Table 4.27 in which the Young's modulus is the second most sensitive to the frequency after the thickness and followed by the

density. Therefore, the Young's modulus is used as the updating parameter for brackets, since the thickness of the plate is already manually corrected.

Table 4.27: Summarised results of the sensitivity analysis with respects to the normalised parameters of brackets

Mode	Frequency	Parameters				
		Thickness	Young's Modulus	Shear Modulus	Poisson's Ratio	Density
1	1.69E+02	1.18E+02	6.75E+01	1.71E+01	4.05E-01	-8.52E+01
2	2.73E+02	1.86E+02	1.06E+02	3.03E+01	1.11E+01	-1.33E+02
3	5.02E+02	4.35E+02	2.28E+02	2.35E+01	-3.61E+01	-2.52E+02

The updated natural frequencies and MAC values of the updated finite element model of bracket 1A are compared with the experimental results. Table 4.28 (column V) shows the reduction in the error which is from 6.98 percent to 2.58 percent. Meanwhile, the MAC values calculated from the updated model are above 0.8. Table 4.29 shows the changes of the initial and updated values of the Young's modulus of bracket 1A with the increment of 4.80 percent from the initial value. The initial changes of the updating parameters from the initial normalised value to convergent value can be seen in Figure 4.14.

Table 4.28: Three comparisons of results between the tested and finite element (FE) model of bracket 1A

Mode	I Experimental bracket 1A (Hz)	II Initial FE bracket 1A (Hz)	III Error (%) [I-II/I]	IV Updated FE bracket 1A (Hz)	V Error (%) [I-IV/I]	VI Updated FE MAC
1	172.14	165.71	3.73	168.85	1.91	0.95
2	273.38	268.69	1.71	273.64	0.10	0.85
3	501.76	494.08	1.53	504.65	0.58	0.92
	Total Error		6.98		2.58	

Table 4.29: Updated value of parameter of bracket 1A

Parameters	Initial Value	Updated Value	Unit
Young's Modulus	210000	220080	MPa

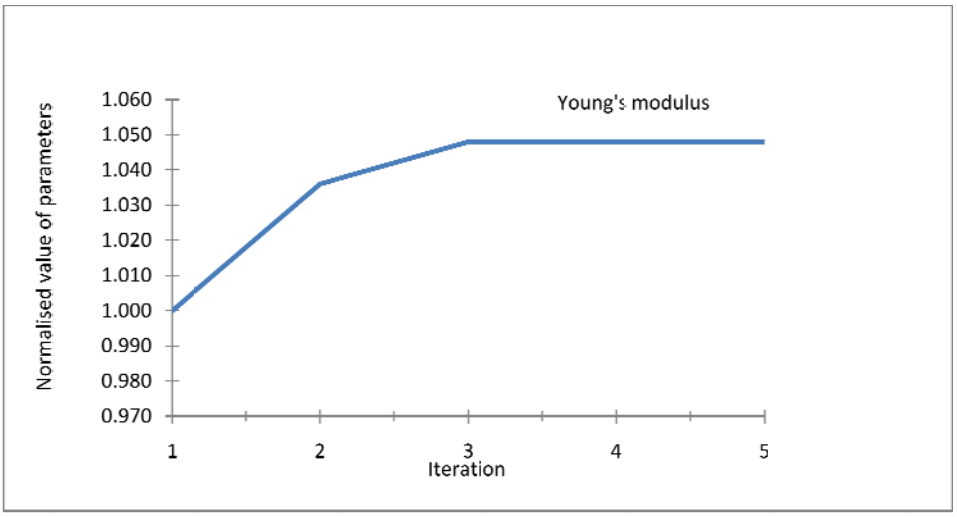

Figure 4.14: The convergence of the updating of bracket 1A

Model updating is applied to bracket 1B. It can be seen from Table 4.30 Column V), the error of updated natural frequencies is reduced from 4.19 percent to 3.45 percent with the MAC values of the updated finite element model are above 0.80.

Table 4.30: Three comparisons of results between the tested and finite element (FE) model of bracket 1B

Mode	I Experimental bracket 1B (Hz)	II Initial FE bracket 1B (Hz)	III Error (%) [I-II/I]	IV Updated FE bracket 1B (Hz)	V Error (%) [I-IV/I]	VI Updated FE MAC
1	171.55	165.71	3.40	168.43	1.82	0.93
2	271.57	268.69	1.06	272.98	0.52	0.90
3	497.71	494.08	0.73	503.26	1.12	0.89
Total Error			5.19		3.45	

Table 4.31 shows the changes of the initial and updated values of the Young's modulus of bracket 1B with the increment of 4.18 percent from the initial value. Meanwhile, the initial changes of the updating parameter from the initial normalised value to convergent value are shown in Figure 4.15.

Table 4.31: Updated value of parameter of bracket 1B

Parameters	Initial Value	Updated Value	Unit
Young's Modulus	210000	218778	MPa

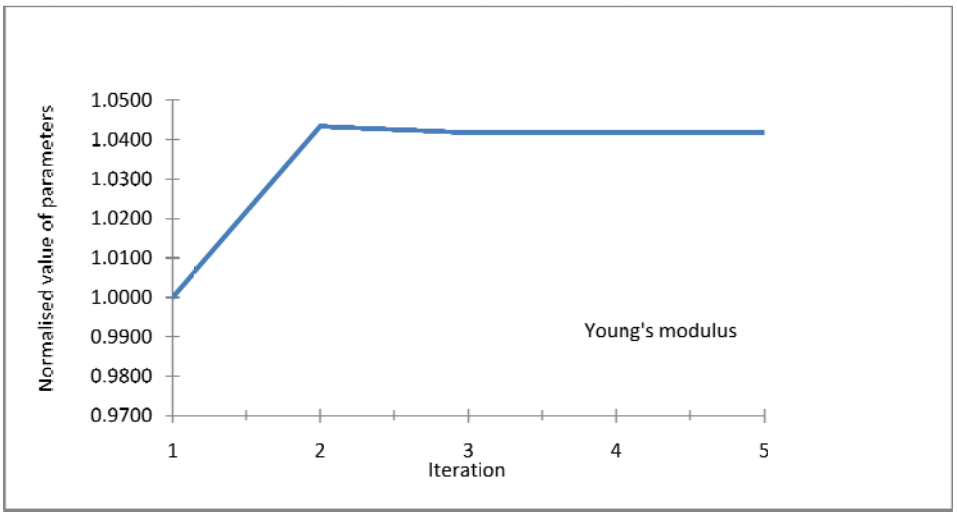

Figure 4.15: The convergence of the updating of bracket 1B

Table 4.32 (Column V) shows the updated result of the finite element model of bracket 2A. The error of bracket 2A is reduced from 4.44 percent to 3.87 percent with MAC values above 0.8. Meanwhile, Table 4.33 shows the changes of the initial and updated values of the Young's modulus of bracket 2A with the increment of 3.77 percent from the initial value. The initial changes of the updating parameters from the initial normalised value to convergent value can be seen in Figure 4.16.

Table 4.32: Three comparisons of results between the tested and finite element (FE) model of bracket 2A

Mode	I Experimental bracket 2A (Hz)	II Initial FE bracket 2A (Hz)	III Error (%) [I-II/I]	IV Updated FE bracket 2A (Hz)	V Error (%) [I-IV/I]	VI Updated FE MAC
1	171.01	165.71	3.10	168.85	1.26	0.93
2	274.37	268.69	2.07	272.58	0.65	0.82
3	492.73	494.08	0.27	502.39	1.96	0.92
	Total Error		5.44		3.87	

Table 4.33: Updated value of parameter of bracket 2A

Parameters	Initial Value	Updated Value	Unit
Young's Modulus	210000	217917	MPa

Figure 4.16: The convergence of the updating of bracket 2A

Table 4.34 (Column V) shows the updated result of the finite element model of bracket 2B. The error of bracket 2B is reduced from 4.85 percent to 3.21 percent. Meanwhile, the MAC values calculated from the updated model are above 0.8. Table 4.35 shows the changes of the initial and updated values of the Young's modulus of bracket 2B with the increment of 3.8 percent from the initial value. The initial changes of the updating parameters from the initial normalised value to convergent value can be seen in Figure 4.17.

Table 4.34: Three comparisons of results between the tested and finite element (FE) model of bracket 2B

Mode	I Experimental bracket 2B (Hz)	II Initial FE bracket 2B (Hz)	III Error (%) [I-II/I]	IV Updated FE bracket 2B (Hz)	V Error (%) [I-IV/I]	VI Updated FE MAC
1	171.31	165.71	3.27	168.44	1.67	0.93
2	271.16	268.69	0.91	273.07	0.70	0.84
3	497.42	494.08	0.67	501.56	0.83	0.91
	Total Error		4.85		3.21	

Table 4.35: Updated value of parameter of bracket 2B

Parameters	Initial Value	Updated Value	Unit
Young's Modulus	210000	217980	MPa

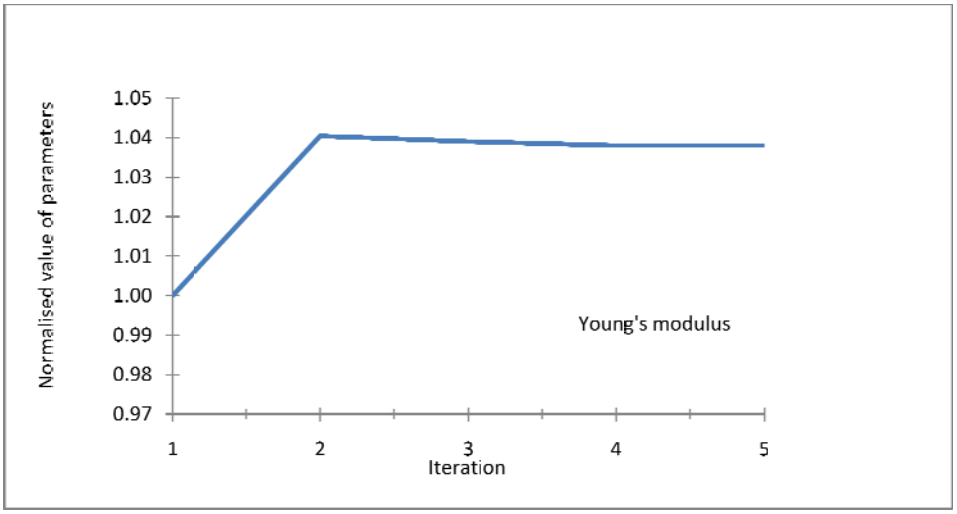

Figure 4.17: The convergence of the updating of bracket 2B

Table 4.36 and Table 4.37 shows the results of bracket 1A and bracket 1B calculated based on the different numbers of the measured frequencies defined in the objective function as shown in Equation 4.8, since the Young's modulus is used as the updating parameter for all brackets. Column I and II represent for the experimental results and the results calculated from the initial finite element model. Meanwhile, columns III is the results calculated from the updated finite element model. Tables shown that the larger the numbers of measured frequencies used in the objective function, the better the results are obtained.

Table 4.36: The comparison of results calculated using different numbers of measured frequencies of bracket 1A in objective function (1^{st} to 3^{th}) multiply by 100

Mode	I	II	III		
	Exp (Hz)	Initial FE (Hz)	Number of the measured frequencies		
			1	2	3
1	172.14	165.71	168.84	168.84	168.84
2	273.38	268.69	273.63	273.64	273.63
3	501.76	494.08	504.66	504.55	504.65
Total Error		0.19	0.0401	0.0398	0.0400

Table 4.37: The comparison of results calculated using different numbers of measured frequencies of bracket 1B in objective function (1^{st} to 3^{th}) multiply by 100

Mode	I	II	III		
	Exp (Hz)	Initial FE (Hz)	Number of the measured frequencies		
			1	2	3
1	171.55	165.71	168.84	168.85	168.43
2	271.57	268.69	273.64	273.64	272.98
3	497.71	494.08	504.65	504.65	503.26
Total Error		0.13	0.0502	0.0500	0.0482

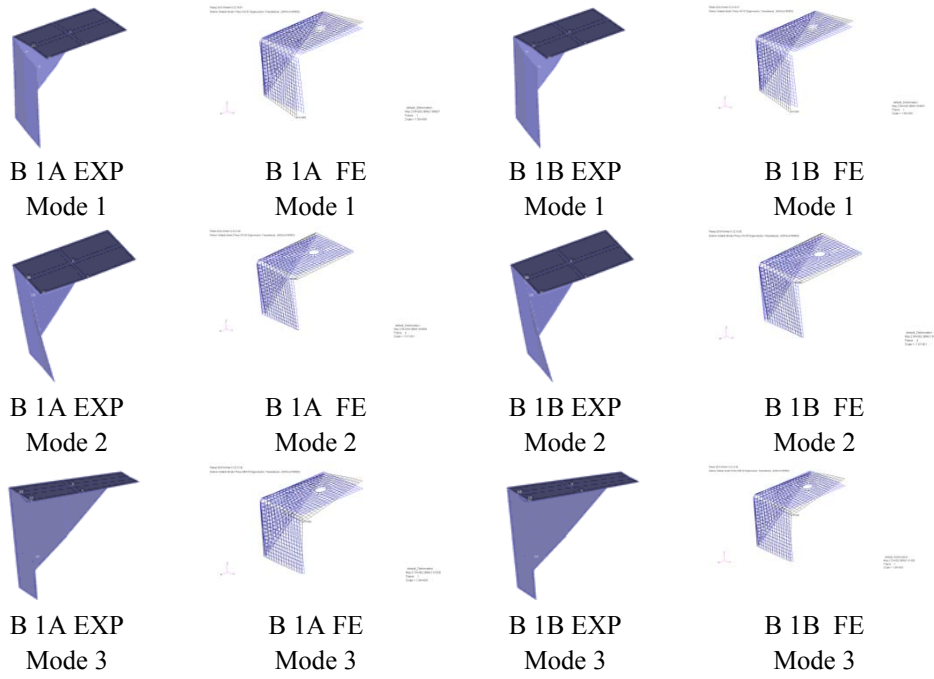

Figure 4.18: Comparison results of mode shapes (1st, 2nd and 3rd) between test and updated FE models of the bracket 1A (B 1A) and bracket 1B (B 1B).

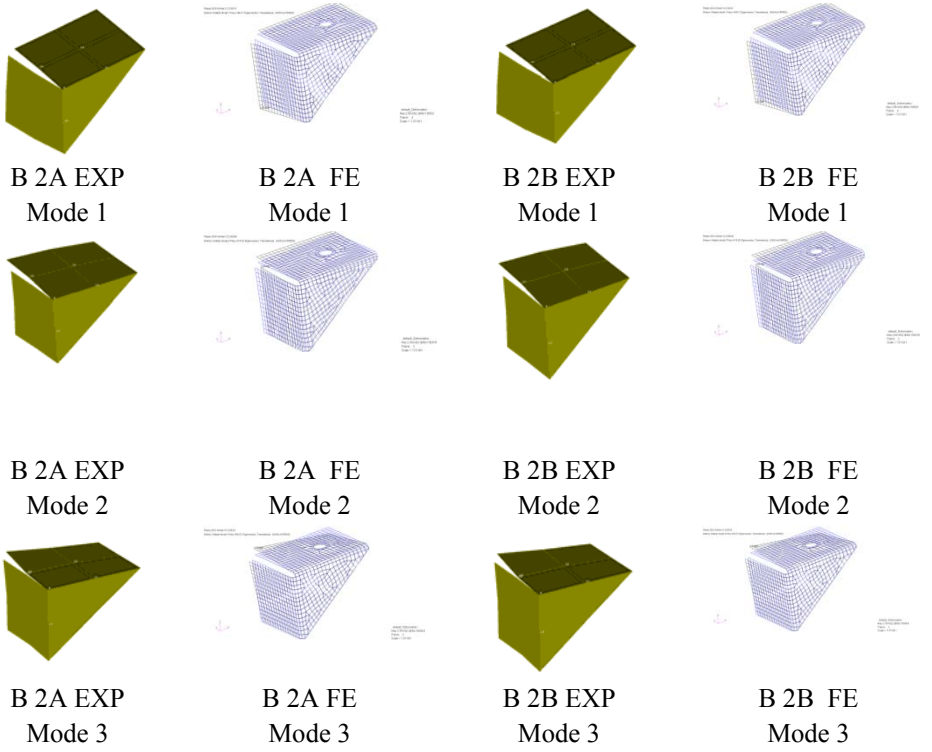

Figure 4.19: Comparison results of mode shapes (1st, 2nd and 3rd) between test and updated FE models of the bracket 2A (B 2A) and bracket 2B (B 2B).

4.10 Finite element modelling of the side supports

The side support A (SS A) and side support B (SS B) are modelled by 1320 CQUAD4 elements. The development of the finite element model of the side supports are shown in Figure 4.20. The nominal values for the material properties of the side supports are shown in Table 3.1. The normal mode analysis of NASTRAN SOL103 is used to calculate the first six natural frequencies and mode shapes of the initial finite element model of the components.

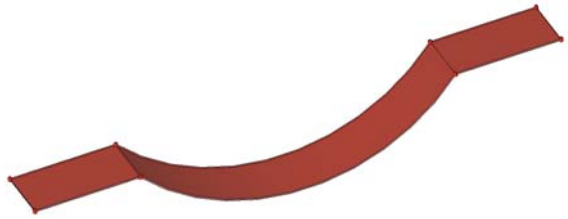

(a) CAD model

(b) Mid-surface model

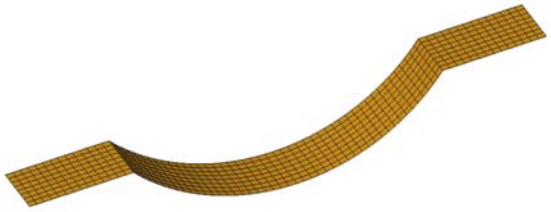

(c) CAE model

Figure 4.20: Visual model of side supports

The computed and experimental natural frequencies are compared as shown in Table 4.38 and Table 4.39. The total of the relative error for the side support A is 13.11 percent. Meanwhile the total relative error for base side support B is 17.03 percent.

Table 4.38: Comparison between measured and FE natural frequencies of side support A

Mode	I Experiment Frequency (Hz)	II Initial F.E Frequency (Hz)	III Relative Error [%] [I-II/I]	IV Initial FE MAC
1	32.66	32.70	0.11	0.86
2	91.73	93.36	1.78	0.92
3	150.24	153.94	2.46	0.79
4	153.24	155.48	1.46	0.71
5	161.89	166.43	2.80	0.88
6	250.63	261.88	4.49	0.76
Total Error			13.11	

Table 4.39: Comparison between measured and FE natural frequencies of side support B

Mode	I Experiment Frequency (Hz)	II Initial F.E Frequency (Hz)	III Relative Error [%] [I-II/I]	IV Initial FE MAC
1	32.66	32.69	0.08	0.91
2	92.10	93.36	1.36	0.84
3	146.62	153.94	4.99	0.83
4	149.55	155.48	3.96	0.78
5	162.24	166.43	2.59	0.92
6	251.72	261.88	4.04	0.85
Total error			17.03	

The updating is performed on the basis of the first five measured frequencies by minimising the objective function (Eq. 4.8). NASTRAN SOL200 is employed to identify the most sensitive parameters. The potential parameters such as the thickness, Young's modulus, shear modulus, density and Poisson's ratio have been listed in the sensitivity analysis. The sensitivities are given in Table 4.40. Meanwhile, Figure 4.23 shows the comparison between the initial finite element mode shapes and the updated mode shapes.

Table 4.40: Summarised results of the sensitivity analysis with respects to the normalised parameters of side support A and side support B

Mode	Frequency	Parameters				
		Thickness	Young's Modulus	Shear Modulus	Poisson's Ratio	Density
1	32.69	8.73E+00	7.39E+00	1.44E-03	9.67E-01	-1.66E+01
2	93.36	8.20E+01	4.19E+01	1.18E-02	5.83E-01	-4.75E+01
3	153.94	1.12E+02	6.16E+01	4.34E-02	1.76E+00	-7.83E+01
4	155.48	6.63E+01	4.80E+01	2.98E-01	-6.97E+00	-7.91E+01
5	166.43	1.44E+02	7.58E+01	5.19E-01	-1.52E+00	-8.46E+01

The Young's modulus is used as the updating parameter for both main side support A and side support B based sensitivity analysis shown in Table 4.40. The updated natural frequencies and MAC values of the updated finite element model of side support A are compared with the experimental results. Table 4.41 (column V) shows the reduction in the error which is from 13.11 percent to 5.0 percent. Meanwhile, the MAC values calculated from the updated model are above 0.8.

Table 4.41: Three comparisons of results between the tested and finite element (FE) model of side support A

Mode	I Experimental side support A (Hz)	II Initial FE side support A (Hz)	III Error (%) [I-II/I]	IV Updated FE side support A (Hz)	V Error (%) [I-IV/I]	VI Updated FE MAC
1	32.66	32.70	0.11	32.33	1.02	0.89
2	91.73	93.36	1.78	91.33	0.43	0.94
3	150.24	153.94	2.46	150.97	0.49	0.81
4	153.24	155.48	1.46	153.13	0.07	0.86
5	161.89	166.43	2.80	162.77	0.54	0.94
6	250.63	261.88	4.49	256.77	2.45	0.84
	Total Error		13.11		5.00	

Table 4.42 shows the changes of the initial and updated value of the Young's modulus with the reduction of 4.76 percent from the initial value. The initial changes of the updating parameters from the initial normalised value to convergent value can be seen in Figure 4.21.

Table 4.42: Updated value of parameter of side support A

Parameters	Initial Value	Updated Value	Unit
Young's Modulus	210000	199849	MPa

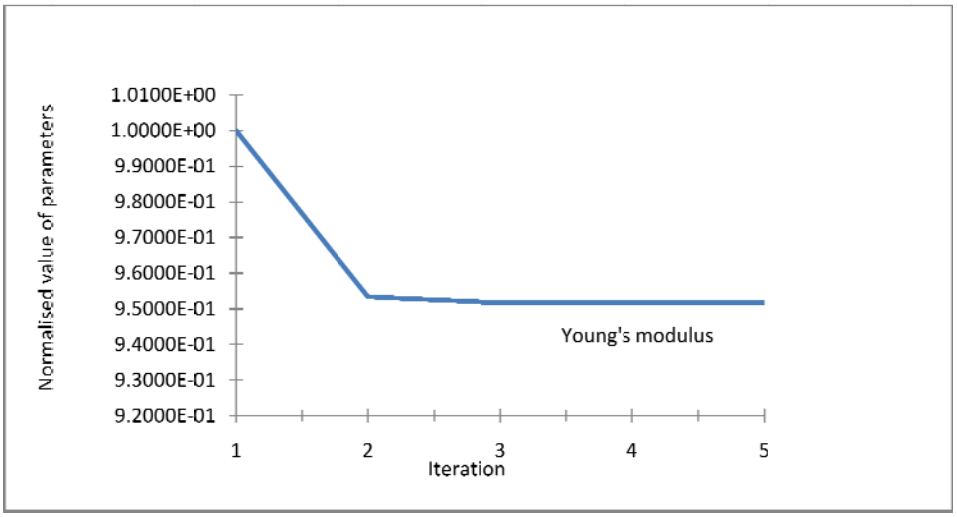

Figure 4.21: The convergence of the updating of side support A

The updating procedure is applied to the component side support B and Young's modulus is used as updating parameter. Table 4.43 (column V) shows the reduction in the error which is from 17.03 percent to 8.84 percent. Meanwhile, the MAC values calculated from the updated model are above 0.8.

Table 4.43: Measured natural frequencies and finite element (FE) predictions in Hz for the side support B

Mode	I Experimental side support B (Hz)	II Initial FE side support B (Hz)	III Error (%) [I-II/I]	IV Updated FE side support B (Hz)	V Error (%) [I-IV/I]	VI Updated FE MAC
1	32.66	32.69	0.08	32.18	1.48	0.92
2	92.10	93.36	1.36	90.47	1.77	0.87
3	146.62	153.94	4.99	149.71	2.11	0.90
4	149.55	155.48	3.96	152.12	1.72	0.83
5	162.24	166.43	2.59	161.23	0.62	0.90
6	251.72	261.88	4.04	254.59	1.14	0.89
	Total error		17.03		8.84	

Table 4.44 shows the changes of the initial and updated value of the Young's modulus with the decrement of 4.83 percent from the initial value. Meanwhile, Figure 4.22 shows the initial changes of the updating parameters from the initial normalised value to convergent value.

Table 4.44: Updated value of parameter of side support B

Parameters	Initial Value	Updated Value	Unit
Young's Modulus	210000	195626	MPa

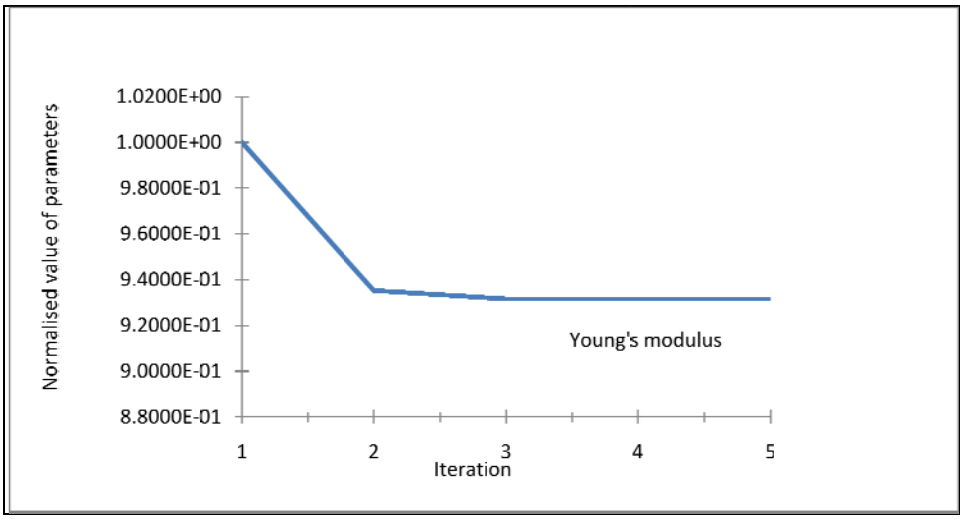

Figure 4.22: The convergence of the updating of side support B

Table 4.45 up to Table 4.46 shows the results of side support A and side support B calculated based on the different number of the measured frequencies defined in the objective function as shown in Equation 4.8. Column I and II represent for the experimental results and the results calculated from the initial finite element model. Meanwhile, columns III is the results calculated from the updated finite element model. Tables shown that the larger the numbers of measured frequencies used in the objective function, the better the results are obtained.

Table 4.45: The comparison of results calculated using different numbers of measured frequencies of side support A (1st to 6th) in the objective function multiply by 100

Mode	I	II	III					
	Exp (Hz)	Initial FE (Hz)	Number of the measured frequencies					
			1	2	3	4	5	6
1	32.66	32.70	32.66	32.45	32.37	32.37	32.33	32.25
2	91.73	93.36	93.14	92.01	91.55	91.53	91.33	90.86
3	150.24	153.94	153.63	151.97	151.30	151.26	150.97	150.29
4	153.24	155.48	155.23	153.93	153.39	153.36	153.13	152.58
5	161.89	166.43	166.05	164.01	163.18	163.13	162.78	161.94
6	250.63	261.88	261.36	258.51	257.35	257.28	256.78	255.60
Total Error		0.3939	0.3408	0.1364	0.0917	0.0894	0.0779	0.0661

Table 4.46: The comparison of results calculated using different numbers of measured frequencies of side support B (1st to 6th) in the objective function multiply by 100

- Mode	I	II	III					
	Exp (Hz)	Initial FE (Hz)	Number of the measured frequencies					
			1	2	3	4	5	6
1	32.663	32.69	32.66	32.51	32.22	32.13	32.17	32.13
2	92.104	93.36	93.15	92.31	90.73	90.24	90.47	90.25
3	146.618	153.94	153.63	152.41	150.01	149.39	149.71	149.39
4	149.552	155.48	155.23	154.28	152.43	151.85	152.11	151.85
5	162.235	166.43	166.05	164.54	161.7	160.83	161.23	160.83
6	251.719	261.88	261.36	259.26	255.27	254.02	254.59	254.04
Total Error		0.65498	0.58776	0.36863	0.15219	0.14280	0.14483	0.14251

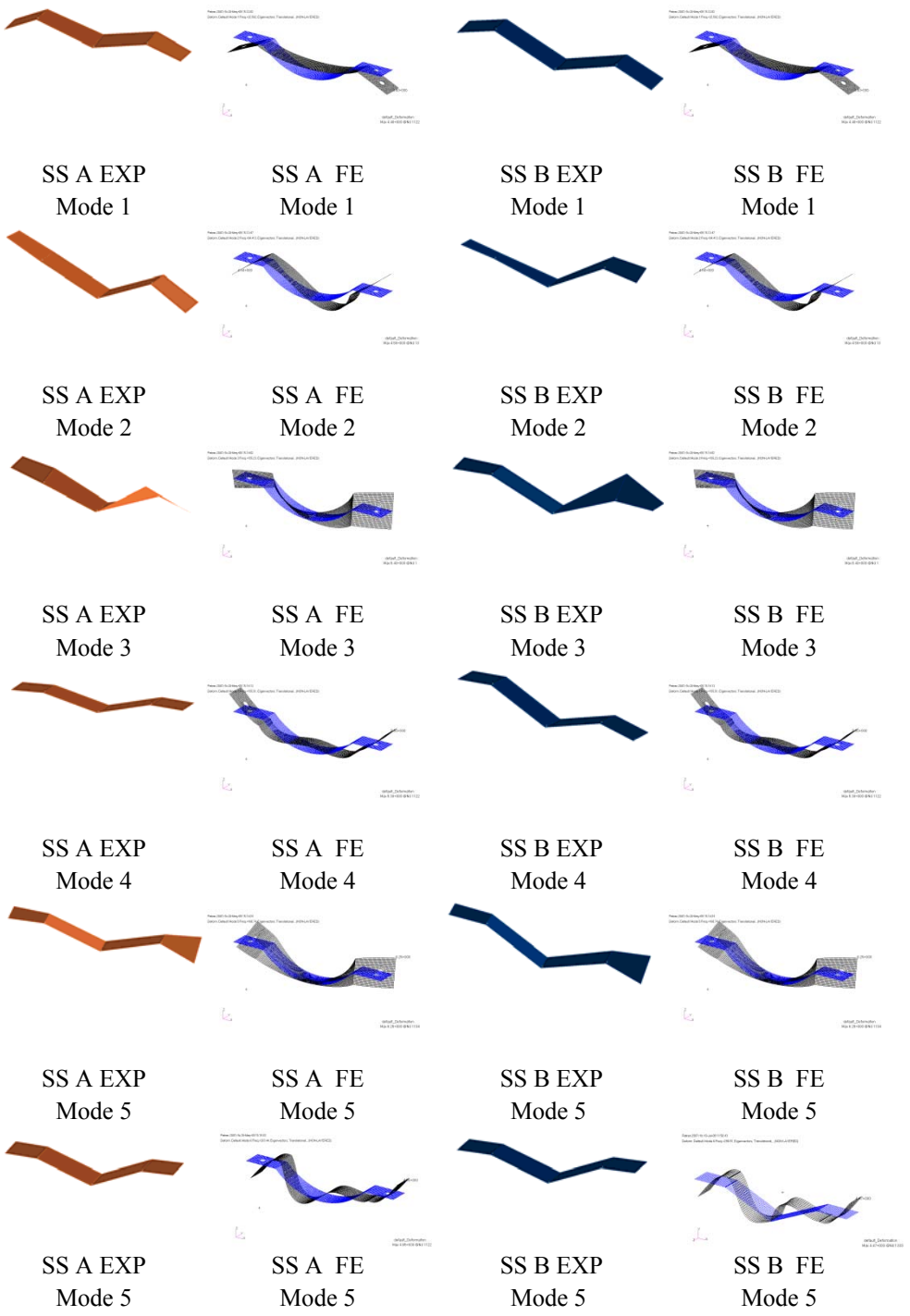

Figure 4.23: Comparison results of mode shapes (1st to 6th) between test and updated FE models of the side support A (SS A) and side support B (SS B).

4.11 Closure

The finite element modelling and updating procedure of components have been demonstrated and discussed theoretically. The errors between the measured and initial finite element models of components are calculated based on the total error of the first ten modes. The parameter of Young's modulus has been identified to be the most sensitive parameter for the components and used as the updating parameter. As a result, the total error of all components has been successfully reduced below than 11 percent.

In this study, it is found that the geometry of the component has a great influence in the calculation of the updated value of the Young's modulus. For example, from Table 4.5, it can be seen that, the initial value of the Young's modulus of main support A has significantly increased for 4.8 percent. On the other hand, the initial values of the Young's modulus of side support A and side support B have decreased for 4.70 percent.

Chapter 5

Finite Element Modelling and Model Updating of the Welded Structures

5.1 Introduction

This chapter presents model updating of the welded structures. The updated finite element models of the components (Chapter 4) are assembled by a number of connector elements to form the welded structures. However, before the finite element models of the components are assembled together, the errors in the models are minimised to acceptable level. In other words, in practise, in updating the finite element models of the components errors must be firstly reduced. This is to ensure any error that may arise in the finite element model of the assembled structure is due to joint modelling.

There are two models of the finite element models, which are called the welded structure A and the welded structure B as shown in Figure 5.1. Each of these welded structures is joined by sixteen spot welds. The CAD system is used to construct the CAD models of both structures before the modelling process of the finite element model of the welded structure A and the welded structure B. Meanwhile, PATRAN which is used as a pre-processor is used in meshing, setting up the boundary conditions and assigning material properties.

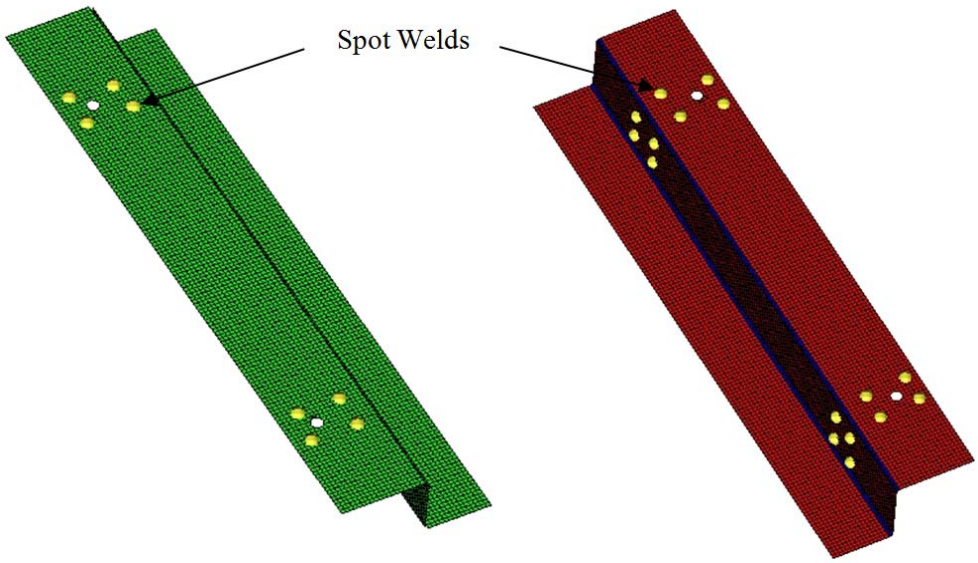

(a) Welded structure A (b) Welded structure B

Figure 5.1: Visual models of the welded A and the welded structure B

This chapter also presents the numerical results calculated from two different types of connector elements namely CWELD element and CFAST element. The CWELD element (ALIGN and ELPAT format) and CFAST element are used to represent the spot weld joints on the welded structure A. In order to validate the accuracy of those connector elements (The CWELD element (ALIGN and ELPAT format) and CFAST element) in representing the physical spot welds, comparisons of natural frequencies between the finite element of the welded structure A and measured data are made. The accuracy of the connector elements (The CWELD element (ALIGN and ELPAT format) and CFAST element) are discussed. The patches are introduced on the finite element of the welded structure A of the CWELD element in ELPAT format in order to further improve on the result of the finite element model of the welded structure A.

Finite element model updating is then employed to the finite element of the welded structure A (CWELD element in ELPAT format) and the finite element of the welded structure A (CWELD element in ELPAT format) with the patches. The effects of parameters that are related to the finite element model of the welded structure such as Young's modulus, diameter of spot weld, and patches are investigated.

The accuracy of the finite element model of the welded structures are discussed and the appropriate model of the connector element that is able to represent the dynamic characteristics of the physical spot welds will be employed in the modelling of the finite element model of the welded structures B and the finite element model of the full welded structure (Chapter 6). They are summarised as follows:

1) Initial finite element model of the welded structure A of CWELD element in ALIGN format.
2) Initial finite element model of welded structure A of CFAST element.

3) Initial finite element model of welded structure A of CWELD element in ELPAT format.

4) The updated finite element model based on the diameter of spot welds and the Young's modulus of patches of welded structure A.

5) The updated finite element model of welded structure A and the welded structure B based on parameters that are related to diameter of spot welds of the welded structure A and welded structure B.

5.2 Spot weld model

Thin sheet structures are used in many areas of engineering such as automotive and aerospace industries. For instance, automotive components such as body panels, B-pillars and floors are formed from thin metal sheets and they are assembled together through many types of joints such as bolted joints and spot welds. These joints are normally used to joint two or more types of sub-components together to form an assembled structure such as a body-in-white (BiW). The behaviour of the joints such as bolted joints and spot welds are known to play an important role in the dynamic behaviour of the structure (Silva et al., 2005).

The finite element method is widely used in automotive industries to predict the dynamic behaviours of spot welds. Accurate predictions can only be obtained when realistic spot weld connections are included in the finite element model. Essentially, before developing a finite element model of the spot weld, engineers and designers should have a sound understanding of the capability of the structural joint elements being used in order to simulate closely the dynamic behaviour of actual joint. The properties and characteristics of structure joints are known to significantly contribute to the overall dynamic behaviour of the structure. Previously, for a number of years, one dimensional element have been widely used in industries to model spot welds (Fang et al., 2000).

Several elements such as rigid body element (RBE), bar, beam and flexible spring are used to represent spot weld in industries. The most common and straight forward approach is to connect the coincident nodes between two surfaces using RBE or spring element. Even though these elements are easy to use, the limitation of these models makes modelling of structural joints become impractical and sometime it is difficult to produce a reliable model of spot welds that has good correlation with a physical structure. In addition, rigid connection and flexible spring elements underestimate the stiffness of real spot welded joint due to the point to point joint Duque et al. (2006) and Kuratani and Yamauchi (2011).

The connector element namely, CWELD element which is available in NASTRAN is used to model the spot weld joints. CWELD element provides more flexibility and capabilities at the connection points and also the way the connector is defined is more versatile such as point to point connection, point to patch connection, patch to patch connection, and multi-element connection. Furthermore, the CWELD element properties include material properties such as the Young's modulus, shear modulus, density, Poisson's ratio's ratio and the diameter of spot welds.

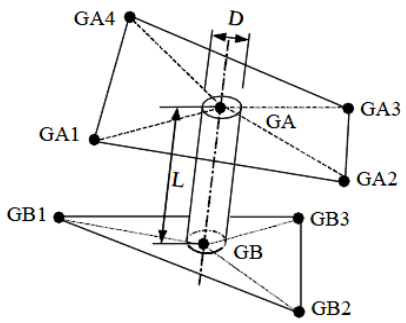

Figure 5.2: The CWELD element in NASTRAN

The main part of the CWELD element is a short beam which connects - points GA to GB with six DOFs per node as shown in Figure 5.2. This beam element is modelled as a special shear flexible beam type element from the Timoshenko beam theory. The element has a cross section diameter (D) and the length (L) from GA to GB. The property of weld is defined in a PWELD property entry and the ratio between the length and diameter of the diameter *(L/D)* is restricted to $0.2 \leq L/D \leq 5.0$ (MSC.NASTRAN, 2001).

The CWELD element has been enhanced to connect more than a single element per sheet and to handle connections other than surface patches (MSC.NASTRAN, 2004). The connection of the spot weld can be established with ease between points, elements, patches, or any of these combinations.

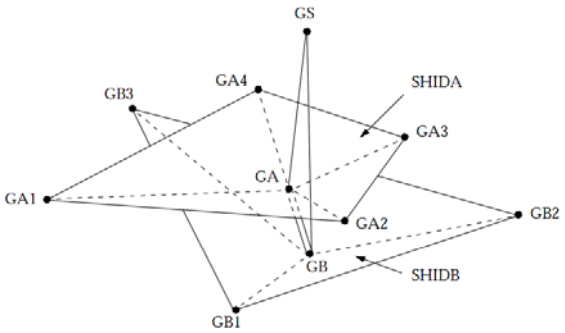

Figure 5.3: CWELD element with ELEMID and GRIDID format for patch to patch connectivity

In the context of CWELD element definition, a patch is a surface to which the weld element will be connected. In this connection, the node of GA and GB are connected to nodes GAi and GBi. The GAi and GBi nodes are bordered by SHIDA and SHIDB which known as element patch (Figure 5.3) respectively. The 3 translational and 3 rotational DOFs from point GA are related to the 3 translational DOFs of each node GAi with constraints from Kirchhoff shell theory:

$$\begin{Bmatrix} u \\ v \\ w \end{Bmatrix}_A = \sum \mathbf{N}_i \left(\xi_A, \eta_A\right). \begin{Bmatrix} u \\ v \\ w \end{Bmatrix}_i \tag{5.1}$$

$$\theta_x^A = \frac{\partial w}{\partial y} = \sum \mathbf{N}_{i,y}.w_i \tag{5.2}$$

$$\theta_y^A = -\frac{\partial w}{\partial x} = -\sum \mathbf{N}_{i,x}.w_i \tag{5.3}$$

$$\theta_z^A = \frac{1}{2}\left(\frac{\partial v}{\partial x} - \frac{\partial u}{\partial y}\right) = \frac{1}{2}\left(\sum \mathbf{N}_{i,x}.v_I - \sum \mathbf{N}_{i,y}u_i\right) \tag{5.4}$$

These equations are written in the local tangent system of the surface patch at point GA, The two tangent direction are *x* and *y*, and the normal direction is z., **N***i*, are the shape functions of the surface patch. Meanwhile, ξ_A and η_A are the normalised coordinates of GA; *u*, *v* and *w* are the displacement DOFs of translation in x, y, z direction. Meanwhile, θ_x, θ_y and θ_z are rotational DOFs in x, y and z direction. Another similar set of equations (Eqn. (5.1)) to (Eqn. (5.4)) are written for node GB resulting in twelve constraint equations.

5.3 Implementation of finite element modelling of the welded structures

Once the experiments of the welded structures are finished, the finite element models of the welded structures are developed in order to evaluate the accuracy of the models. In generating the finite element models of the welded structures, each updated component (Chapter 5) is assembled in a CAD system as the welded structures. The geometries of welded structures are constructed in the CAD system (Figure 5.4 (a)) in order to shorten the modelling process in the CAE system.

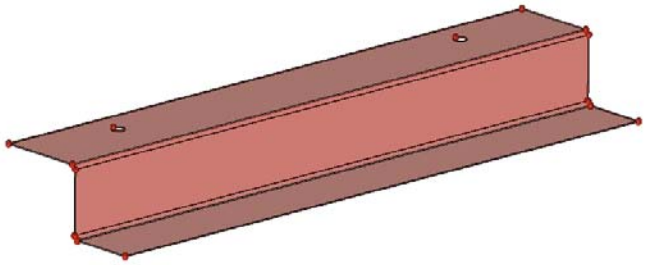

(a) CAD model

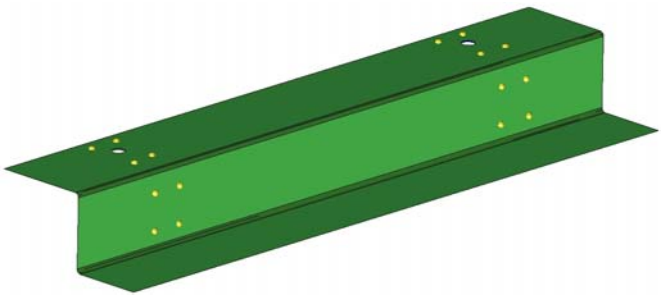

(b) Mid-surface model

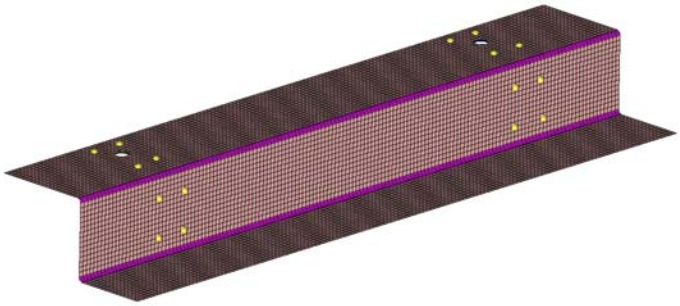

(c) CAE model

Figure 5.4: Visual model of the welded structures

PATRAN is used as a pre-processor to construct the finite element models of the welded structures as shown in Figure 5.4 (b) and Figure 5.4 (c). Meanwhile, the MSC NASTRAN SOL103 is used as a finite element solver to predict the natural frequencies and mode shapes of the welded structures. For representing the spot welds in the finite element model of the welded structure, three type of elements are used to model spot welds for the welded structure namely CWELD (ALIGN and ELPAT format) and CFAST elements. The finite element models of the welded structure A and the welded structure B have 9864 CQUAD4 elements and 16 connector elements as shown in Figure 5.4 (c). The nominal material values (Table 3.1) and spot weld diameter are the parameters considered in the modelling work of the spot welds. Results are discussed and the appropriate element for representing the spot welds will be used in modelling the welded structures.

5.4 CWELD element in ALIGN format

Traditionally, the CWELD element in ALIGN format that is available in MSC.NASTRAN connection can be created from node to node connection. The node to node connection requires congruent mesh and the connection can be established by connecting two point normals (GA and GB) in direction of the weld axis. The direction of the weld axis is automatically defined by 'ALIGN' format in PWELD entry (Figure 5.5).

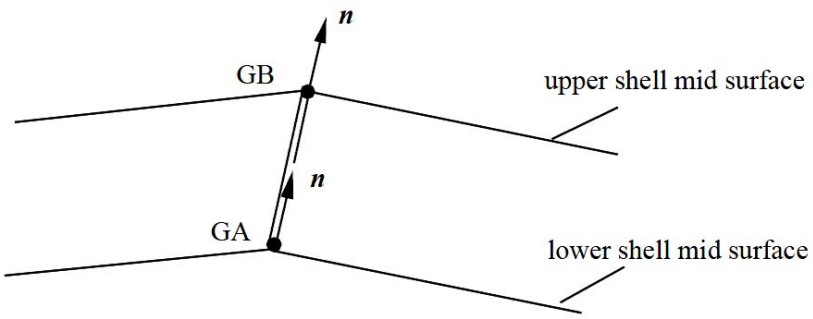

Figure 5.5: CWELD element node to node connectivity with ALIGN format

However, Palmonella et al. (2005) and Donders et al. (2006) revealed that the node to node connection is physically inconsistent and may imprecise and unstable results, this is because the node to node connection of structural joint often underestimates its stiffness. Point to point connection is also impractical and time consuming because two grids of elements have to be congruent with each others. In addition, all components attached to a new component have to re-meshed to make them congruent to the new part.

The calculated results of the first ten modes are compared with the experimentally derived frequencies as shown in Table 5.1. As summarised in Table 5.1, the total error is 28.85 percent (column III) and it can be seen that the 3rd frequencies shows the highest error of 4.78 percent.

Table 5.1: Comparison of results between the tested and the CWELD element in ALIGN format model of welded structure A

Mode	I Experiment Frequency (Hz)	II Initial F.E Frequency (Hz)	III Relative Error [%] [I-II/I]
1	43.44	42.59	1.95
2	143.42	140.62	1.95
3	196.40	187.02	4.78
4	200.01	191.62	4.20
5	213.17	205.93	3.40
6	218.79	213.16	2.58
7	252.37	244.62	3.07
8	262.93	255.08	2.99
9	276.43	267.94	3.07
10	294.80	295.61	0.27
ALIGN	Total Error		28.85

5.5 CFAST element

CFAST element is the enhanced version of the CWELD element which is available in the library of MSC.NASTRAN (2005a) . It is used to model spot weld joints of structure A. CFAST element enables the user to connect surfaces with different mesh densities. It provides more flexibility and capabilities at the connection points (MSC.NASTRAN, 2005a). The versatility of these elements offers point to point connection, point to patch connection, patch to patch connection, and multi-elements connection.

CFAST defines a flexible connection between two surface patches or more depending on the location of the piercing points GA and GB, and also the size of the bolt diameter D (in the case of a bolted joint) as shown in Figure 5.6. The element connectivity is defined using the CFAST Bulk Data entry and properties

are defined in the corresponding PFAST entry and also by the element properties of shells.

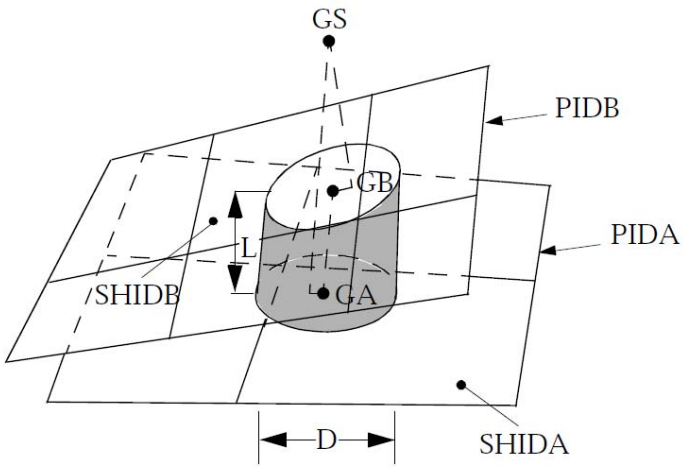

Figure 5.6: CFAST element with PROP and ELM formats connectivity

The first ten frequencies that are calculated from CFAST welded structure are compared with the experimental result as shown in Table 5.2. It can be seen that the 3rd frequency shows the highest error. Meanwhile the lowest error is from the 10th frequency with an error of 0.51 percent of error. The total relative error is 35.92 percent as shown in column (III).

Table 5.2: Comparison of results between the tested and the CFAST format model of welded structure A

Mode	I Experiment Frequency (Hz)	II Initial F.E Frequency (Hz)	III Relative Error [%] [I-II/I]
1	43.43	42.34	2.52
2	143.41	140.29	2.18
3	196.39	183.49	6.57
4	200.01	191.02	4.50
5	213.16	201.16	5.63
6	218.79	212.96	2.67
7	252.37	242.45	3.93
8	262.93	254.45	3.23
9	276.43	264.88	4.18
10	294.80	293.30	0.51
CFAST	Total Error		35.92

5.6 CWELD element in ELPAT format

CWELD elements in PARTPAT and ELPAT formats have been developed to overcome the modelling issues such as non-congruent meshes. The connection can be established easily between points, elements, patches, or any of these combinations. In the context of CWELD element definition, a patch is a surface to which the weld element will be connected. In this connection, nodes of GA and GB are connected to nodes GAi and GBi. The GAi and GBi nodes are bordered by SHIDA and SHIDB which known as element patch (Figure 5.7) respectively. The 3 translational and 3 rotational DOFs from point GA are related to the 3 translational DOFs of each node GAi with constraints from Kirchhoff shell theory.

Then the enhanced patch to patch connection format was introduced by MSC.NASTRAN (2004) and can be defined by using new connection format known as the 'PARTPAT' and 'ELPAT' formats. These connection formats are most versatile, which allows the size of mesh elements smaller than the single element size of spot weld and permit connection up to 3x 3 elements per shell sheet.

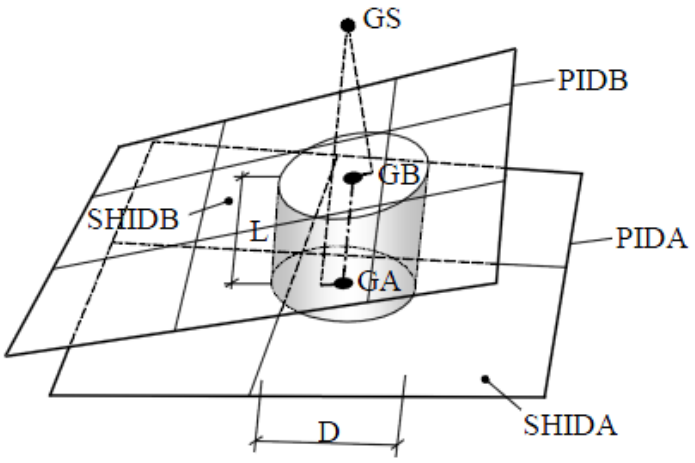

Figure 5.7: CWELD element with 'PARTPAT' and 'ELPAT' formats for patch to patch connectivity

The 'PARTPAT' format and the 'ELPAT' format can be established by connecting two shell element patches with shell identifications SHIDA and SHIDB or two patches identification PIDA and PIDB. The first ten frequencies that are calculated from the CWELD elements in ELPAT format of welded structure are compared with experimental result as shown in Table 5.3. It can be seen that the 4th frequency shows the highest error. Meanwhile the lowest error is from the 8th frequency with an error of 2.65 percent. The total relative error is 14.53 percent as shown in column (III).

Table 5.3: Comparison of results between the tested and the CWELD element in ELPAT format model of welded structure A

Mode	I Experiment Frequency (Hz)	II Initial F.E Frequency (Hz)	III Relative Error [%] [I-II/I]
1	43.43	43.48	0.10
2	143.41	142.20	0.85
3	196.39	193.48	1.49
4	200.01	195.65	2.18
5	213.16	213.68	0.24
6	218.79	214.09	2.15
7	252.37	248.92	1.37
8	262.93	255.97	2.65
9	276.43	272.32	1.49
10	294.80	300.76	2.02
ELPAT	Total Error		14.53

5.7 Results and discussion of CWELD (ALIGN and ELPAT format) and CFAST elements model

The two types of spot weld models (CWELD ALIGN and ELPAT format) and CFAST fastener element are compared in order to model spot weld joints. From Table 5.2 large discrepancies can be observed between the CFAST finite element model and the experimental data of welded structure A. The total error calculated from the finite element model using CFAST connector is 35.92 percent with the largest error contributor partly from the 3rd frequency which is 6.57 percent. Meanwhile, the CWELD elements in ALIGN format shows the second highest relative error with the 28.85 percent. However, the total error calculated from CWELD elements in ELPAT format show the lowest error in comparison with other connecter elements (CWELD element in ALIGN format and CFAST

element) with the relative error of 14.53 percent. From the comparison, it can be seen that the CWELD element in ELPAT format shows a better capability to represent the dynamics characteristics of the spot welds. Therefore, the CWELD element in ELPAT format is used to model the spot welds. Even though the CWELD element in ELPAT format is used for further spot weld modelling, model updating needs to be performed to the finite element model of the welded structures. This is because the parameters of the spot weld model are merely based on nominal values. Therefore, the parameters such as the Young's modulus, Poisson's ratio, shear modulus and diameter of spot weld need to be corrected in order to obtained the correct dynamic characteristic of the welded structures.

5.8 Finite element modelling and updating of the welded structure (CWELD element in ELPAT format) with patches

The CWELD element in ELPAT format is used to model spot welds on the welded structures since the model shows better capability and flexibility in presenting the physical model of spot welds as discussed in the last section. Typically, in the fusion process of resistance spot welds, the surface resistance of metal sheets is utilised to generate an intense localised heat under pressure with a high current (Khanna and Long, 2008). The areas of the heat affected zone of spot welds are numerically manipulated in order to adjust stiffness of the finite element model of spot welds. Patches which are used to represent the heat affected zone areas of the spot welds by Palmonella et al. (2004) and Abu Husain et al. (2010) are introduced to the finite element model of welded structure A. Eight square patches are constructed at the upper and lower element of the welded structure A as shown in Figure 5.8.

In this approach, the patches are treated as a new entity of the model with new material properties and they are assumed to be the same with nominal values of mild steel, as shown in Table 3.1. The initial predicted natural frequencies of the welded structure A is shown in Table. 5.4.

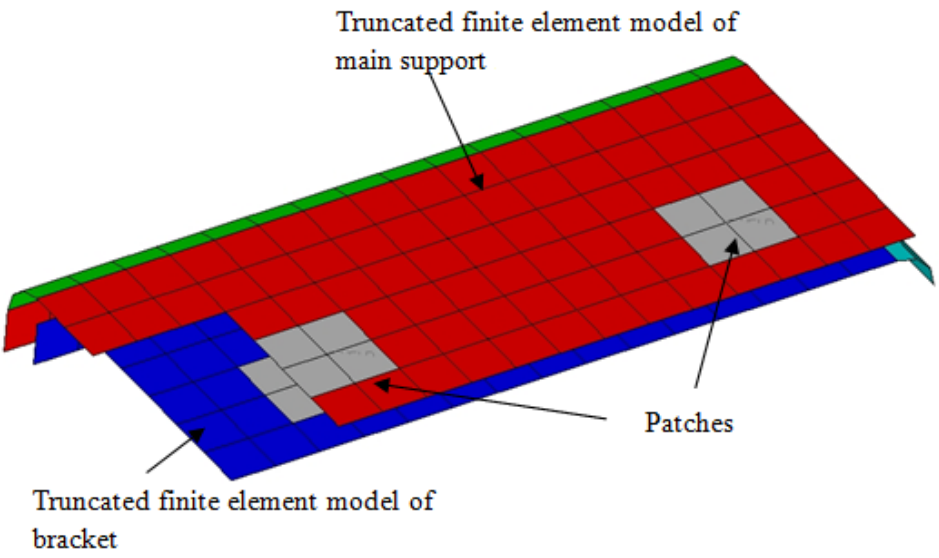

Figure 5.8: Finite element model of patches from the truncated finite element model of the welded structure.

Table 5.4: Comparison of results between the tested and the CWELD element in ELPAT format model of welded structure A with patches

Mode	I Experiment Frequency (Hz)	II Initial F.E Frequency (Hz)	III Relative Error [%] [I-II/I]
1	43.43	43.69	0.59
2	143.41	142.92	0.35
3	196.39	193.80	1.32
4	200.01	196.96	1.53
5	213.16	213.70	0.25
6	218.79	214.28	2.06
7	252.37	248.61	1.49
8	262.93	256.69	2.38
9	276.43	273.29	1.14
10	294.80	301.42	2.24
Total Error			13.34

In order to identify the most sensitive parameters to the frequencies, NASTRAN SOL200 is used to compute the sensitivity based on the parameters of spot welds and patches as shown in Table 5.5 and Table 5.6. From the results of the sensitivity analysis (Table 5.5 and Table 5.6) , it can be seen that the first five frequencies are sensitive to the Young's modulus of spot welds, diameter of spot welds and the shear modulus of patches. Therefore, a combination of these parameters is used as updating parameters for the finite element model of the welded structure A.

Table 5.5: Summarised results of the sensitivity analysis with respects to the normalised parameters of welded structure A (spot weld and patches)

Mode	Frequency	Parameters of Spot Welds			
		Spot Weld Diameter	Young's Modulus	Shear Modulus	Poisson's Ratio
1	4.37E+01	4.00E-01	2.32E-02	1.11E-01	0.00E+00
2	1.43E+02	7.89E-01	3.30E-02	1.78E-01	0.00E+00
3	1.94E+02	2.08E+00	2.04E-01	4.38E-01	0.00E+00
4	1.97E+02	2.11E+00	7.05E-02	5.47E-01	0.00E+00
5	2.14E+02	1.01E+00	1.41E-01	1.29E-01	0.00E+00

Table 5.6: Summarised results of the sensitivity analysis with respects to the normalised parameters of welded structure A (spot weld and patches)

Mode	Frequency	Parameters of Patch			
		Patch's Thickness	Young's Modulus	Shear Modulus	Poisson's Ratio
1	4.37E+01	1.37E+00	7.54E-01	3.18E-02	0.00E+00
2	1.43E+02	1.73E+00	8.85E-01	2.90E-02	0.00E+00
3	1.94E+02	9.20E+00	3.90E+00	2.21E-01	0.00E+00
4	1.97E+02	5.64E+00	2.59E+00	7.90E-02	0.00E+00
5	2.14E+02	4.94E+00	1.97E+00	1.25E-01	0.00E+00

The accuracy of the finite element models of the welded structure with patches and the finite element model of welded structure without patches are compared. The updated values of the natural frequencies of the finite element model of welded structure A with patches are shown in Table 5.7. From the table, it is clearly shown that by considering the patches as a structural component in the updating parameters, the total error of the updated natural frequencies is slightly reduced from 13.34 percent to 12.66 percent and MAC values are above 0.8.

Table 5.7: Three comparisons of results between the tested and finite element model of welded structure A (spot weld and patches)

Mode	I Experiment (Hz)	II Initial FE (Hz)	III Error (%) [I-II/I]	IV Updated FE A (Hz)	V Error (%) [I-IV/I]	VI Updated FE MAC
1	43.43	43.69	0.59	43.79	0.82	0.85
2	143.41	142.92	0.35	143.14	0.19	0.98
3	196.39	193.80	1.32	194.27	1.08	0.90
4	200.01	196.96	1.53	197.53	1.24	0.86
5	213.16	213.70	0.25	213.92	0.35	0.89
6	218.79	214.28	2.06	214.52	1.96	0.94
7	252.37	248.61	1.49	248.87	1.39	0.86
8	262.93	256.69	2.38	256.77	2.35	0.96
9	276.43	273.29	1.14	273.72	0.98	0.98
10	294.80	301.42	2.24	301.61	2.31	0.82
Total Error			13.34		12.66	

In order to determine the accuracy of the finite element model of the welded structure A (CWELD element in ELPAT format) and the finite element model of the welded structure A (CWELD element in ELPAT format with patches), the finite element model updating is performed to the finite element model of the welded structure A (CWELD element in ELPAT format). The sensitivity analysis results of the first five frequencies are shown in Table 5.8.

Table 5.8: Summarised results of the sensitivity analysis with respects to the normalised parameters of the welded structure A without patches (WS A)

Mode	Frequency	Parameters				
		Spot Weld Diameter	Young's Modulus	Shear Modulus	Poisson's Ratio	Density
1	4.34E+01	3.87E-01	2.18E-02	1.08E-01	0.00E+00	0.00E+00
2	1.42E+02	7.54E-01	3.11E-02	1.68E-01	0.00E+00	0.00E+00
3	1.93E+02	2.13E+00	1.94E-01	4.43E-01	0.00E+00	0.00E+00
4	1.95E+02	2.00E+00	6.62E-02	5.08E-01	0.00E+00	0.00E+00
5	2.14E+02	1.91E-01	1.17E-02	4.88E-02	0.00E+00	0.00E+00

The updated natural frequencies of the finite element model of welded structure A without including patches is shown in Table 5.9 (Column V). Meanwhile, by considering the Young's modulus and the diameter of spot welds as the updating parameter the error is reduced from 14.98 percent to 14.10 percent and the average MAC values are above 0.85.

Table 5.9: Three comparisons of results between the tested and finite element model of the welded structure A without patches (WS A)

Mode	I Experiment (Hz)	II Initial FE (Hz)	III Error (%) [I-II/I]	IV Updated FE A (Hz)	V Error (%) [I-IV/I]	VI Updated FE MAC
1	43.43	43.42	0.03	43.51	0.17	0.85
2	143.41	142.10	0.92	142.31	0.77	0.96
3	196.39	193.16	1.65	193.63	1.41	0.94
4	200.01	195.39	2.31	195.92	2.05	0.88
5	213.16	213.66	0.23	213.70	0.25	0.90
6	218.79	213.84	2.27	214.27	2.07	0.93
7	252.37	248.77	1.43	249.00	1.34	0.88
8	262.93	255.95	2.66	256.03	2.63	0.97
9	276.43	272.21	1.53	272.58	1.39	0.98
10	294.80	300.59	1.96	300.79	2.03	0.83
Total Error			14.98		14.10	

Based on the comparison of results between the updated finite element models of the welded structure (patches and without patches), the total error of the finite element model of the welded structure without patches (Table 5.9 column V) is reduced by about 0.9 percent. Meanwhile, the reduction in the total error of the finite element model of the welded structure A with patches (Table 5.7 column V) is merely 0.7 percent which is a very small improvement.

It can be concluded that, introducing patches to the finite element model of spot welds could only lead to a very small improvement in the finite element model of the welded structure. Abdul Rani (2012) revealed that generally there was no significant improvement when including patches to the finite element model of the welded structure and a detailed modelling of spot welds and patches requires a large amount of effort of computational time. Thus, modelling each spot welded joint in detail is often impractical because a typical vehicle body-in-white usually consists of several thousand spot welds and it is impossible to have a detailed representation of each spot weld (Lamouroux et al., 2007 and Kuratani and Yamauchi, 2011). As a result patches are not considered the finite element of the welded structures. Therefore, in this work, CWELD element in ELPAT format is used to construct the finite element model of the welded structure and the finite element model of the full welded structure in Chapter 7.

CWELD elements in ELPAT format is used to construct the finite element model of the welded structure B as shown in Figure 5.1. The NASTRAN SOL103 is used to calculate the natural frequencies and mode shapes and the results of the natural frequencies and MAC values are tabulated in Table 5.10.

Table 5.10: Comparison of results between measured frequencies and FE natural frequencies of the welded structure B (WS B)

Mode	I Experiment Frequency (Hz)	II Initial F.E Frequency (Hz)	III Relative Error [%] [I-II/I]
1	43.43	43.51	0.17
2	142.36	142.37	0.01
3	196.31	194.20	1.07
4	198.79	197.26	0.77
5	216.49	213.31	1.47
6	218.56	213.46	2.33
7	251.37	249.96	0.56
8	263.59	255.50	3.07
9	274.10	273.43	0.24
10	306.65	299.73	2.26
Total Error			11.96

NASTRAN SOL200 is then utilised to identify the most sensitive parameters of the frequencies that are related to the spot welds such the Young's modulus, diameter of spot welds, shear modulus and the Poisson's ratio. Table 5.11 shows the summary of the sensitivity analysis of the welded structure B. In the sensitivity results, the Young's modulus is found to be most influential to frequencies and followed by shear modulus and diameter of spot welds. The Young's modulus and the diameter of spot welds are used as the updating parameters for the welded structure B, instead of shear modulus because of the direct relation between the Young's modulus and shear modulus in the calculation of the natural frequency.

Table 5.11: Summarised results of the sensitivity analysis with respects to the normalised parameters of the welded structures

Mode	Frequency	Parameters			
		Spot Weld Diameter	Young's Modulus	Shear Modulus	Poisson's Ratio
1	4.34E+01	3.87E-01	2.18E-02	1.08E-01	0.00E+00
2	1.42E+02	7.54E-01	3.11E-02	1.68E-01	0.00E+00
3	1.93E+02	2.13E+00	1.94E-01	4.43E-01	0.00E+00
4	1.95E+02	2.00E+00	6.62E-02	5.08E-01	0.00E+00
5	2.14E+02	1.91E-01	1.17E-02	4.88E-02	0.00E+00

Table 5.12 shows the comparison between the initial natural frequencies and updated natural frequencies of welded structure B. It can be seen, that the error of updated natural frequencies is reduced from 11.96 percent to 10.76 percent and MAC values are improved to above than 0.8.

Table 5.12: Three comparisons of results between the tested and finite element (FE) model of the welded structure B (WS B)

Mode	I Experiment (Hz)	II Initial FE (Hz)	III Error (%) [I-II/I]	IV Updated FE A (Hz)	V Error (%) [I-IV/I]	VI Updated FE MAC
1	43.43	43.51	0.17	43.61	0.41	0.83
2	142.36	142.37	0.01	142.62	0.18	0.96
3	196.31	194.20	1.07	194.87	0.73	0.90
4	198.79	197.26	0.77	198.01	0.39	0.86
5	216.49	213.31	1.47	213.42	1.42	0.84
6	218.56	213.46	2.33	213.93	2.12	0.90
7	251.37	249.96	0.56	250.40	0.39	0.84
8	263.59	255.50	3.07	255.91	2.91	0.99
9	274.10	273.43	0.24	274.06	0.01	0.97
10	306.65	299.73	2.26	299.90	2.20	0.82
Total error			11.96		10.76	

The initial changes of updated value of the Young's modulus and diameter of spot weld of welded structure A and welded structure B are shown in Table 5.13 and Table 5.14. The initial change of the updating parameters from the initial normalised value to convergent value of welded structure is also shown (Figure 5.9) due to the same parameters are used in the updating procedure for both structures (welded structure A and the welded structure B). The comparison between the initial finite element mode shapes and the updated mode shapes is shown in Figure 5.10 and Figure 5.11.

Table 5.13: Updated value of parameter of the welded structure A (WS A)

Parameters	Initial Value	Updated Value	Unit
Young's Modulus	210000	222600	MPa
Spot Weld	4	5.50	mm

Table 5.14: Updated value of parameter of the welded structure B (WS B)

Parameters	Initial Value	Updated Value	Unit
Young's Modulus	210000	222600	MPa
Spot Weld	4	5.50	mm

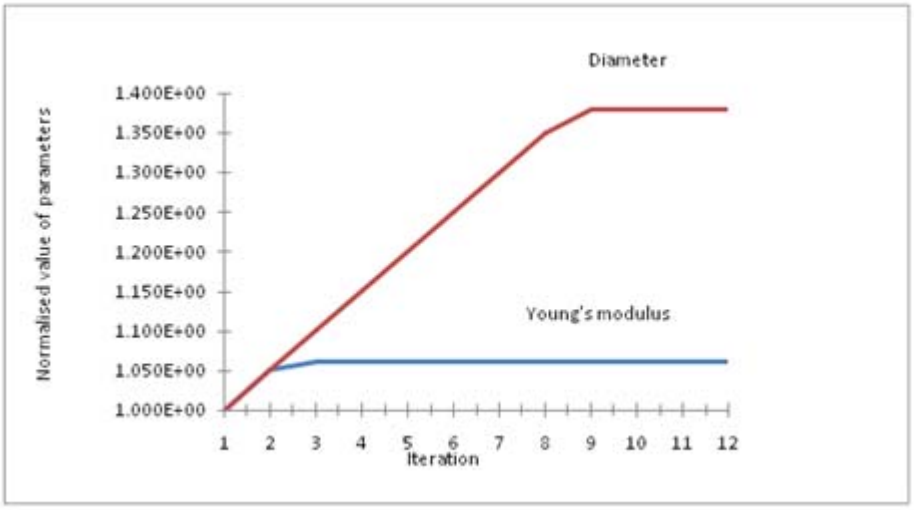

Figure 5.9: The convergence of the updating of the welded structure A and the welded structure B

The comparison of the results of welded structure A and welded structure B that is calculated based on the different numbers of the measured frequencies defined in the objective function (Equation 5.8) are shown in Tables 5.15 up to Table 5.18. Column I and II in Table 5.15 up to Table 5.18 represent the experimental results and the numerical results calculated from the initial finite element model. Meanwhile, column III gives the results calculated from the updated finite element model. These tables show that the larger the numbers of measured frequencies used in the objective function, the better the results are obtained.

Table 5.15: The comparison of results calculated using different numbers of measured frequencies (1st to 5th) of the welded structure A (WS A) in the objective function multiply by 100

Mode	I	II	III				
	Exp (Hz)	Initial FE (Hz)	Number of the measured frequencies				
			1 (Hz)	2 (Hz)	3 (Hz)	4 (Hz)	5 (Hz)
1	43.44	43.42	43.43	43.5100	43.51	43.51	43.51
2	143.42	142.10	142.11	142.30	142.30	142.30	142.31
3	196.40	193.16	193.19	193.62	193.63	193.62	193.63
4	200.01	195.39	195.42	195.92	195.92	195.92	195.92
5	213.17	213.66	213.66	213.70	213.70	213.70	213.70
6	218.80	213.84	213.87	214.26	214.26	214.26	214.27
7	252.38	248.77	248.79	249.00	249.00	249.00	249.00
8	262.94	255.95	255.96	256.03	256.03	256.03	256.03
9	276.43	272.21	272.23	272.58	272.58	272.58	272.58
10	294.81	300.59	300.60	300.70	300.00	300.70	300.79
Total Error			0.29125	0.25812	0.24904	0.25812	0.25890

Table 5.16: The comparison of results calculated using different numbers of measured frequencies (6th to 10th) of the welded structure A (WS A) in the objective function multiply by 100

Mode	I	II	III				
	Exp (Hz)	Initial FE (Hz)	Number of the measured frequencies				
			6 (Hz)	7 (Hz)	8 (Hz)	9 (Hz)	10 (Hz)
1	43.44	43.42	43.51	43.51	43.51	43.51	43.51
2	143.42	142.10	142.30	142.30	142.30	142.30	142.30
3	196.40	193.16	193.62	193.63	193.62	193.62	193.63
4	200.01	195.39	195.92	195.92	195.92	195.92	195.92
5	213.17	213.66	213.70	213.70	213.70	213.70	213.70
6	218.80	213.84	214.26	214.26	214.26	214.26	214.26
7	252.38	248.77	249.00	249.00	249.00	249.00	249.00
8	262.94	255.95	256.03	256.03	256.03	256.03	256.03
9	276.43	272.21	272.58	272.58	272.58	272.58	272.58
10	294.81	300.59	300.79	300.79	300.79	300.79	300.79
Total Error			0.25935	0.25920	0.25935	0.25935	0.25920

Table 5.17: The comparison of results calculated using different numbers of measured frequencies (1st to 5th) of the welded structure B (WS B) in the objective function multiply by 100

Mode	I	II	III				
	Exp (Hz)	Initial FE (Hz)	Number of the measured frequencies				
			1 (Hz)	2 (Hz)	3 (Hz)	4 (Hz)	5 (Hz)
1	43.43	43.51	43.44	43.45	43.61	43.61	43.61
2	142.36	142.37	142.23	142.24	142.62	142.62	142.62
3	196.31	194.20	193.73	193.77	194.88	194.88	194.88
4	198.79	197.26	196.85	196.88	198.02	198.02	198.02
5	216.49	213.31	212.93	212.97	213.42	213.42	213.42
6	218.56	213.46	213.35	213.35	213.93	213.93	213.93
7	251.37	249.96	249.67	249.69	250.40	250.40	250.40
8	263.59	255.50	255.44	255.45	255.59	255.59	255.59
9	274.10	273.43	273.04	273.08	274.07	274.07	274.07
10	306.65	299.73	299.50	299.52	299.96	299.96	299.96
Total Error			0.26675	0.26455	0.21493	0.21493	0.21493

Table 5.18: The comparison of results calculated using different numbers of measured frequencies (6th to 10th) of the welded structure B (WS B) in the objective function multiply by 100

Mode	I	II	III				
	Exp (Hz)	Initial FE (Hz)	Number of the measured frequencies				
			6 (Hz)	7 (Hz)	8 (Hz)	9 (Hz)	10 (Hz)
1	43.43	43.51	43.61	43.61	43.61	43.61	43.61
2	142.36	142.37	142.62	142.62	142.62	142.62	142.62
3	196.31	194.20	194.88	194.88	194.88	194.88	194.88
4	198.79	197.26	198.02	198.02	198.02	198.02	198.03
5	216.49	213.31	213.42	213.42	213.42	213.42	213.42
6	218.56	213.46	213.93	213.93	213.93	213.93	213.94
7	251.37	249.96	250.40	250.40	250.40	250.40	250.41
8	263.59	255.50	255.59	255.59	255.59	255.59	255.59
9	274.10	273.43	274.07	274.07	274.07	274.07	274.07
10	306.65	299.73	299.96	299.96	299.96	299.96	299.96
Total Error			0.21493	0.21493	0.21493	0.21493	0.21467

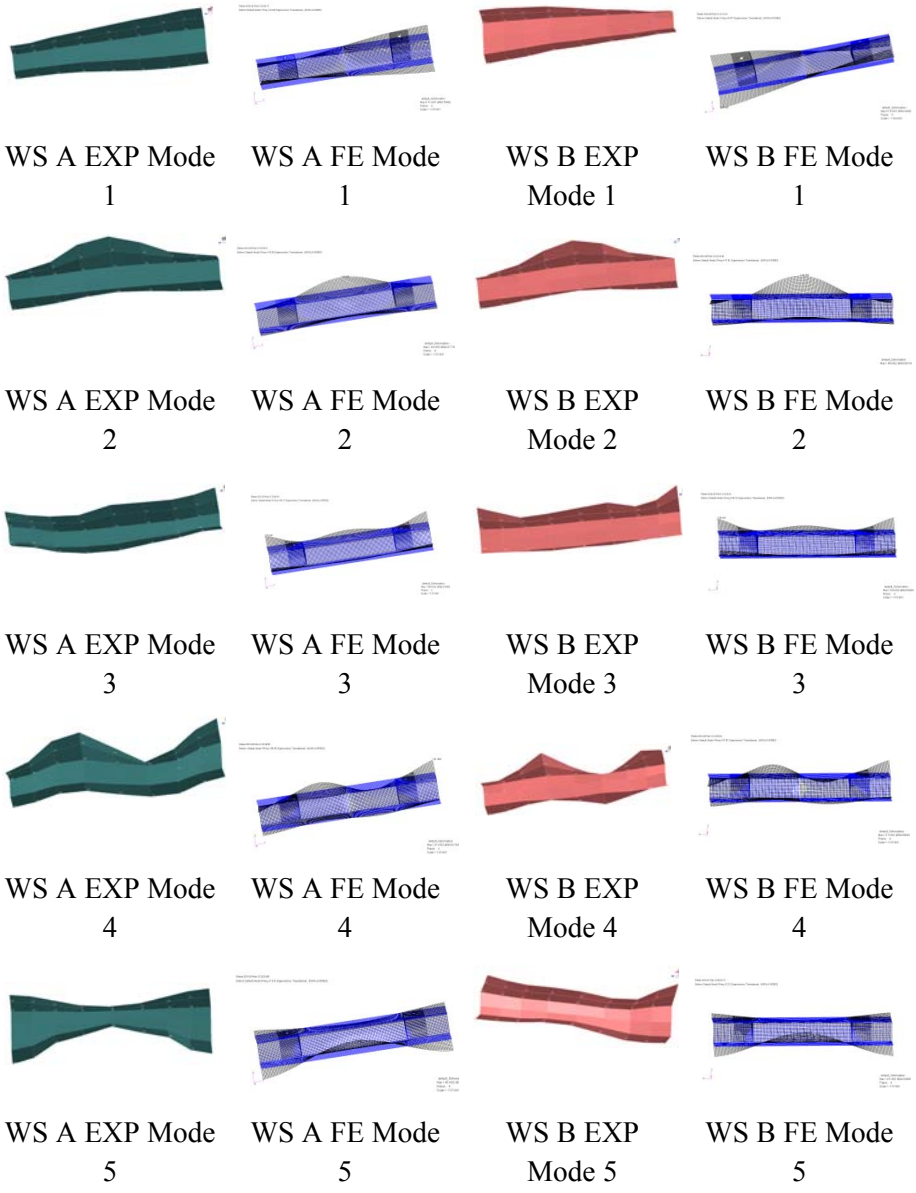

Figure 5.10: Comparison results of mode shapes (1st to 5th) between test and updated FE models of the welded structure A (WS A) and the welded structure B (WS B).

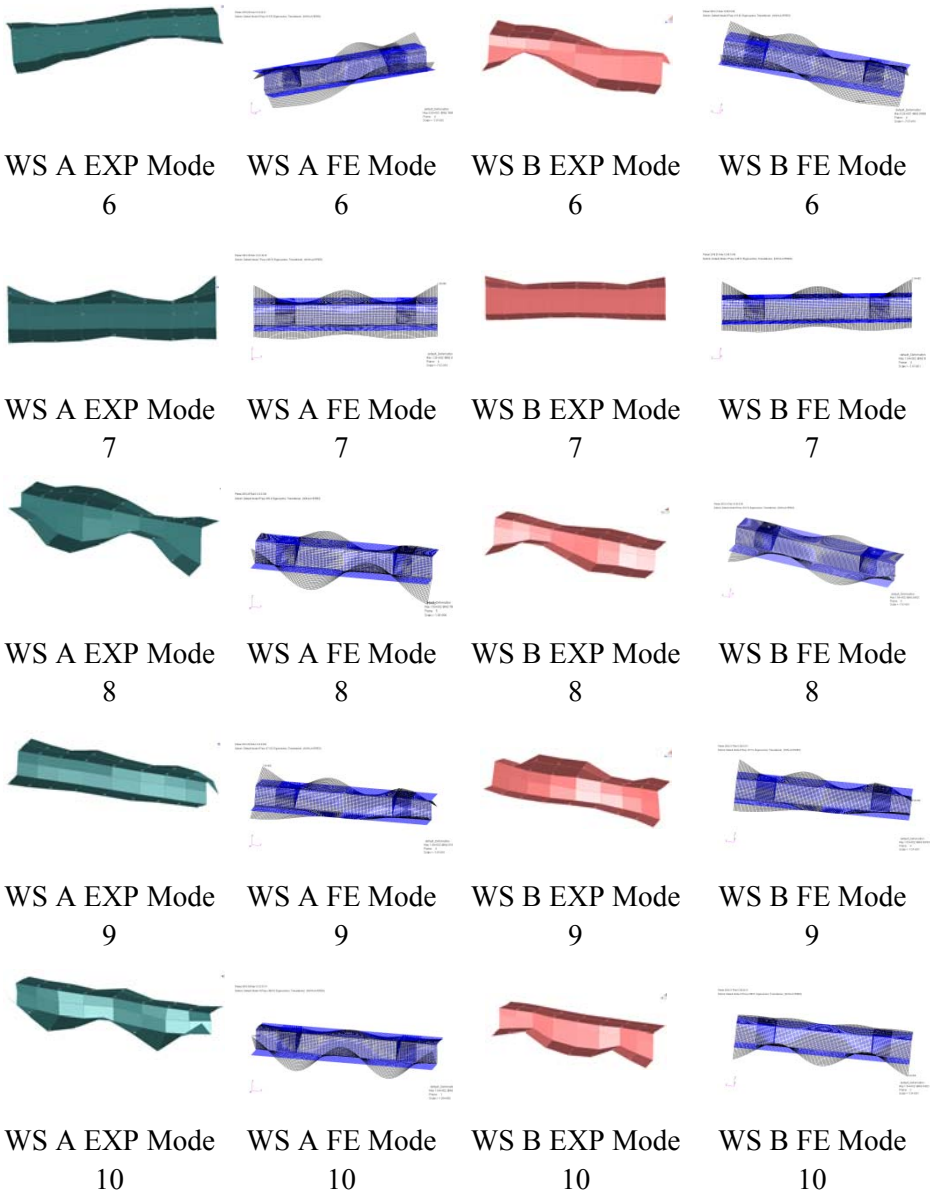

Figure 5.11: Comparison results of mode shapes (6^{th} to 10^{th}) between test and updated FE models of the welded structure A (WS A) and the welded structure B (WS B).

5.9 Closure

The finite element modelling and model updating of the welded structures have been investigated and discussed. Three types of connector elements namely CWELD element in ELPAT format, CWELD element in Align format and CFAST connector element have been utilised to model the spot weld joints of the structures. The results calculated from those element connectors (CWELD and CFAST) are investigated in order to find the most appropriate model that can be used to construct the finite element model of the welded structure.

In this work, CWELD element in ELPAT format has been chosen to be the most appropriate model of spot welds. It is used to construct the finite element model of the welded structures. In addition, the element connector has been successfully used in updating work of the welded structure.

Chapter 6

Finite Element Modelling and Model Updating of the Full Welded Structure

6.1 Introduction

This chapter presents the procedures and approaches used in the finite element modelling and model updating of the full welded structure. The updated finite element models of the components as elaborated in Chapter 5, namely base bent support A, base bent support B, side support A and side support B are joined together with the updated finite element models of welded structure A and welded structure B (Chapter 6) in order to form assembled structures namely, the full welded structure. Due to the complexity of the structure, the assembly processes of the full welded structure have been performed in the CAD system, rather than in the CAE pre-processor.

The CAE pre-processor, PATRAN is used for creating the mid-surface of the full welded structure and then meshing the mid surface of the structure, assigning the properties of the elements and setting-up the boundary conditions of the full welded structure. The finite element model of the full welded structure is built using approximately 30400 CQUAD4 elements as shown in Figure 6.1 (c) and 72 CWELD elements are used in representing the physical spot welds on the structures.

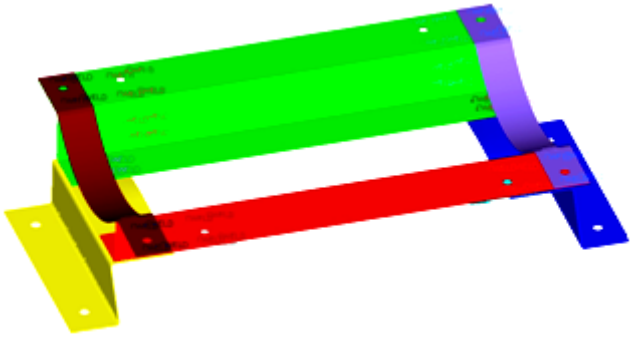

(a) CAD Model

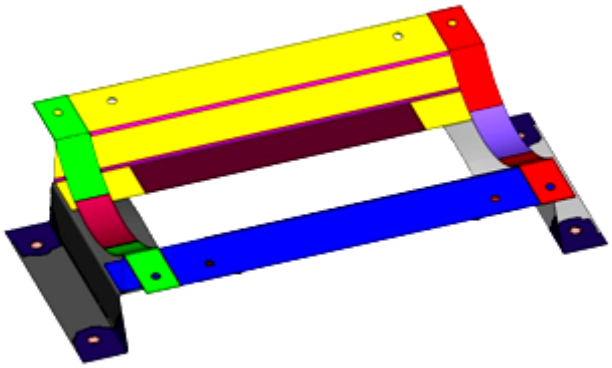

(b) Mid –surface model

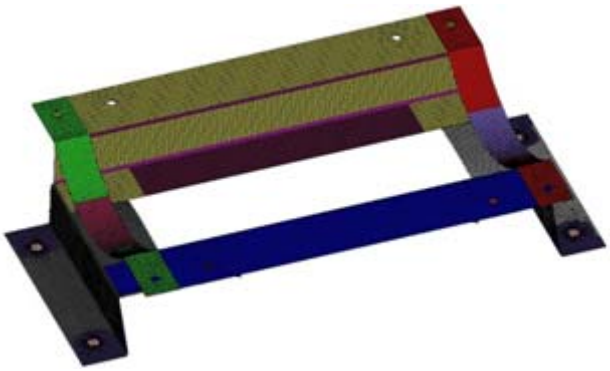

(c) CAE model

Figure 6.1: Visual model of the full welded structure

Figure 6.1 (a) and Figure 6.1 (b) show the CAD model of the full welded structure and the mid-surface model of the full welded structure. Meanwhile, Figure 6.1 (c) shows the CAE model of the full welded structure.

This chapter also presents the analysis results calculated from different types of boundary conditions used in the experiment. Two boundary conditions are considered in the finite element model of the full welded structure, namely free-free boundary conditions and fixed boundary conditions.

The finite element model of the full welded structure with free-free boundary conditions without considering the effect of the suspension spring and this effect - are investigated. The initial natural frequencies of the finite element models are compared with the experimental results and their accuracy is discussed.

The finite element model of the full welded structure with bolted joints (fixed boundary conditions) is modelled and the effects of the bolted joints, washers contact area and the initial curvatures due to fabrication process are investigated. The natural frequencies of the initial finite element models are compared with the experimental results and their accuracy is discussed. They are summarised as follows:

1) The finite element modelling and model updating of the full welded structure based on free-free boundary conditions (diameter of spot welds).

2) The finite element modelling and model updating of the full welded structure based on free-free boundary conditions (diameter of spot welds and spring)

3) The finite element modelling and model updating of the full welded structure based on bolted joints of the full welded structure.

6.2 Application of boundary conditions

In modal testing, the set up and the instrumentation used for the modal testing may affect experimental results (Ewins, 2000). To obtain the accurate experimental results, modal testing should be carried out in free-free boundary conditions. Modal testing with free-free boundary conditions is very popular because it is easy to simulate analytically and approximate experimentally in comparison with fixed boundary conditions. Soft springs are normally used to approximate free-free boundary conditions of the test structures. The effect of soft springs on the test structure is often negligible (Simmermacher et al., 1997).

Since, past few decades, the effects of suspension stiffness on the modal parameters of the test structures have gained attention from many researchers. For example, Wolf (1984) discussed the effects of support stiffness with regards to modal testing of automotive structures. His studies showed that stiff supports had led to significant errors in the measured modal frequencies. Furthermore, he also suggested that the rule of thumb to implement the experiment with free-free boundary conditions was to design the support system so that the rigid body frequencies are not more than one-tenth of the frequency of the lowest elastic mode. Munsi et al. (2002) investigated the effect of the support on the dynamic properties of a light structure and Purekar (2005) used the COMB14 spring element in ANSYS to model the stiffness of the bungee cord for the finite element model of a H-shaped structure.

Carne and Dohrmann (1998) and Carne et al. (2007) revealed that the stiffness and damping of the suspension cord may have significantly altered the modal parameters of the elastic modes of the test structure, if the separation between rigid body and deformation modes was not achieved. He also reported that the stiff bungee cords provided different support stiffness on the structures and thus changed the natural frequencies of the structure. Abdul Rani (2012) used CELAS to represent the springs and strings to approximate free-free boundary conditions and he successfully minimised the large discrepancies between the FE and experimental results. It has been shown that the stiffness of suspension springs is

enough to affect the measured modal properties (frequencies and mode shapes). Consequently, the stiffness of suspension spring must be included in the finite element modelling of the structure.

In this study, the spring element CBUSH in MSC.NASTRAN (2004) is used to model the stiffness of the soft springs so that the real boundary conditions can be implemented for theoretical modal analysis of the structure.

6.3 Finite element modelling and updating of the full welded structure with free-free boundary conditions

SOL103 is used to calculate the natural frequencies and mode shapes of the initial finite element model of the full welded structure. The first ten initial natural frequencies of the finite element model of the full welded structure are compared with those experimental results. Table 6.1 shows the total error of first ten frequencies which is 27.98 percent and the average MAC values which is above 0.75. It can be seen that the largest error is in the first frequency at 6.38 percent.

Table 6.1: Comparison of results between the measured and the initial finite element model of the full welded structure (free-free boundary conditions)

Mode	I Experiment Frequency (Hz)	II Initial F.E Frequency (Hz)	III Relative Error [%] [I-II/I]	IV Initial FE MAC
1	14.55	13.62	6.38	0.78
2	28.96	28.63	1.14	0.91
3	44.92	44.56	0.79	0.88
4	46.62	45.15	3.16	0.93
5	47.96	46.45	3.15	0.87
6	52.66	51.25	2.68	0.96
7	67.35	64.63	4.03	0.86
8	80.74	78.80	2.41	0.92
9	89.48	85.91	3.99	0.81
10	133.72	134.05	0.25	0.76
Total Error			27.98	

In order to identify the sensitive parameters of the initial finite element model of the full welded structure, a list of potential parameters of the CWELD element such as the Young's modulus, shear modulus, Poisson's ratio and the diameter are listed in sensitivity analysis. SOL200 is used to compute the sensitivity analysis. It can be seen (Table 6.2) that the first frequency is sensitive to Young's modulus, followed by shear modulus and the diameter of spot welds. However, the Young's modulus and the diameter are used in the updating since shear modulus and Young's modulus have a direct relationship. The Young's modulus and the shear modulus can be used as updating parameters but the right range of the Poisson's ratio must be maintained. Normally, a large variation of the Poisson's ratio is not reasonable and it is constrained to be close to initial value of 0.3 (Brockenbrough and Merritt, 2011).

Table 6.2: Summarised results of the sensitivity analysis of the full welded structure (free-free boundary conditions)

Mode	Frequency	Parameters			
		Young's Modulus	Shear Modulus	Spot Weld Diameter	Poisson's Ratio
1	1.36E+01	9.91E-03	3.34E-02	2.74E-01	0.0E+00
2	2.86E+01	2.36E-02	6.65E-02	5.31E-01	0.0E+00
3	4.46E+01	2.69E-02	5.34E-02	5.17E-01	0.0E+00
4	4.52E+01	4.73E-02	9.91E-02	9.33E-01	0.0E+00
5	4.65E+01	4.57E-02	1.01E-01	9.25E-01	0.0E+00

Table 6.3 shows (Column V) the discrepancies between the updated the finite element results and the experimental results of the full welded structure. Reduction in the discrepancies is seen from 27.98 percent to 23.63 percent. The first frequency still shows the highest error in the updated results of the finite element model of the full welded structure. Meanwhile, the updated values of the updating parameters are shown in Table 6.4 in which the initial value of the Young's modulus has increased by 5 percent and the diameter of spot welds has increased from 5 mm to 7.1 mm.

Table 6.3: Three comparisons of results between the measured and finite element results of the full welded structure (free-free boundary conditions)

Mode	I Experiment (Hz)	II Initial FE (Hz)	III Error (%) [I-II/I]	IV Updated FE (Hz)	V Error (%) [I-IV/I]	VI Updated FE MAC
1	14.55	13.62	6.38	13.69	5.90	0.82
2	28.96	28.63	1.14	28.89	0.24	0.93
3	44.92	44.56	0.79	44.79	0.28	0.91
4	46.62	45.15	3.16	45.40	2.62	0.94
5	47.96	46.45	3.15	46.70	2.63	0.95
6	52.66	51.25	2.68	51.54	2.13	0.97
7	67.35	64.63	4.03	64.89	3.65	0.88
8	80.74	78.80	2.41	79.02	2.14	0.95
9	89.48	85.91	3.99	86.13	3.74	0.84
10	133.72	134.05	0.25	134.11	0.29	0.87
Total Error			27.98		23.63	

Table 6.4: Updated values of the parameters of the full welded structure

Parameters	Initial Value	Updated Value	Unit
Young's Modulus	210000	220500	MPa
Spot Weld	5	7.10	mm

It can be seen that the parameters (Young's modulus, and the diameter of spot welds) used in reconciling the initial finite element model of the full welded structure with the test structure are still not good enough to reduce the discrepancies especially the error in the first frequency. Obviously, in practice it is not feasible to perform experiment of the structure completely in free-free boundary conditions. The effect of the soft springs that are used to support the test

structure must be considered in the finite element modelling. Therefore, it is essential to include the effect of suspension springs (as elaborated in Section 6.2) in the finite element model updating of the full welded structure. The CBUSH element that is available in NASTRAN is used to replicate the soft springs that are used in the experiment. The initial finite element model of the full welded structure considering the effect of the suspension spring is shown in Figure 6.2.

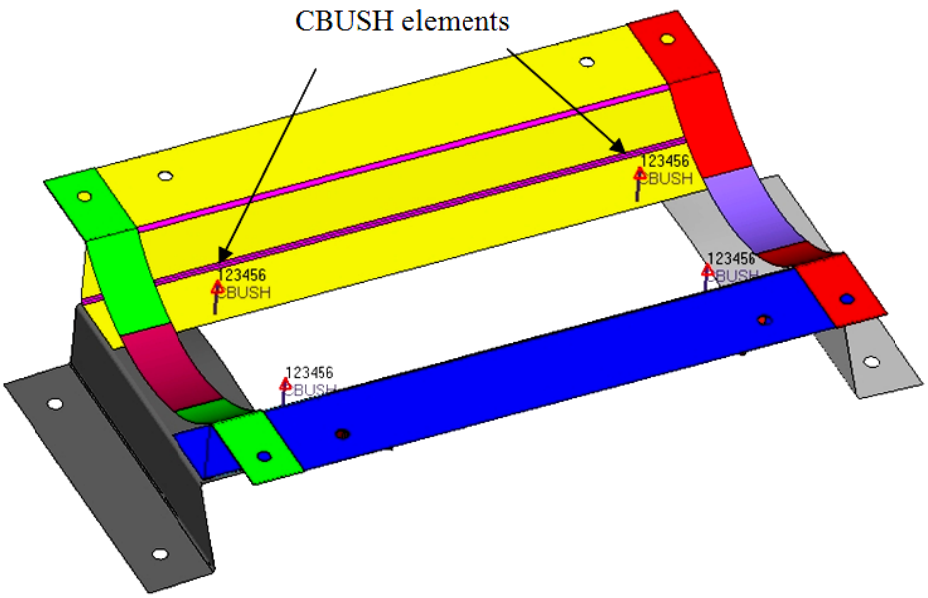

Figure 6.2: Finite element modelling of the full welded structure considering the effect of boundary conditions

A new parameter known as PBUSH (the elastic property of CBUSH elements) is introduced and included in the finite element model of the full welded structure. A new sensitivity analysis based on the new parameters is performed. Table 6.5 to Table 6.6 show a summary of the new sensitivity analysis results based on CBUSH element. From the tables, it is shown that the CBUSH merely influences the first and second frequencies. Based on five the parameters that are listed in the sensitivity analysis, only three of them are used as updating parameters of the full welded structure. These parameters are the Young's modulus, diameter of spot

welds and the CBUSH. Meanwhile, Poisson's ratio is found not sensitive to the first five frequencies.

Table 6.5: Summarised results of the sensitivity analysis of the full welded structure (suspension spring)

Mode	Frequency	Parameters		
		Young's Modulus	Shear Modulus	Spot Weld Diameter
1	4.35E+01	4.68E-02	1.01E-01	9.48E-01
2	1.42E+02	4.45E-02	9.53E-02	8.71E-01
3	1.94E+02	4.41E-02	1.27E-01	1.04E+00
4	1.97E+02	7.23E-02	8.56E-02	1.13E+00
5	2.13E+02	4.43E-02	6.05E-02	7.68E-01

Table 6.6: Summarised results of the sensitivity analysis of the full welded structure (suspension spring)

Mode	Frequency	Parameters	
		PBUSH	Poisson's Ratio
1	4.35E+01	2.36E-01	0.0E+00
2	1.42E+02	4.07E-01	0.0E+00
3	1.94E+02	1.73E-01	0.0E+00
4	1.97E+02	1.87E-01	0.0E+00
5	2.13E+02	3.32E-02	0.0E+00

Table 6.7: Three comparisons of results between the measured, the initial finite element model and the updated finite element model (with Young's modulus and PBUSH as updating parameters) of the full welded structure.

Mode	I Experiment (Hz)	II Initial FE (Hz)	III Error (%) [I-II/I]	IV Updated FE (Hz)	V Error (%) [I-IV/I]	VI Updated FE MAC
1	14.55	13.62	6.38	14.57	0.15	0.95
2	28.96	28.63	1.14	29.26	1.03	0.96
3	44.92	44.56	0.79	44.61	0.68	0.94
4	46.62	45.15	3.16	45.86	1.64	0.97
5	47.96	46.45	3.15	47.45	1.06	0.97
6	52.66	51.25	2.68	51.87	1.51	0.90
7	67.35	64.63	4.03	65.23	3.14	0.87
8	80.74	78.80	2.41	79.08	2.06	0.91
9	89.48	85.91	3.99	86.42	3.42	0.89
10	133.72	134.05	0.25	134.01	0.22	0.86
Total Error			27.98		14.90	

The updating procedure of the full welded structure is performed on the first five frequencies. The first ten frequencies of the updated finite element model of the full welded structure based on updating parameters of PBUSH, the Young's modulus and the diameter of spot welds are compared with the experimental results and are shown in Table 6.7. It can be seen, that the total error between the updated and the measured frequencies is reduced from 27.98 percent to 14.90 percent. Obviously, the error of the first frequency is significantly reduced from 6.38 percent to almost 0 percent. The significant improvement is as a result of including the effect of boundary conditions in the finite element modelling. On top of that, the correlation between the updated and the measured natural frequencies are simultaneously improved from mode 4th up to mode 10^{th}, which gives confidence in the quality of the updated model. Furthermore, the average updated MAC values for the updated finite element model of the full welded structure are improved in comparison with those calculated from the initial finite element model.

Table 6.8: Updated value of parameter of the full welded structure (suspension spring)

Parameters	Initial Value	Updated Value	Unit
Young's Modulus	210000	220500	MPa
Spot Weld	5	7.10	mm
PBUSH	1.6	1.97	N/mm

Table 6.8 shows the changes in the initial values and updated values of the parameters used in updating the finite element model of the full welded structure. It can be observed that the value of the Young's modulus has increased to 5 percent from the initial value. The diameter of spot weld has increased from 5 mm to 7.10 mm as depicted in Figure 6.3. The stiffness of PBUSH has also increased from 1.6 N/mm to 1.97 N/mm as depicted in Figure 6.4.

Figure 6.3: The measurement of the diameter of the physical spot weld

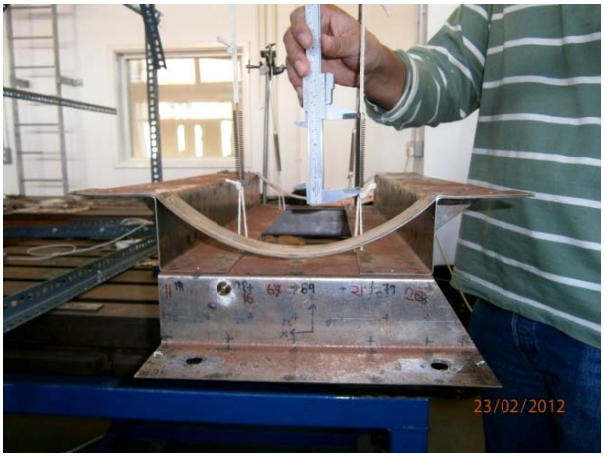

Figure 6.4: The measurement of the length of the physical suspension springs

Figure 6.5 shows the changes in the updating parameters from the initial normalised values to final values of the Young's modulus, diameter of spot welds and the PBUSH. It can be seen that the Young's modulus has converged in two iterations, followed by the diameter of spot welds into nine iterations and the PBUSH in twenty iterations.

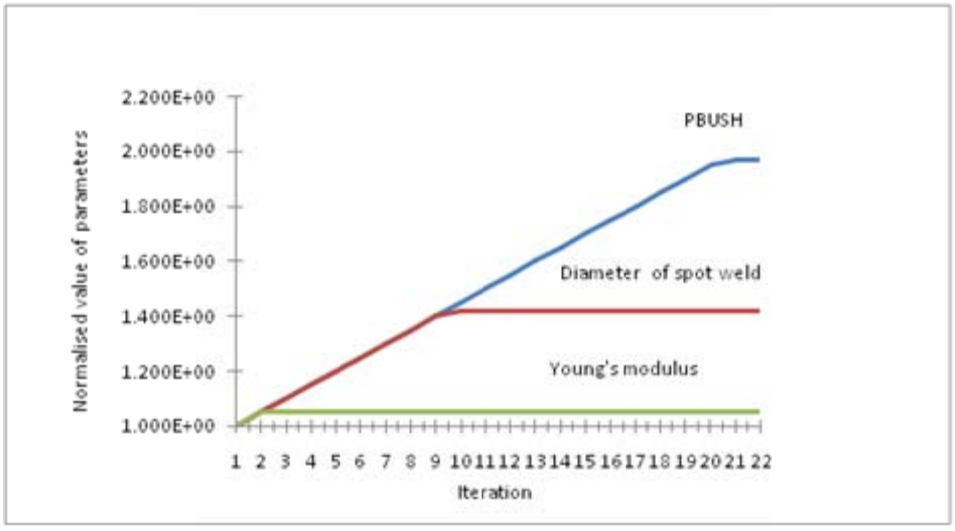

Figure 6.5: The convergence of the updating parameters of the full welded structure (suspension spring)

Tables 6.9 and Table 6.10 show the comparison of the results of the full welded structure calculated based on the different numbers of the measured frequencies defined in the objective function as shown in Equation 5.8. Column I and II represent the experimental results and the results calculated from the initial finite element model respectively. Meanwhile, column III presents the results calculated from the updated finite element model. These tables show that the larger the numbers of the measured frequencies used in the objective function, the better the results are obtained. Meanwhile, the comparison between the initial finite element mode shapes and the mode shapes of the updated full welded structure with PBUSH is shown in Figure 6.6 and Figure 6.7.

Table 6.9: The comparison of results calculated using different numbers of measured frequencies (1^{st} to 5^{th}) of the full welded structure in the objective function multiply by 100 (suspension spring)

Mode	I	II	III				
	Exp (Hz)	Initial FE (Hz)	Number of the measured frequencies				
			1 (Hz)	2 (Hz)	3 (Hz)	4 (Hz)	5 (Hz)
1	14.55	14.08	14.55	14.52	14.50	14.53	14.57
2	28.96	28.80	29.24	29.06	29.20	29.23	29.26
3	44.92	44.39	44.60	44.34	44.58	44.59	44.60
4	46.62	45.42	45.87	45.39	45.83	45.87	45.88
5	47.96	46.80	47.42	47.09	47.35	47.40	47.44
6	52.66	51.41	51.86	51.34	51.81	51.85	51.87
7	67.35	64.74	65.22	64.65	65.16	65.21	65.23
8	80.74	78.83	79.08	78.67	79.05	79.08	79.08
9	89.48	86.04	86.41	86.00	86.37	86.41	86.42
10	133.72	133.85	134.01	133.68	133.99	134.01	134.01
Total Error			0.33633	0.56120	0.35523	0.33864	0.33404

Table 6.10: The comparison of results calculated using different numbers of measured frequencies (6^{th} to 10^{th}) of the full welded structure in the objective function multiply by 100 (suspension spring)

Mode	I	II	III				
	Exp (Hz)	Initial FE (Hz)	Number of the measured frequencies				
			6 (Hz)	7 (Hz)	8 (Hz)	9 (Hz)	10 (Hz)
1	14.55	14.08	14.59	14.62	14.62	14.64	14.62
2	28.96	28.80	29.28	29.30	29.30	29.32	29.30
3	44.92	44.39	44.61	44.61	44.61	44.62	44.61
4	46.62	45.42	45.89	45.90	45.91	45.91	45.91
5	47.96	46.80	47.46	47.50	47.50	47.52	47.50
6	52.66	51.41	51.88	51.89	51.89	51.90	51.89
7	67.35	64.74	65.23	65.25	65.25	65.26	65.25
8	80.74	78.83	79.08	79.09	79.09	79.09	79.09
9	89.48	86.04	86.43	86.44	86.44	86.45	86.45
10	133.72	133.85	134.01	134.00	134.01	134.01	134.01
Total Error			0.3329	0.3300	0.3294	0.3293	0.3286

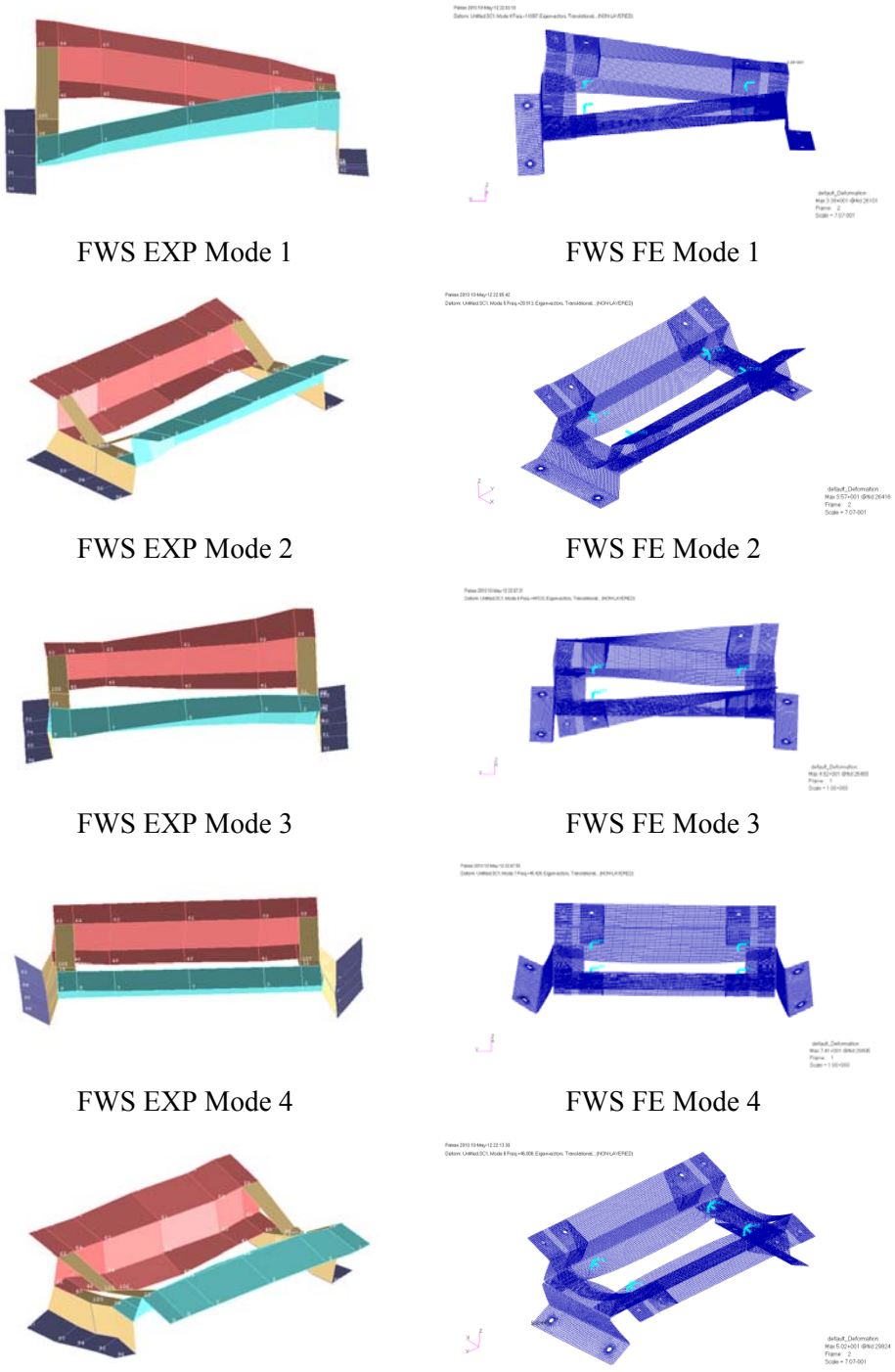

Figure 6.6: Comparison results of mode shapes (1st to 5th) between test and updated FE models of the full welded structure (suspension spring)

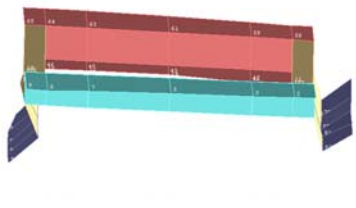

FWS EXP Mode 6

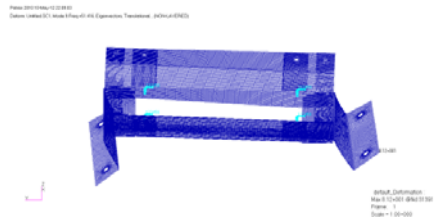

FWS FE Mode 6

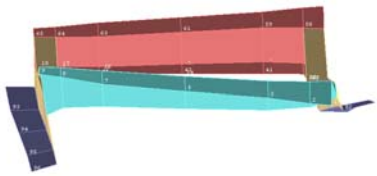

FWS EXP Mode 7

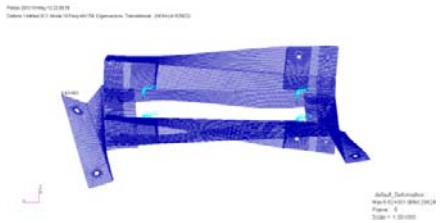

FWS FE Mode 7

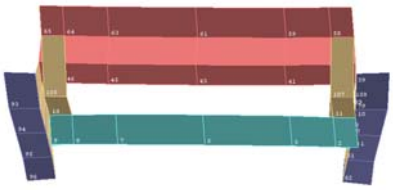

FWS EXP Mode 8

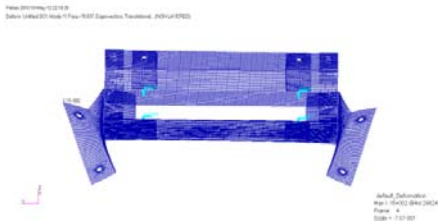

FWS FE Mode 8

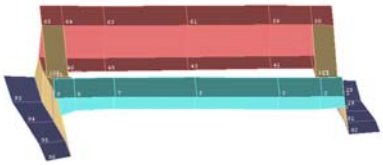

FWS EXP Mode 9

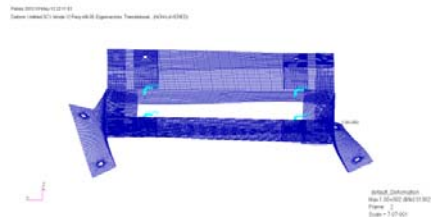

FWS FE Mode 9

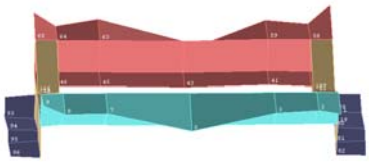

FWS EXP Mode 10

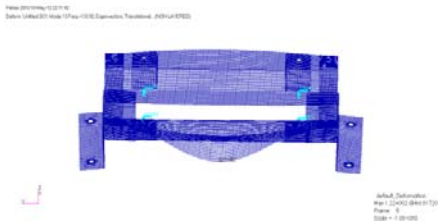

FWS FE Mode 10

Figure 6.7: Comparison results of mode shapes (6^{th} to 10^{th}) between test and updated FE models of the full welded structure (suspension spring)

6.4 Finite element modelling and updating of the full welded structure fixed boundary conditions due to bolted joints

Modelling a structure with bolted joints is very difficult and challenging. The dynamic behaviour of a structure can be significantly affected by the mass, stiffness, and damping effects of bolted joints (He and Zhu, 2011). Tsai and Chou (1988) found the mass effect of bolted joints can be easily included in the finite element model of the structure. However, the stiffness and the damping effects of a bolted joint, which are mainly related to the clamping force at each bolted connection, the pre-loadings caused by assembling the structure, and the surface properties of contact interfaces are usually difficult to model. Therefore, it is difficult to directly model a bolted joint by taking into account all the parameters mentioned above.

The limitation on model size has made modelling of a bolted joint in detail is impractical and costly in computational time. Therefore, many analysts have chosen other methods to model bolted joints. For instance, Montgomery (2002) and Kim et al. (2007) investigated the modelling techniques of bolted joints using alternative approaches such as a solid bolt model, a coupled bolt model, a spider bolt model and a no bolt model. Meanwhile, Rutman et al. (2007) and Rutman et al. (2009) utilised the combination of different types of connector elements to model the bolted joint of plates. Bograd et al. (2011) revealed that there exists no universal technique for modelling the dynamics of joints so that each application has to be examined on case-by-case basis, however each of them has advantages in some applications and limitations in others. Therefore, application of the finite element model for the analysis and design of bolted joints mechanical systems remains a difficult task.

The previous section has discussed, finite element model updating for full welded structure in free-free boundary condition. An improved finite element model of the full weld structure presented in the last section is then used in the attempt to update the finite element model with fixed boundary conditions due to bolted joints.

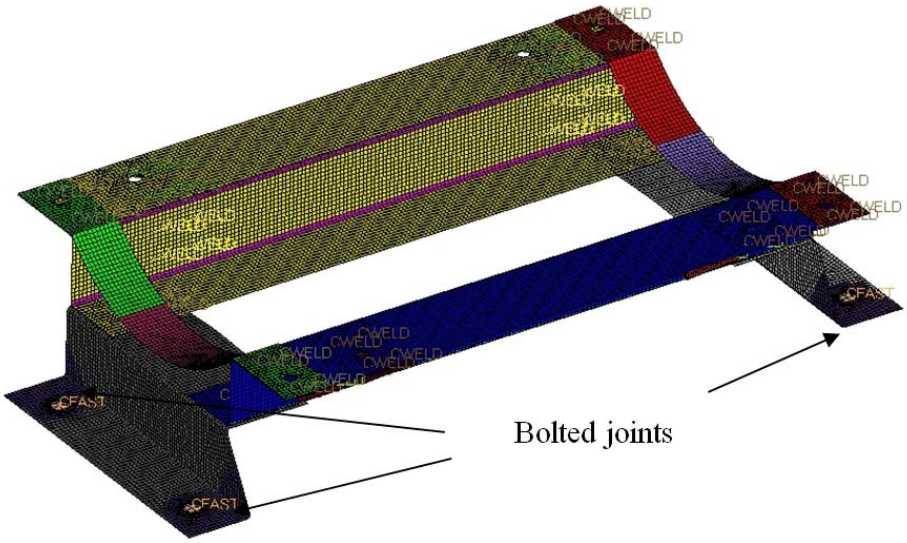

Figure 6.8: CAE Model of the full welded structure with bolted joints

CFAST elements in MSC.NASTRAN (2005a) are used to represent the bolted joints. To the author's best knowledge, modelling CFAST elements in modelling bolted joints have never been reported. An updated finite element model of the full welded structure in free-free boundary conditions as described in previous section is then modelled with fixed boundary conditions. CFAST elements are used to represent the bolted joints on the steel bar of the test bed as shown in Figure 6.10. In this work, the model updating procedure is used to improve the natural frequencies of the full welded structure up to a frequency of about 120 Hz. The initial natural frequencies and modes shapes of the full welded structure with bolted joints are computed using SOL103 of NASTRAN as shown in Table 6.11. The results show the total error of natural frequencies is approximately 35 percent and the average MAC value is above 0.7.

Table 6.11: Comparison of results between measured and the finite element model of the full welded structure with fixed boundary conditions due to bolted joints

Mode	I Experiment Frequency (Hz)	II Initial F.E Frequency (Hz)	III Relative Error [%] [I-II/I]	IV Initial FE MAC
1	26.38	25.37	3.83	0.88
2	28.41	28.37	0.15	0.83
3	34.61	33.12	4.30	0.85
4	43.50	43.45	0.11	0.79
5	45.02	44.69	0.74	0.83
6	68.67	67.49	1.71	0.78
7	84.64	76.99	9.04	0.80
8	101.48	95.24	6.15	0.73
9	124.76	113.89	8.71	0.70
Total Error			34.74	

In order to reduce the error between the initial finite element model and the measured structure, NASTRAN SOL200 is used to identify the most sensitive parameters to the frequencies. In the first attempt to update the finite element model of the full welded structure with bolted joints, parameters that are available in the properties of CFAST elements are listed in the sensitivity analysis as shown in Table 6.12 and Table 6.13. The first eight measured frequencies are used in the objective function (Equation 5.8) that is defined in NASTRAN SOL200. Table 6.12 and Table 6.13 show the sensitivity analysis results of the finite element model of the full welded structure with fixed boundary condition due to bolted joints. It can be seen that the frequencies of the finite element model of the full welded structure with fixed boundary condition due to bolted joints are sensitive to the stiffness of bolt in translation X, the rotational stiffness around the X axis, rotational stiffness around the Y axis and rotational stiffness around the Z axis. Therefore, these parameters are then used in the updating procedure of the full welded structure of fixed boundary conditions with bolted joint.

Table 6.12: Summarised results of the sensitivity analysis (diameter, the stiffness in the translations of X, Y and Z directions) of the full welded structure with fixed boundary conditions due to bolted joints

Mode	Frequency	Bolt stiffness			Diameter (mm)
		Translation in X direction (T1)	Translation in Y direction (T2)	Translation in Z direction (T3)	Bolt
1	2.54E+01	1.12E-04	6.27E-04	5.54E-04	9.94E-03
2	2.84E+01	8.36E-06	4.13E-05	5.17E-06	3.72E-04
3	3.31E+01	1.49E-07	1.78E-04	3.69E-03	-1.81E-02
4	4.35E+01	1.82E-04	2.13E-03	9.60E-04	1.49E-02
5	4.47E+01	8.99E-06	9.28E-05	5.00E-05	4.26E-04
6	6.75E+01	1.00E-03	4.18E-04	5.24E-03	1.50E-01
7	7.70E+01	6.35E-04	2.47E-03	1.87E-03	2.20E-02

Table 6.13: Summarised results of the sensitivity analysis (the rotational stiffness around the X axis, rotational stiffness around the Y axis and rotational stiffness around the Z axis) of the full welded structure with fixed boundary conditions due to bolted joints

Mode	Frequency	Bolt Stiffness		
		Rotational stiffness around X axis (R1)	Rotational stiffness around Y axis (R2)	Rotational stiffness around Z axis (R3)
1	2.54E+01	3.01E-06	1.56E-05	3.43E-07
2	2.84E+01	5.66E-07	1.27E-06	2.93E-08
3	3.31E+01	1.94E-05	3.87E-05	2.62E-06
4	4.35E+01	5.05E-06	2.71E-05	5.53E-07
5	4.47E+01	1.91E-06	6.68E-07	9.32E-10
6	6.75E+01	7.43E-06	1.19E-04	1.65E-06
7	7.70E+01	1.57E-05	7.67E-05	1.11E-06

Table 6.14 shows the updated natural frequencies of the finite element model of the full welded structure with fixed boundary conditions due to bolted joints. It can be seen that parameters of PFAST alone is unable to reduce the error as shown in Table 6.14 in column (V).

Table 6.14: Three comparisons of results between the measured and the initial finite element (FE) model of the full welded structure with fixed boundary conditions due to bolted joints

Mode	I Experiment (Hz)	II Initial FE (Hz)	III Error (%) [I-II/I]	IV Updated FE (Hz)	V Error (%) [I-IV/I]	VI Updated FE MAC
1	26.38	25.37	3.83	25.37	3.83	0.90
2	28.41	28.37	0.15	28.37	0.15	0.83
3	34.61	33.12	4.30	33.12	4.30	0.87
4	43.50	43.45	0.11	43.45	0.11	0.82
5	45.02	44.69	0.74	44.70	0.72	0.87
6	68.67	67.49	1.71	67.49	1.71	0.79
7	84.64	76.99	9.04	76.99	9.04	0.83
8	101.48	95.24	6.15	95.24	6.15	0.74
9	124.76	113.89	8.71	113.89	8.71	0.72
Total Error			34.74		34.72	

Table 6.15 shows that the updated diameter of CFAST is increased to 11.28 mm and the largest increment in CFAST stiffness is found to be in translation X direction by 1.52 percent. Meanwhile Figure 6.9 shows the initial changes of the updating parameters from the initial normalised value to convergent value.

Table 6.15: Updated value of parameter of the full welded structure with fixed boundary conditions due to bolted joints

Parameters	Initial Value (N)	Fractional Value	Updated Values (N)
Diameter of Bolt (mm)	11	1.03	11.28
Stiffness translation in X direction (KT1)	5.17E+06	1.52	7.88E+06
Stiffness rotational in X direction (KR1)	1.72E+09	1.36	2.35E+09
Stiffness rotational in Y direction (KR2)	1.63E+10	1.36	2.22E+10
Stiffness rotational in Y direction (KR3)	1.63E+10	1.45	2.36E+10

Figure 6.9: The convergence of the updating parameters of the full welded structure with fixed boundary conditions due to bolted joints

It can be seen from Table 6.14 that the usage of the parameters of CFAST alone as the updating parameters has proved to be incapable of reducing the discrepancy between the measured and predicted frequencies. Therefore, other potential parameters that may contribute to the errors are investigated.

A new approach is used to improve the correlation between the measured and the finite element model of the full welded structure with fixed boundary conditions with bolted joints by updating the parameters that related to the bolted joints of the structure. The approach includes the inclusion of washers in the assembly of the structure with fixed boundary conditions. An assumption is made by assuming the areas between the washer and the base supports are firmly tightened by the bolts and washers. The chief of the new approach are to develop and use a simple modelling method for the bolted joints of the full welded structure, through which detailed phenomena such as slip, loosing, or clearance effect, are not considered because they are believed to have less effect on the dynamic characteristic of the full welded structure with bolted joints. Therefore, the details of the finite element model of the washers are not included in the finite element model of the full assembled structure.

The initial stress ratio in MSC.NASTRAN (2005b) that has been elaborated and successfully used by Abdul Rani (2012) in investigating the effect of the clamp load during welding process is then used to represent the effect of the preload due to the bolts and washers. On top of that, the initial stress ratio is also used to investigate the effect of fabrication process of the full welded structure because the structure is made from thin metal sheets and it is very susceptible to initial curvatures due to its low flexible stiffness or fabrication error.

Even though the individual component such as the side supports and the base bent supports have been updated individually, due to uncertainties in the fabrication process and different boundary conditions they are no longer useful and new parameters need to be considered. Based on the visual inspection and the engineering judgement new regions are introduced in addition to the PFAST

proprieties. The new regions are known as initial stress ratio of washer base (Figure 6.10) and of plate centre (Figure 6.11). Different properties such as the Young's modulus, density, shear modulus and the Poisson's ratio are assigned to the new regions based on Table 3.1. The simplified model of the washer is then used to verify the accuracy of the finite element model with the measured data.

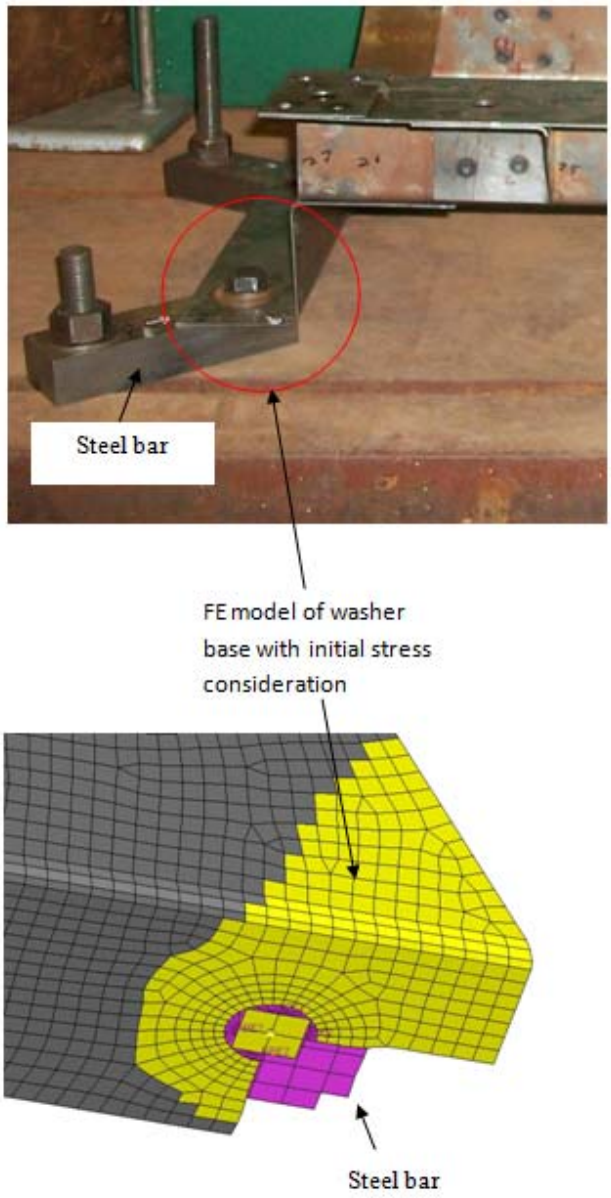

Figure 6.10: The detail of the region of the bolted joints with fixed boundary conditions

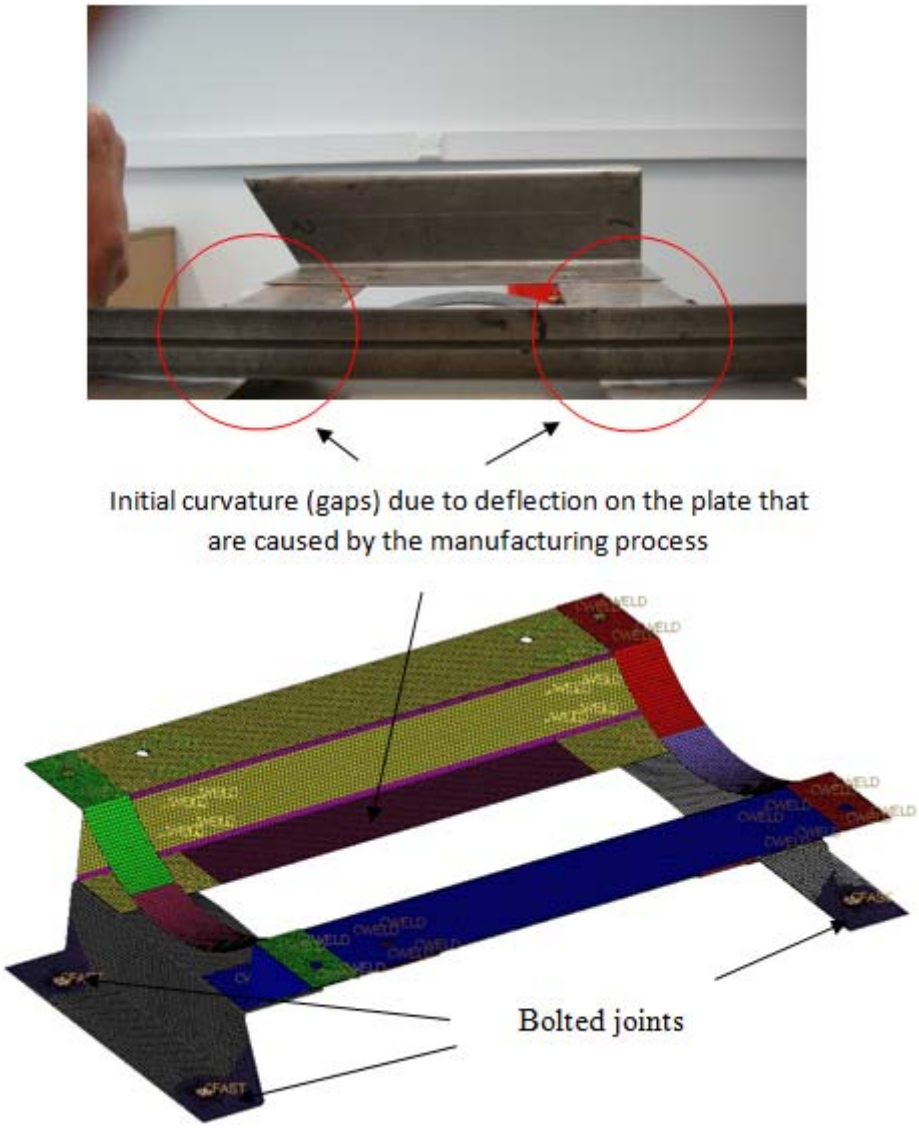

Figure 6.11: Initial curvature/gap on the centre plate of the structure.

In order to identify the sensitivity parameters, SOL200 is used to make the sensitivity analysis. The parameters that are related to CFAST, washer base and the plate centre are listed in the sensitivity analysis as shown in Table 6.16 up to Table 6.18. The first nine measured frequencies are used in the objective function (Equation 5.8) that is defined in SOL200. Table 6.16 up to Table 6.18 show the results of the sensitivity analysis of the full welded structure with initial stress ratio.

Table 6.16: Summarised results of the sensitivity analysis (Initial stress ratio and diameter) of the full welded structure with fixed boundary conditions due to bolted joints

Mode	Frequency	Initial stress ratio		Diameter (mm)
		Washer	Plate	Bolt
1	2.54E+01	9.49E-01	7.06E-01	9.94E-03
2	2.84E+01	8.32E-02	6.14E-01	3.72E-04
3	3.31E+01	4.00E+00	6.79E-02	-1.81E-02
4	4.35E+01	1.57E+00	5.66E-01	1.49E-02
5	4.47E+01	9.84E-02	5.38E-01	4.26E-04
6	6.75E+01	6.72E+00	5.61E-01	1.50E-01
7	7.70E+01	4.93E+00	1.39E+00	2.20E-02

Table 6.17: Summarised results of the sensitivity analysis (translation in X, Y and Z directions) of the full welded structure with fixed boundary conditions due to bolted joints

Mode	Frequency	Bolt Stiffness		
		Translation in X direction (K1)	Translation in Y direction (K2)	Translation in Z direction (K3)
1	2.54E+01	1.12E-04	6.27E-04	5.54E-04
2	2.84E+01	8.36E-06	4.13E-05	5.17E-06
3	3.31E+01	1.49E-07	1.78E-04	3.69E-03
4	4.35E+01	1.82E-04	2.13E-03	9.60E-04
5	4.47E+01	8.99E-06	9.28E-05	5.00E-05
6	6.75E+01	1.00E-03	4.18E-04	5.24E-03
7	7.70E+01	6.35E-04	2.47E-03	1.87E-03

Table 6.18: Summarised results of the sensitivity analysis (the rotational stiffness around the X axis, rotational stiffness around the Y axis and rotational stiffness around the Z axis) of the full welded structure with fixed boundary conditions due to bolted joints

Mode	Frequency	Bolt Stiffness		
		Rotational stiffness around X axis (R1)	Rotational stiffness around Y axis (R2)	Rotational stiffness around Z axis (R3)
1	2.54E+01	3.01E-06	1.56E-05	3.43E-07
2	2.84E+01	5.66E-07	1.27E-06	2.93E-08
3	3.31E+01	1.94E-05	3.87E-05	2.62E-06
4	4.35E+01	5.05E-06	2.71E-05	5.53E-07
5	4.47E+01	1.91E-06	6.68E-07	9.32E-10
6	6.75E+01	7.43E-06	1.19E-04	1.65E-06
7	7.70E+01	1.57E-05	7.67E-05	1.11E-06

CFAST parameters such as the stiffness in translation X, the rotational stiffness around the X axis, rotational stiffness around the Y axis and rotational stiffness around the Z axis that have been used in the first attempt of finite element model updating of fixed boundary conditions. The first and second frequencies are found sensitive to parameters of the initial stress ratio of the washer base and the centre of the plate in comparison with other frequencies.

Table 6.19 (Column V) shows the updated results of finite element model of the full welded structure with fixed boundary conditions due to bolted joints. The first seven measured frequencies and six parameters are used in the updating procedure of the finite element model of the full welded structure with bolted joints. It can be seen that the error of the updated finite element model of the full welded structure with fixed boundary conditions due to bolted joints is reduced from 34.74 percent to 21.74 percent (Table 6.19 column V) and the improvement can be seen for the 1st, 3rd and 7th to 9th frequencies.

Table 6.19: Three comparisons of the results between the measured and the initial finite element model of the full welded structure with fixed boundary conditions due to bolted joints (initial stress ratio)

Mode	I Experiment (Hz)	II Initial FE (Hz)	III Error (%) [I-II/I]	IV Updated FE (Hz)	V Error (%) [I-IV/I]	VI Updated FE MAC
1	26.38	25.37	3.83	26.22	0.61	0.92
2	28.41	28.37	0.15	28.85	1.53	0.88
3	34.61	33.12	4.30	34.76	0.44	0.91
4	43.50	43.45	0.11	44.44	2.17	0.86
5	45.02	44.69	0.74	45.19	0.37	0.90
6	68.67	67.49	1.71	70.16	2.18	0.86
7	84.64	76.99	9.04	79.59	5.97	0.85
8	101.48	95.24	6.15	99.14	2.30	0.88
9	124.76	113.89	8.71	117.07	6.16	0.87
Total Error			34.74		21.74	

Obviously, based on the updated result, the combination of CAST elements and the initial stress ratio can be used to model the effect of contact and force area the washers and overall improve the correlation between the finite element model of the full welded structure and measured data. Based on Table 6.20, it can be seen that the initial stress ratio at the washer areas is increased to 1.45 mm from 1.0 mm and the bent base plate is increased to 1.95 mm from value of 1.0 m (Figure 6.12).

Table 6.20: Updated value of parameter of the full welded structure with fixed boundary conditions (initial stress ratio)

Parameters	Initial Value	Fractional Value	Updated Values
Initial stress ratio of washer (mm)	1.0	1.45	1.45
Initial stress ratio of plate (mm)	1.0	1.95	1.95
Diameter of Bolt (mm)	11	0.90	9.90
Bolt stiffness translation in X direction, T1 (N)	5.17E+06	1.48	7.63E+06
Rotational stiffness around Y axis, R2 (N)	1.63E+10	1.41	2.30E+10
Rotational stiffness around Z axis, R3 (N)	1.63E+10	1.40	2.28E+10

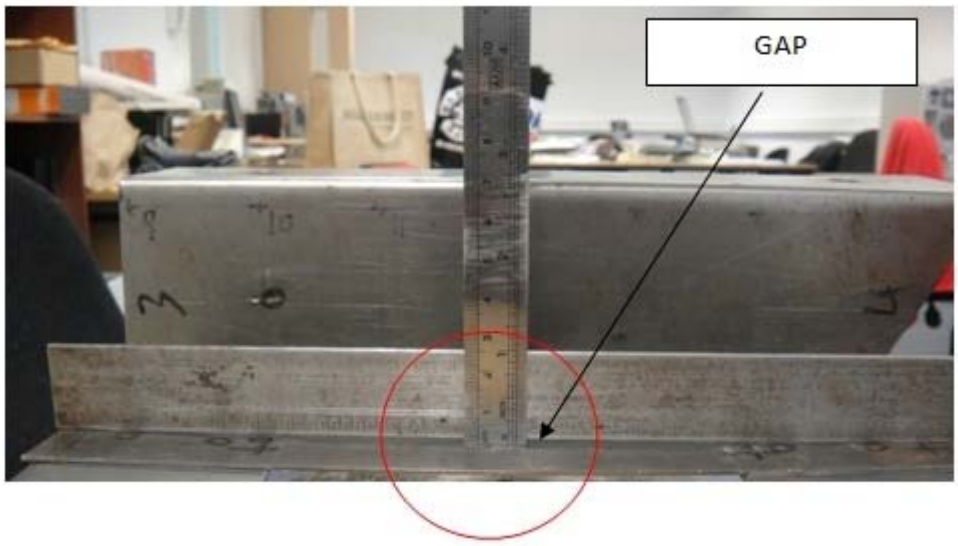

Figure 6.12: The measurement of the initial stress ratio (curvature) of the physical structure

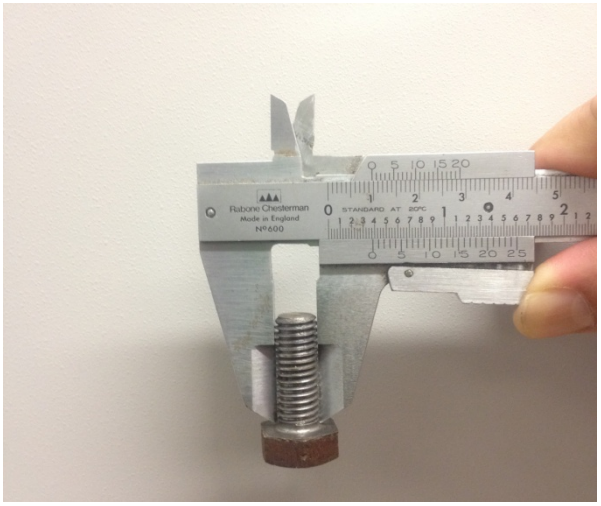

Figure 6.13: The measurement of the diameter of the physical bolt

Meanwhile, among the updated parameters of CFAST, the bolt diameter is reduced to 9.90 mm from 11.0 mm (Figure 6.13) and the stiffness in translation X direction is increased by 48 percent. Meanwhile, the rotational stiffness around the Y axis and rotational stiffness around the Z axis are also increased by 41 percent and 40 percent respectively. Figure 6.14 depicts the changes of the updating parameters from the initial normalised values to convergence value.

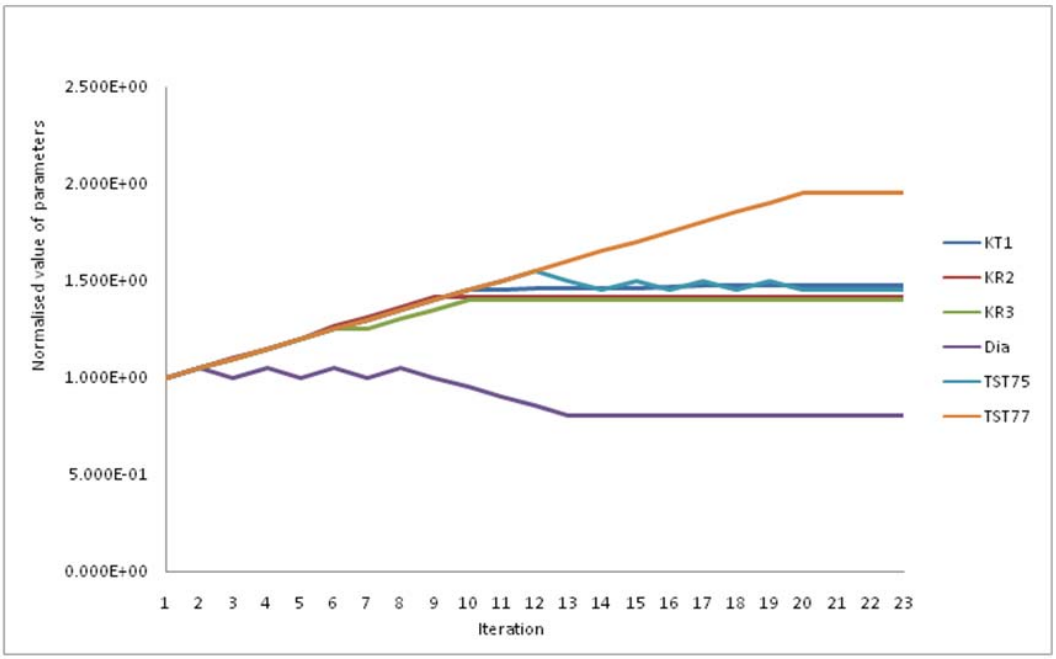

Figure 6.14: The convergence of the updating parameters of the finite element model of the full welded structure with fixed boundary conditions due to bolted joints (initial stress ratio)

Tables 6.21 up to Table 6.22 shows the comparison of the results of the finite element model of the full welded structure with fixed boundary conditions calculated based on the different numbers of the measured frequencies defined in the objective function as shown in Equation 5.8. Column I and II present the experimental results and the results calculated from the initial finite element model. Meanwhile, column III gives the results calculated from the updated finite element model. These tables show that the larger the numbers of measured frequencies used in the objective function, the better the results are obtained. Meanwhile, the comparison between the initial finite element mode shapes and the updated mode shapes of full welded structure with fixed boundary conditions is shown in Figure 6.15 and Figure 6.16.

Table 6.21: The comparison of results calculated using different numbers of measured frequencies (1^{st} to 5^{th}) of the full welded structure with fixed boundary conditions (initial stress ratio) in the objective function multiply by 100 percent

Mode	I	II	III				
	Exp (Hz)	Initial FE (Hz)	Number of the measured frequencies used				
			1 (Hz)	2 (Hz)	3 (Hz)	4 (Hz)	5 (Hz)
1	26.38	25.37	26.40	26.62	26.07	25.97	25.97
2	28.41	28.37	28.85	28.61	28.73	28.64	28.64
3	34.61	33.12	36.05	37.48	34.74	34.73	34.74
4	43.50	43.45	44.71	44.66	44.30	44.21	44.21
5	45.02	44.69	45.22	45.03	45.06	44.97	44.97
6	68.67	67.49	71.72	72.85	70.12	70.05	70.05
7	84.64	76.99	80.56	80.95	79.34	79.17	79.17
8	101.48	95.24	101.56	103.42	99.15	99.08	99.08
9	124.76	113.89	118.30	118.82	116.84	116.66	116.66
Total Error			0.97575	1.59859	0.95468	0.99474	0.99496

Table 6.22: The comparison of results calculated using different numbers of measured frequencies (6^{th} to 9^{th}) of the full welded structure with fixed boundary conditions (initial stress ratio) in the objective function multiply by 100 percent

Mode	I	II	III			
	Exp (Hz)	Initial FE (Hz)	Number of the measured frequencies used			
			6 (Hz)	7 (Hz)	8 (Hz)	9 (Hz)
1	26.38	25.37	25.85	26.21	26.18	26.36
2	28.41	28.37	28.59	28.85	28.76	28.91
3	34.61	33.12	34.41	34.76	35.20	35.21
4	43.50	43.45	44.06	44.44	44.44	44.62
5	45.02	44.69	44.91	45.19	45.10	45.27
6	68.67	67.49	69.54	70.16	70.71	70.84
7	84.64	76.99	78.78	79.58	79.77	80.07
8	101.48	95.24	98.31	99.14	100.00	100.02
9	124.76	113.89	116.17	117.07	117.37	117.68
Total Error			1.1323	0.9160	0.8893	0.8653

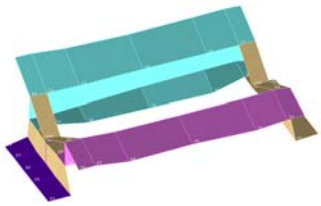

FWSBC EXP Mode 1

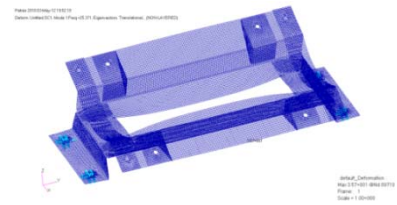

FWSBC FE Mode 1

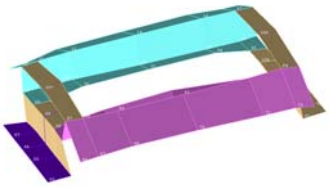

FWSBC EXP Mode 2

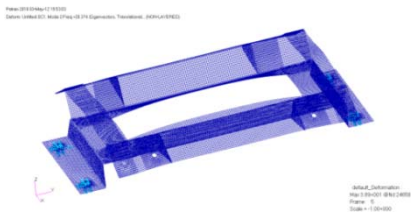

FWSBC FE Mode 2

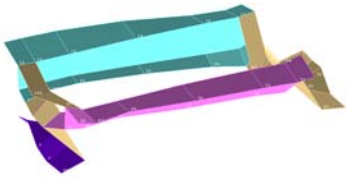

FWSBC EXP Mode 3

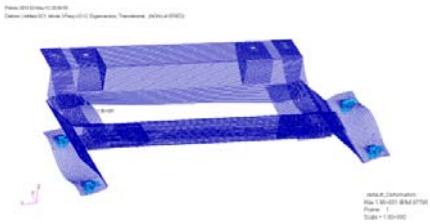

FWSBC FE Mode 3

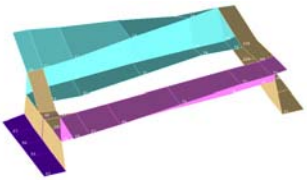

FWSBC EXP Mode 4

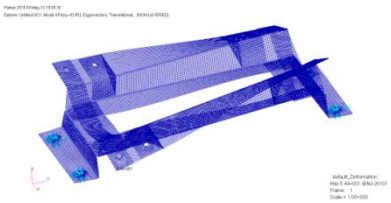

FWSBC FE Mode 4

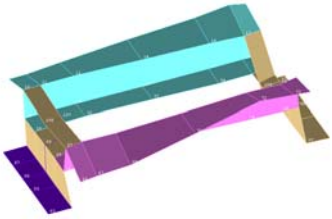

FWSBC EXP Mode 5

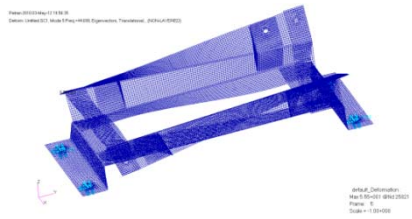

FWSBC FE Mode 5

Figure 6.15: Comparison results of mode shapes (1st to 5th) between test and updated FE models of the full welded structure with fixed boundary conditions (FWSBC)

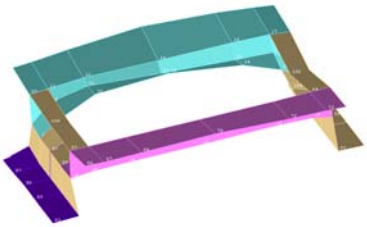

FWSBC EXP Mode 6

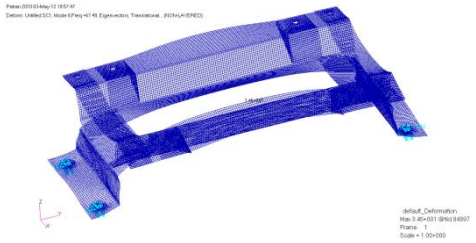

FWSBC FE Mode 6

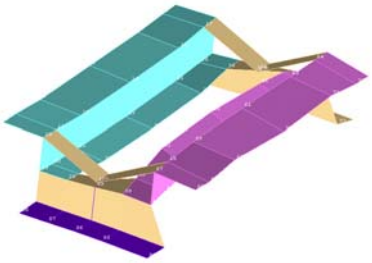

FWSBC EXP Mode 7

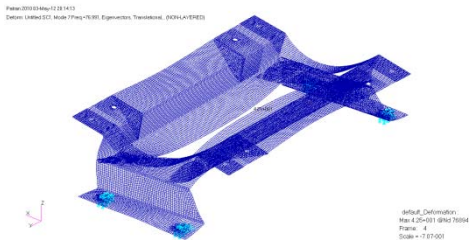

FWSBC FE Mode 7

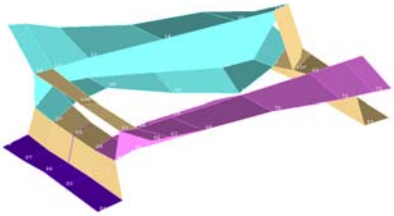

FWSBC EXP Mode 8

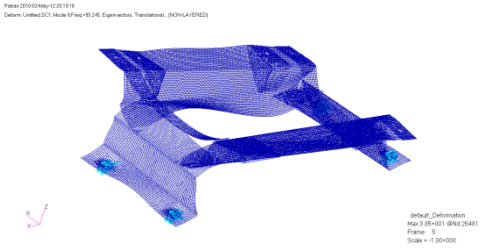

FWSBC FE Mode 8

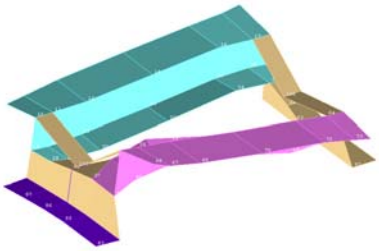

FWSBC EXP Mode 9

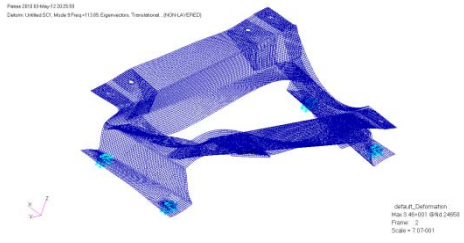

FWSBC FE Mode 9

Figure 6.16: Comparison results of mode shapes (6^{th} to 9^{th}) between test and updated FE models of the full welded structure with fixed boundary conditions (FWSBC)

6.5 Response Surface Methodology

6.5.1 Introduction

The finite element method is widely used to model large and complex structures, structural components and also to perform different types of analyses (Sinha and Friswell, 2002). However, this method is based on the approximation of the physical structure. The use of inappropriate boundary conditions, material properties and geometrical property are the factors that lead to the errors of the finite element model (Mottershead et al., 1995). On the other hand, the nominal parameter values obtained from text books for the material properties such as the Young's Modulus and shear modulus cannot guarantee to obtain accurate predicted dynamic behaviour of the actual structures.

The degree of the accuracy of a finite element model is normally verified by comparing the initial finite element model with the measured data. The lack of the credibility on the predicted results obtained from the finite element model has required the finite element model to be corrected based on the measured data. The finite element model updating is the most predominant method for improving the correlation between the initial finite element model and the measured data in order to reflect better approximation model than the initial finite element model (Titurus and Friswell, 2008 and Friswell, 2008). During the updating process the values of the model parameters such as the Young's modulus and the geometry of the model (diameter of spot welds) are systematically adjusted. The finite element model is then reformed by using the new updated parameters and the updating process is repeated until the convergence criteria are achieved. However, in model updating, the change of parameters of the finite element model should remain within the range of expected variance of the input parameters and this can be achieved by satisfying the proper parameter constraints and also by updating the most sensitive parameters of the finite element model. Dascotte and Guggenberger (2005) revealed that the results and the performance of model updating highly depended on the on the objective function, the optimization method and respective

number of parameters to be modified. On the other hand, Teughels et al. (2003) were of the opinion that the success of the application of the updating method depended on the accuracy of the numerical finite element model, the quality of the measured data, the definition of the optimisation problem and also the mathematical capabilities of the optimisation algorithm.

In iterative model updating, the recalculation of sensitivity is performed in each iteration. The sensitivity analysis is essential for iterative based optimisation methods in order to find the local minima. The iterative based methods have been widely used in model updating by many researchers because it is easy to be implemented in several commercial codes (Friswell and Mottershead, 1995a). However, the calculation of the sensitivity can be time consuming because it needs to be sequentially evaluated due to the minimisation of errors in the objective function. Therefore, model updating for a large and complex structure such as automotive structures require a large amount of computational resources both in memory requirements and CPU time due to a large number of components and different types of joints.

The function surface of the finite element model of a complex structure that is generated by the function can be rough or complex and it also consists of several local minima. Therefore, the algorithm of iterative based methods can get stuck in local minima rather than a global optimum leading to ill-conditioning (Zingg et al., 2008). The problem of getting trapped in a local minimum can be an alternatively solved by implementing the global optimisation algorithm such as evolutionary algorithm such as genetic algorithm (GA*),* simulated annealing (SA) and particle swarm optimization (PSO). Mean while the response surface method (RSM) can be used to replace the expensive the computational analysis. The RSM is a surrogate model is often used in optimisation and uncertainty quantification. The sampling method such as Latin Hypercube cube sampling is often used to generate samples of the input variables.

6.5.2 Numerical Sampling

The principle of design optimisation is to define the best possible product under certain restriction (Moens and Vandepitte, 2004). Samplings are used to generate the numerical models in order to obtain the most accurate representation of the tested model that is based on the assigned constraints. The initial sampling is also used to provide an informative picture of the function at minimum cost (Chaloner and Verdinelli, 1995). Latin hypercube sampling is one of the popular sampling methods for constructing the numerical samples. LHS is widely used as sampling technique for the propagation of uncertainty in analyses due to its simplicity and versatility (Rutherford, 2002). The Latin hypercube sampling (LHS) is an extension of the stratified sampling which ensures that each input variable has all portions of its range represented. Furthermore, LHS requires less computational effort in generating and coping with many input variables (Stein, 1987) . This technique provides more evenly distributed sampling points than random sampling techniques by ensuring a good coverage of the random parameter space (McKay et al., 1979 and Simpson et al., 2001a) . The idea is to divide the parameter space in subspaces of equal probability and the samples are taken from each subspace ensuring that every parameter is covered equally. Iman and Helton (1988) revealed that the LHS sampling exercise randomly covered the entire range of each input variable in comparison with normal sampling method.

In this section, LHS is used to create the numerical sample of the finite element model of the full welded structure with fixed boundary conditions due to bolted joints. The initial finite element model of the full welded structure with fixed boundary conditions due to bolted joints can be completely replaced by the surrogate model that is constructed based on data obtained from the numerical sample. In generating the sample, MATLAB 2011 is used. In order to obtain the reasonable values of the sample, the system parameters are allowed to vary ± 10% from the initial values. Twenty one samples are generated based on two variables namely, initial stress of bolted region and initial stress of plate region as shown in Table 6.23 up to Table 6.25.A response surface approximation is then generated based on these samples.

Table 6.23: Random sample produced by Latin hypercube sampling (sample 1 up to sample 7)

Parameters	Sample 1	Sample 2	Sample 3	Sample 4	Sample 5	Sample 6	Sample 7
Initial stress bolts (mm)	1.22	1.44	1.23	1.31	1.37	1.36	1.34
Initial stress plate (mm)	1.73	1.76	1.93	1.64	1.68	1.71	1.91

Table 6.24: Random sample produced by Latin hypercube sampling (sample 8 up to sample 14)

Parameters	Sample 8	Sample 9	Sample 10	Sample 11	Sample 12	Sample 13	Sample 14
Initial stress bolts (mm)	1.41	1.42	1.43	1.28	1.40	1.25	1.27
Initial stress plate (mm)	1.84	1.61	1.79	1.66	1.83	1.78	1.63

Table 6.25: Random sample produced by Latin hypercube sampling (sample 15 up to sample 21)

Parameters	Sample 15	Sample 16	Sample 17	Sample 18	Sample 19	Sample 20	Sample 21
Initial stress bolts (mm)	1.38	1.24	1.29	1.30	1.35	1.33	1.21
Initial stress plate (mm)	1.94	1.86	1.81	1.74	1.69	1.89	1.88

6.5.3 Response Surface Method

Response surface methodology (RSM) is a methodology that combines design of experiments (DOE) and statistical techniques and was initially developed and described by Box and Wilson (1951). RSM have been used in many areas of engineering such as chemical and mechanical industries in order to replace the experimental work (Rutherford et al., 2005). In automotive industries a vehicle structure are made from a large number of components and they are assembled with a different types of joints. Therefore to perform the finite element analysis on this type of structure, it is often time consuming and computationally expensive. RSM is a well known approach for constructing simple and fast approximations of complex computational analysis which is numerically generated by space filling method such as LHS. Alternatively, RSM is often used as inexpensive replacements for computationally expensive simulations and excessive computational time. The initial finite element model can be completely replaced by the surrogate model that is constructed based on data obtained from the numerical sampling.

The real relationship between the response and the independent variables is relatively unknown (Myers and Montgomery, 2002 and Alvarez et al., 2009) . For that reason, the first step in RSM is to find an approximation of the true functional relationship between the response and the independent variables. The function can be approximated by first order or second order polynomial (Myers et al., 1989 and Fang and Perera, 2009). In this study, the second order is used for the model fitting and it can be expressed by(Khuri and Cornell, 1987):

$$y = \beta_0 + \sum_{i=1}^{k} \beta_i x_i + \sum_{i<j} \sum \beta_{ij} x_i x_j + \sum_{i=1}^{k} \beta_{ii} x_i^2 + \varepsilon \qquad (6.1)$$

Where y is the response function of a set of design variables x_i, x_j....x_n are design variables .Meanwhile β_{ij} coefficients of unknown parameter set (i=1, 2,...k;

j =1,2,...k) from the sampling data. The parameter set can be estimated by the regression analysis and the least square method is used to estimate the regression coefficients and ε represents the model error.

In this work, there are twenty one samples that are generated from LHS based on the finite element model of the full welded structure. The samples include two variables which are the initial stress at the bolted region and the initial stress at the plate region as shown in Table 6.23 and Table 6.25. A second order polynomial function is used to fit the sample data in order to construct the surface response model. Figure 6.17 shows the response surface which is constructed based on the design variables tabulated in Table 6.23 and Table 6.25. Meanwhile Table 6.26 shows the natural frequencies obtained from the RSM. Column III shows the total error which is 22.2 %.

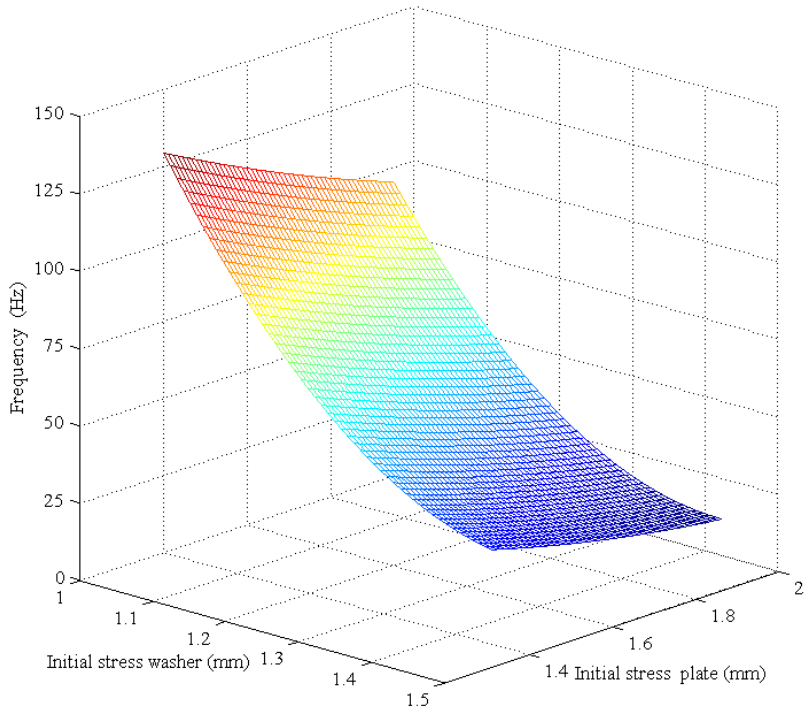

Figure 6.17: Response surface fit to the LHS design samples

Table 6.26: Comparison of results between the measured and the RSM of the full welded structure with fixed boundary conditions due to bolted joints

Mode	I Experiment Frequency (Hz)	II RSM Frequency (Hz)	III Error (%) [I-II/I]
1	26.38	26.2844	0.37
2	28.41	28.9192	1.78
3	34.61	34.9557	1.01
4	43.50	44.5120	2.34
5	45.02	45.2745	0.56
6	68.67	70.4055	2.53
7	84.64	79.8324	5.68
8	101.48	99.4485	2.00
9	124.76	117.4018	5.89
Total Error (RSM)			22.158

Table 6.27 shows the comparison of the CPU time for each method. It can be observed that iterative method is required about 4000 seconds for the model updating process. Meanwhile, the response surface method (RSM) required about 30 seconds in comparison to the iterative based method. Although the iterative based method is required a large computational efforts, however in term of accuracy the iterative based method has show a slightly better correlation (Table 6.28, column V) in comparison with RSM (Table 6.28, column VII).

Table 6.27: The comparison of results between two methods

Iterative method (seconds)	RSM (second)
4131.6	30.5

Table 6.28: Comparisons of results between the measured and the initial finite element (FE) model and RSM of the full welded structure with fixed boundary conditions due to bolted joints

Mode	I	II	III	IV	V	VI	VII
	Experiment (Hz)	Initial FE (Hz)	Error (%) [I-II/I] Initial FE	RSM (Hz)	Error (%) [I-IV/I] Updated FE	RSM (Hz)	Error (%) [I-IV/I] RSM
1	26.38	25.37	3.83	26.22	0.61	26.2844	0.37
2	28.41	28.37	0.15	28.85	1.53	28.9192	1.78
3	34.61	33.12	4.30	34.76	0.44	34.9557	1.01
4	43.50	43.45	0.11	44.44	2.17	44.5120	2.34
5	45.02	44.69	0.74	45.19	0.37	45.2745	0.56
6	68.67	67.49	1.71	70.16	2.18	70.4055	2.53
7	84.64	76.99	9.04	79.59	5.97	79.8324	5.68
8	101.48	95.24	6.15	99.14	2.30	99.4485	2.00
9	124.76	113.89	8.71	117.07	6.16	117.4018	5.89
Total Error			34.74		21.738		22.158

6.6 Closure

In this chapter, finite element modelling and updating of the full welded structure have been presented and discussed. Finite element model updating based on the iterative based method is used to minimise the discrepancies of dynamic behaviour results between the finite element models of the full welded structure and the actual structure. In these updating procedures, two finite element models of the full welded structures are used namely, the finite element model of the full welded structure with free-free boundary conditions and the finite element model of the full welded structure with fixed boundary conditions due to bolted joints.

The work has revealed that the stiffness values of the spring suspensions have a big influence on the first frequency of the finite element model of the full welded structure with free-free boundary conditions. The inclusion of the suspension stiffness as the updating parameters (boundary conditions) has significantly improved the accuracy of the first predicted frequency. The PBUSH which specifies the stiffness of CBUSH is used to represent the stiffness of the suspension springs.

A simple approach is used to represent the detailed phenomena of the bolted joints such as slip, loosening and clearance effect at the mating areas of the washers and of the bolts of the full welded structure. PFAST the properties of the CFAST element are used to represent the bolted joints of the finite element model of the full welded structure due to bolted joints. Meanwhile the initial stress ratio is used to represent the local effects in the area of the mating point of the washer, bolt and the structure. The use of the initial stress ratio which is based on engineering judgement and observation in representing the local effects has led to good agreement between updated results and the measured data.

In this work, the non deterministic optimisations namely response surface method is used (RSM) to update the full welded structure with fixed boundary conditions due to bolted joint. The efficiency and accuracy of both methods (iterative based method and RSM)) are compared.

Chapter 7

Conclusions and Future Work

7.1 Conclusions

This section presents a summary of the conclusions, main contributions and also recommendations for the future work.

7.1.1 Introduction

Thin metal sheets are widely used in manufacturing engineering products such as domestic appliances and automotive components due to their flexibility and easy to form into a variety of different shapes. However, little work has been done on finite element model updating of complex structures that are made from thin metal sheets and assembled with different types of jointing methods. Therefore, this research has sought to investigate the invalid assumptions of the initial finite element models of the components and the welded structures that are made from thin metal sheets and are joined by a number of spot welds and bolted joints.

7.1.2 Experimental Modal Analysis

Experimental modal analysis has been performed on the simplified structure of the natural gas vehicle compartment. The full welded structure consists of ten components and they are assembled by seventy two spot welds. The experimental model analyses are successfully performed in two stages (1) on the component levels and (2) the structure levels for the evaluation of the natural frequencies and the mode shapes of the components and the structures.

Several factors related to the experiments such as the number of accelerometers and measuring points, hanging orientation and excitation methods as

demonstrated and discussed in Chapter 4 are considered before performing the tests. The systematic arrangement of the accelerometers during each experiment is vital to avoid any mass loading issues. The method of roving accelerometers is preferable and used in the experiment because firstly the design of the structure is complex and secondly the structure is made from thin metal sheets which are easy to bounce back during the excitation process.

Prior to performing the experiment, the initial prediction of dynamic properties of the components and the welded structures is firstly performed. The natural frequencies and mode shapes calculated from the initial finite element is used for the selection of the excitation points (reference points) and the locations of measuring points of the components, the welded structures and the full welded structure. This is to ensure that the selected points are the optimum points that are used for the reference and also covering all the mode shapes of interest.

Two types of boundary conditions are used in the experiments namely: (1) free-free boundary conditions and (2) fixed boundary conditions. In free-free boundary conditions, a suspension spring is used to hang the structure. Meanwhile, the bolted jointed is used to fix the full welded structure to the test bed. The finite element results are compared with the measured data for verification.

7.1.3 Finite element modelling and model updating

The finite element models of the components, welded structures, and the full welded structure are developed based on CAD models. However, physical parameters of the components, welded structures and full welded structure may slightly differ from these drawings due to the fabrication issues. The fabrication issues such as machining and jointing process can cause the welded structures to deform locally. In the automotive industry, a typical body-in-white is joined by a few types of joints such as spot welds and bolted joints.

In addition, in finite element model of the bolted joint, it is very often that very fine meshes are used to at the contact region between the washers, bolt and the structure. However this leads to the time consuming and also require lot data storage. The new modelling techniques for the bolted joints which are utilising the combination of the CFAST element and the initial stress ratio has demonstrated a simple approach in modelling bolted joints and local effect especially on the thin metal sheet. Based on the updated results, the modelling method has given a good insight into the modelling of the assembled structure using the bolted joints especially for structure that is made from thin metal sheets.

In this research, finite element model updating is divided into three stages namely, the components (Chapter 5), the welded structures (Chapter 6) and the full welded structure (Chapter 7). The sensitivity analysis is used to identify the sensitive parameters of the components, the welded structures and the full welded structures. However, to identify the potential parameters to be included in the sensitivity analysis of a complex joined structure is highly based on the engineering judgement and technical observation.

Model updating is firstly performed on the components and this is to ensure that uncertainty at the component levels are minimised prior to the assembly process. Therefore, the main source of uncertainty in the welded structures is largely due to the joints. In this thesis, three connector elements (CFAST element, CWELD element ALIGN format and CWELD element ELPAT format have been investigated in representing bolted joints and spot weld especially for the automotive structure and components.
The results show that the total error of the first ten modes of CWELD element ELPAT format is 14.53 percent (Table 5.3) of the total error in comparison with CWELD element ALIGN format and CFAST element, which is 28.85 percent (Table 5.1) and 35.92 percent (Table 5.2) respectively.

Finite element model updating of the full welded structure with free-free boundary conditions revealed that the stiffness of support springs used in the

experiment is highly influential in the first mode, which is a torsional one. The error in the first frequency has reduced significantly from 13.62 percent to 0.15 percent. Based on the engineering judgement and observation, the low frequencies are seen to be highly influenced by boundary conditions especially when the structure is suspended at four corners by suspension spring/ cords. The CBUSH element is used to model the suspension springs and it is also used as the updating parameter in the updating of the full welded structure with free-free boundary conditions.

Modelling and model updating of the full welded structure with fixed boundary conditions due to bolted joint are seen to be very challenging. This is because the local phenomena especially in the mating area where the washer, bolt and the structure contact each other is normally associated with nonlinearity and it is very difficult to model. A simple and reliable procedure is required to simplify the modelling process. To update the finite element model of the full welded structure with fixed boundary conditions due to bolted joints, CFAST connector element available in NASTRAN is used to model the bolted joints. Meanwhile, the effects of loosening, the contacting area of the washer and bolt to the structure is modelled using the initial stress ratio. By including the parameters of CFAST element and initial stress ratio in the updating procedure, the total error of the finite element model of the full welded structure has reduced from 37.74 percent to 21.74 percent (Table 6.19).

The iterative finite element model updating methods which are based on the minimization of the total error in objective function are seen to be computationally expensive due to repeated calculations of the sensitivity matrix. In this research, the response surface model updating is applied to the finite element model of the full welded structure with fix boundary conditions due to bolted joints. Response surface model (RSM) is constructed in order to replace the finite element model of the full welded structure with fixed boundary conditions due to bolted joints. The Latin Hypercube Sampling technique is used to ensure the validity of the data sampling.

The efficiency of this response surface method is investigated based on its CPU time and capability of minimising the error in the initial finite element model. The results calculated from response surface method have demonstrated a reasonable outcome in comparison with those calculated from the iterative method. The comparison of the results of both methods is tabulated in Table 6.27 On top of that, in terms of CPU time, the results of the iterative methods have converged with 4131.6 second and those obtained from the response surface method have converged with 30.5 second as shown in Table 6.27. In addition, model updating via the response surface method has been successfully used in determining the optimum configuration of the initial stress ratio at the bolted joints and the plate areas

7.1.4 Contributions of the research

The contributions of this research are follows:

1. In this research, the systematic reconciliation method known as finite element model updating has been used to reconcile the initial finite element model of the components, the welded structures and the full welded structure with the measured data. The initial finite element model that is used for the structural dynamic analysis is inaccurate because of the invalid assumptions on the material properties, physical parameters, fabrication process and boundary conditions. The structural optimisation code in MSC NASTRAN (SOL 200) is used intensively in the model updating process. In this work also modal testing using impact hammer and roving accelerometers are used intensively in measuring the dynamic behaviour of the components and structures.

2. The accuracy of the results obtained from three types of connector elements (CFAST element, CWELD element ALIGN format and CWELD element ELPAT format) in MSC NASTRAN are compared. Based on

calculated results, the CWELD element in ELPAT format have shown a much better representation of spot welds and is used in representing the spot welds on the welded structures and the full welded structure.

3. The use of a new simple joint modelling technique which is the combination between CFAST element in representing bolted joints and the initial stress ratio in representing the effect of mating area of washers, bolt and the structure of the bolted joints structure has led to good agreement with the experimental results.

4. The effects of the suspension springs in the experiment of the free-free boundary conditions are investigated. The use of the CBUSH element in representing the stiffness of the suspension springs has shown good agreement with the measured data.

5. The response surface method is used to replace an excessive computer analysis of the finite element method. The accuracy and computational time on both methods (SOL 200 and response surface method) are demonstrated.

.

7.5 Recommendations for future work

The study undertaken in this thesis which covers the application of finite element modelling and model updating of the components, the welded structures and the full welded structure is presented and discussed. The application of two model updating methods namely the iterative method (SOL 200) and the response surface method (RSM) in minimising the discrepancies between the finite element models and the real structure has been investigated, demonstrated and discussed. The updated results have shown very good agreement with the measured data. Further improvement that can be done is listed below.

1. In this study, both methods are merely applied to a simplified structure of the natural gas platform due to the limited period of time. Therefore, a

complete set of the natural gas platform including tank, tank support and straps can be considered in the future work. In addition, the connector elements such as CBUSH elements can be probably used to model the effects of the gap between tank, meanwhile CFAST elements can be used to model the bolted straps.

2. Although finite element modelling and finite element model updating of the bolted joints have been performed successfully, modelling the effects of the joint interfaces between washer and structure clearly demands great attention. Therefore, the versatility of linear spring elements can be considered to be the simplest alternative method for modelling these joint interfaces.

3. The response surface method (RSM) has been successfully used as an alternative model updating to the iterative model updating method (SOL 200) which is computationally expensive. The combination of evolutionary algorithm such as genetic algorithm (GA) and response surface method (RSM) can be used for the global search with less computational effort.

4. The variability of spot welds in the full welded structure has been identified as an opportunity for performing stochastic model updating and also estimating the variability in the full welded structure.

5. The manufacturing variability that exists in spot welds has been identified as another opportunity for performing damage assessment on the structure.

Appendix A: NASTRAN input files for SOL103

Appendix A:
NASTRAN input file (.bdf) for Normal Modes analysis (SOL 103) of the full welded structure with fixed boundary conditions due to bolted joints

```
$ Direct Text Input for Nastran System Cell Section
$ Normal Modes Analysis, Database
SOL 103
CEND
TITLE = THIS IS A DEFAULT SUBCASE.
ECHO = NONE
RESVEC = NO
SUBCASE 1
  TITLE=This is a default subcase.
  METHOD = 1
  SPC = 1
  VECTOR(PRINT,PUNCH,SORT1,REAL)=1
$ Direct Text Input for this Subcase
BEGIN BULK
PARAM   AUTOSPC YES
PARAM    POST    -1
PARAM   COUPMASS 1
$PARAM    WTMASS .001
PARAM   PRTMAXIM YES
PARAM   BAILOUT  -1
EIGRL,    1,      1.,        ,    10,      0,        ,            ,  MASS
$ Elements and Element Properties for region : pshell.75
%PSHELL, 75 ,    75  ,   1.18  ,   75  ,   %1.0    , 75   , .833333  ,
$ Elements and Element Properties for region : pshell.77
%PSHELL, 77 ,    77  ,   1.18  ,   77  ,   %1.0    , 77   , .833333  ,
INCLUDE 'model.dat'
$ Fastener elements and properties for region : pfast.21
```

```
$ Pset: "pfast.21" will be imported as: "pfast.21"
%PFAST,21,%10.,-1,,1.65+9,1.80+9,1.80+9,1.72+9
,3.62+7,1.36+10,0.

$ Loads for Load Case : Default
$SPCADD,   2 ,   1
$ Displacement Constraints of Load Set : spc.1
SPC1     1       123456  170693  170701  170709  170717  170885  170893
         170901  170909  171077  171085  171093  171101  171273  171281
         171289  171297
$ Referenced Coordinate Frames
ENDDATA d22b8a73
```

Appendix B: NASTRAN input files for SOL200

Appendix B:
NASTRAN input file (.bdf) for SOL 200 (optimisation code) of the full welded structure with fixed boundary conditions due to bolted joints

```
SOL 200
TIME 600
$ Direct Text Input for Executive Control
CEND
SET 1 = 9
TITLE = MD Nastran job created on 11-Apr-08 at 12:17:04
ECHO = NONE
MAXLINES = 999999999
DESOBJ(MIN) = 60

DSAPRT (START=1,END=LAST,EXPORT)=ALL
ANALYSIS = MODES
SUBCASE 1
  METHOD = 1
  SPC = 2
  VECTOR(SORT1,REAL)=1
  SPCFORCES(SORT1,REAL)=1
BEGIN BULK
PARAM,GRDPNT,0
PARAM    POST    0
PARAM   COUPMASS 1
PARAM   OPEXIT   4
PARAM   IUNIT    13
PARAM   PRTMAXIM YES
EIGRL    1       1.      200.     10      0                    MASS
$ Elements and Element Properties for region : pshell.12
PSHELL   12      12      1.18     12              12
$ Pset: "pshell.12" will be imported as: "pshell.12"
CQUAD4   123600  12      25898   25866   25867   25901   0.      0.
.
.
.
GRID     171664          -31.751 -114.   -68.2
$ Loads for Load Case : Default
SPCADD   2       1
$ Displacement Constraints of Load Set : spc.1
SPC1     1       123456  170693  170701  170709  170717  170885  170893
```

```
      170901  170909  171077  171085  171093  171101  171273  171281
      171289  171297

$ ...DESIGN VARIABLE DEFINITION
$ K_PFAST_1
DESVAR   1     KT1     1.      1.0E-1  40.5     .01
.
.
.
$ K_PFAST_5
DESVAR   5     KR2     1.      1.0E-1  20.5     .01
.
$ K_PFAST_6
DESVAR   6     KR3     1.      1.0E-1  20.5     .01
.
$ Dia_PFAST_21
DESVAR   7     Dia     1.      .8      1.10     .01
.
$ TST_9
DESVAR   10    TST75   1.      .05     4.0      .01
.
$ TST_11
DESVAR   13    TST77   1.      .05     4.0      .01

$ ...DEFINITION OF DESIGN VARIABLE TO ANALYSIS MODEL
PARAMETER RELATIONS

DVPREL1  1      PFAST   21      KT1
      1      5.172+06
.
.
.
DVPREL1  5      PFAST   21      KR2
      5      1.63+10
.
DVPREL1  6      PFAST   21      KR3
      6      1.63+10
.
DVPREL1  7      PFAST   21      D
      7      11.
.
DVPREL1 10     PSHEll   75      6
      10     1.0
.
DVPREL1 13     PSHEll  77      6
      13     1.0
.
$ ...STRUCTURAL RESPONSE IDENTIFICATION
```

```
DRESP1,1      ,FREQ_1 ,FREQ   ,      ,      ,1
DRESP1,2      ,FREQ_2 ,FREQ   ,      ,      ,2
DRESP1,3      ,FREQ_3 ,FREQ   ,      ,      ,3
DRESP1,4      ,FREQ_4 ,FREQ   ,      ,      ,4
DRESP1,5      ,FREQ_5 ,FREQ   ,      ,      ,5
DRESP1,6      ,FREQ_6 ,FREQ   ,      ,      ,6
DRESP1,7      ,FREQ_7 ,FREQ   ,      ,      ,7
DRESP2,60     ,SUU    ,70
        DRESP1  1     2        3        4        5        6
                7
DEQATN  70     SUU(F1,F2,F3,F4,F5,F6,F7)=
           (F1/26.40-1.)**2+(F2/28.44-1.)**2 +
           (F3/34.70-1.)**2+(F4/43.50-1.)**2 +
                (F5/45.04-1.)**2+(F6/68.66-1.)**2 +
                (F7/84.64-1.)**2

$ ...OPTIMIZATION CONTROL
DOPTPRM  DESMAX 30      FSDMAX  0      P1     0      P2     1
      METHOD  1      OPTCOD  MSCADS  CONV1  .001    CONV2  1.-20
      CONVDV .001    CONVPR .01      DELP   .2      DELX   .5
      DPMIN  .01     DXMIN  .05      CT     -.03    GMAX   .005
      CTMIN  .003
ENDDATA
```

References

ABDUL RANI, M. N., STANCIOIU, D., YUNUS, M. A., OUYANG, H., DENG, H. & JAMES, S. 2011. Model updating for a welded structure made from thin steel sheets. *Applied Mechanics and Materials,* 70**,** 117-122.

ABU HUSAIN, N., KHODAPARAST, H. H. & OUYANG, H. 2010. FE model updating of welded structures for identification of defects. *International Journal of Vehicle Noise and Vibration,* 6**,** 163-175.

ABU HUSAIN, N., HADDAD KHODAPARAST, H. & OUYANG, H. 2012. Parameter selection and stochastic model updating using perturbation methods with parameter weighting matrix assignment. *Mechanical Systems and Signal Processing,* 32**,** 135-152.

ABU HUSAIN, N., KHODAPARAST, H. H., SNAYLAM, A., JAMES, S., DEARDEN, G. & OUYANG, H. 2010. Finite-element modelling and updating of laser spot weld joints in a top-hat structure for dynamic analysis. *Proceedings of the Institution of Mechanical Engineers, Part C: Journal of Mechanical Engineering Science,* 224**,** 851-861.

ABU HUSAIN, N., SNAYLAM, A., KHODAPARAST, H. H., JAMES, S., DEARDEN, G. & OUYANG, H. 2009. FE model updating for damage detection - Application to a welded structure. *Key Engineering Materials,* 413-414**,** 393-400.

AGILENT TECHNOLOGIES 2000. *The Fundamentals of Modal Testing*.

AHMADIAN, H., MOTTERSHEAD, J. E., JAMES, S., FRISWELL, M. I. & REECE, C. A. 2006. Modelling and updating of large surface-to-surface joints in the AWE-MACE structure. *Mechanical Systems and Signal Processing,* 20**,** 868-880.

AKULA, V. R. & GANGULI, R. 2003. Finite element model updating for helicopter rotor blade using genetic algorithm. *AIAA JOURNAL,* 41**,** 554-556.

ALVAREZ, M. J., ILZARBE, L., VILES, E. & TANCO, M. 2009. The use of genetic algorithms in response surface methodology. *Quality Technology and Quantitative Management,* 6**,** 295-307.

ARGYRIS, J. H. 1954. Energy theorems and structural analysis a generalized discourse with applications on energy principles of structural analysis including the effects of temperature and non-linear stress-strain relations. *Aircraft Engineering and Aerospace Technology,* 26**,** 347 - 356.

ARORA, V. 2011. Comparative study of finite element model updating methods. *Journal of Vibration and Control,* 17**,** 2023-2039.

ASMA, F. & BOUAZZOUNI, A. 2005. Finite element model updating using FRF measurements. *Shock and Vibration,* 12**,** 377-388.

BARUCH, M. 1978. Optimization procedure to correct stiffness and flexibility matrices using vibration tests. *AIAA J,* 16**,** 1208-1210.

BATHE, K. J. 1982. *Finite element procedures in engineering analysis [by] Klaus-Jurgen Bathe*, Englewood Cliffs N.J.: Prentice-Hall, 1982.

BAUMAL, A. E., MCPHEE, J. J. & CALAMAI, P. H. 1998. Application of genetic algorithms to the design optimization of an active vehicle suspension system. *Computer Methods in Applied Mechanics and Engineering,* 163**,** 87-94.

BERMAN, A. & FLANNELLY, W. G. 1971. Theory of incomplete models of dynamic structures. *AIAA JOURNAL,* 9**,** 1481-1487.

BERMAN, A. & NAGY, E. J. 1983. Improvement of a large analytical model using test data. *AIAA JOURNAL,* 21**,** 1168-1173.

BHATTI, Q. I., OUISSE, M. & COGAN, S. 2011. An adaptive optimization procedure for spot-welded structures. *Computers and Structures,* 89**,** 1697-1711.

BLAKELY, K. 1991. Updating MSC/NASTRAN models to match test data. *The MSC 1991 World Users' Conf. Proc.,* 2.

BLEVINS, R. D. 1979. *Formulas for natural frequency and mode shape,* Malabar (Fla), Krieger publishing company.

BLOT, B. 1996. Amélioration des résultats de calcul de caisse. *Third International SIA Congress*.

BOGRAD, S., REUSS, P., SCHMIDT, A., GAUL, L. & MAYER, M. 2011. Modeling the dynamics of mechanical joints. *Mechanical Systems and Signal Processing,* 25**,** 2801-2826.

BOX, G. E. P. & WILSON, K. B. 1951. On the experimental attainment of optimum conditions. *Journal of the Royal Statistical Society. Series B (Methodological),* 1.

BREHM, M., ZABEL, V. & BUCHER, C. 2010. An automatic mode pairing strategy using an enhanced modal assurance criterion based on modal strain energies. *Journal of Sound and Vibration,* 329**,** 5375-5392.

BRIAN, J. S. & MARK, H. R. 1999. Experimental modal analysis. *CSI Reliability Week.* Orlando, FL.

BROCKENBROUGH, R. & MERRITT, F. S. 2011. *Structural steel designers' handbook Frederick S. Merritt: editor*, New York: McGraw-Hill, 2011.

BROWNJOHN, J. M. W., PAN, T. C. & DENG, X. Y. 2000. Macro-updating of finite element modelling for core systems of tall buildings. *The 14th ASCE Engineering Mechanics Conference.* Austin, Texas

BROWNJOHN, J. M. W. & XIA, P. Q. 2000. Dynamic assessment of curved cable-stayed bridge by model updating. *Journal of structural engineering New York, N.Y.,* 126**,** 252-260.

BURNETT, M. A. & YOUNG, W. G. Modal correlation and updating of a vehicle body-in-white. *In:* SAS, P. & BERGEN, B., eds., 2008. Leuven, ISMA, 1825-1838.

CANYURT, O. E., KIM, H. R. & LEE, K. Y. 2008. Estimation of laser hybrid welded joint strength by using genetic algorithm approach. *Mechanics of Materials,* 40**,** 825-831.

CARLO, P., VALENTINO, P., ALBERTO, C. & GRANT, S. 2002. The use of design of experiments (DOE) and response surface analysis (RSA) in PSO. *Product and System Optimization.* Copenhagen: FENET NAFEMS.

CARNE, T. G. & DOHRMANN, C. R. Support conditions, their effect on measured modal parameters. 1998. United States, SPIE International Society of Optical, 477-483.

CARNE, T. G., GRIFFITH, D. T. & CASIAS, M. E. 2007. Support conditions for experimental modal analysis. *Sound & Vibration,* 41**,** 10-16.

CEASER, B. 1987. Updating system matrices using modal test data. *Proceedings of the fifth IMAC,* 12**,** 453–459.

CHALONER, K. & VERDINELLI, I. 1995. Bayesian experimental design: a review. *Statistical Science,* 10**,** 273-304.

CHAMBERS, L. 2001. *The practical handbook of genetic algorithms : applications / edited by Lance Chambers*, Boca Raton, Fla. ; Chapman & Hall/CRC 2001. 2nd ed.

CHANG, D. C. 1974. Effect of flexible connections on body structural response. *SAE Technical papers,* 83**,** 233-244.

CHELLINI, G., DE ROECK, G., NARDINI, L. & SALVATORE, W. 2008. Damage detection of a steel-concrete composite frame by a multilevel approach: Experimental measurements and modal identification. *Earthquake Engineering and Structural Dynamics,* 37**,** 1763-1783.

CLOUGH, R. W. The finite element method in plane stress analysis. Proceedings Second ASCE Conference on Electronic Computation, 1960 Pittsburgh, PA., 345-378.

COLEY, D. A. 1999. *An introduction to genetic algorithms for scientists and engineers / David A. Coley*, Singapore ; World Scientific, 1999.

COOK, R. R. 1983. Modern automotive structural analysis. *Shock & Vibration Digest,* 15**,** 39-39.

CORREIA, D. S., GONÇALVES, C. V., DA CUNHA JR, S. S. & FERRARESI, V. A. 2005. Comparison between genetic algorithms and response surface methodology in GMAW welding optimization. *Journal of Materials Processing Technology,* 160**,** 70-76.

CUNHA, A., CAETANO, E. & DELGADO, R. 2001. Dynamic tests on targe cable-stayed bridge. *Journal of Bridge Engineering,* 6**,** 54-62.

DASCOTTE, E. Practical applications of finite element tuning using experimental modal data. Proceedings of the 8th International Modal Analysis Conference, 1990 Orlando, Florida., 1032-1037.

DASCOTTE, E. & GUGGENBERGER, J. 2005. In search of simulating reality validation and updating of FE models for structural Analysis. *23rd CADFEM Users' Meeting 2005 International Congress on FEM Technology with ANSYS CFX & ICEM CFD Conference.* International Congress Center Bundeshaus Bonn, Germany.

DAVID-WEST, O. S., WANG, J. & COOPER, R. 2010. Finite element model updating of a thin wall enclosure under impact excitation. 24-25**,** 337-342.

DE ALBA, R. O., FERGUSON, N. S. & MACE, B. R. 2009a. Dynamic analysis of structures with uncertain point connections. *Noise and Vibration Emerging Methods : NOVEM 2009,* 17**,** 1-12.

DE ALBA, R. O., FERGUSON, N. S. & MACE, B. R. (eds.) 2009b. *A multipoint constraint model for the vibration of spot welded structures*: ISVR Technical Memorandum 982.

DE FARIA, A. R. & DE ALMEIDA, S. F. M. 2006. The maximization of fundamental frequency of structures under arbitrary initial stress states. *International Journal for Numerical Methods in Engineering,* 65**,** 445-460.

DENG, X., CHEN, W. & SHI, G. 2000. Three-dimensional finite element analysis of the mechanical behavior of spot welds. *Finite Elements in Analysis and Design,* 35**,** 17-39.

DONDERS, S., BRUGHMANS, M., HERMANS, L., LIEFOOGHE, C., VAN DER AUWERAER, H. & DESMET, W. 2006. The robustness of dynamic vehicle performance to spot weld failures. *Finite Elements in Analysis and Design,* 42**,** 670-682.

DONDERS, S., BRUGHMANS, M., HERMANS, L. & TZANNETAKIS, N. 2005. The effect of spot weld failure on dynamic vehicle performance. *Sound and Vibration,* 39**,** 16-25.

DUQUE, O. A. S., DE MUNCK, M., STENTI, A., MOENS, D. & SENIN, A. R. The fuzzy parameterization method for model updating: application to welded joints. *In:* SAS, P. & DE MUNCK, M., eds. Proceedings of the International Conference on Noise and Vibration Engineering ISMA 2006, 2006 Leuven, Belgium. Department Werktuigkunde Katholieke Universiteit Leuven, Heverlee Belgium, 2567-2578.

DYER, S. A. 2001. *Survey of instrumentation and measurement,* Canada, John Wiley and Sons.

EWINS, D. J. 2000. *Modal testing : theory, practice, and application / D.J. Ewins*, Baldock : Research Studies Press, 2000. 2nd ed.

EWINS, D. J. & IMREGUN, M. 1986. State of the art assessment of structural dynamic response analysis models (DYNAS). *Shock and Vibration Bulletin,* 56**,** 59-90.

EWINS, D. J., SILVA, J. M. & MALECI, G. 1980. Vibration analysis of a helicopter with an externally-attached structure. *Shock and Vibration Bulletin,* 50**,** 155-170.

FANG, J., HOFF, C., HOLMAN, B., MUELLER, F. & WALLERSTEIN, D. 2000. Weld modelling with MSC.NASTRAN. *Second MSC Worldwide Automotive User Conference.* Dearborn, MI, USA: MSC Software.

FANG, S. E. & PERERA, R. 2009. A response surface methodology based damage identification technique. *Smart Materials and Structures,* 18**,** 1-14.

FARRAR, C. R., WORDEN, K., TODD, M. D., PARK, G., NICHOLS, J., ADAMS, D. E., BEMENT, M. T. & FARINHOLT, K. 2007. Nonlinear system identification for damage detection. Los Alamos National Laboratory: Los Alamos National Security, LLC, for the National Nuclear Security Administration of the U.S. Department of Energy.

FONG, K. L. J. 2005. *A study of curvature effects on guided elastic wave.* PhD, Imperial College London, University of London.

FOX, R. L. & KAPOOR, M. P. 1968. Rates of change of eigenvalues and eigenvectors. *AIAA JOURNAL,* 6**,** 2426-2429.

FRISWELL, M. I. 2008. Inverse problems in structural dynamics. *Second International Conference on Multidisciplinary Design Optimization and Applications*, 1-12.

FRISWELL, M. I. & MOTTERSHEAD, J. E. 1995a. Best practice in finite element model updating. *International Forum on Aeroelasticity and Structural Dynamics,* 2**,** 1-11.

FRISWELL, M. I. & MOTTERSHEAD, J. E. 1995b. *Finite element model updating in structural dynamics*, Kluwer Academic, Dordrecht, 1995.

FRISWELL, M. I. & MOTTERSHEAD, J. E. 2001. Physical understanding of structures by model updating. *International Conference on Structural System Indentification,* 1**,** 81-96.

FRISWELL, M. I., MOTTERSHEAD, J. E. & AHMADIAN, H. 2001. Finite–element model updating using experimental test data: parametrization and regularization. *Philosophical Transactions of the Royal Society of London. Series A: Mathematical, Physical and Engineering Sciences,* 359**,** 169-186.

FRISWELL, M. I., PENNY, J. E. T. & GARVEY, S. D. 1997. Parameter subset selection in damage location. *Inverse Problems in Engineering,* 5**,** 189-215.

FRITZEN, C. P., JENNEWEIN, D. & KIEFER, T. 1998. Damage detection based on model updating methods. *Mechanical Systems and Signal Processing,* 12**,** 163-186.

GAUL, L. & NITSCHE, R. 2001. The role of friction in mechanical joints. *Applied Mechanics Reviews,* 54**,** 93-106.

GIUNTA, A. A., GOLIVIDOV, O., KNILL, D. L., GROSSMAN, B., MASON, W. H. & WATSON, L. T. 1997. Multidisciplinary design optimazation of advanced aircraft configurations. Germany, : Springer.

GUPTA, K. K. & MEEK, J. L. 1996. A brief history of the beginning of the finite element method. *International Journal for Numerical Methods in Engineering,* 39**,** 3761-3774.

HAUPT, R. 1995. Comparison between genetic and gradient-based optimisation algorithms for solving electromagnetics problems. *IEEE Transaction of Magnetics,* 31**,** 1932-1935.

HE, J. & EWINS, D. J. 1986. Analytical stiffness matrix correction using measured vibration modes. *The international Journal of Analytical and Experimental Modal Analysis,* 1**,** 9-14.

HE, K. & ZHU, W. D. 2009. Modeling of fillets in thin-walled beams using shell/plate and beam finite elements. *Journal of Vibration and Acoustics,* 131**,** 051002.

HE, K. & ZHU, W. D. 2011. Finite element modeling of structures with L-shaped beams and bolted joints. *Journal of Vibration and Acoustics -Transaction of The ASME,* 133.

HEISERER, D., SIELAFF, J. & CHARGIN, M. (eds.) 1999. *High performance, process oriented, weld spot approach,* 1st MSC Worldwide Automotive User Conference.

HELTON, J. C. & DAVIS, F. J. 2003. Latin hypercube sampling and the propagation of uncertainty in analyses of complex systems. *Reliability Engineering and System Safety,* 81**,** 23-69.

HEMEZ, F. M. & DOEBLING, S. W. 2001. Review and assessment of model updating for non-linear, transient dynamics. *Mechanical Systems and Signal Processing,* 15**,** 45-74.

HEYLEN, W., LAMMENS, S. & SAS, P. 1998. *Modal analysis theory and testing / Ward Heylen, Stefan Lammens, Paul Sas , 2nd ed,* Leuven, Belgium, Belgium : Katholieke Universiteit Leuven.

HILL, W. J. & HUNTER, W. G. 1966. A Review of response surface methodology: A literature survey. *Technometrics***,** 571.

HOLLAND, J. H. 1975. *Adaptation in natural and artificial systems: an introductory analysis with applications to biology, control, and artificial intelligence*, Ann Arbor: University of Michigan Press, 1975.

HORTON, B., GURGENCI, H., VEIDT, M. & FRISWELL, M. I. Finite element model updating of the welded joints in a tubular H-frame. IMAC XVII-Proceedings of the 17th International Modal Analysis Conference, 1999. 1556-1562.

IBRAHIM, R. & PETTIT, C. 2005. Uncertainties and dynamic problems of bolted joints and other fasteners. *Journal of Sound and Vibration,* 279**,** 857-936.

IMAN, R. L. & HELTON, J. C. 1988. An Investigation of uncertainty and sensitivity analysis techniques for computer models. *Risk Analysis,* 8**,** 71-90.

IMREGUN, M. & VISSER, W. J. 1991. A Review of model updating techniques. *Shock & Vibration Digest*, 23**,** 9-20

KHAN, Z. & PRASAD, B. 1997. Machining condition optimization by genetic algorithms and simulated annealing. *Computers & Operations Research,* 24**,** 647-657.

KHANNA, S. K. & LONG, X. 2008. Residual stresses in resistance spot welded steel joints. *Science and technology of welding and joining,* 13**,** 278-288.

KHODAPARAST, H. H. 2010. *Stochastic finite element model updating and its application in aeroelasticity*, Liverpool : Thesis Ph.D., 2010.

KHOO, L. P. & CHEN, C. H. 2001. Integration of response surface methodology with genetic algorithms. *International Journal of Advanced Manufacturing Technology,* 18**,** 483-489.

KHURI, A. I. & CORNELL, J. A. 1987. *Response surfaces: designs and analyses*, New York: Dekker, 1987.

KIM, D., RHEE, S. & PARK, H. 2002. Modelling and optimization of a GMA welding process by genetic algorithm and response surface methodology. *International Journal of Production Research,* 40**,** 1699-1711.

KIM, J., YOON, J. C. & KANG, B. S. 2007. Finite element analysis and modeling of structure with bolted joints. *Applied Mathematical Modelling,* 31**,** 895-911.

KNIGHT, C. E. 1993. *Finite element method in mechanical design*, Belmont (Calif.): Wadsworth, 1993.

KOCIS, L. & WHITEN, W. J. 1997. Computational investigations of low-discrepancy sequences. *ACM Transactions on Mathematical Software,* 23**,** 266-294.

KOMZSIK, L. 2005. *What every engineer should know about computational techniques of finite element analysis* Boca Raton, Fla. , Taylor & Francis, 2005.

KURATANI, F. & YAMAUCHI, T. 2011. Simplified model for spot welded joints using multi-point constraint and its dynamic characteristics. *The Japan Society of Mechanical Engineers,* 77**,** 1748-1758.

KWAK, H. G. & KIM, J. An integrated genetic algorithm complemented with direct search for optimum design of RC frames. *Computer-Aided Design,* 41**,** 490-500.

LAMOUROUX, E., COUTELLIER, D., DOELLE, N. & KUEMMERLEN, P. 2007. Detailed model of spot-welded joints to simulate the failure of car assemblies. *International Journal on Interactive Design and Manufacturing (IJIDeM),* 1**,** 33-40.

LARDEUR, P., LACOUTURE, E. & BLAIN, E. Spot weld modelling techniques and performances of finite element models for the vibrational behaviour of automotive structures. *In:* SAS, P. & MOENS, D., eds. ISMA25 Conference, 2000 Leuven, Belgium. Departement Werktuigkunde Katholieke Universiteit Leuven, 387-394.

LEE, U. 2001. Dynamic characterization of the joints in a beam structure by using spectral element method. *Shock and Vibration,* 8**,** 357-366.

LEISSA, A. W. & KADI, A. S. 1971. Curvature effects on shallow shell vibrations. *Journal of Sound and Vibration,* 16**,** 173-187.

LEVIN, R. I. & LIEVEN, N. A. J. 1998. Dynamic finite element model updating using simulated annealing and genetic algorithms. *Mechanical Systems and Signal Processing,* 12**,** 91-120.

LIM, S. H., NIISAWA, J., TOMIOKA, N. & KOISO, A. 1990. On stress distribution of spot weld welded box beams with a longitudinal partition subjected to torsion. *International Journal of Materials and Product Technology,* 5**,** 95-108.

LINK, M. Identification and correction of errors In analytical models using test data theoretical and practical bounds. Proceedings of the 8th International Modal Anlysis Conference, 1990 Orlando, FL. Society for Experimental Mechanics, 570–578.

LIU, X., PAUROBALLY, R. & PAN, J. 2008. The effect of prestress on vibration behavior of structures in impedance method damage detection. *Advanced Materials Research* 41-42**,** 401-406.

MAGUIRE, J. R. 1996. A correlation benchmark for dynamic analysis. *Proceedings of the DTA/NAFEMS/SECED Second International***,** 1-12.

MAIA, N. M. M. & SILVA, J. M. M. 1997. *Theoretical and experimental modal analysis* Taunton, Somerset : Research Studies Press, 1997.

MALONEY, J. G., SHELTON, M., T. & UNDERHILL, D. A. 1970. Structural dynamic properties of tactical missile joints *Phase I,* . Port Royal Road, Springfield Va., 22151: General Dynamics Pomona Calif Electro Dynamic Div.

MARES, C., MOTTERSHEAD, J. E. & FRISWELL, M. I. Stochastic model updating of a spot welded structure. Proceedings of ISMA 2004: International Conference on Noise and Vibration Engineering, 2004 Leuven, Belgium. Leuven, ISMA Publications, 1885-1898.

MARWALA, T. 2004. Finite Element Model Updating Using Response Surface Method. *AIAA-Structures, structural dynamics, and materials conference***,** 5165-5173.

MARWALA, T. 2010. *Finite-element-model updating using computional intelligence techniques : applications to structural dynamics*, London ; Springer-Verlag, 2010.

MARWALA, T. & HEYNS, P. S. 1998. Multiple-criterion method for determining structural damage. *AIAA JOURNAL,* 36**,** 1494-1501.

MCKAY, M. D. 1992. Latin hypercube sampling as a tool in uncertainty analysis of computer models. *Winter Simulation Conference***,** 557.

MCKAY, M. D., BECKMAN, R. J. & CONOVER, W. J. 1979. A comparison of three methods for selecting values of input variables in the analysis of output from a computer code. *Technometrics,* 21**,** 239-245.

METROPOLIS, N. & ULAM, S. 1949. The Monte Carlo method. *Journal Of The American Statistical Association,* 44**,** 335-341.

MODAK, S. V., KUNDRA, T. K. & NAKRA, B. C. 2002a. Comparative study of model updating methods using simulated experimental data. *Computers and Structures,* 80**,** 437-447.

MODAK, S. V., KUNDRA, T. K. & NAKRA, B. C. 2002b. Prediction of dynamic characteristics using updated finite element models. *Journal of Sound and Vibration,* 254**,** 447-467.

MOENS, D. & VANDEPITTE, D. Non-probabilistic approaches for non-deterministic dynamic FE analysis of imprecisely defined structures. *In:* SAS, P. & DE MUNCK, M., eds., 2004. Leuven, ISMA Publications, 3095-3120.

MONTGOMERY, J. 2002. Methods for modeling bolts in the bolted joint. *International ANSYS User's Conference 2002,* 8**,** 1-15.

MOON, Y. M., JEE, T. H. & PARK, Y. P. 1999. Development of an automotive joint model using an analytically based formulation. *Journal of Sound and Vibration,* 220**,** 625-640.

MORDINI, A., SAVOV, K. & WENZEL, H. 2007. The finite element model updating: A powerful tool for structural health monitoring. *Structural Engineering International,* 17**,** 352-358.

MOTTERSHEAD, J. E. & FRISWELL, M. I. 1993. Model updating in structural dynamics: A survey. *Journal of Sound and Vibration,* 167**,** 347-375.

MOTTERSHEAD, J. E., GOH, E. L. & SHAO, W. 1995. On the treatment of discretization errors in finite-element model updating. *Mechanical Systems and Signal Processing,* 9**,** 101-112.

MOTTERSHEAD, J. E., LINK, M. & FRISWELL, M. I. 2011. The sensitivity method in finite element model updating: A tutorial. *Mechanical Systems and Signal Processing,* 25**,** 2275-2296.

MOTTERSHEAD, J. E., MARES, C., FRISWELL, M. I. & JAMES, S. 2000. Selection and updating of parameters for an aluminium space-frame model. *Mechanical Systems and Signal Processing,* 14**,** 923-944.

MOTTERSHEAD, J. E., MARES, C., JAMES, S. & FRISWELL, M. I. 2006. Stochastic model updating: Part 2—application to a set of physical structures. *Mechanical Systems and Signal Processing,* 20**,** 2171-2185.

MOTTRAM, J. T. & ZHENG, Y. 1996. State of the art review on the design of beam to column connections for pultruded frames. *Composite Structures,* 35**,** 387-401.

MSC.NASTRAN 2001 MSC.Nastran 2001 Release Guide.

MSC.NASTRAN 2004. MSC.Nastran 2004 Release Guide.

MSC.NASTRAN 2005a. MSC.Nastran 2005r2 Release Guide.

MSC.NASTRAN 2005b. MSC.Nastran 2005r3 Design Sensitivity and Optimization User's Guide.

MUNSI, A. S. M. Y., WADDELL, A. J. & WALKER, C. A. 2002. Modal analysis of a lightweight structure-investigation of the effects of the supports on the structural dynamics. *Mechanical Systems and Signal Processing,* 16**,** 273-284.

MYERS, R. H., KHURI, A. I. & CARTER, W. H. 1989. Response surface methodology: 1966-1988. *Technometrics***,** 137.

MYERS, R. H. & MONTGOMERY, D. C. 2002. *Response surface methodology : process and product optimization using designed experiments*, New York : J. Wiley, 2002, 2nd ed.

NICOLAI, R. P., DEKKER, R., PIERSMA, N. & VAN OORTMARSSEN, G. J. Automated response surface methodology for stochastic optimization models with unknown variance. 2004. IEEE, 491-499.

NIED, H. A. 1984. Finite element modelling of the resistance spot welding process. *Welding Journal (Miami, Fla),* 63**,** 123-132.

OLDFIELD, M., OUYANG, H. & MOTTERSHEAD, J. E. 2005. Simplified models of bolted joints under harmonic loading. *Computers and Structures,* 84**,** 25-33.

OLSSON, A., SANDBERG, G. & DAHLBLOM, O. 2003. On Latin hypercube sampling for structural reliability analysis. *Structural Safety,* 25**,** 47-68.

ORTS, D. H. 1981. Fatigue strength of spot welded joints in a HSLA steel. *SAE Technical Paper*.

OUYANG, H., OLDFIELD, M. & MOTTERSHEAD, J. E. 2006. Experimental and theoretical studies of a bolted joint excited by a torsional dynamic load. *International Journal of Mechanical Sciences,* 48**,** 1447-1455.

PAL, K. & CRONIN, D. L. 1995. Static and dynamic characteristics of spot welded sheet metal beams. *Journal of engineering for industry,* 117**,** 316-322.

PALMONELLA, M., FRISWELL, M. I., MARES, C. & MOTTERSHEAD, J. E. 2003. Improving spot weld models in structural dynamics. *ASME Design Engineering Technical Conferences and Computer and Information in Engineering Conference,* 1 379-388.

PALMONELLA, M., FRISWELL, M. I., MOTTERSHEAD, J. E. & LEES, A. W. 2004. Guidelines for the implementation of the CWELD and ACM2 spot weld models in structural dynamics. *Finite Elements in Analysis and Design,* 41**,** 193-210.

PALMONELLA, M., FRISWELL, M. I., MOTTERSHEAD, J. E. & LEES, A. W. 2005. Finite element models of spot welds in structural dynamics: Review and updating. *Computers and Structures,* 83**,** 648-661.

PEETERS, B., VAN DER AUWERAER, H., GUILLAUME, P. & LEURIDAN, J. 2004. The PolyMAX frequency-domain method: A new standard for modal parameter estimation. *Shock and Vibration,* 11**,** 395-409.

PENNY, J. E. T., FRISWELL, M. I. & GARVEY, S. D. 1994. Automatic choice of measurement locations for dynamic testing. *AIAA JOURNAL,* 32**,** 407-414.

PERERA, R. & RUIZ, A. 2008. A multistage FE updating procedure for damage identification in large-scale structures based on multiobjective evolutionary optimization. *Mechanical Systems and Signal Processing,* 22**,** 970-991.

PULA, W. & BAUER, J. 2007. Application of the response surface method. *Courses and Lectures - International Centre for Mechanical Sciences,* 491**,** 147-168.

PUREKAR, D. M. 2005. *A study of modal testing measurement errors, sensor placement and modal complexity on the process of finite element correlation.* Master Thesis, University of Cincinnati.

RAICH, A. M. & LISZKAI, T. R. 2007. Improving the performance of structural damage detection methods using advanced genetic algorithms. *Journal of Structural Engineering,* 133**,** 449-461.

RAO, M. K., ZEBROWSKI, M. P. & CRABB, H. C. 1983. Automotive body joint analysis for improved vehicle response. *Proceedings of International Symposium on Automotive Technology and Automation,* 2**,** 953-973.

RAO, S. S. 2004. *Mechanical vibrations / Singiresu S. Rao,* Upper Saddle River, New Jersey Pearson/Prentice Hall, 2004

RAPHAEL, B. & SMITH, I. F. C. 2000. A probabilistic search algorithm for finding optimally directed solutions. *Proceedings of Construction Information Technology 2000.* Icelandic Building Research Institute, Reykjavik.

REN, W. X. & CHEN, H. B. 2010. Finite element model updating in structural dynamics by using the response surface method. *Engineering Structures,* 32**,** 2455-2465.

REN, W. X., FANG, S. E. & DENG, M. Y. 2011. Response surface-based finite-element-model updating using structural static responses. *Journal of Engineering Mechanics,* 137**,** 248-257.

ROSSETTO, E., ROSSI, F., VASCHETTO, L. & ATZORI, B. 1987. Fatigue limit of spot-welded lap joints. *SAE International Congress and Exposition***,** 23-27.

RUTHERFORD, A. C., INMAN, D. J., PARK, G. & HEMEZ, F. M. 2005. Use of response surface metamodels for identification of stiffness and damping coefficients in a simple dynamic system. *Shock and Vibration,* 12**,** 317-331.

RUTHERFORD, A. C., MAUPIN, R. D. & HEMEZ, F. M. Latin hypercube sampling vs. metamodel Monte Carlo for propagating uncertainty through transient dynamics simulations. IMAC-XXIV: Conference & Exposition on Structural Dynamics, 2006 St Louis, Missouri, USA.: Curran Associates, Inc. (Jun 2006).

RUTHERFORD, B. 2002. Response-modeling for the design of computer experiments. *IMAC XX20th International Modal Analysis Conference* 4753 I**,** 683-688.

RUTHERFORD, B. 2006. A response-modeling alternative to surrogate models for support in computational analyses. *Reliability Engineering and System Safety,* 91**,** 1322-1330.

RUTMAN, A., BOSHERS, C., PEARCE, L. & PARADY, J. 2007. Fastener modeling for joining parts modeled by shell and solid elements. *Americas Virtual Product Development Conference***,** 1-26.

RUTMAN, A., BOSHERS, C., PEARCE, L. & PARADY, J. 2009. Fastener modeling for joining composite parts. *Americas Virtual Product Development Conference***,** 1-28.

SAMUELSSON, A. & ZIENKIEWICZ, O. C. 2006. History of the stiffness method. *International Journal for Numerical Methods in Engineering,* 67**,** 149-157.

SCHEDLINSKI, C., WAGNER, F., BOHNERT, K., FRAPPIER, J., IRRGANG, A., LEHMANN, R. & MÜLLER, A. 2005. Test-based computational model updating of a car body in white. *Sound & Vibration,* 39**,** 19-23.

SCHULZ, M. J. & INMAN, D. J. 1994. Model updating using constrained eigensstructure assigment. *Journal of Sound and Vibration,* 178**,** 113-130.

SIDHU, J. & EWINS, D. J. Correlation of finite element and modal test studies of a practical structures. Proceedings of the International Modal Analysis Conference & Exhibit 2, 1984 Orlando, FL, USA. 756-762.

SILVA, J. M. M., BATISTA, F. C. & MAIA, N. M. M. 2005. Dynamics modelling of spot welded joints. *Twelfth International Congress on Sound and Vibration***,** 1-10.

SIMMERMACHER, T., JAMES, S. & HURTADO, J. E. 1997. Structural Health Monitoring of Wind Turbines. *Proceedings of the international workshop on structural health monitoring***,** 788-797.

SIMPSON, T. W., LIN, D. K. J. & CHEN, W. 2001a. Sampling strategies for computer experiments: Design and analysis. *International Journal of Reliability and Applications,* 2**,** 209-240.

SIMPSON, T. W., PEPLINSKI, J. D., KOCH, P. N. & ALLEN, J. K. 2001b. Metamodels for computer-based engineering design: survey and recommendations. *Engineering with Computers,* 17**,** 129-150.

SINHA, J. K. & FRISWELL, M. I. 2002. Model Updating: A tool for reliable modelling, design modification and diagnosis. *Shock & Vibration Digest,* 34**,** 27-35.

SINHA, J. K., FRISWELL, M. I. & EDWARDS, S. 2002. Simplified models for the location of cracks in beam structures using measured vibration data. *Journal of Sound and Vibration,* 251**,** 13-38.

STEIN, M. 1987. Large sample properties of simulations using Latin hypercube sampling. *Technometrics,* 9.

STEWART, P., FLEMING, P. J. & MACKENZIE, S. A. On the response surface methodology and designed experiments for computationally intensive distributed aerospace simulations. *In:* YUCESAN, E., ed. Proceedings of the 2002 Winter Simulation Conference, 2002 San Diego, California, USA. IEEE, 476-482.

TEUGHELS, A., DE, R., G. & SUYKENS, J. A. K. 2003. Global optimization by coupled local minimizers and its application to FE model updating. *Computers and Structures,* 81**,** 2337-2351.

TITURUS, B. & FRISWELL, M. I. 2008. Regularization in model updating. *International Journal for Numerical Methods in Engineering,* 75**,** 440-478.

TORSTEN, E. & ROLF, S. 2007. *Modelling of spot welds for NVH simulations in view of refined panel meshes.* Master's Thesis, Chalmers University of Technology.

TSAI, J. S. & CHOU, Y. F. 1988. The identification of dynamic characteristics of a single bolt joint. *Journal of Sound and Vibration,* 125**,** 487-502.

VENTER, G. 2010. Review of optimization techniques. *Encyclopedia of Aerospace Engineering.* John Wiley & Sons, Ltd.

VENTURA, C. E., BRINCKER, R., DASCOTTE, E. & ANDERSEN, P. FEM Updating of the Heritage Court Building Structure. International modal analysis conference; Proceedings of IMAC-XIX a conference on structural dynamics, 2001 Orlando, FL, USA. Society for Experimental Mechanics, 324-330.

VOPEL, H. G. & HILLMANN, J. 1996. Berücksichtigung der schweipunkte bei der FEM-modellierung von karosserien. *VDI-Berichte,* 1283**,** 171-181.

WOLF, J. A. 1984. The influence of mounting stiffness on frequencies measured in a vibration test. *SAE Technical Paper* 840480**,** 1-10.

XU, S. & DENG, X. 2004. An evaluation of simplified finite element models for spot-welded joints. *Finite Elements in Analysis & Design,* 40**,** 1175-1194.

YOO, J., HONG, S. J., CHOI, J. S. & KANG, Y. J. 2009. Design guide of bolt locations for bolted-joint plates considering dynamic characteristics. *Proceedings of the Institution of Mechanical Engineers, Part C: Journal of Mechanical Engineering Science,* 223**,** 363-375.

YU, Q., MOSTAGHEL, N. & FU, K. C. 1994. Effect of initial curvature on natural frequency of thin-plate on hinge supports. *Journal of Engineering Mechanics* 120**,** 796-813.

YUNUS, M. A., ABDUL RANI, M. N., OUYANG, H., DENG, H. & JAMES, S. 2011. Identification of damaged spot welds in a complicated joined structure. *Journal of Physics: Conference Series,* 305**,** 1-10.

ZABEL, V. & BREHM, M. Model updating methods - A comparative study. Conference Proceedings of the Society for Experimental Mechanics Series, 2009 Orlando, FL. 27th Conference and Exposition on Structural Dynamics, IMAC XXVII, 1-11.

ZANG, C., CHEN, G. & EWINS, D. J. 2006a. Finite element model updating with modal data. *Conference: 2006 IMAC-XXIV: Conference & Exposition on Structural Dynamics,* 5**,** 1-10.

ZANG, C., CHEN, G. & EWINS, D. J. 2006b. A review of advances in developments in FE model validation. *Conference: 2006 IMAC-XXIV: Conference & Exposition on Structural Dynamics***,** 1-12.

ZHANG, Q. & LALLEMENT, G. 1987. Dominant error localisation in a finite element model of a mechanical structure. *Mechanical Systems and Signal Processing,* 1**,** 141-149.

ZIAEI-RAD, S. & IMREGUN, M. 1996. On the accuracy required of experimental data for finite element model updating. *Journal of Sound and Vibration,* 196**,** 323-335.

ZIENKIEWICZ, O. C., TAYLOR, R. L., NITHIARASU, P. & ZHU, J. Z. 2005. *The finite element method / O. C. Zienkiewicz, R. L. Taylor, J. Z. Zhu*, Oxford : Elsevier/Butterworth-Heinemann, 2005. 6th ed.

ZINGG, D. W., NEMEC, M. & PULLIAM, T. H. 2008. A comparative evaluation of genetic and gradient-based algorithms applied to aerodynamic optimization. *European Journal of Computational Mechanics/Revue Européenne de Mécanique Numérique,* 17**,** 103-126.

ŽIVANOVIĆ, S., PAVIC, A. & REYNOLDS, P. 2007. Finite element modelling and updating of a lively footbridge: The complete process. *Journal of Sound and Vibration,* 301**,** 126-145.